united nations
educational, scientific
and cultural
organization

international atomic
energy agency

the
abdus salam
international centre for theoretical physics
40th anniversary 1964 2004

H4.SMR/1586-23

"7th Workshop on Three-Dimensional Modelling of Seismic Waves Generation and their Propagation"

25 October - 5 November 2004

Study of Active Tectonic Regions

F. WU

State University of New York
Department of Geological Sciences
New York, U.S.A.

New Zealand geology

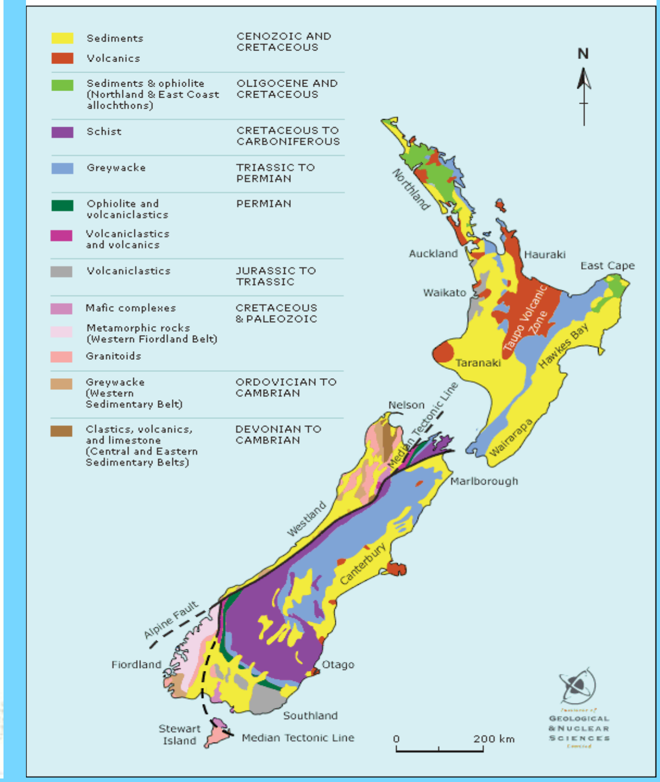

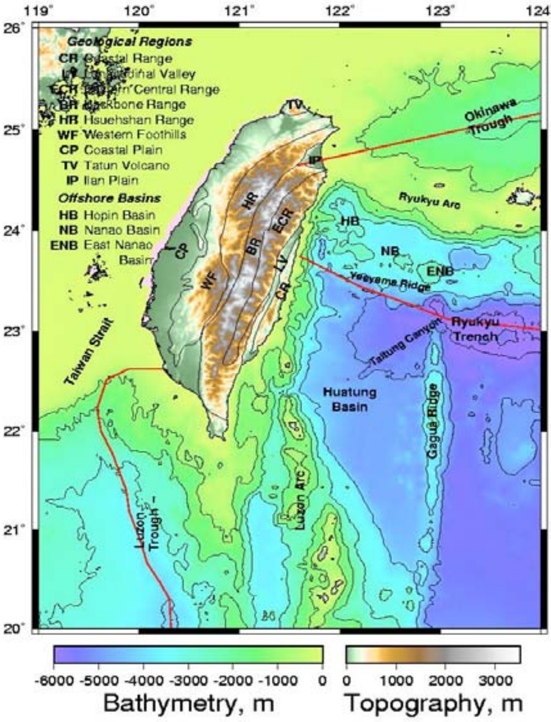

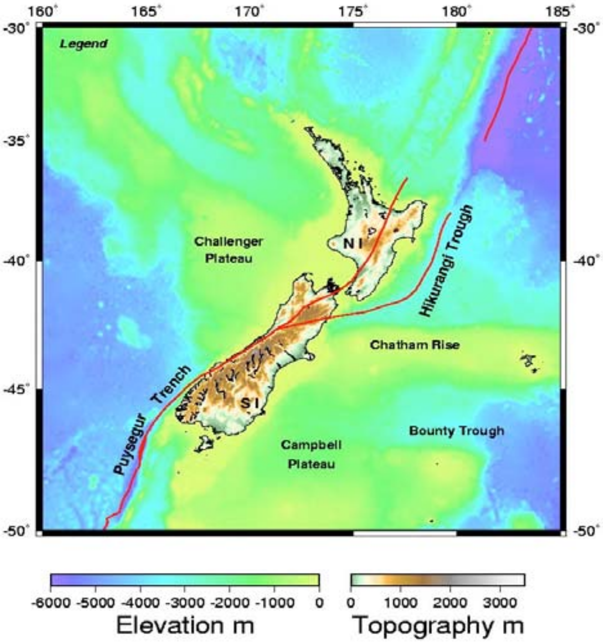

Seismicity of New Zealand

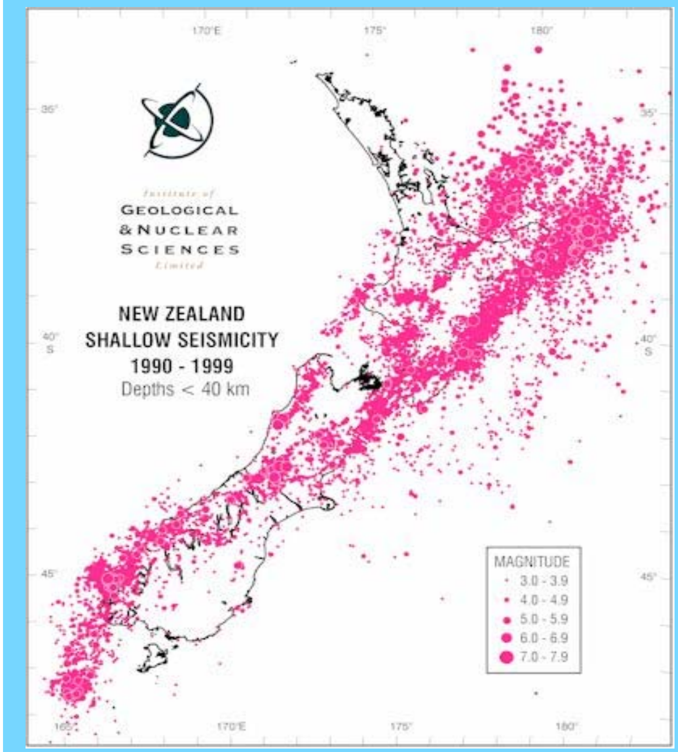

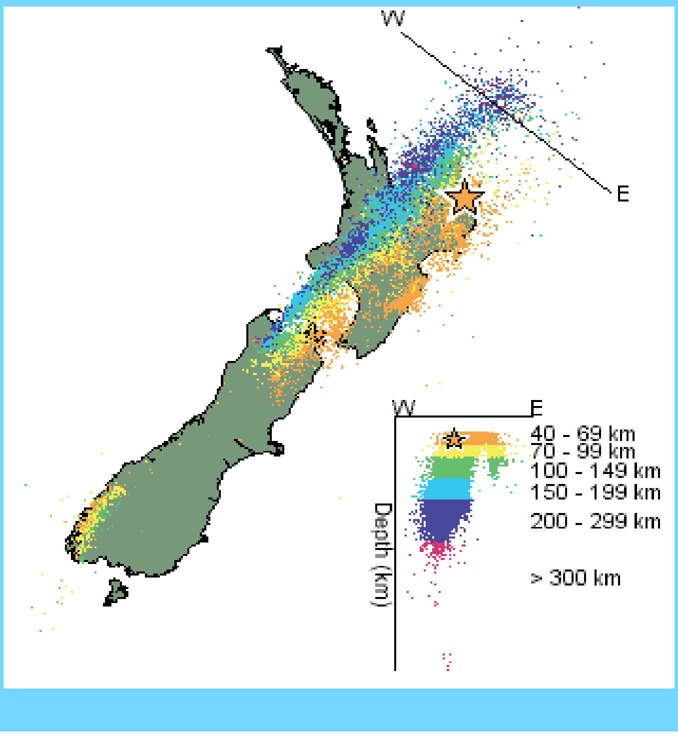

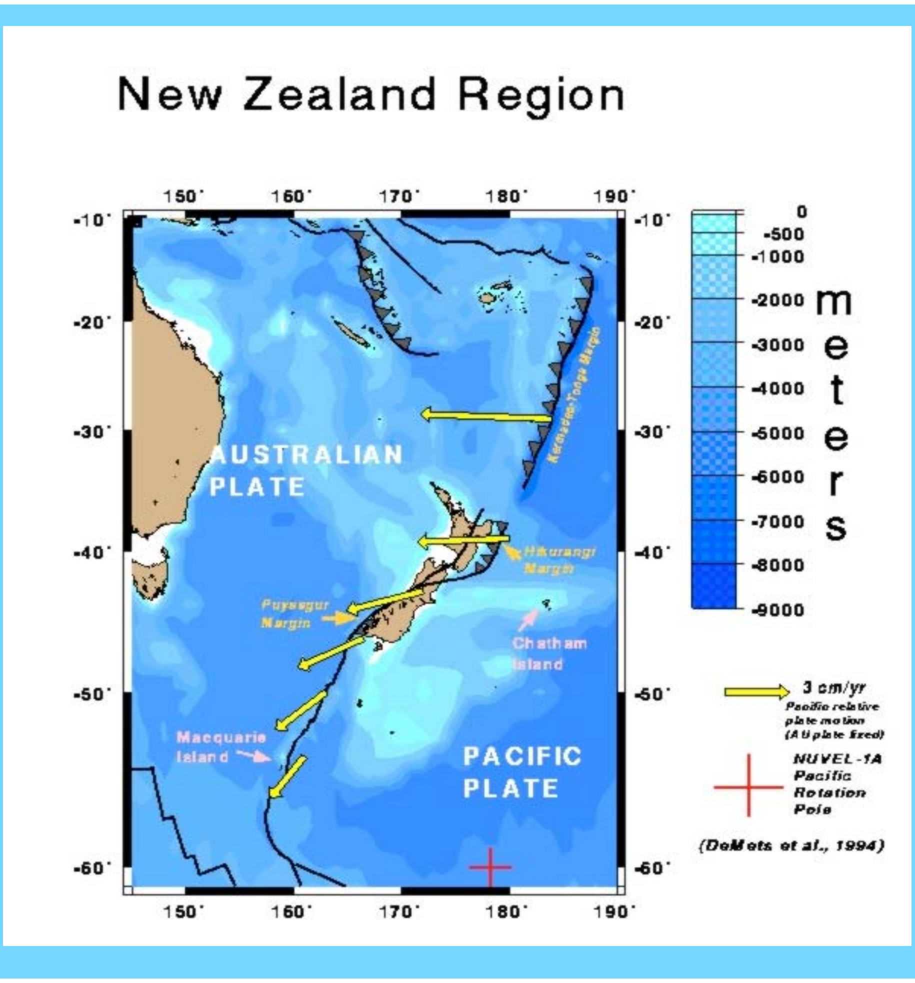

The plate boundaries around New Zealand. Notice the change of polarities from the northern zone to the southern zone. The yellow vectors indicate plate motions.

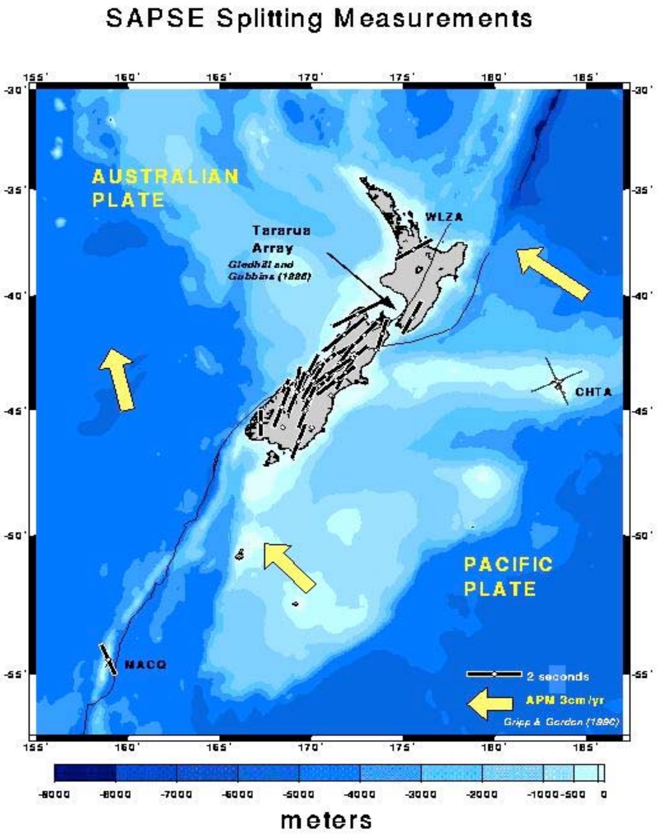

the regional distribution of S wave splitting obtained in the 1995-1997 experiment. Note the trend-parallel fast directions on the South Island and the lack of clear splitting on Chatham and the plate motion-parallel vector on Macquarie Island.

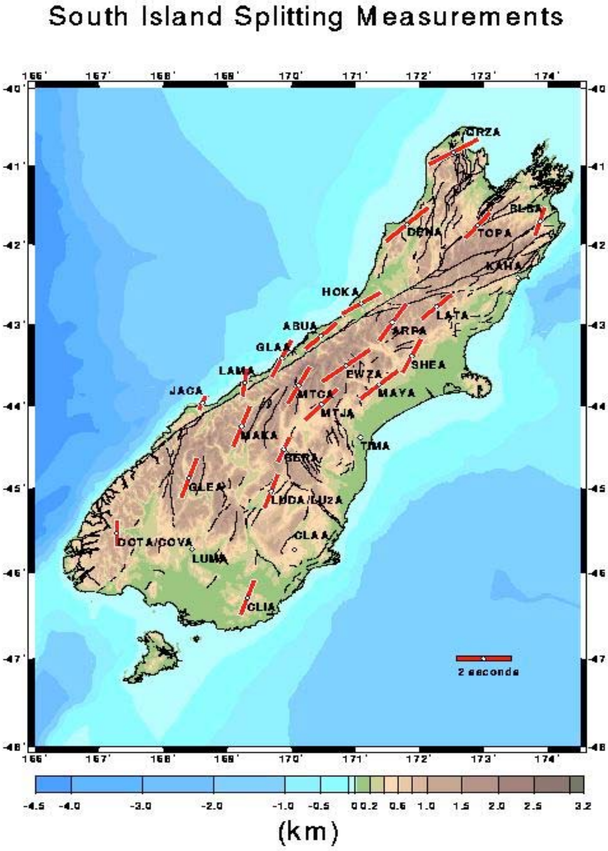

On the South Island the fast S-splitting direction can clearly be seen as parallel to the local structural trend.

knowing that the S-splitting delays are too large for the source of delays to be in the crust, these measurements imply an upper mantle source for the splitting.

A simple interpretation is that the plate boundary shearing causes the splitting and this shearing is coherent through the crust and the uppermMantle.

Because there is no OBS measurements it is not know where do the splitting anomalies stop offshore.

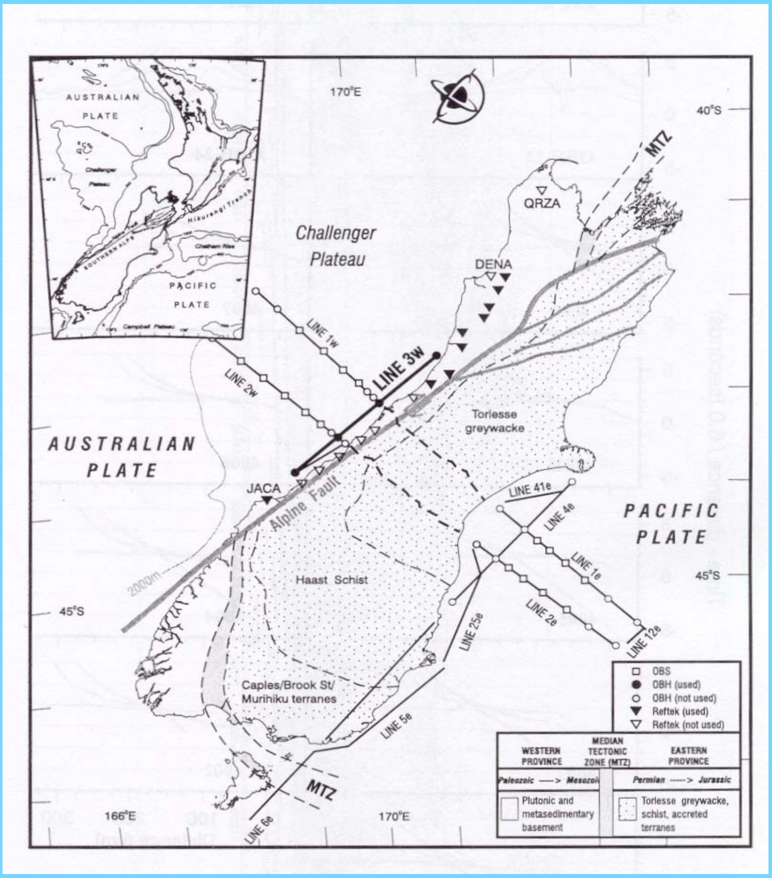

During the 1995-1996 sea-land two Profile lines were obtained. The Airguns shot over the line of OBS (circles) as well as recorded as Multiple channel marine seismic Lines. Along the dashed lines on Land 3-component instruments at A spacing of about 1 km interval Were used to record the airguns. At The same time reflection profiling Using explosives were also shot.

The combined data were used to Derive the crustal profiles shown Next.

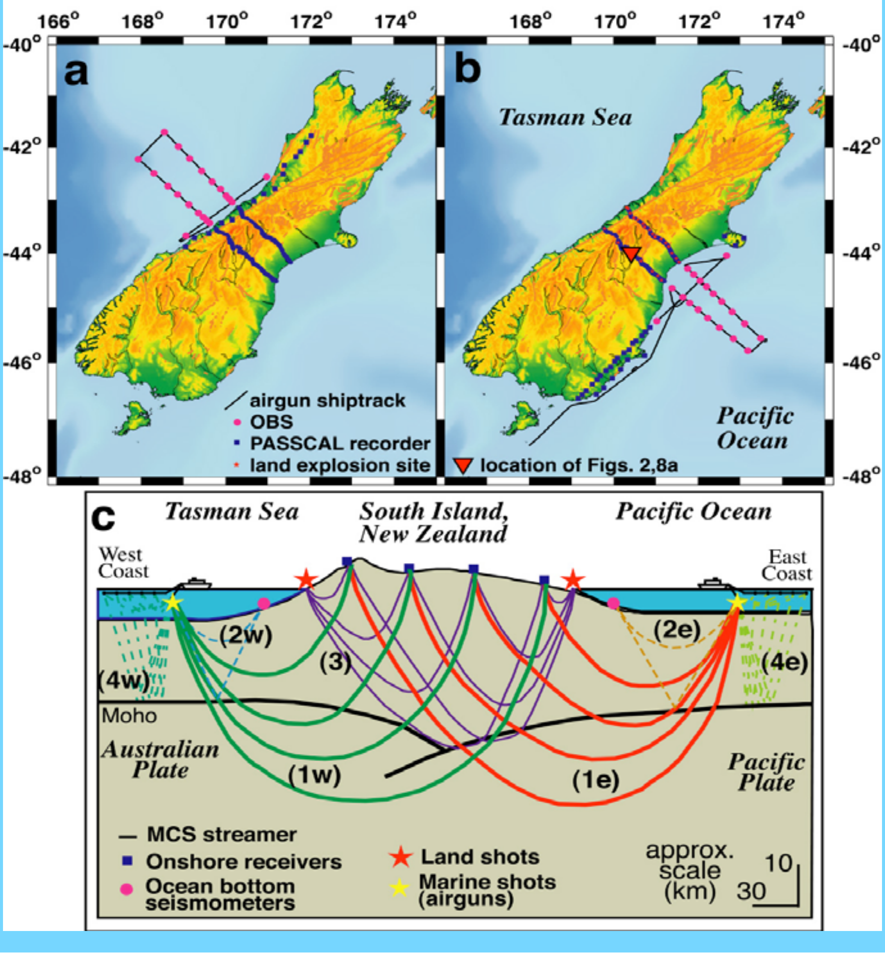

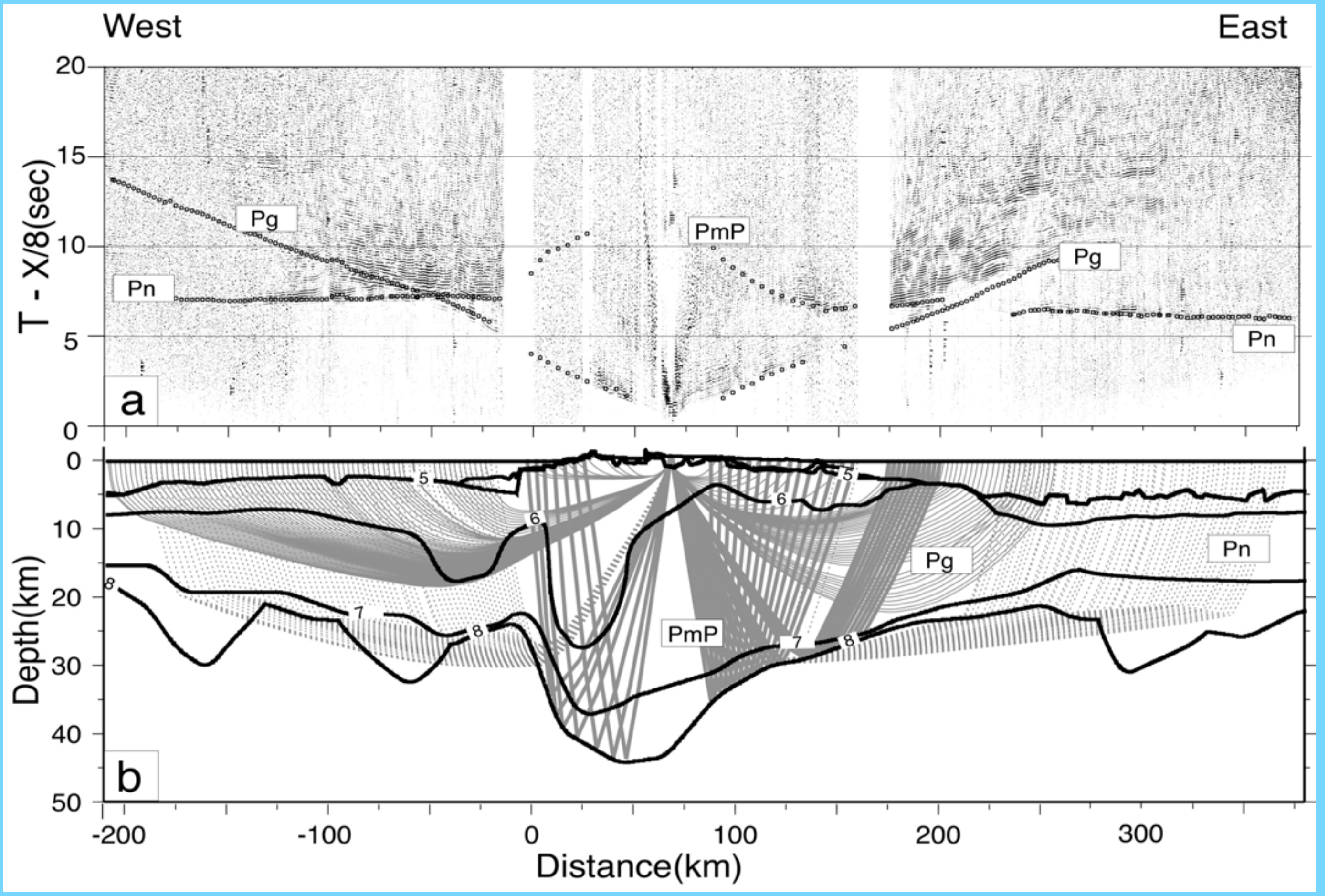

West
East
T - X/8(sec)
20
15
10
5
0
Pg
Pn
PmP
Pg
Pn
a
Depth(km)
0
10
20
30
40
50
5
6
7
8
5
6
7
8
Pg
Pn
PmP
b
-200
-100
0
100
200
300
Distance(km)

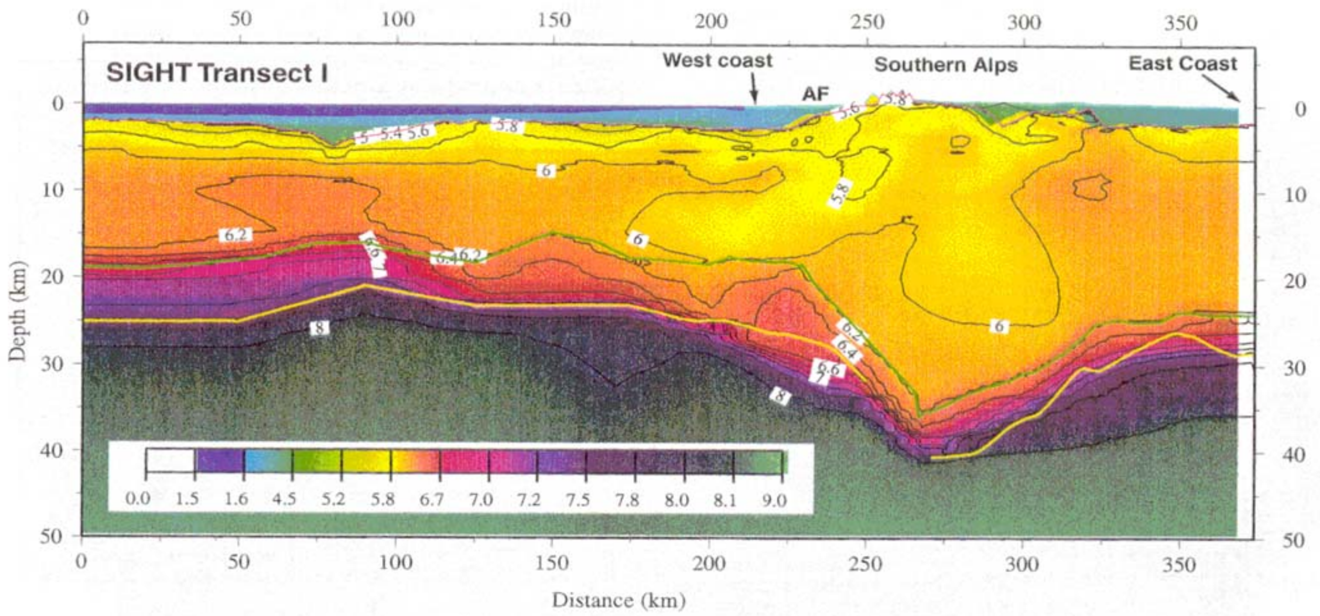

SIGHT Transect I
West coast
Southern Alps
East Coast
AF
0
50
100
150
200
250
300
350
Depth (km)
0
10
20
30
40
50
5.4
5.6
5.8
6
6.2
6.4
6.6
7
8
0.0
1.5
1.6
4.5
5.2
5.8
6.7
7.0
7.2
7.5
7.8
8.0
8.1
9.0
Distance (km)

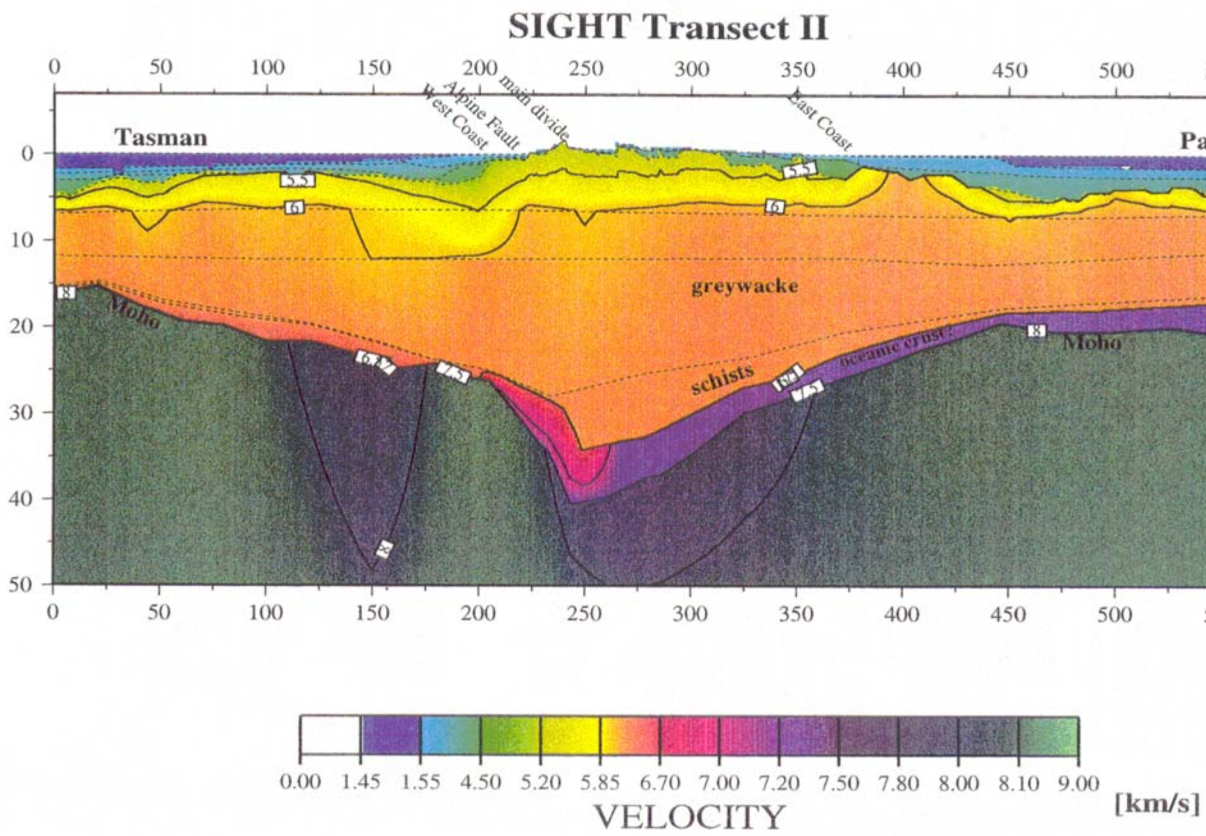

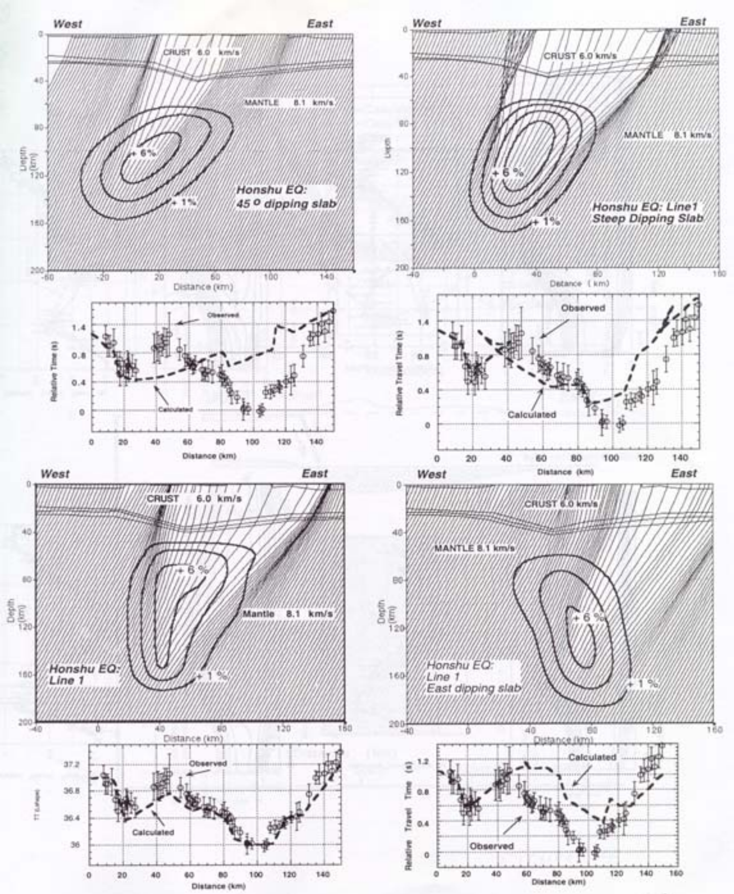

While waiting for R/V Ewing to go From one side of the island to the Other the 3-component instruments Also recorded signals from three Teleseisms. The delays times at the Line of stations, after the crustal Effects were removed, show early Arrivals in central parts of the island.

The early arrivals indicate the presence Of a high velocity body. This body is Directly under the island and cannot Be explained as subducted lithosphere.

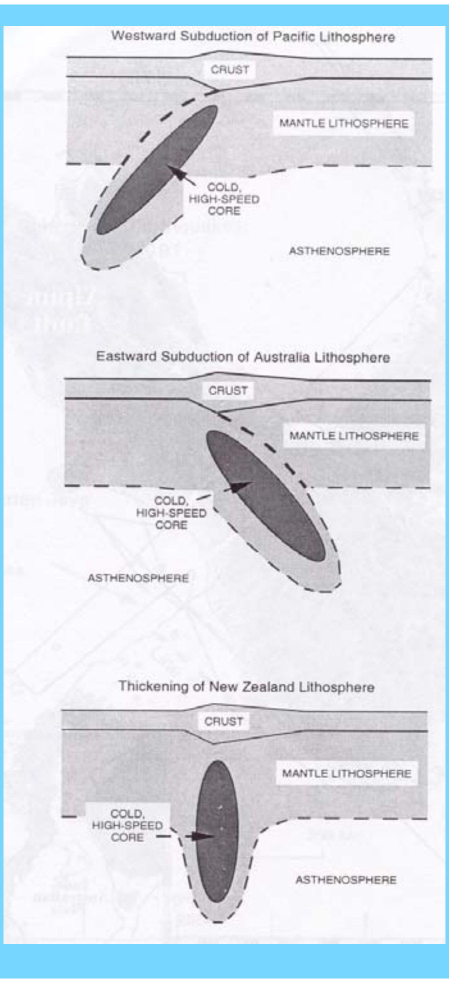

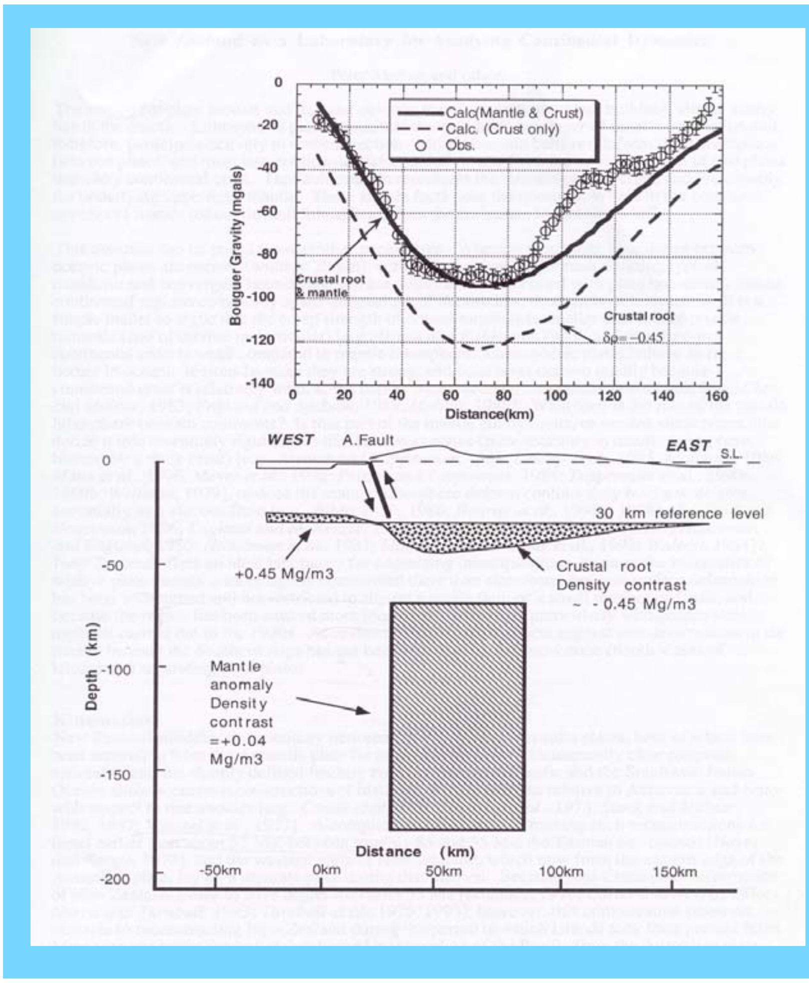

From the gravity data it is evident
That the additional mass in mantle
Compensates for the excessively
Deep crust.

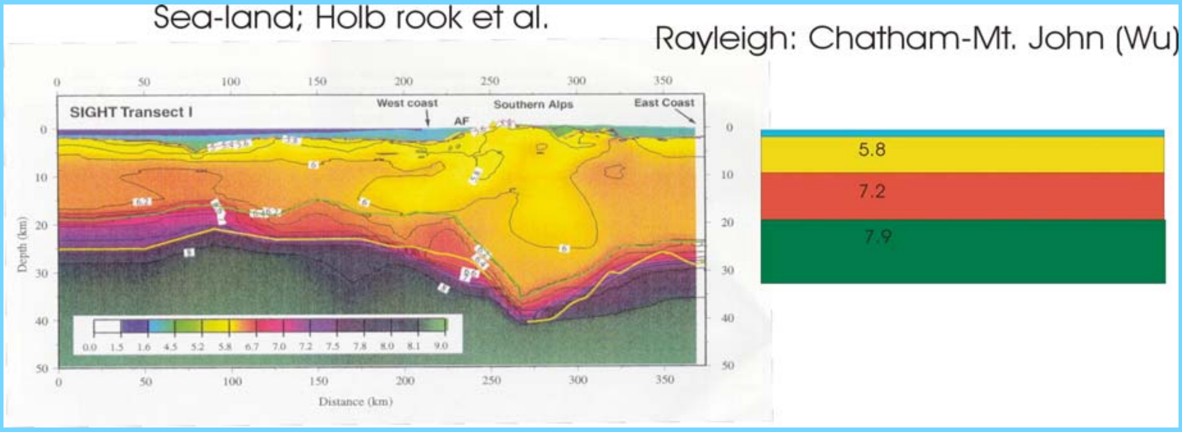

Balancing of crustal thickening and effect of shortening

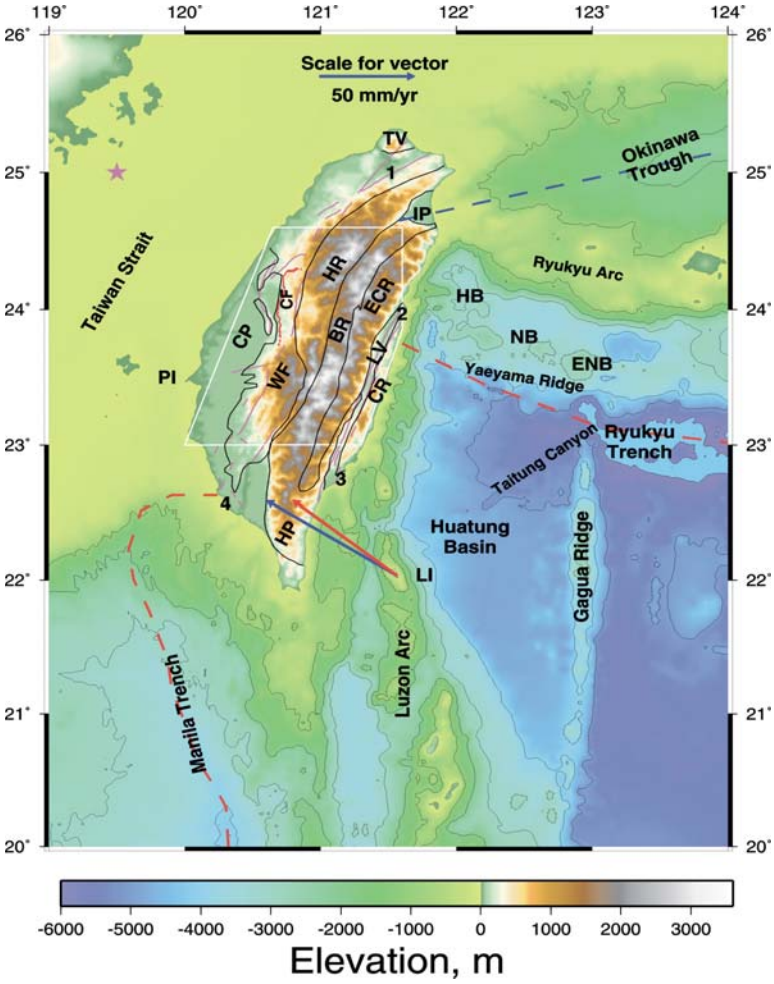

CR=Coastal R.
LV=Long. Valley
ECR=E. Central R.
BR=Backbone R.
HR=Hsueshan R.
WF=W. Foothills
CP=Coastal Plain
IP=Ilan Plain
TV=Tatun Volc.
PI=Penghu Is.
LI=Lanhsu I.
HB=Huatung B.
NB=Nanao B.
ENB=E. Nanao B.


臺灣地質圖
GEOLOGIC MAP OF TAIWAN
中華民國七十五年 (1986)
比例尺 五十萬分之一
SCALE 1:500,000
0 10 20 30 40 50 Kilometers
經濟部中央地質調查所編印
PUBLISHED BY
CENTRAL GEOLOGICAL SURVEY, MINISTRY OF ECONOMIC AFFAIRS
所長 詹新甫
SHIN-FU TSAN, DIRECTOR
何春蓀 編製
COMPILED BY C. S. HO
臺灣海峽
TAIWAN STRAIT
太平洋
PACIFIC OCEAN
圖例 LEGEND

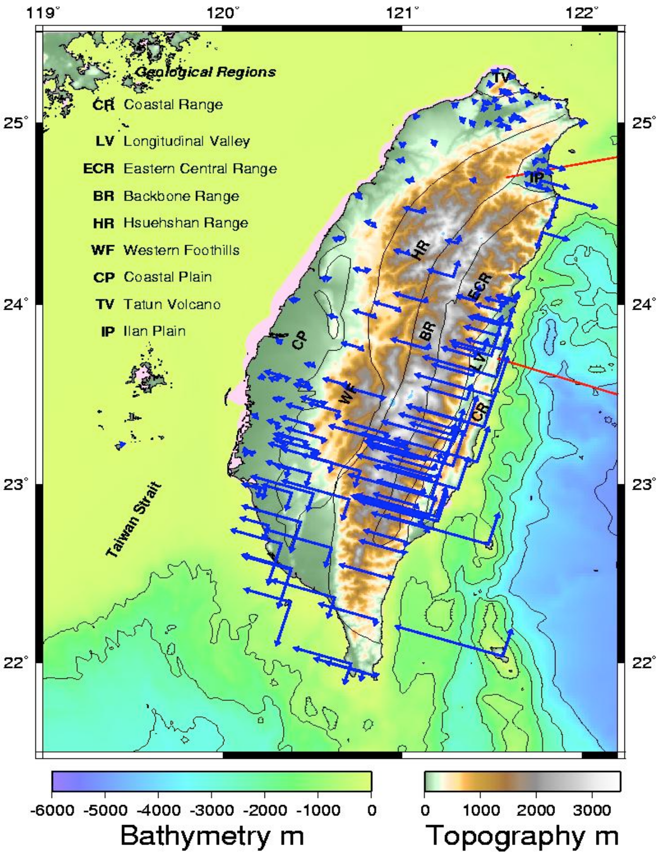
119°
120°
121°
122°
25°
24°
23°
22°
Geological Regions
CR Coastal Range
LV Longitudinal Valley
ECR Eastern Central Range
BR Backbone Range
HR Hsuehshan Range
WF Western Foothills
CP Coastal Plain
TV Tatun Volcano
IP Ilan Plain
TV
IP
HR
ECR
BR
CP
LV
WF
CR
Taiwan Strait
-6000
-5000
-4000
-3000
-2000
-1000
0
Bathymetry m
0
1000
2000
3000
Topography m

Active Deformation of Taiwan Orogen

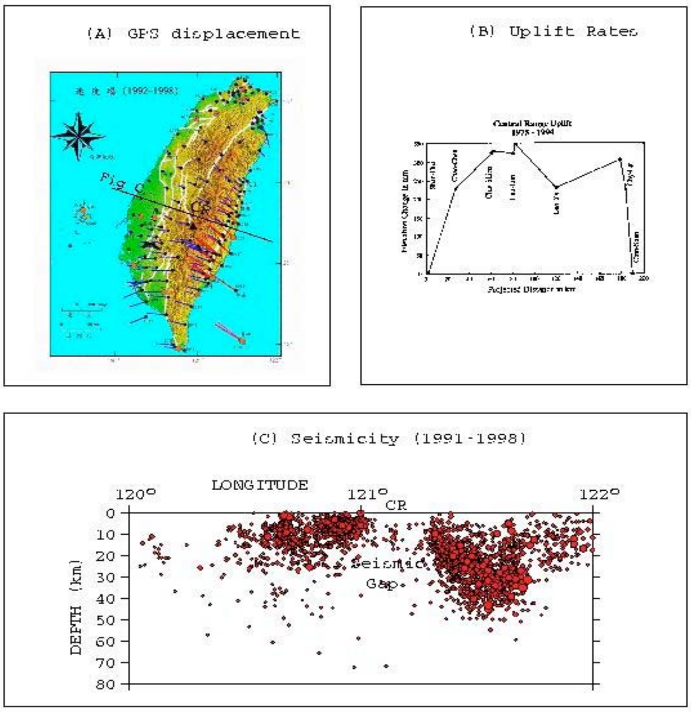

Figure 2

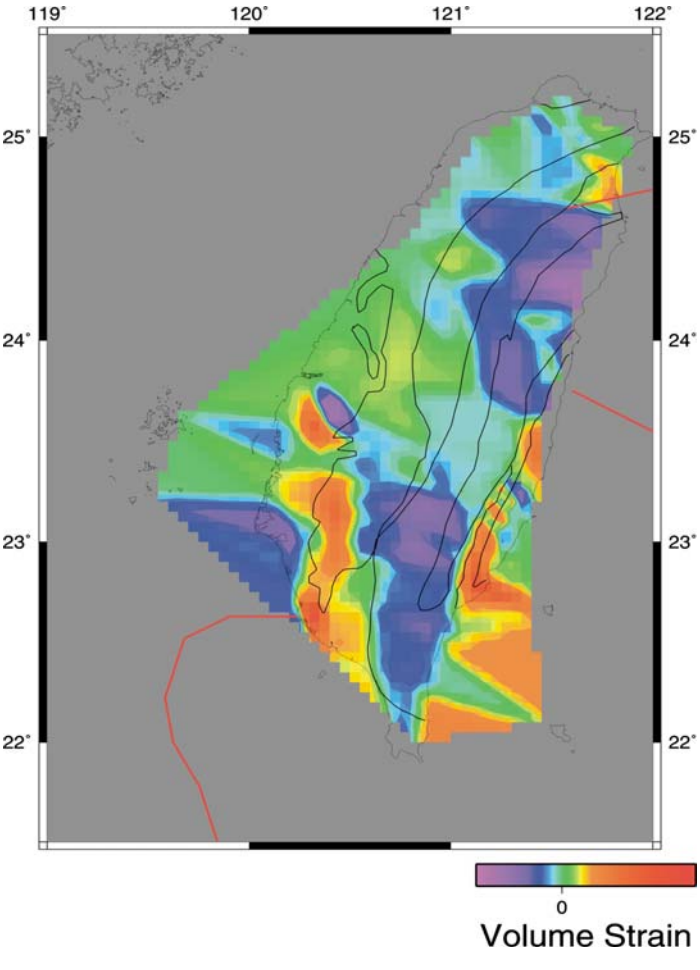

1999 Chi-Chi Earthquake

- Magnitude 7.6
- Mainly NS-trending reverse fault dipping east at about 25-30^{O}.
- Maximum ~9 m horizontal and ~4 m vertical displacements of the hangwall block
- But it does **not** contribute directly to mountain building

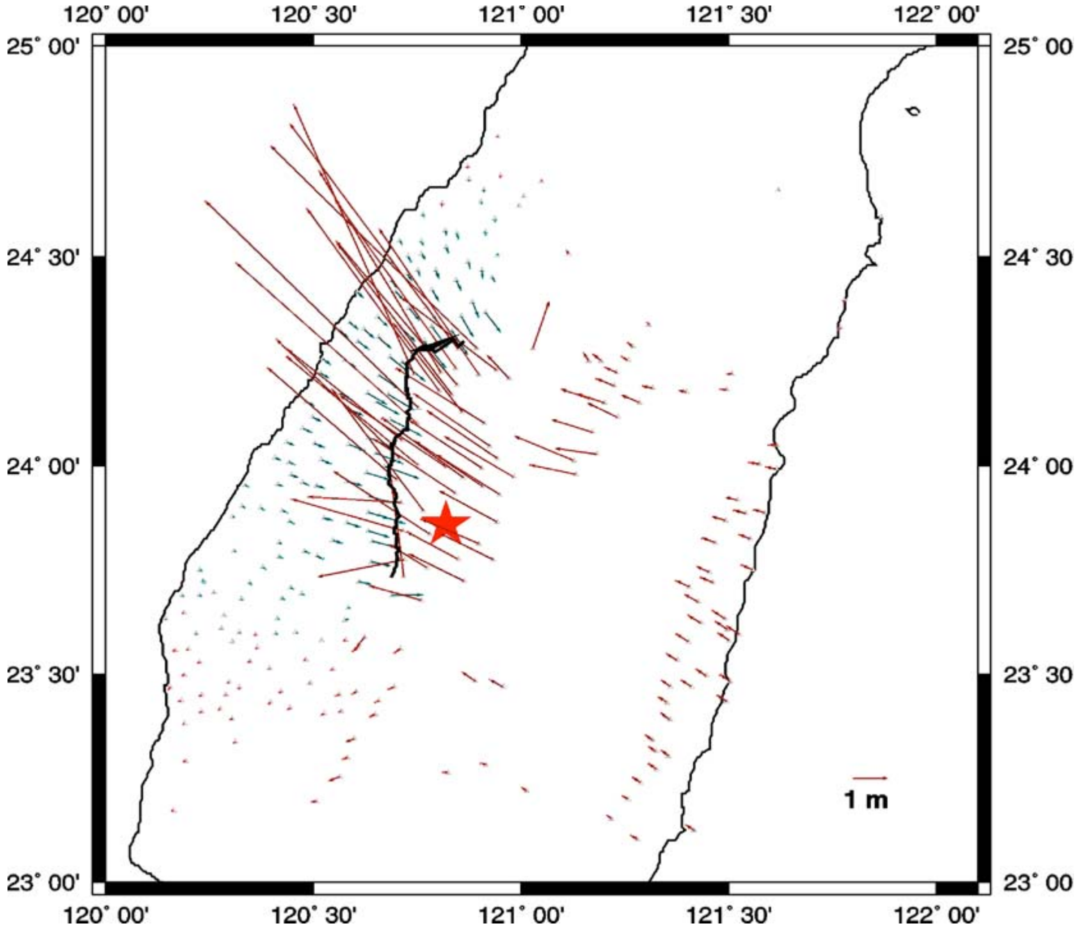
120° 00'
120° 30'
121° 00'
121° 30'
122° 00'
25° 00'
24° 30'
24° 00'
23° 30'
23° 00'
1 m

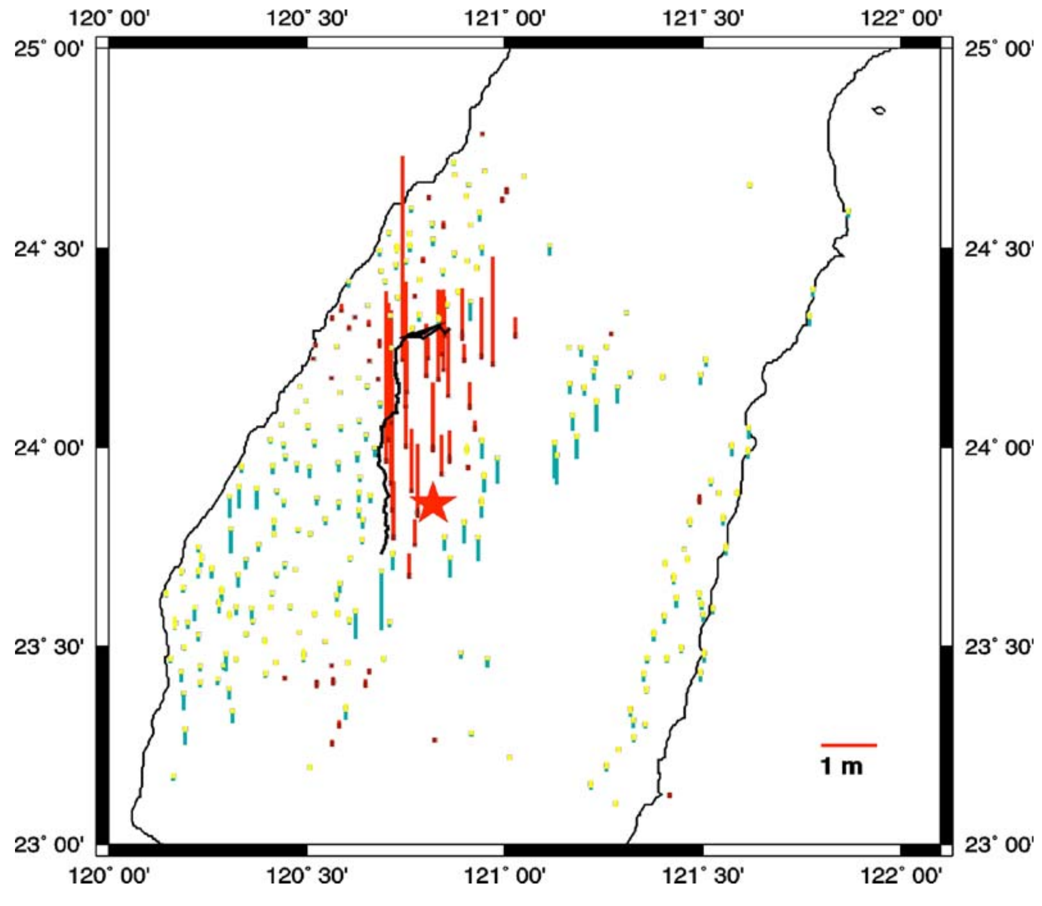
120° 00'
120° 30'
121° 00'
121° 30'
122° 00'
25° 00'
24° 30'
24° 00'
23° 30'
23° 00'
1 m

Mechanism of Rebound Thrust

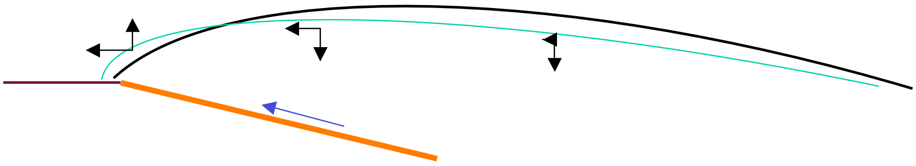

Following the Chi-Chi earthquake the Central Range subsided by about 60 cm. But the uplift rate of the Central Range is > 1 cm/yr. If recurrence is about 1000 years, then the mountain is still going up at the rate of 10m-.6m during this time!

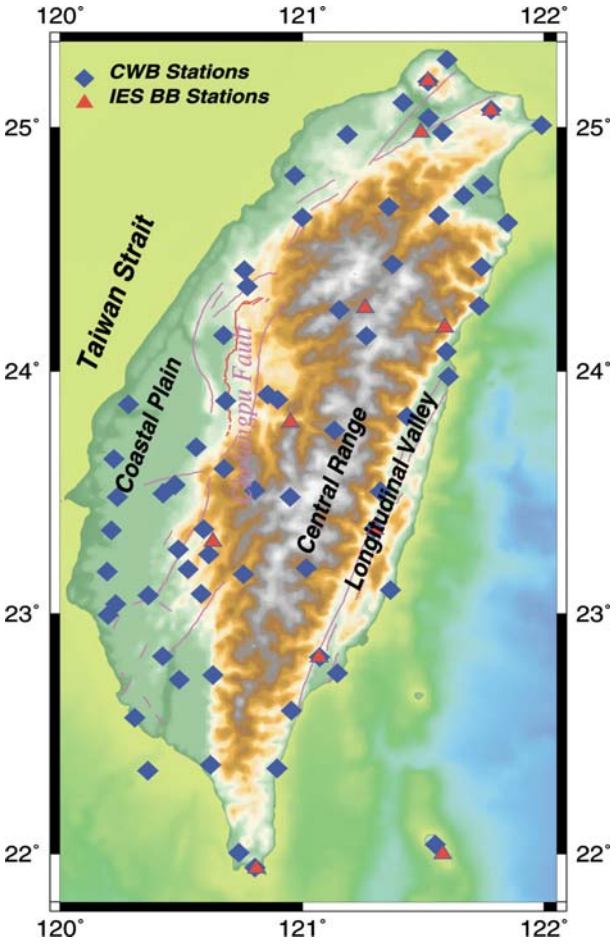

Precise Hypocentral Relocation with Double-Difference Relocation

---

Double Difference Eq Location

(Waldhauser and Ellsworth, 2000)

If the hypocentral separation of two events is small compared to

(a) the station-event distance and

(b) the spatial scale of velocity variations

then the ray paths for a common station recording both events are similar.

=> $\Delta tt \propto \Delta d$

- Network catalog times can be used
- Better results will be obtained with more accurate relative arrival times (correlation)
- travel time residual for event j and station k:

$$\frac{\partial t_k^j}{\partial m}\Delta m^j = r_k^j$$

$$r_k^j = (t^{obs} - t^{cal})^j$$

$$\Delta m^j = (\Delta x^j, \Delta y^j, \Delta z^j, \Delta \boldsymbol{\tau}^j)$$

- Relative hypocentral parameters between two closeby events i and j (where slowness does not change between events):

$$\frac{\partial t_k^{ij}}{\partial m}\Delta m^{ij} = dr_k^{ij}$$

$$dr_k^{ij} = (t_k^i - t_k^j)^{obs} - (t_k^i - t_k^j)^{cal}$$

$$\Delta m^{ij} = (\Delta dx^{ij}, \Delta dy^{ij}, \Delta dz^{ij}, \Delta d\boldsymbol{\tau}^{ij})$$

- In General, where velocity varies sufficiently different slowness for each events has to be used:

$$\frac{\partial t_k^i}{\partial m}\Delta m^i - \frac{\partial t_k^j}{\partial m}\Delta m^j = dr_k^{ij}$$

Combining near and distant events in the inversion for location of all events with respect to a centroid location:

$\mathbf{G}\mathrm{m}=\mathrm{d}$

Or, with weights,

$\mathbf{WG}\mathrm{m}=\mathbf{W}\mathrm{d}$

- Temporal sequence of faulting
- Distribution of foci; rheology or fluid?
- Focal mechanisms and kinematics

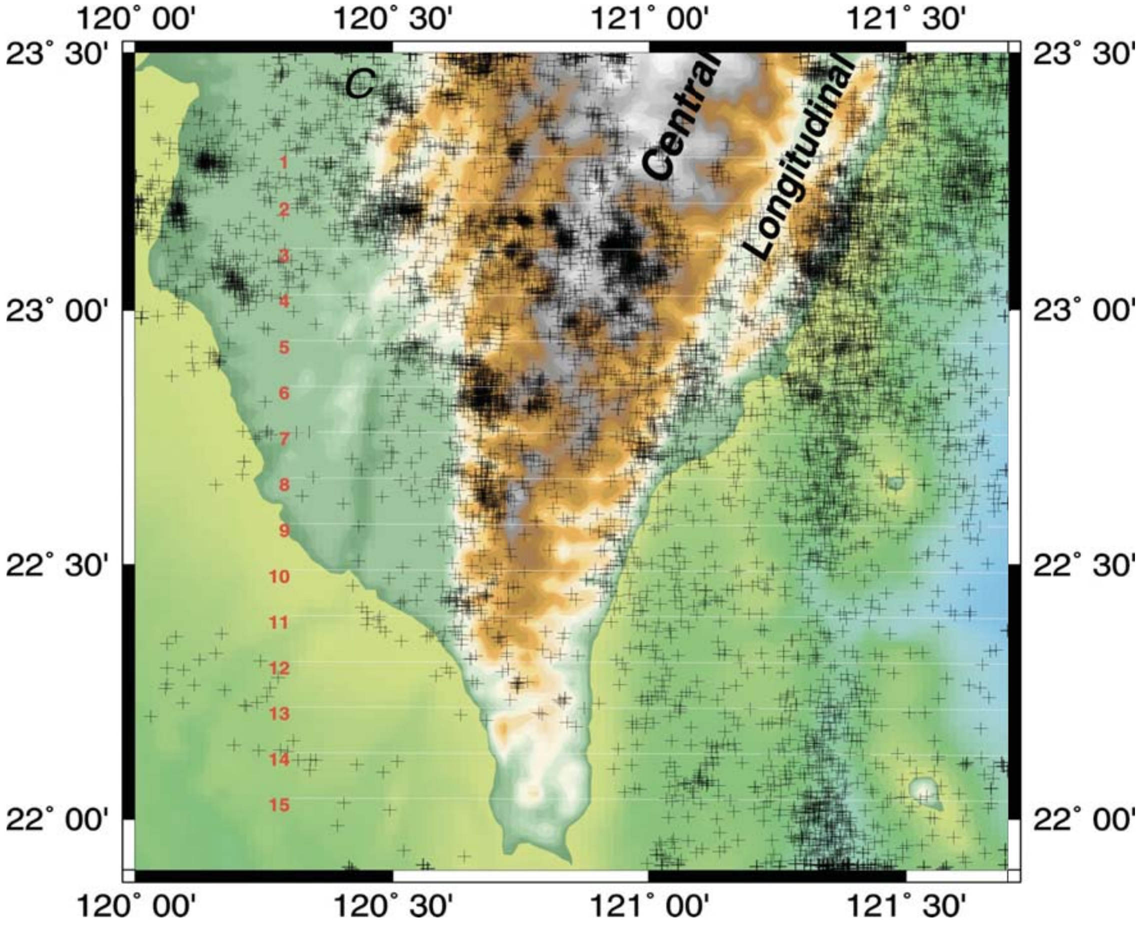

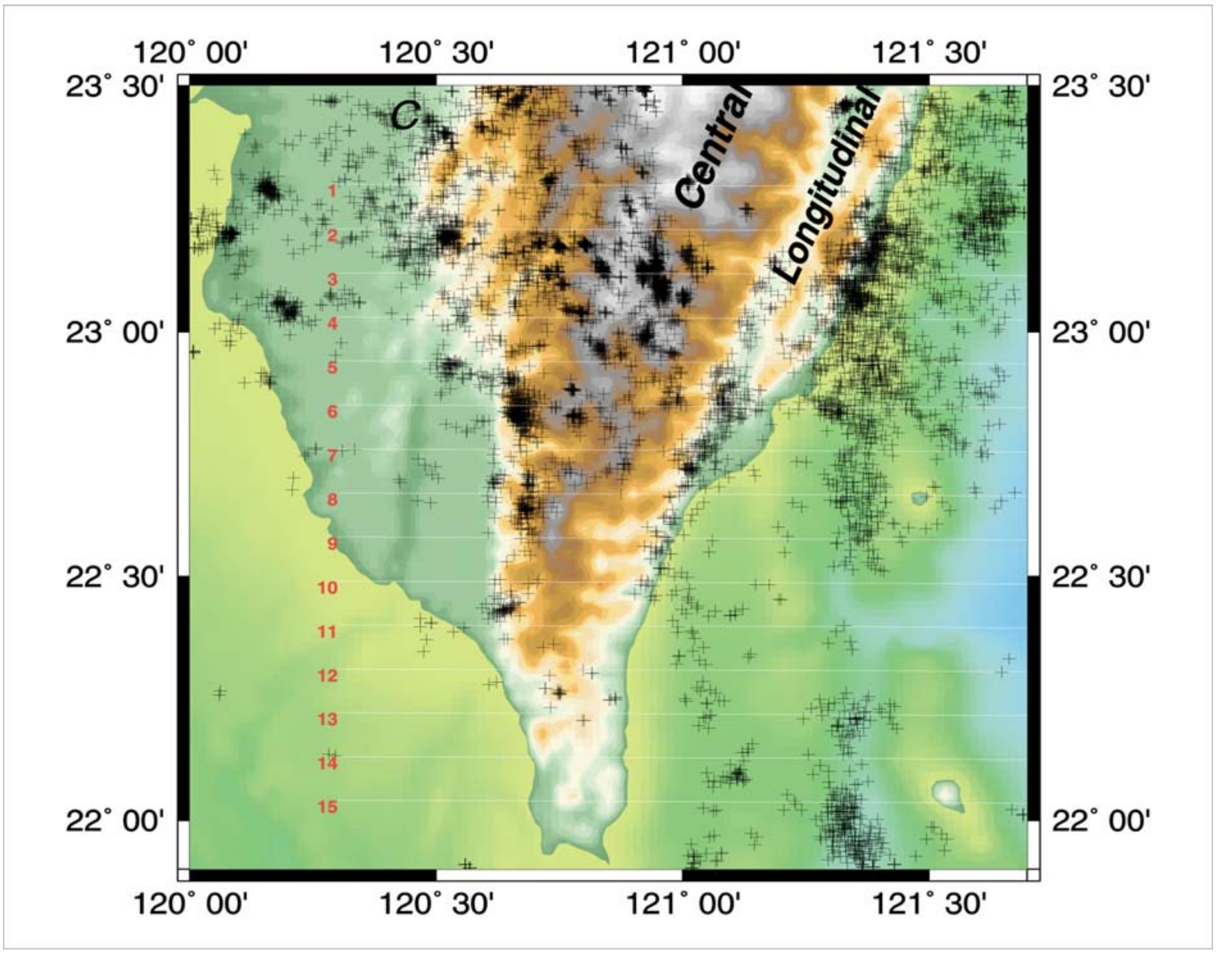
120° 00'
120° 30'
121° 00'
121° 30'
23° 30'
23° 00'
22° 30'
22° 00'
C
Central
Longitudinal
1
2
3
4
5
6
7
8
9
10
11
12
13
14
15

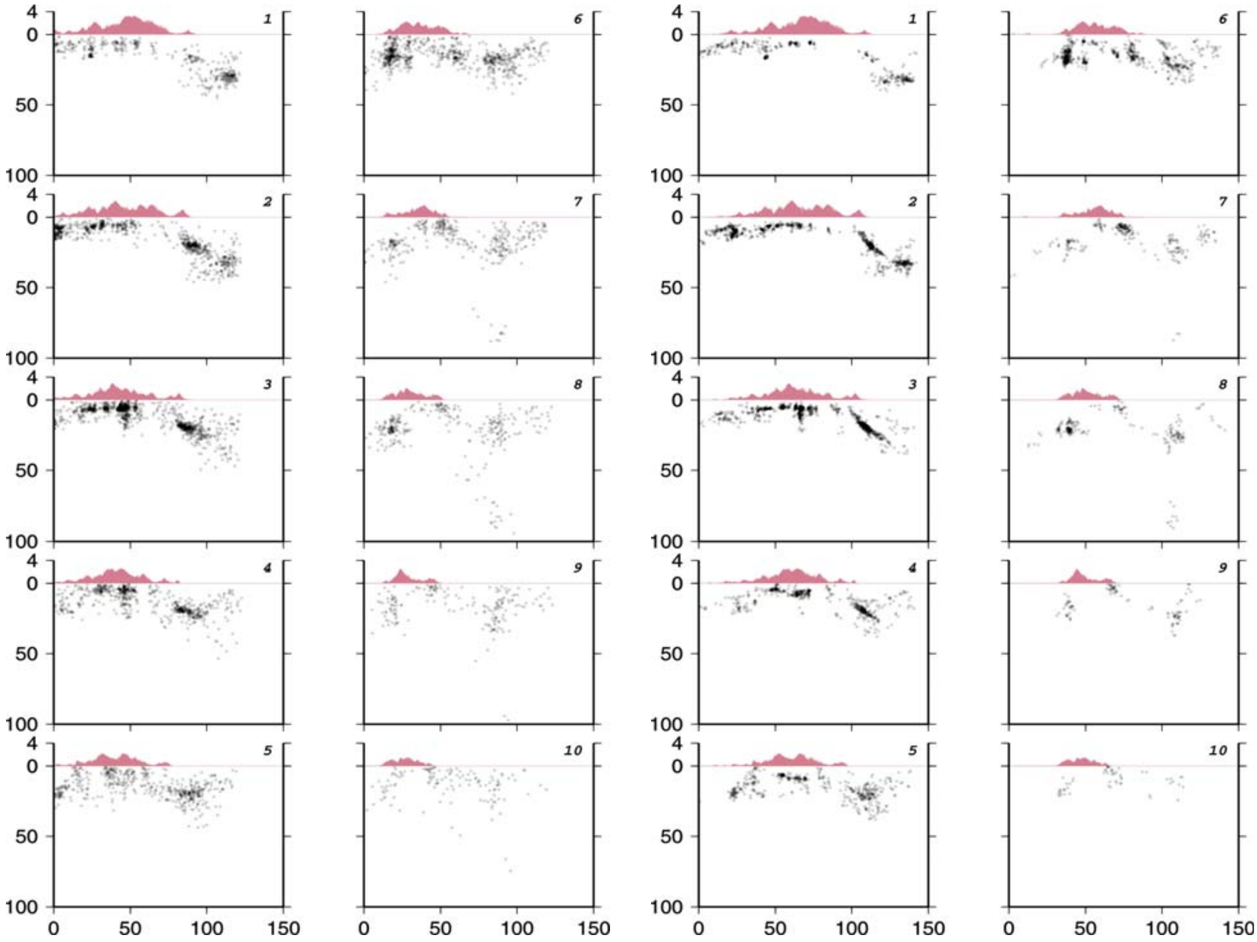
4
0
50
100
1
2
3
4
5
6
7
8
9
10
0
50
100
150

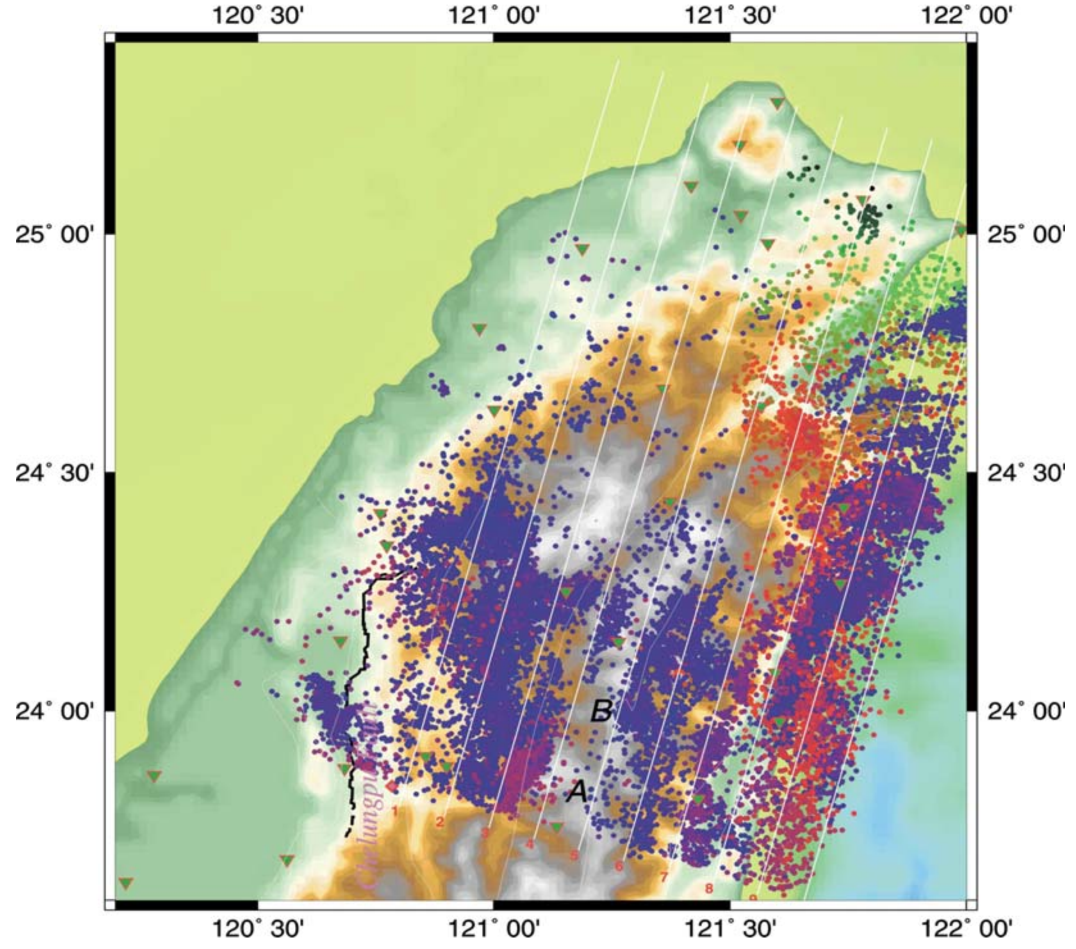

120° 30'
121° 00'
121° 30'
122° 00'
25° 00'
24° 30'
24° 00'
Chelungpu
A
B
1
2
3
4
5
6
7
8
9

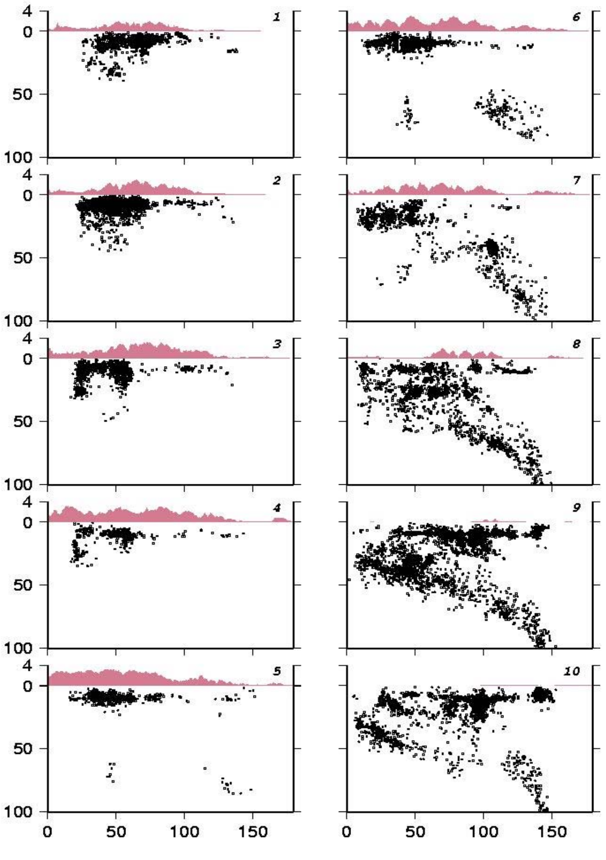

1
2
3
4
5
6
7
8
9
10
4
0
50
100
0
50
100
150

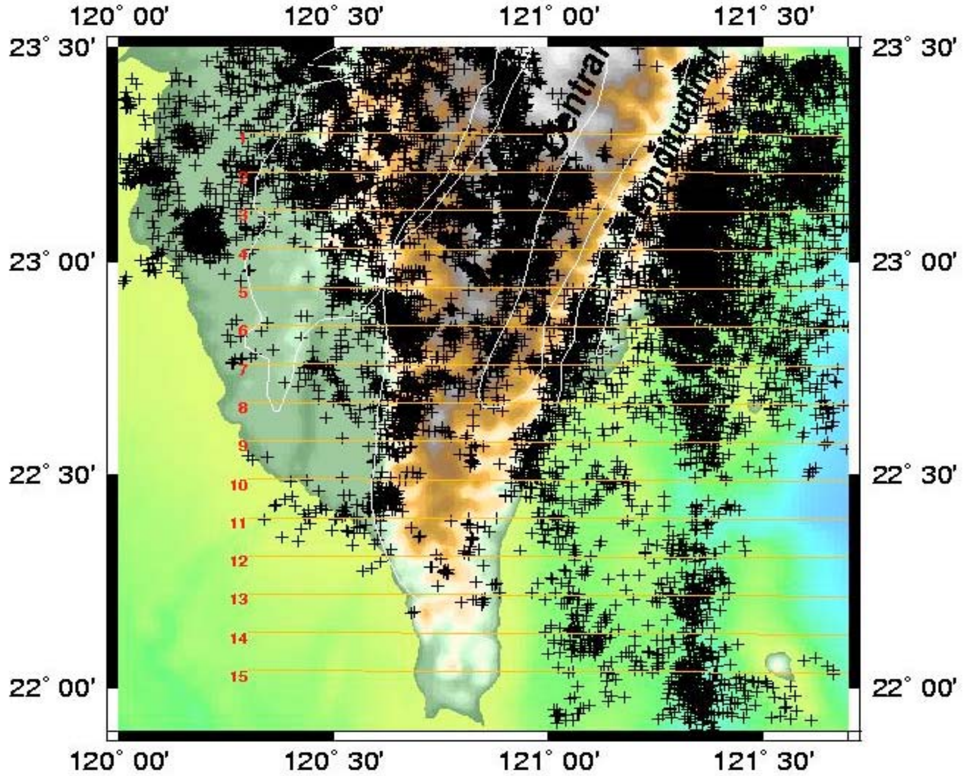
120° 00'
120° 30'
121° 00'
121° 30'
23° 30'
23° 00'
22° 30'
22° 00'
Central
Longitudinal
1
2
3
4
5
6
7
8
9
10
11
12
13
14
15

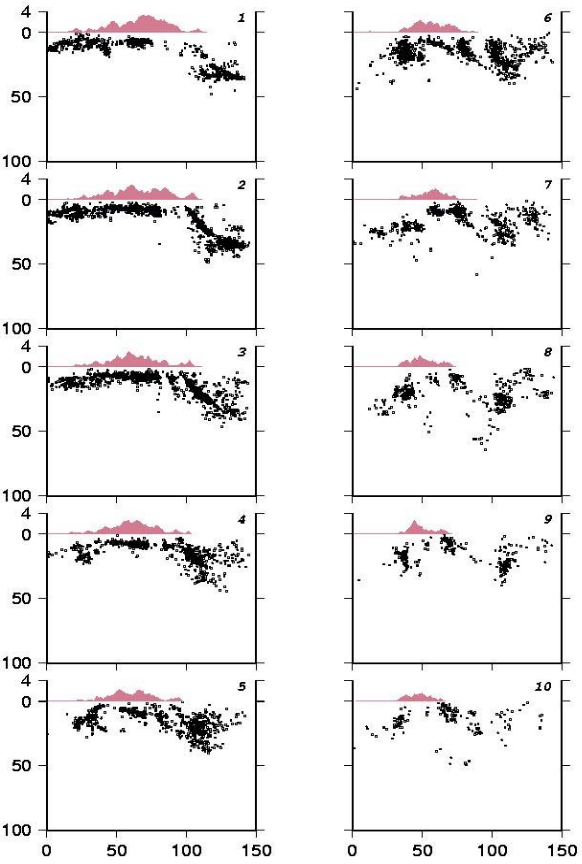
4
0
50
100
0
50
100
150
1
2
3
4
5
6
7
8
9
10

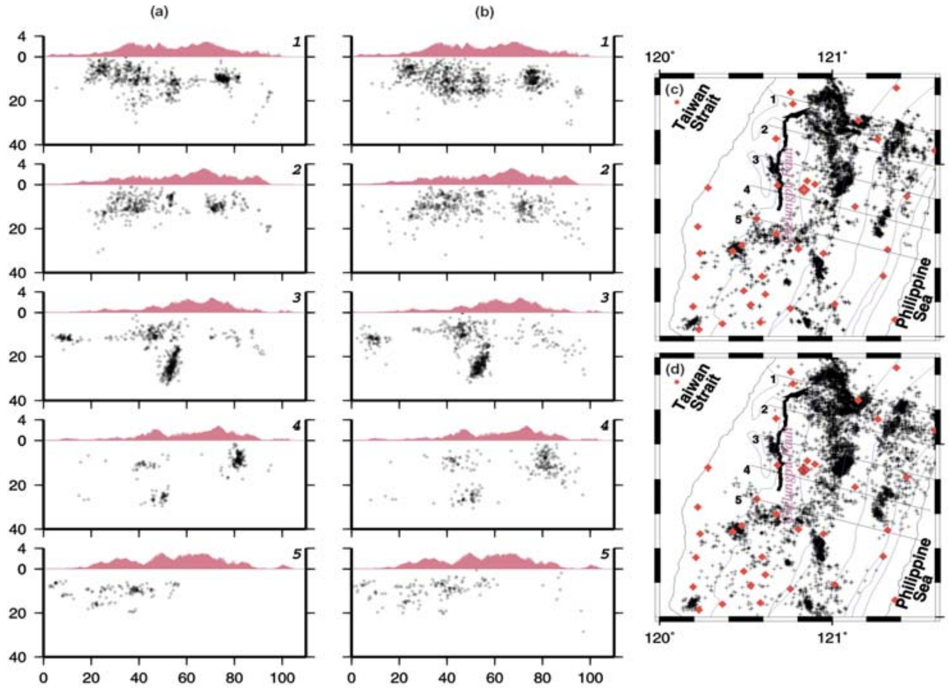

Fig. 3. Comparisons of CWB catalog and relocated event locations in map view and in cross-sections. Aftershocks in 2000 are used. The five left panels show the relocated events and to their right the corresponding catalog locations are shown; the locations of the profiles are shown in the maps on the right, the top figure shows the relocated and the bottom the catalog epicenters. Note that the relocated events are more tightly clustered. In the two maps at right the top one show the relocated and bottom one the catalog epicenters. The diamonds in this and later figures indicate the locations of the CWB network.

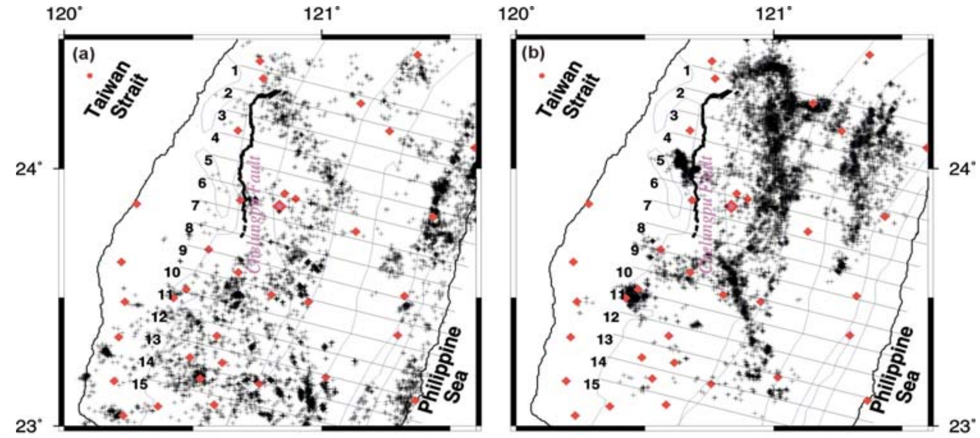

1994.1.1-1999.9.20

1999.9.20-1999.12.31

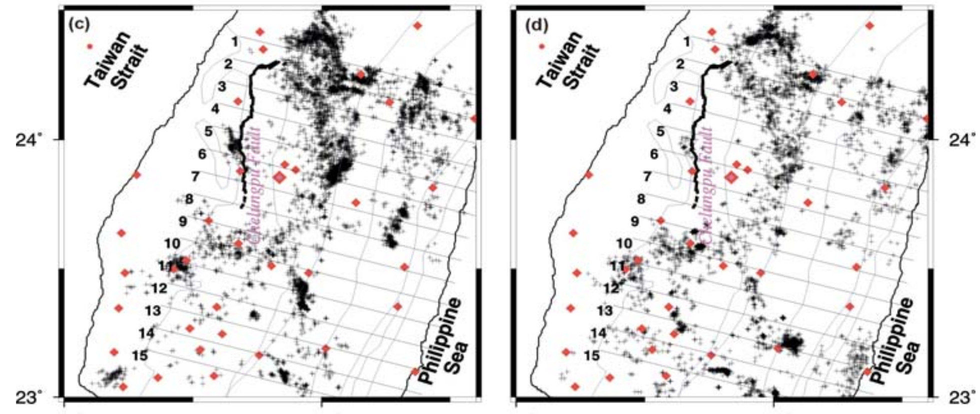

2000.1.1.-2000.12.31

2001.1.1-2002.12.31

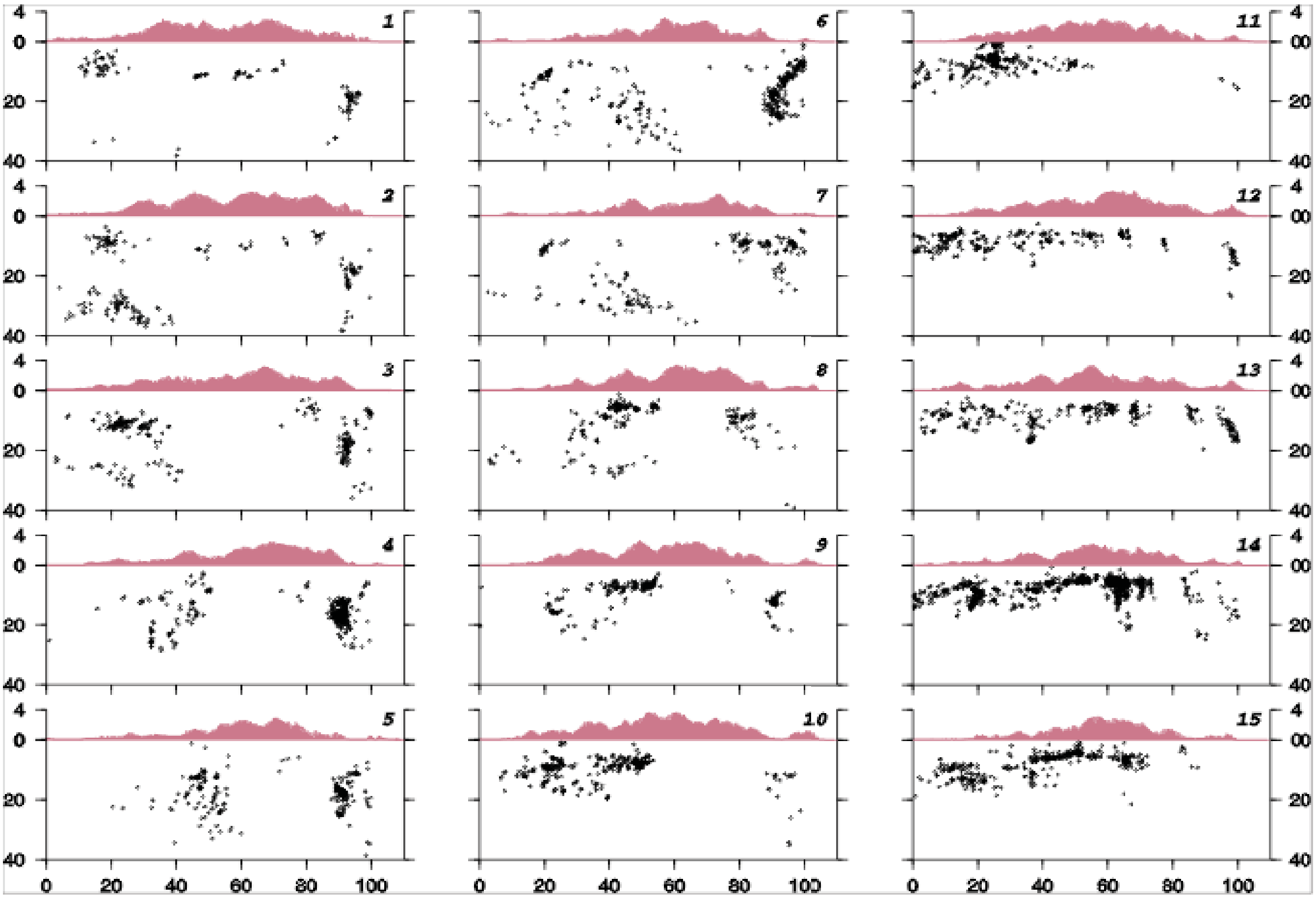
1
2
3
4
5
6
7
8
9
10
11
12
13
14
15
4
0
20
40
0
20
40
60
80
100

1993.7-1999.9

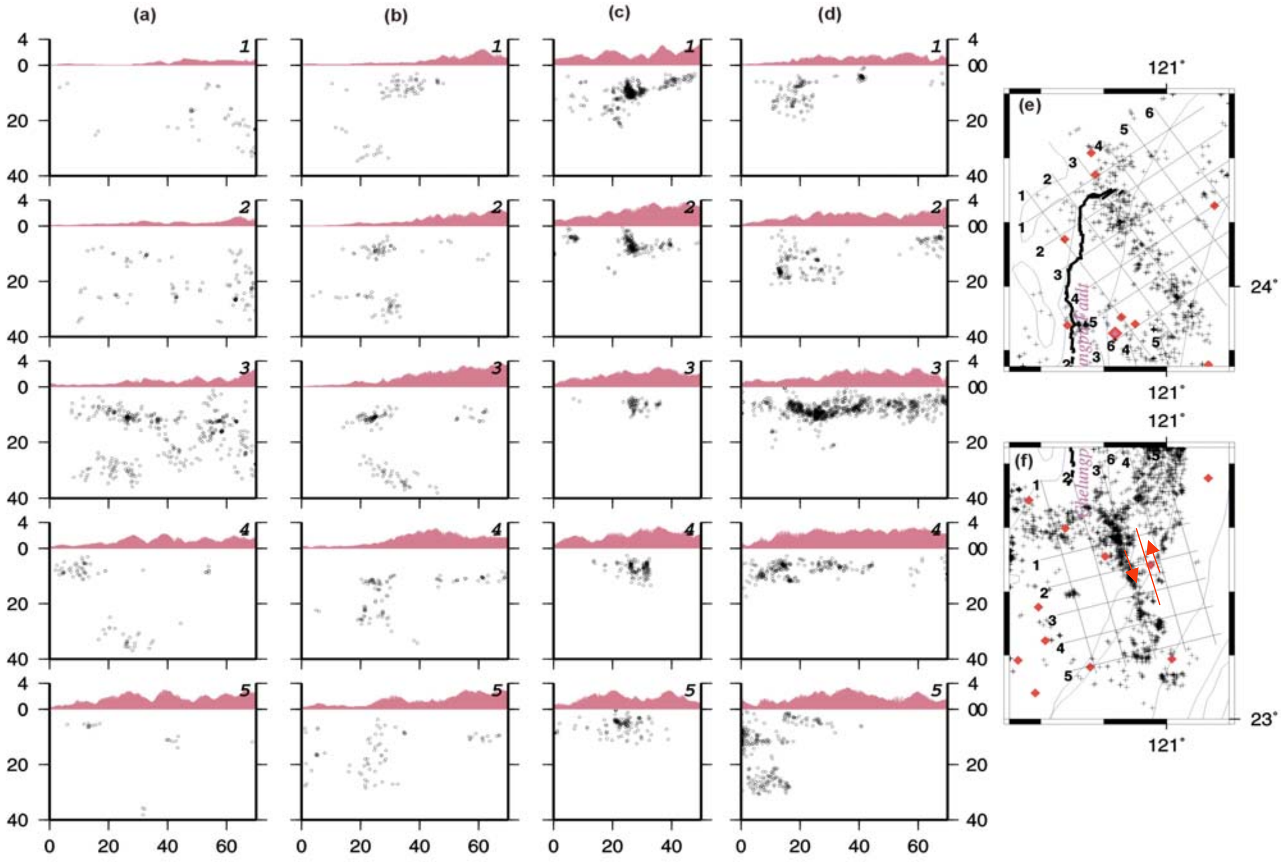
(a)
(b)
(c)
(d)
(e)
(f)
1
2
3
4
5
4
0
20
40
0
20
40
60
121°
24°
23°

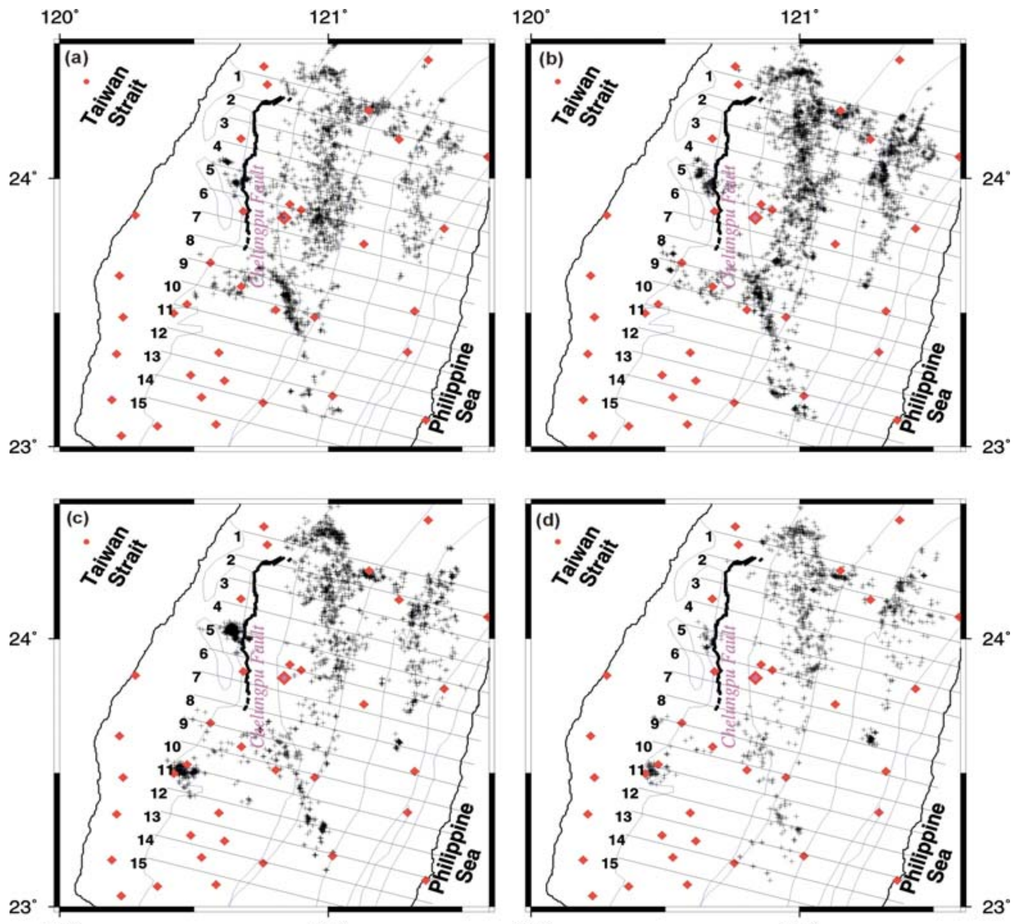

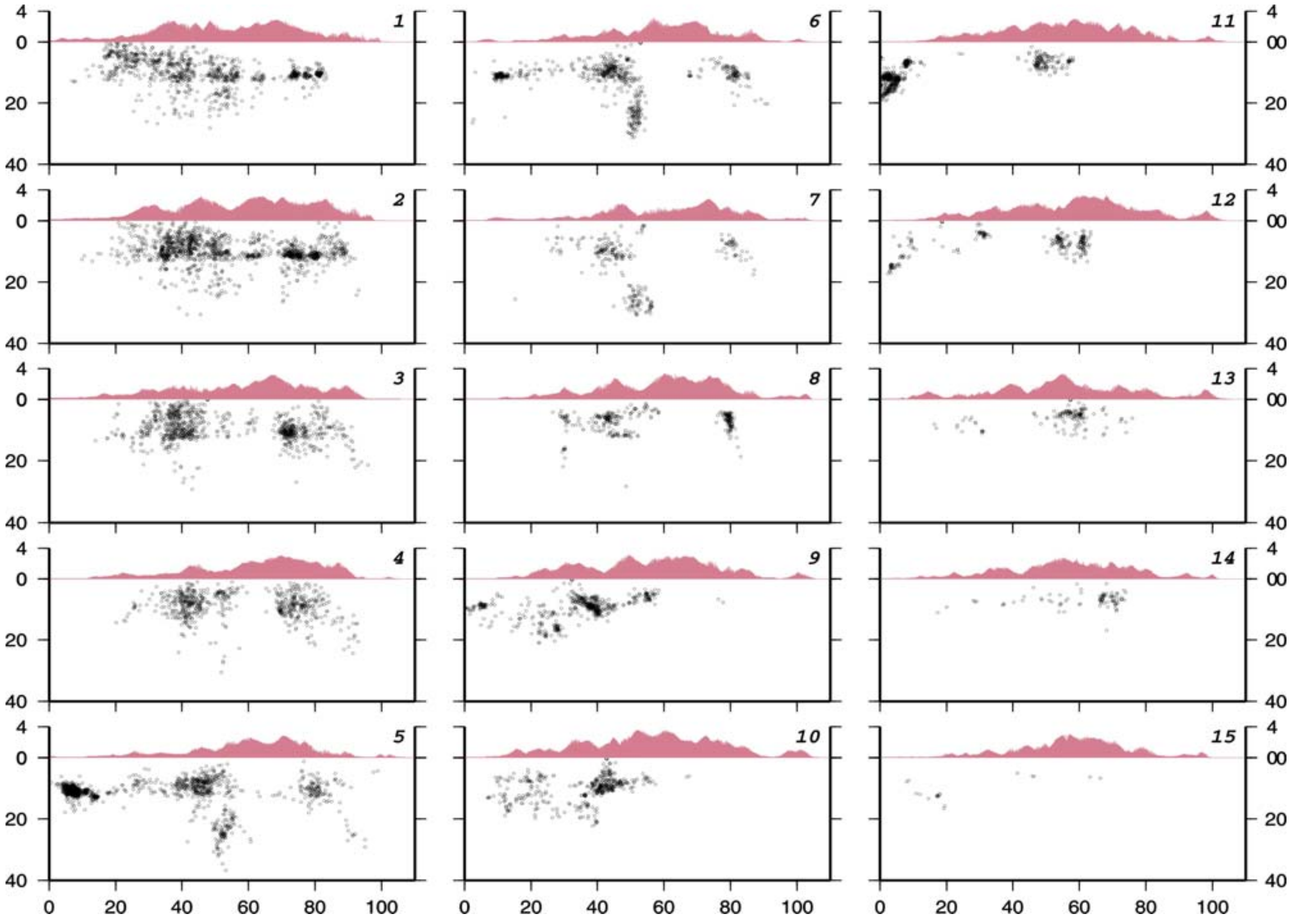

1999.9.20-1999.12.31

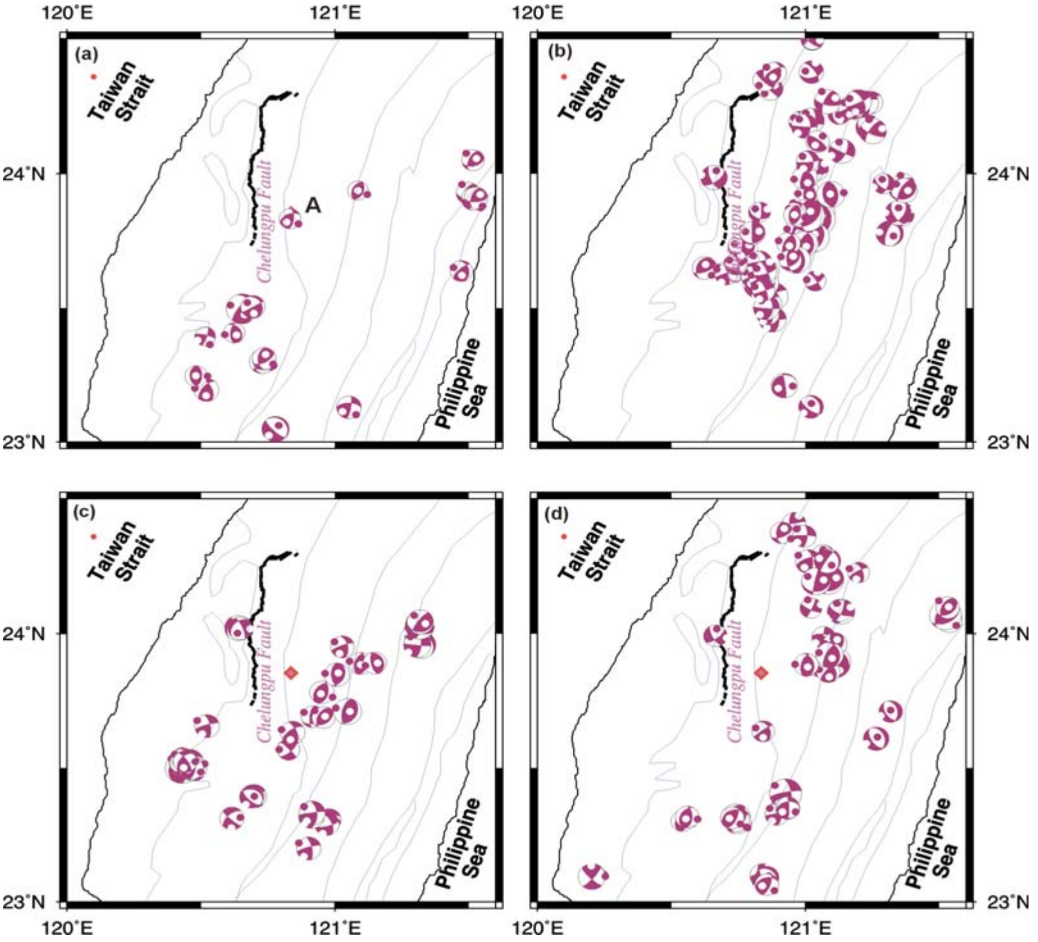

120°E
121°E
24°N
23°N
(a)
(b)
(c)
(d)
Taiwan Strait
Philippine Sea
Chelungpu Fault
A

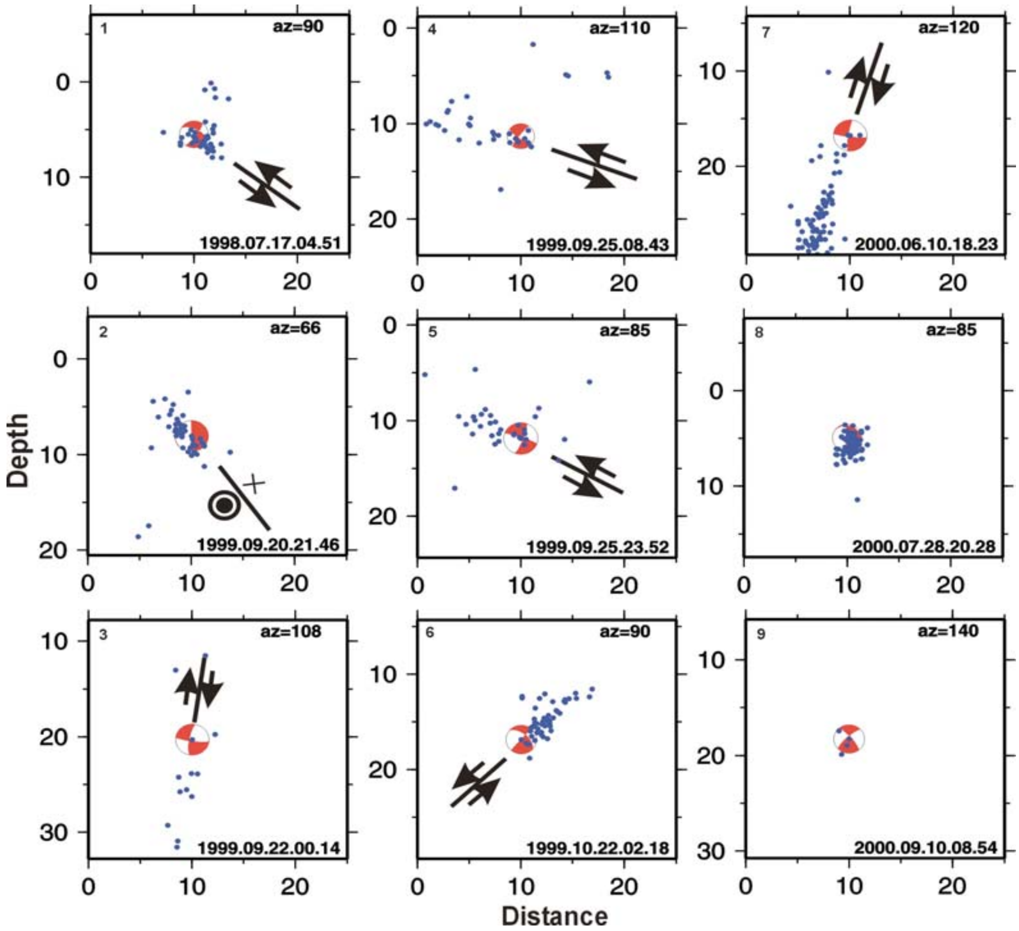

1
az=90
1998.07.17.04.51
2
az=66
1999.09.20.21.46
3
az=108
1999.09.22.00.14
4
az=110
1999.09.25.08.43
5
az=85
1999.09.25.23.52
6
az=90
1999.10.22.02.18
7
az=120
2000.06.10.18.23
8
az=85
2000.07.28.20.28
9
az=140
2000.09.10.08.54
Depth
Distance
0
10
20
30

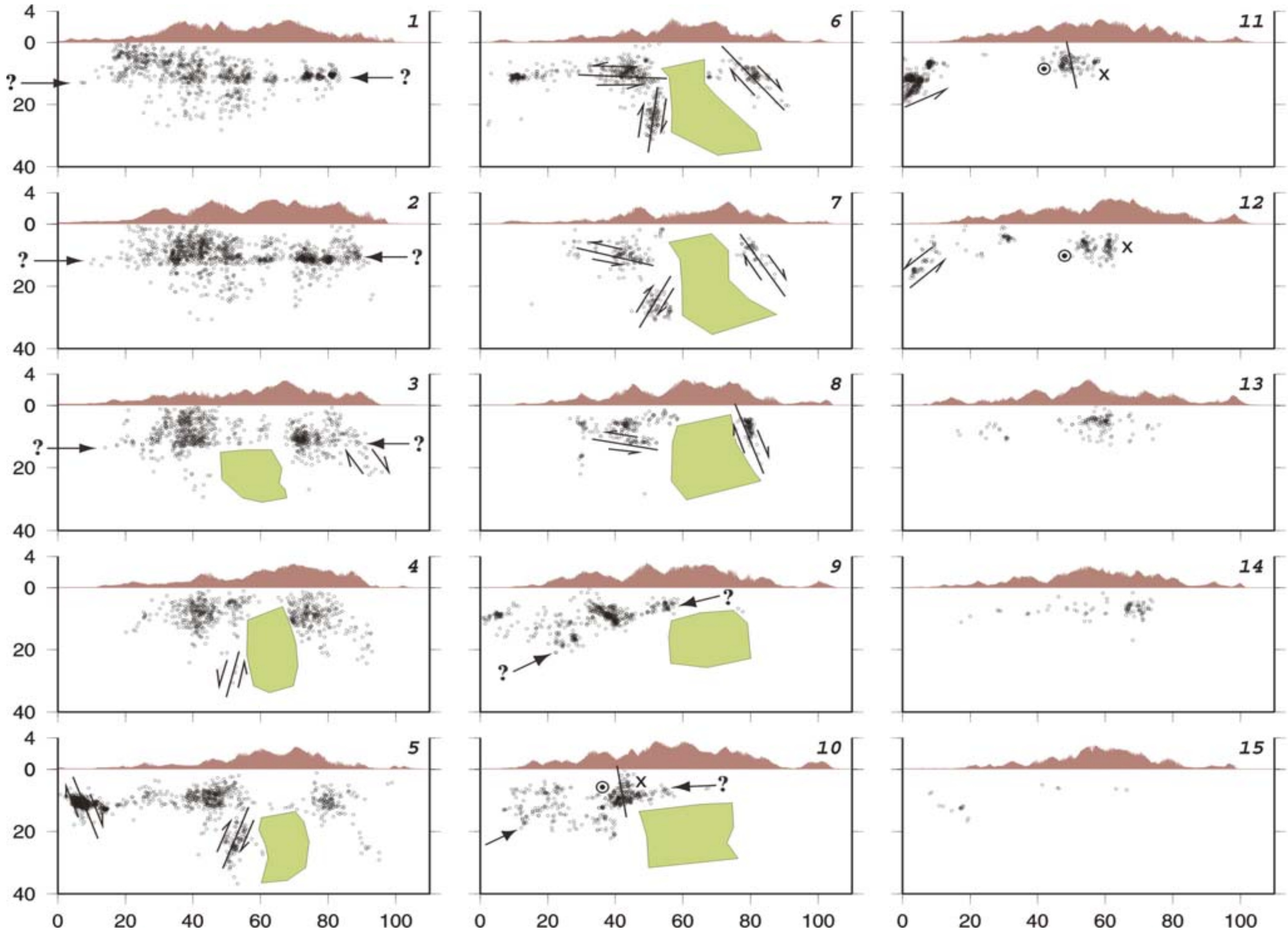
1
2
3
4
5
6
7
8
9
10
11
12
13
14
15
?
4
0
20
40
00
0
20
40
60
80
100

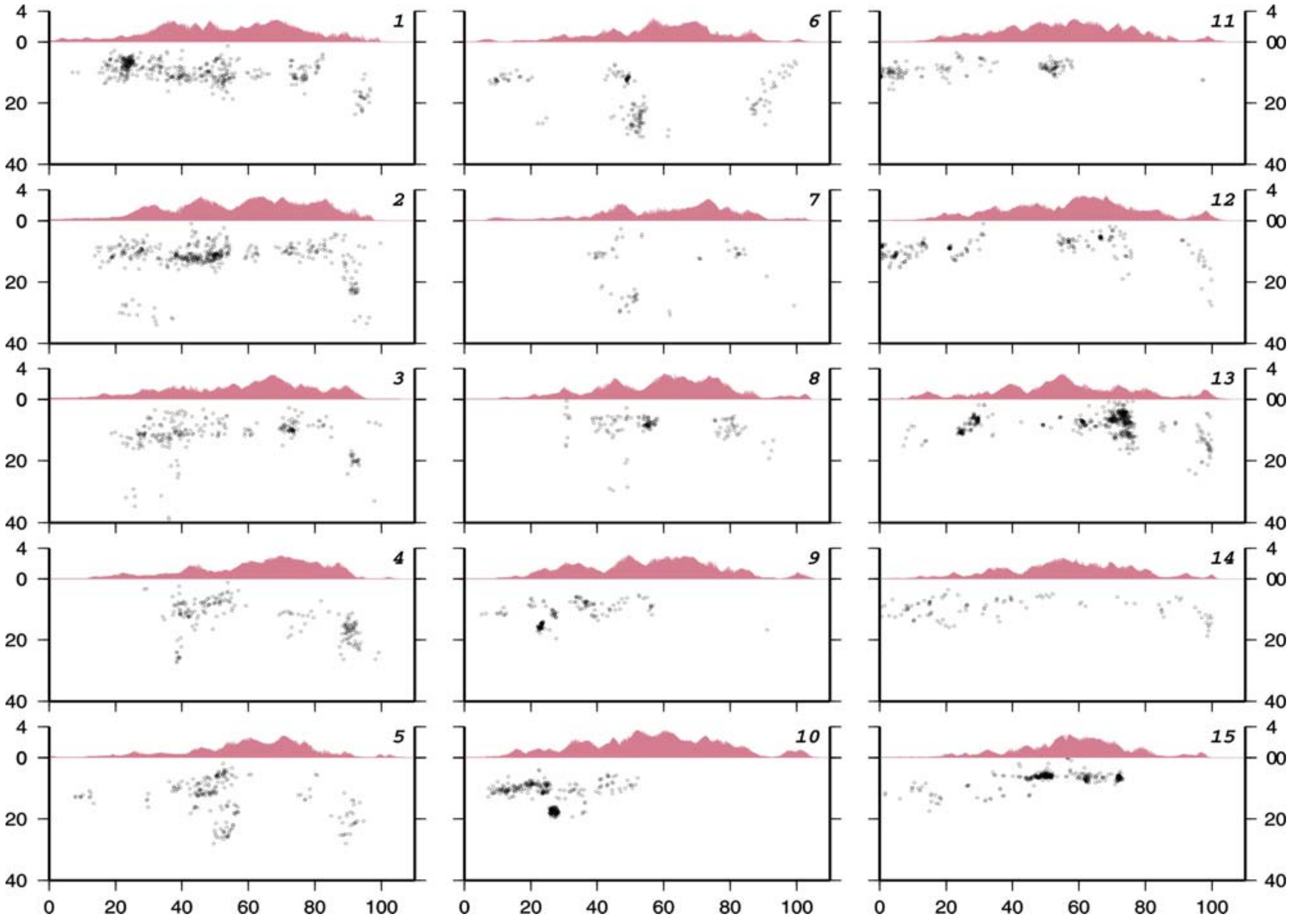
1
2
3
4
5
6
7
8
9
10
11
12
13
14
15
4
0
20
40
00
0
20
40
60
80
100

Local Earthquake Tomography

- Depends on local seismicity; some areas of interest may not be illuminated
- Determines velocity structure and earthquake location iteratively
- Network density and widely distributed earthquakes key to success

---

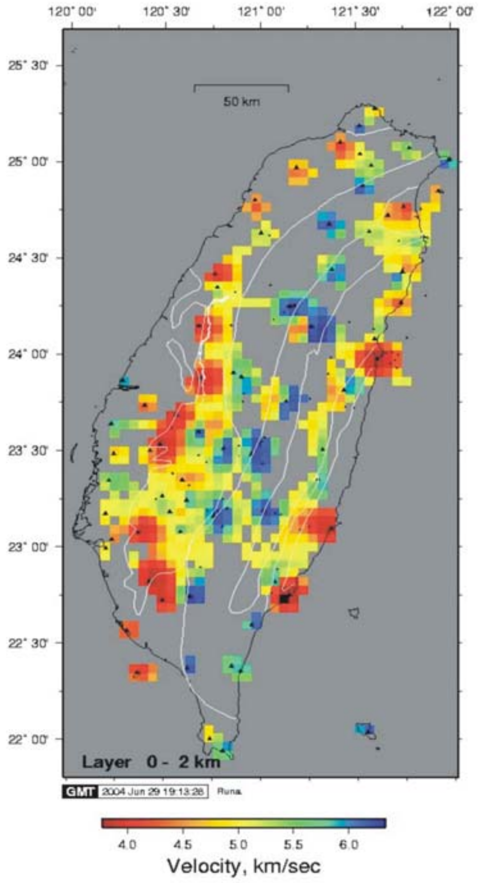

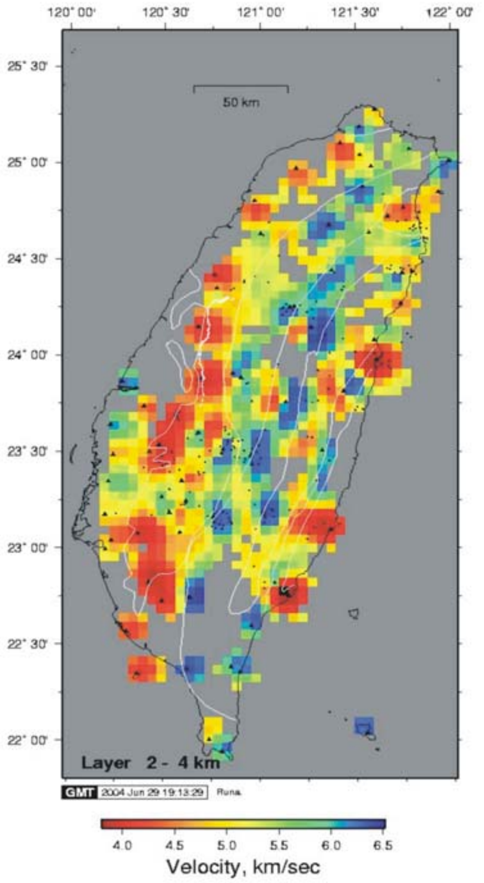

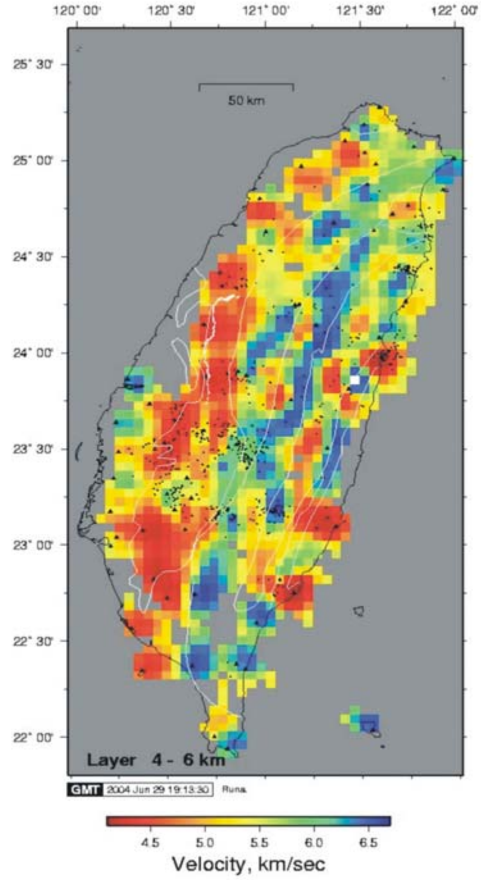
120° 00'
120° 30'
121° 00'
121° 30'
122° 00'
25° 30'
25° 00'
24° 30'
24° 00'
23° 30'
23° 00'
22° 30'
22° 00'
50 km
Layer 4 - 6 km
GMT 2004 Jun 29 19:13:30 Runa.
4.5
5.0
5.5
6.0
6.5
Velocity, km/sec

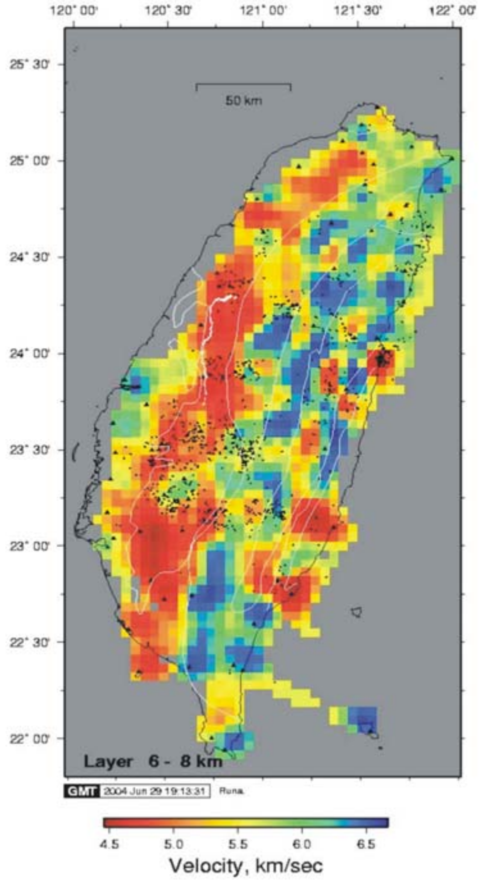
120° 00'
120° 30'
121° 00'
121° 30'
122° 00'
25° 30'
25° 00'
24° 30'
24° 00'
23° 30'
23° 00'
22° 30'
22° 00'
50 km
Layer 6 - 8 km
GMT 2004 Jun 29 19:13:31 Runa.
4.5
5.0
5.5
6.0
6.5
Velocity, km/sec

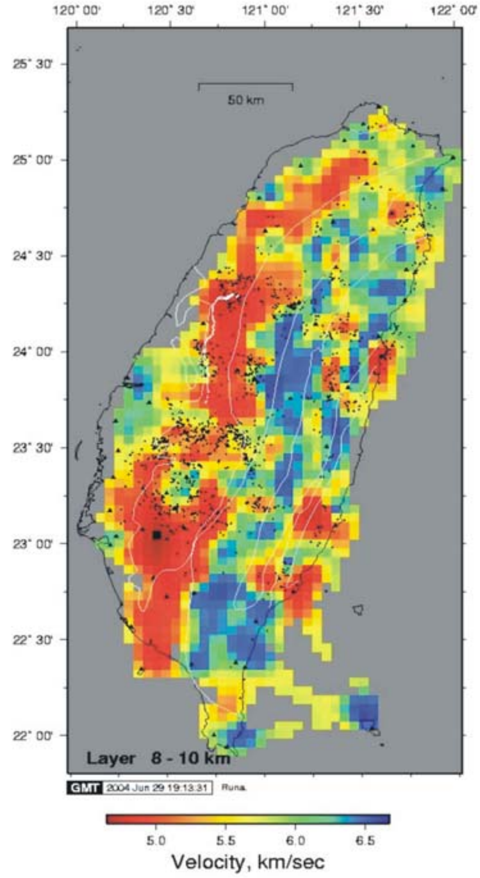
120° 00'
120° 30'
121° 00'
121° 30'
122° 00'
25° 30'
25° 00'
24° 30'
24° 00'
23° 30'
23° 00'
22° 30'
22° 00'
50 km
Layer 8 - 10 km
GMT 2004 Jun 29 19:13:31 Runa.
5.0
5.5
6.0
6.5
Velocity, km/sec

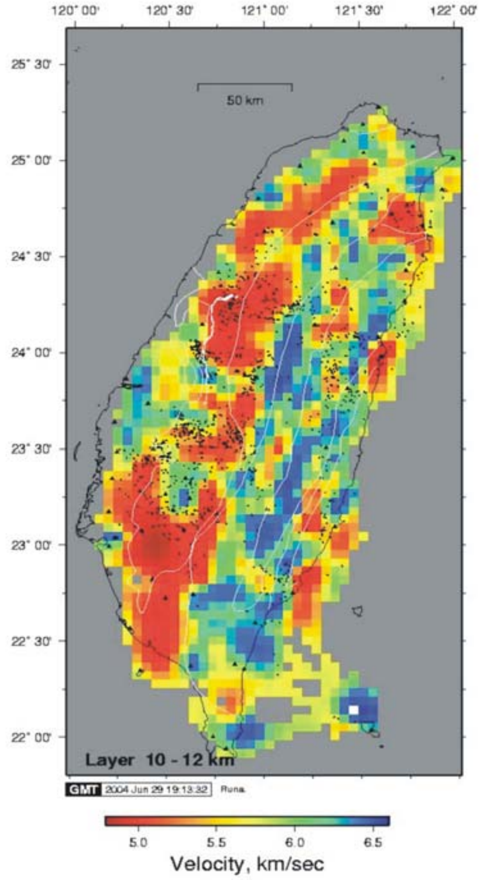
120° 00'
120° 30'
121° 00'
121° 30'
122° 00'
25° 30'
25° 00'
24° 30'
24° 00'
23° 30'
23° 00'
22° 30'
22° 00'
50 km
Layer 10 - 12 km
GMT 2004 Jun 29 19:13:32 Runa.
5.0
5.5
6.0
6.5
Velocity, km/sec

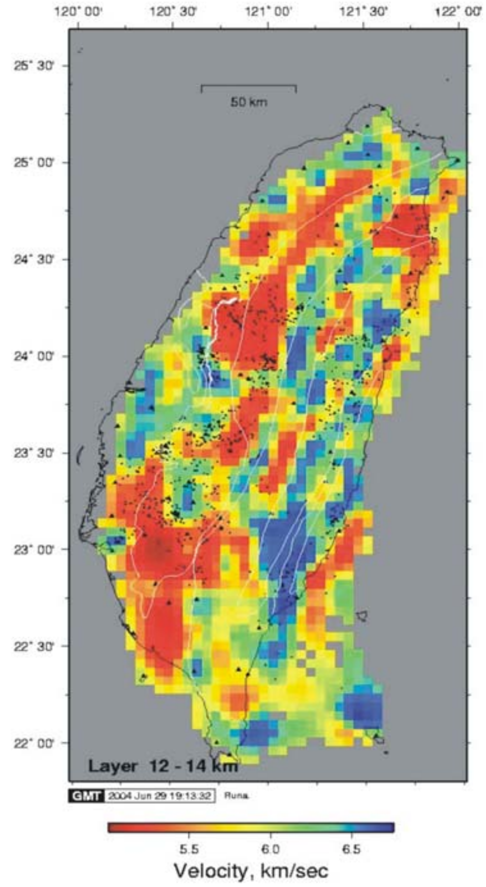
120° 00'
120° 30'
121° 00'
121° 30'
122° 00'
25° 30'
25° 00'
24° 30'
24° 00'
23° 30'
23° 00'
22° 30'
22° 00'
50 km
Layer 12 - 14 km
GMT 2004 Jun 29 19:13:32 Runa
5.5
6.0
6.5
Velocity, km/sec

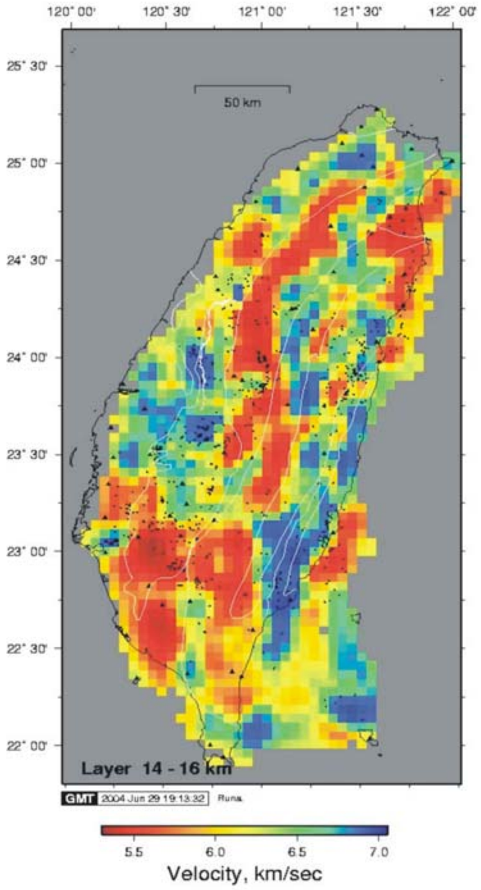
120° 00'
120° 30'
121° 00'
121° 30'
122° 00'
25° 30'
25° 00'
24° 30'
24° 00'
23° 30'
23° 00'
22° 30'
22° 00'
50 km
Layer 14 - 16 km
GMT 2004 Jun 29 19:13:32 Runa
5.5
6.0
6.5
7.0
Velocity, km/sec

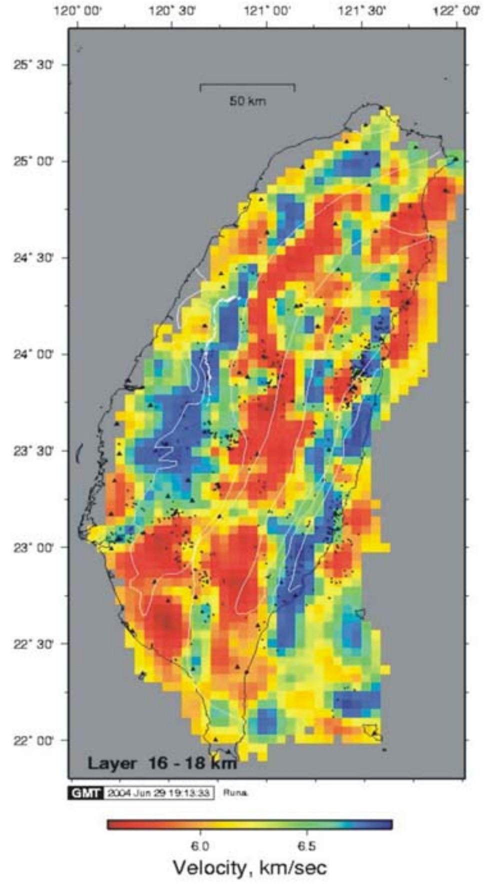
120° 00'
120° 30'
121° 00'
121° 30'
122° 00'
25° 30'
25° 00'
24° 30'
24° 00'
23° 30'
23° 00'
22° 30'
22° 00'
50 km
Layer 16 - 18 km
GMT 2004 Jun 29 19:13:33 Runa
6.0
6.5
Velocity, km/sec

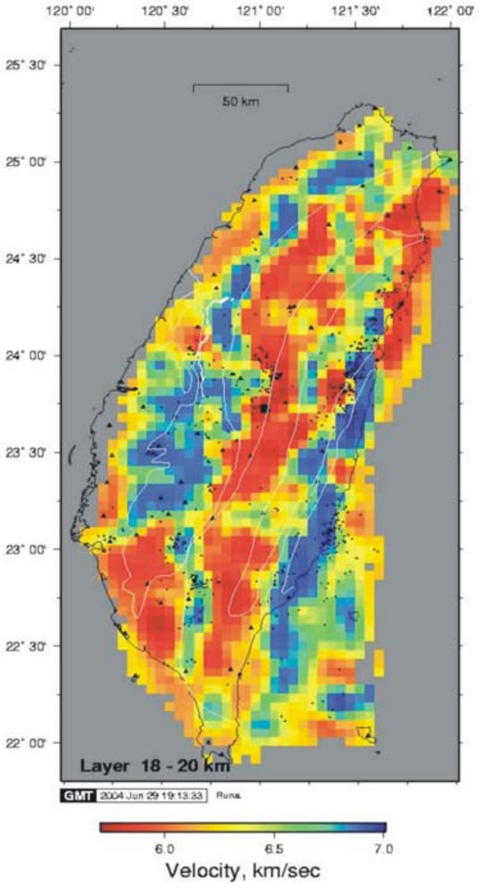
120° 00'
120° 30'
121° 00'
121° 30'
122° 00'
25° 30'
25° 00'
24° 30'
24° 00'
23° 30'
23° 00'
22° 30'
22° 00'
50 km
Layer 18 - 20 km
GMT 2004 Jun 29 19:13:33 Runa
6.0
6.5
7.0
Velocity, km/sec

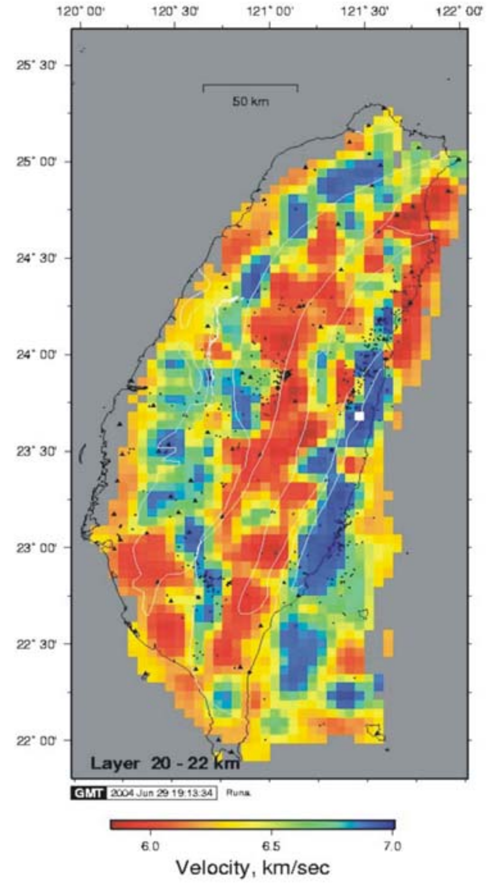
120° 00'
120° 30'
121° 00'
121° 30'
122° 00'
25° 30'
25° 00'
24° 30'
24° 00'
23° 30'
23° 00'
22° 30'
22° 00'
50 km
Layer 20 - 22 km
GMT 2004 Jun 29 19:13:34 Runa
6.0
6.5
7.0
Velocity, km/sec

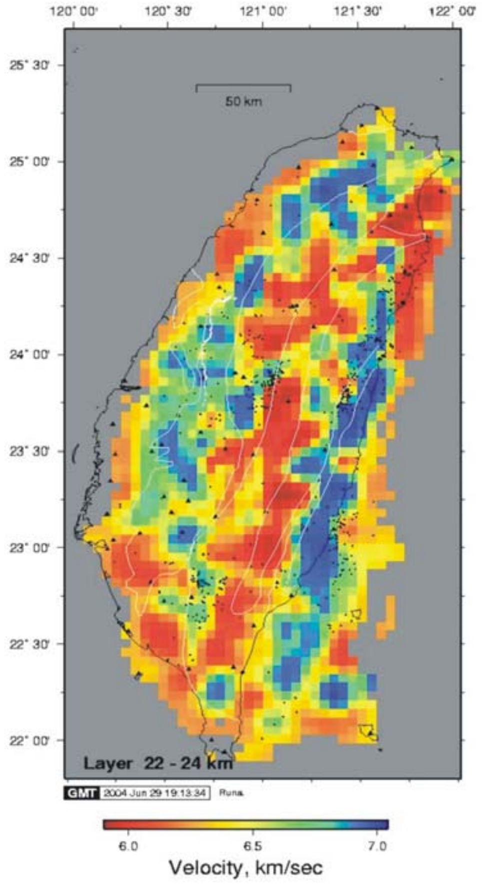
120° 00'
120° 30'
121° 00'
121° 30'
122° 00'
25° 30'
25° 00'
24° 30'
24° 00'
23° 30'
23° 00'
22° 30'
22° 00'
50 km
Layer 22 - 24 km
GMT 2004 Jun 29 19:13:34 Runa
6.0
6.5
7.0
Velocity, km/sec

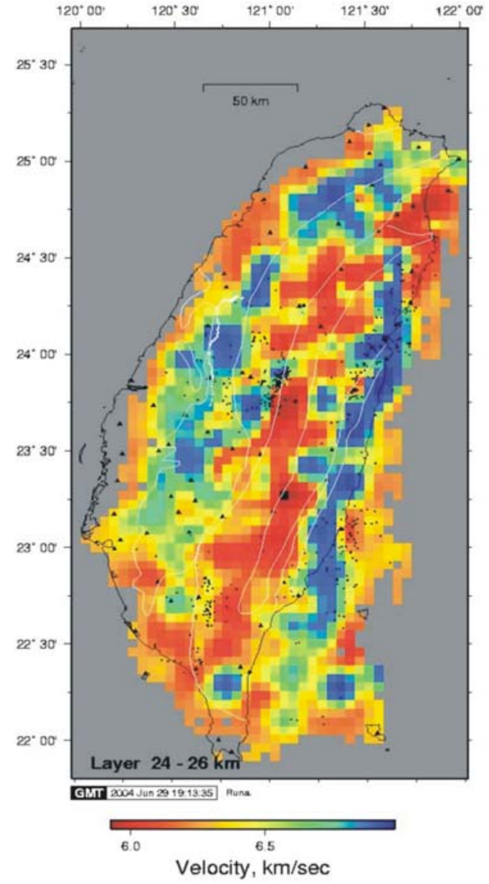
120° 00'
120° 30'
121° 00'
121° 30'
122° 00'
25° 30'
25° 00'
24° 30'
24° 00'
23° 30'
23° 00'
22° 30'
22° 00'
50 km
Layer 24 - 26 km
GMT 2004 Jun 29 19:13:35 Runa
6.0
6.5
Velocity, km/sec

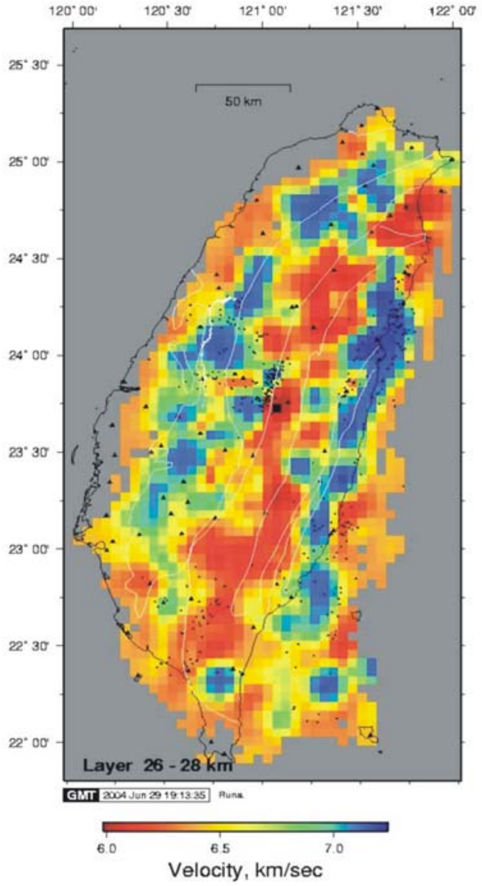
120° 00'
120° 30'
121° 00'
121° 30'
122° 00'
25° 30'
25° 00'
24° 30'
24° 00'
23° 30'
23° 00'
22° 30'
22° 00'
50 km
Layer 26 - 28 km
GMT 2004 Jun 29 19:13:35 Runa
6.0
6.5
7.0
Velocity, km/sec

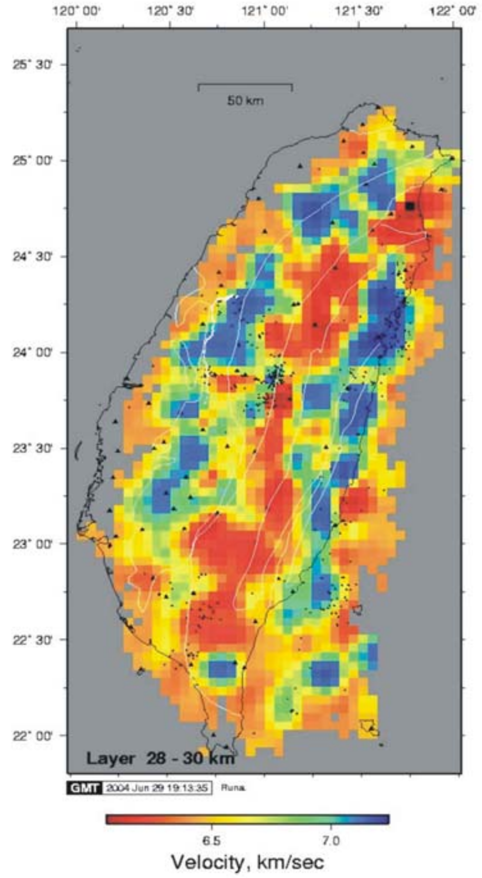
120° 00'
120° 30'
121° 00'
121° 30'
122° 00'
25° 30'
25° 00'
24° 30'
24° 00'
23° 30'
23° 00'
22° 30'
22° 00'
50 km
Layer 28 - 30 km
GMT 2004 Jun 29 19:13:35 Runa
6.5
7.0
Velocity, km/sec

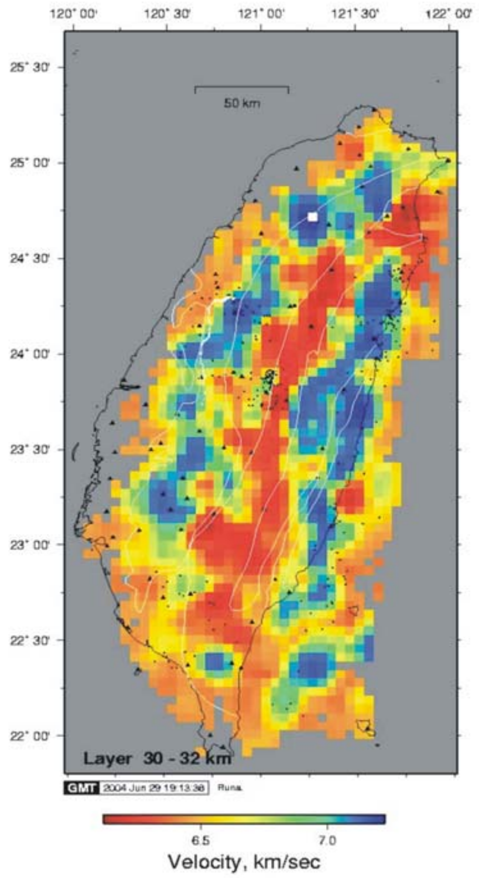
120° 00'
120° 30'
121° 00'
121° 30'
122° 00'
25° 30'
25° 00'
24° 30'
24° 00'
23° 30'
23° 00'
22° 30'
22° 00'
50 km
Layer 30 - 32 km
GMT 2004 Jun 29 19:13:36 Runa
6.5
7.0
Velocity, km/sec

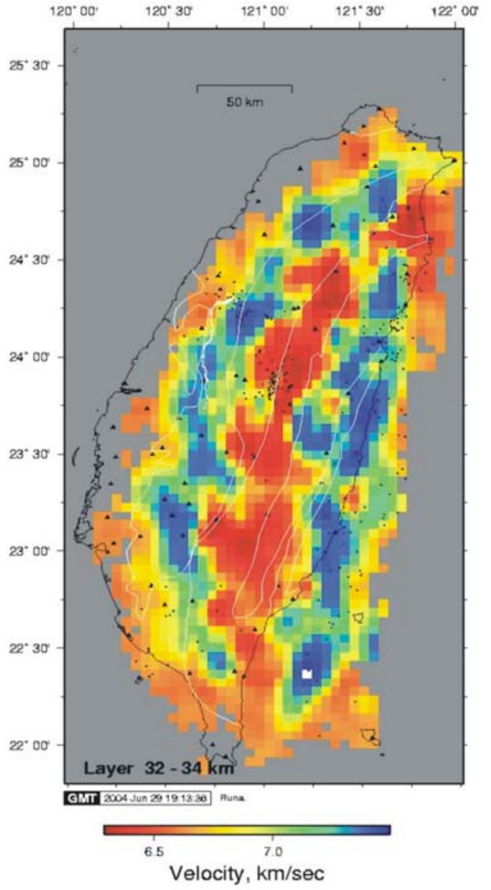
120° 00'
120° 30'
121° 00'
121° 30'
122° 00'
25° 30'
25° 00'
24° 30'
24° 00'
23° 30'
23° 00'
22° 30'
22° 00'
50 km
Layer 32 - 34 km
GMT 2004 Jun 29 19:13:36 Runa
6.5
7.0
Velocity, km/sec

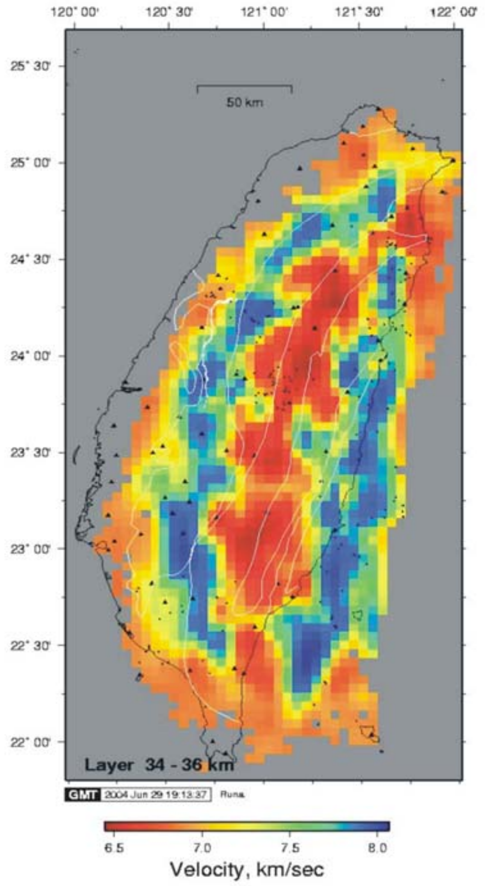
120° 00'
120° 30'
121° 00'
121° 30'
122° 00'
25° 30'
25° 00'
24° 30'
24° 00'
23° 30'
23° 00'
22° 30'
22° 00'
50 km
Layer 34 - 36 km
GMT 2004 Jun 29 19:13:37 Runa
6.5
7.0
7.5
8.0
Velocity, km/sec

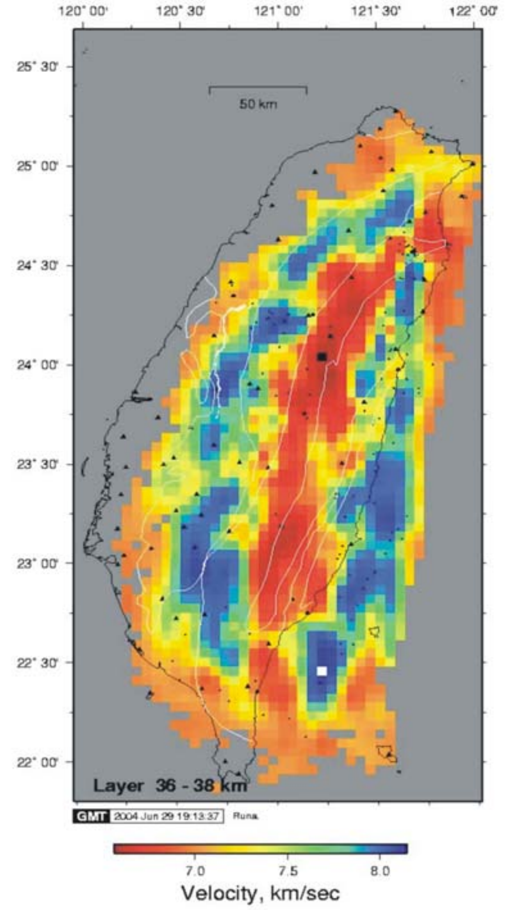
120° 00'
120° 30'
121° 00'
121° 30'
122° 00'
25° 30'
25° 00'
24° 30'
24° 00'
23° 30'
23° 00'
22° 30'
22° 00'
50 km
Layer 36 - 38 km
GMT 2004 Jun 29 19:13:37 Runa.
7.0
7.5
8.0
Velocity, km/sec

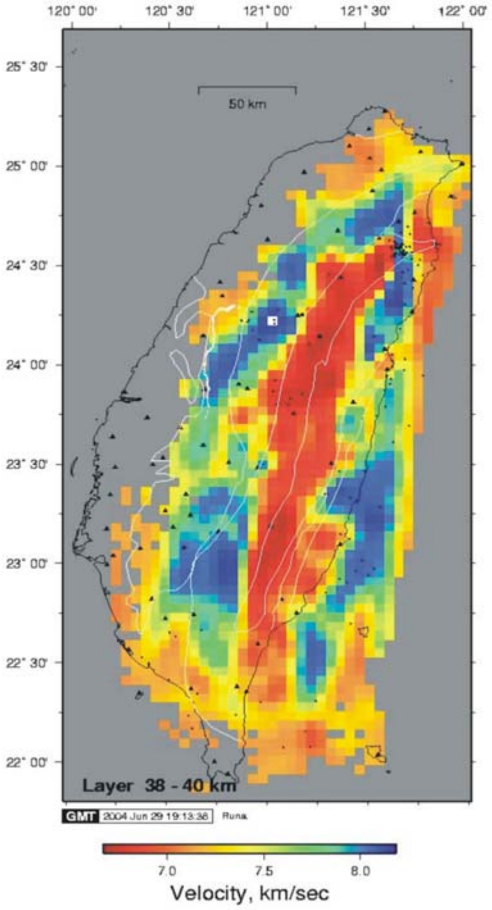
120° 00'
120° 30'
121° 00'
121° 30'
122° 00'
25° 30'
25° 00'
24° 30'
24° 00'
23° 30'
23° 00'
22° 30'
22° 00'
50 km
Layer 38 - 40 km
GMT 2004 Jun 29 19:13:38 Runa.
7.0
7.5
8.0
Velocity, km/sec

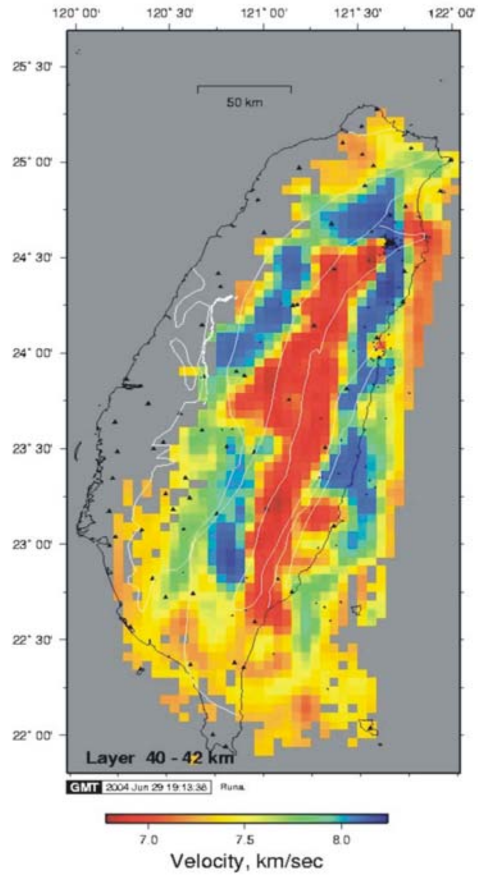
120° 00'
120° 30'
121° 00'
121° 30'
122° 00'
25° 30'
25° 00'
24° 30'
24° 00'
23° 30'
23° 00'
22° 30'
22° 00'
50 km
Layer 40 - 42 km
GMT 2004 Jun 29 19:13:38 Runa.
7.0
7.5
8.0
Velocity, km/sec

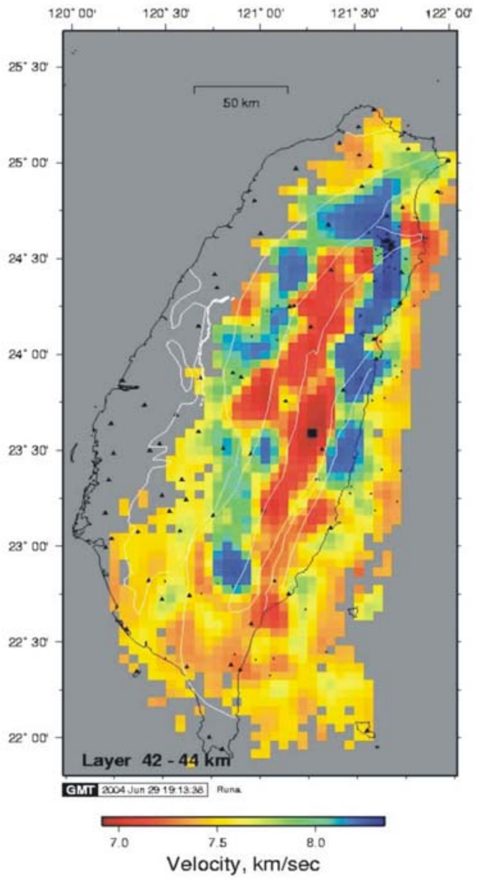
120° 00'
120° 30'
121° 00'
121° 30'
122° 00'
25° 30'
25° 00'
24° 30'
24° 00'
23° 30'
23° 00'
22° 30'
22° 00'
50 km
Layer 42 - 44 km
GMT 2004 Jun 29 19:13:38 Runa.
7.0
7.5
8.0
Velocity, km/sec

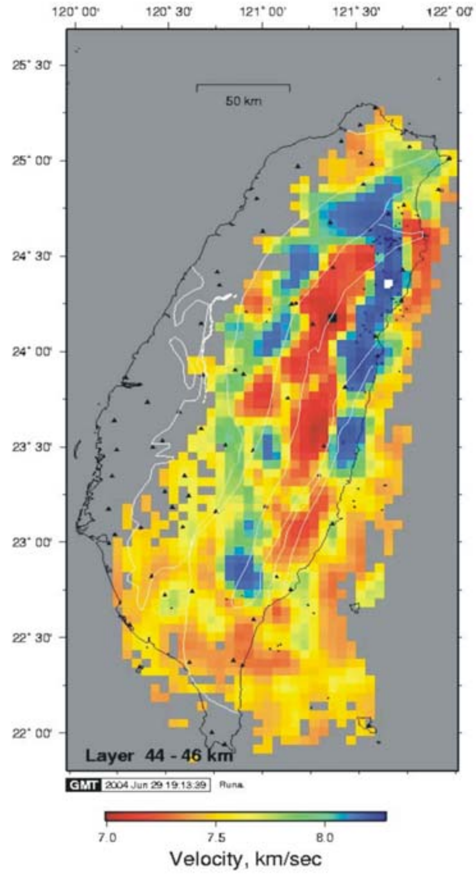
120° 00'
120° 30'
121° 00'
121° 30'
122° 00'
25° 30'
25° 00'
24° 30'
24° 00'
23° 30'
23° 00'
22° 30'
22° 00'
50 km
Layer 44 - 46 km
GMT 2004 Jun 29 19:13:39 Runa.
7.0
7.5
8.0
Velocity, km/sec

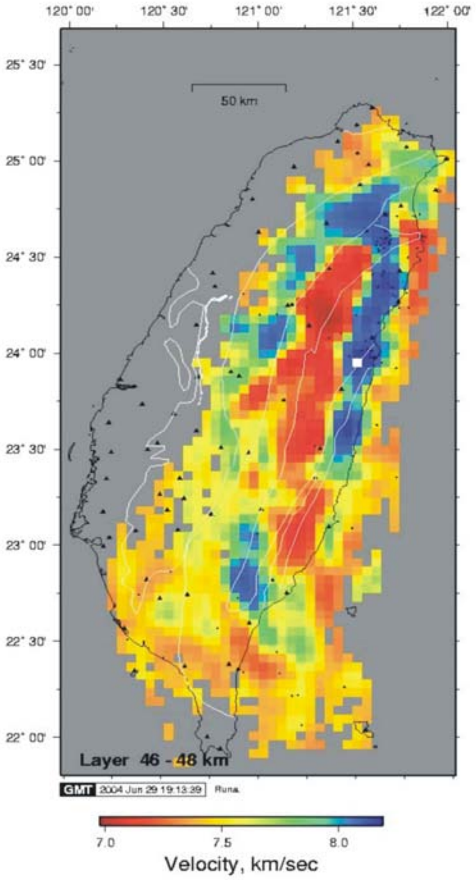
120° 00'
120° 30'
121° 00'
121° 30'
122° 00'
25° 30'
25° 00'
24° 30'
24° 00'
23° 30'
23° 00'
22° 30'
22° 00'
50 km
Layer 46 - 48 km
GMT 2004 Jun 29 19:13:39 Runa.
7.0
7.5
8.0
Velocity, km/sec

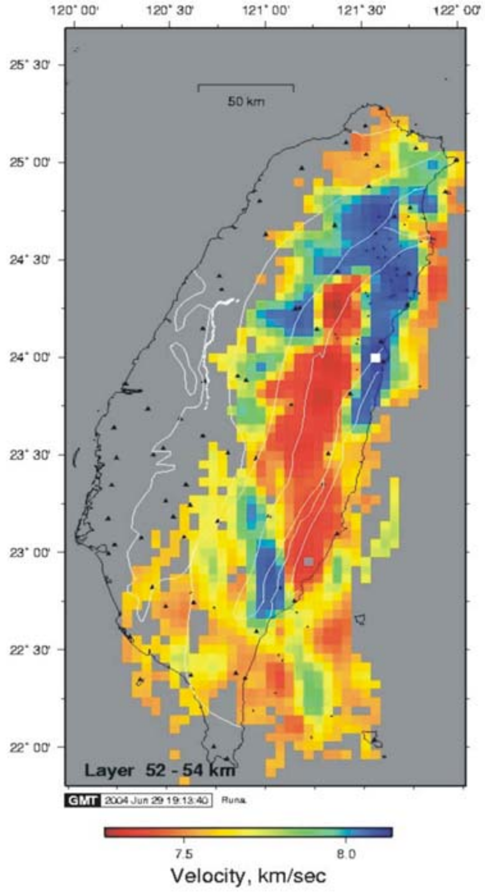
120° 00'
120° 30'
121° 00'
121° 30'
122° 00'
25° 30'
25° 00'
24° 30'
24° 00'
23° 30'
23° 00'
22° 30'
22° 00'
50 km
Layer 52 - 54 km
GMT 2004 Jun 29 19:13:40 Runa.
7.5
8.0
Velocity, km/sec

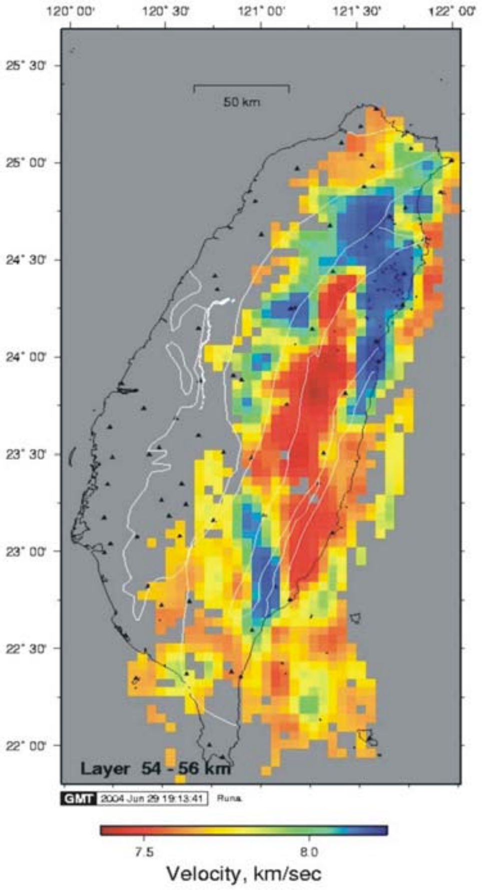
120° 00'
120° 30'
121° 00'
121° 30'
122° 00'
25° 30'
25° 00'
24° 30'
24° 00'
23° 30'
23° 00'
22° 30'
22° 00'
50 km
Layer 54 - 56 km
GMT 2004 Jun 29 19:13:41 Runa.
7.5
8.0
Velocity, km/sec

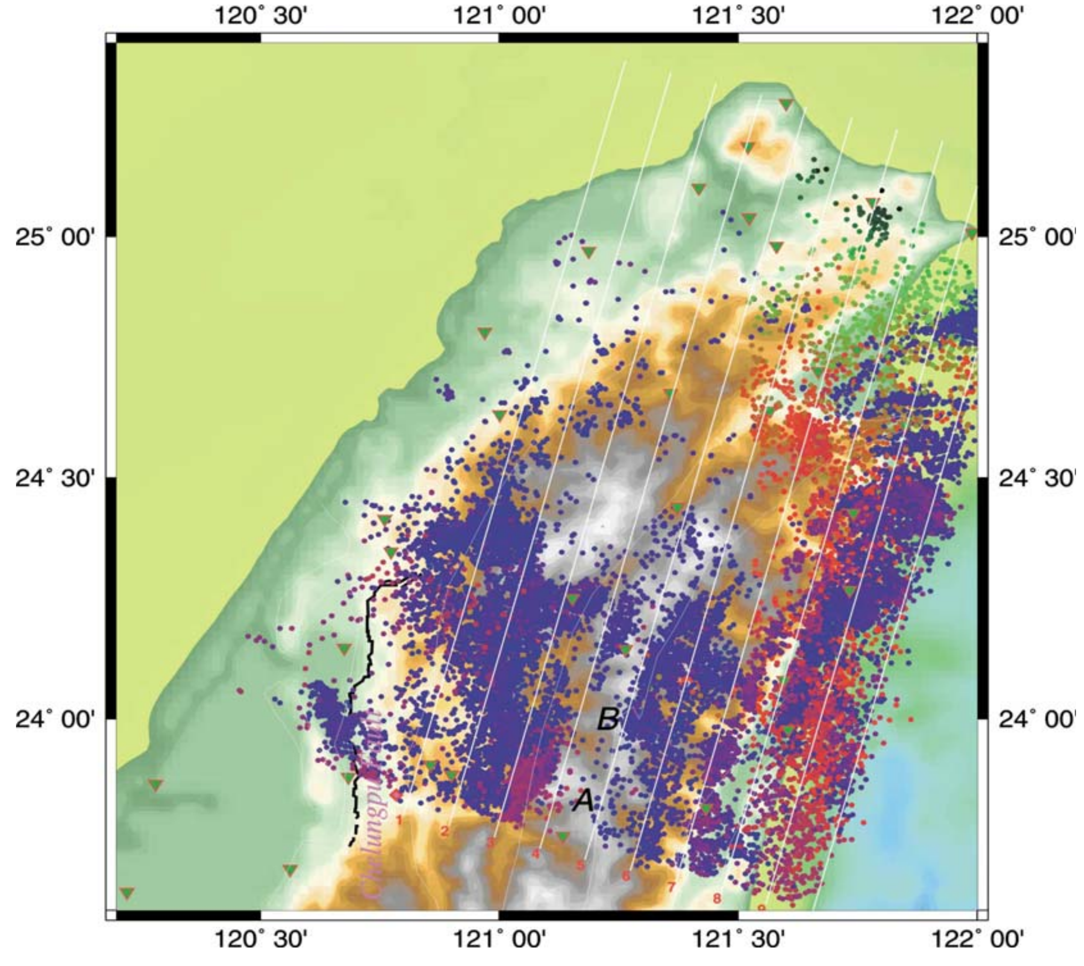
120° 30'
121° 00'
121° 30'
122° 00'
25° 00'
24° 30'
24° 00'
B
A
Chelungpu
1
2
3
4
5
6
7
8
9

N4

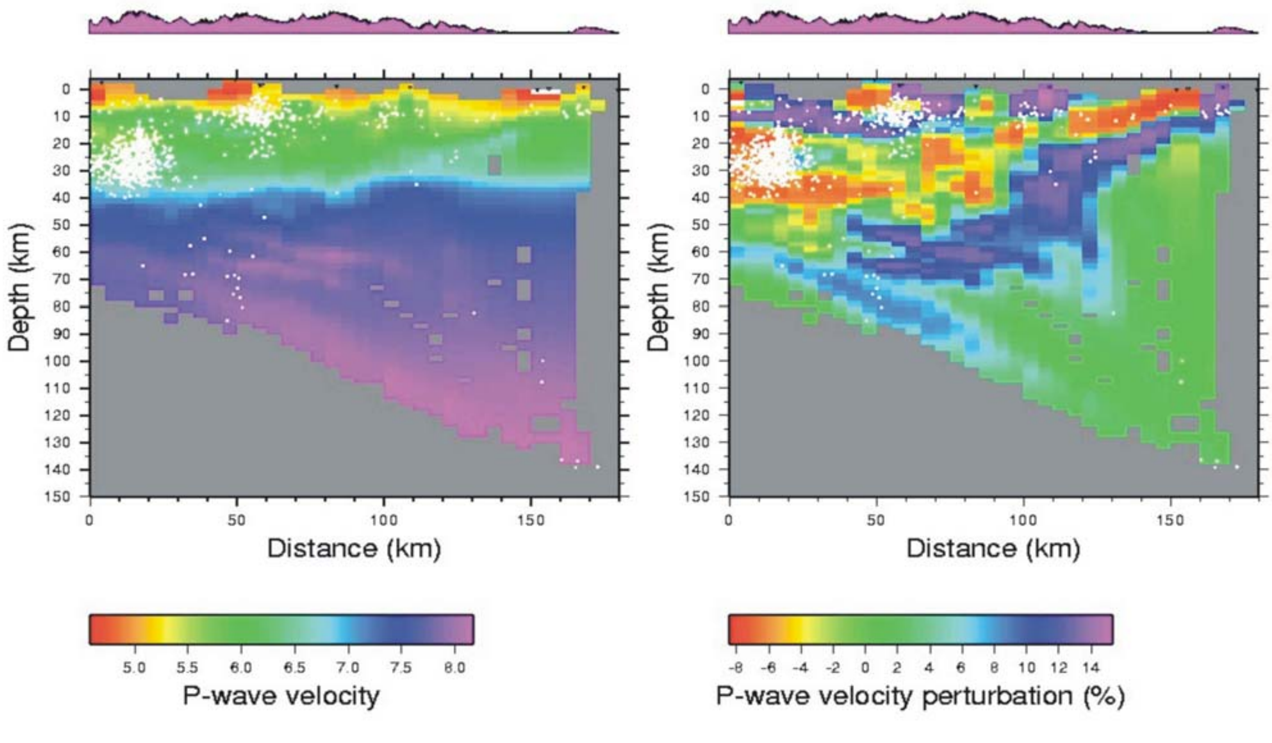
Depth (km)
0
10
20
30
40
50
60
70
80
90
100
110
120
130
140
150
Distance (km)
0
50
100
150
5.0
5.5
6.0
6.5
7.0
7.5
8.0
P-wave velocity
-8
-6
-4
-2
0
2
4
6
8
10
12
14
P-wave velocity perturbation (%)

N5

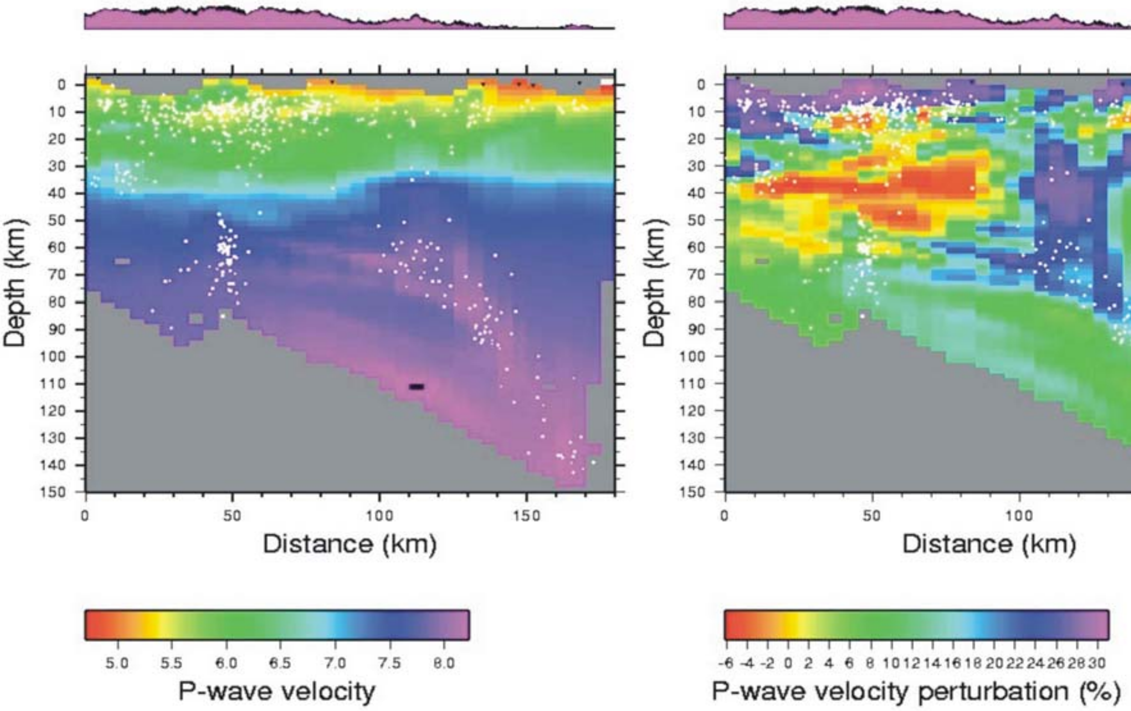
Depth (km)
0
10
20
30
40
50
60
70
80
90
100
110
120
130
140
150
0
50
100
150
Distance (km)
5.0
5.5
6.0
6.5
7.0
7.5
8.0
P-wave velocity
-6 -4 -2 0 2 4 6 8 10 12 14 16 18 20 22 24 26 28 30
P-wave velocity perturbation (%)

N6

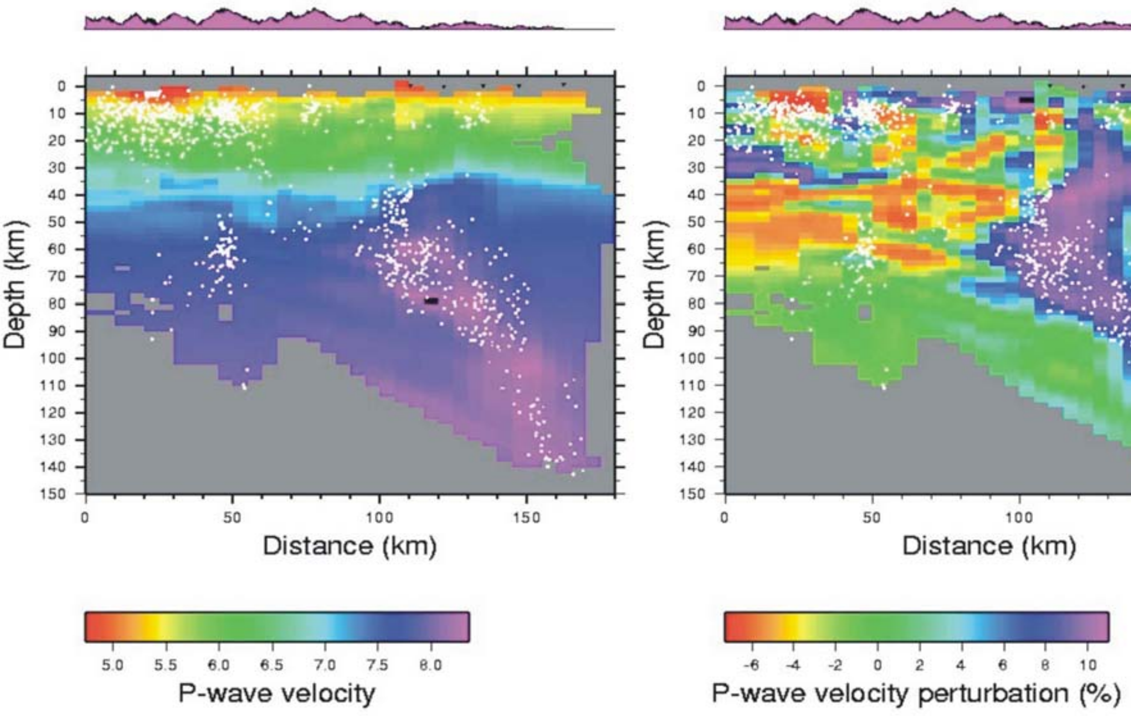
Depth (km)
0
10
20
30
40
50
60
70
80
90
100
110
120
130
140
150
0
50
100
150
Distance (km)
5.0
5.5
6.0
6.5
7.0
7.5
8.0
P-wave velocity
-6
-4
-2
0
2
4
6
8
10
P-wave velocity perturbation (%)

N7

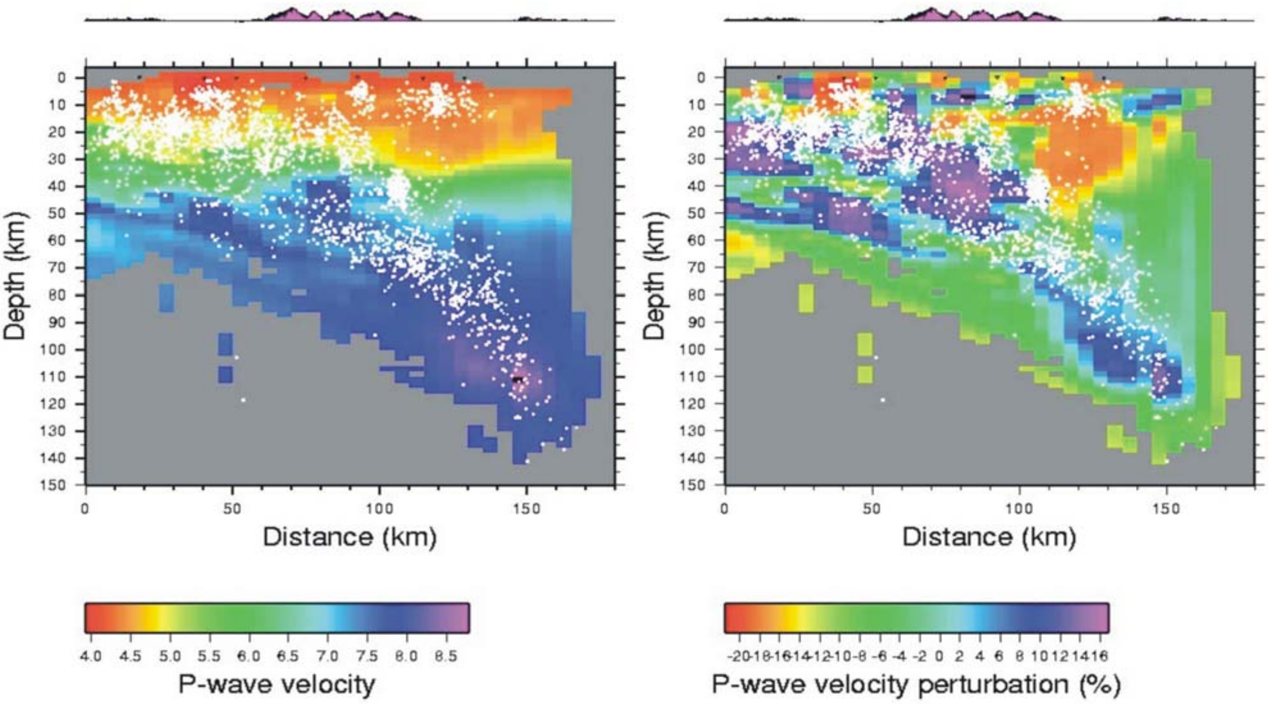
Depth (km)
0
10
20
30
40
50
60
70
80
90
100
110
120
130
140
150
Distance (km)
0
50
100
150
4.0 4.5 5.0 5.5 6.0 6.5 7.0 7.5 8.0 8.5
P-wave velocity
-20 -18 -16 -14 -12 -10 -8 -6 -4 -2 0 2 4 6 8 10 12 14 16
P-wave velocity perturbation (%)

S3

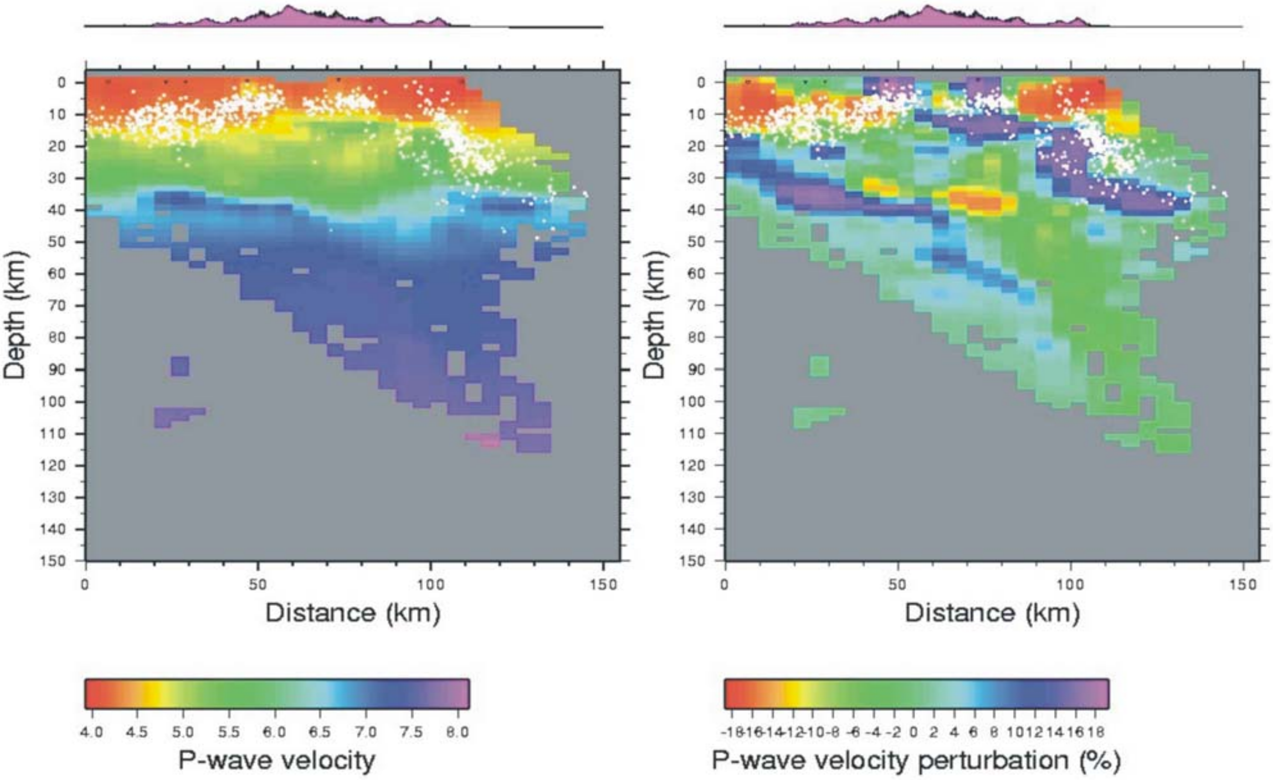
Depth (km)
0
10
20
30
40
50
60
70
80
90
100
110
120
130
140
150
Distance (km)
0
50
100
150
4.0 4.5 5.0 5.5 6.0 6.5 7.0 7.5 8.0
P-wave velocity
-18 -16 -14 -12 -10 -8 -6 -4 -2 0 2 4 6 8 10 12 14 16 18
P-wave velocity perturbation (%)

S6

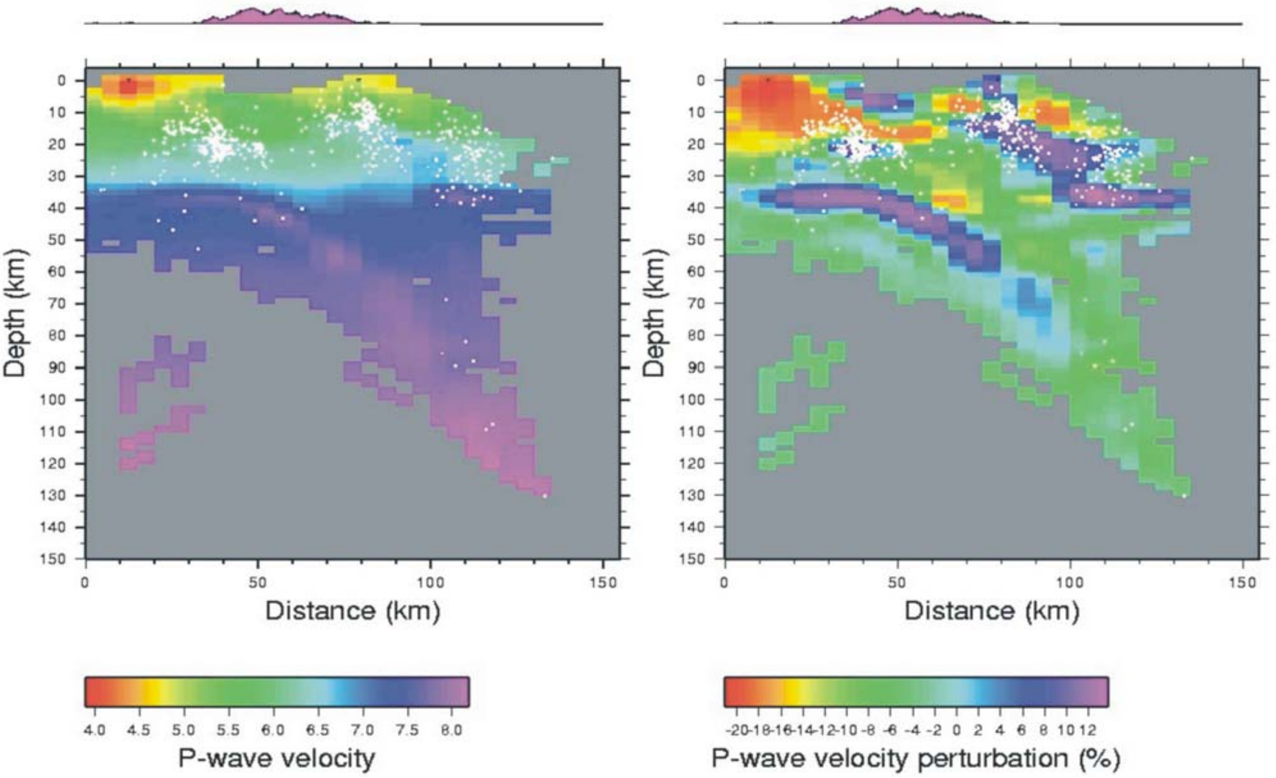
Depth (km)
0
10
20
30
40
50
60
70
80
90
100
110
120
130
140
150
Distance (km)
0
50
100
150
4.0 4.5 5.0 5.5 6.0 6.5 7.0 7.5 8.0
P-wave velocity
-20 -18 -16 -14 -12 -10 -8 -6 -4 -2 0 2 4 6 8 10 12
P-wave velocity perturbation (%)

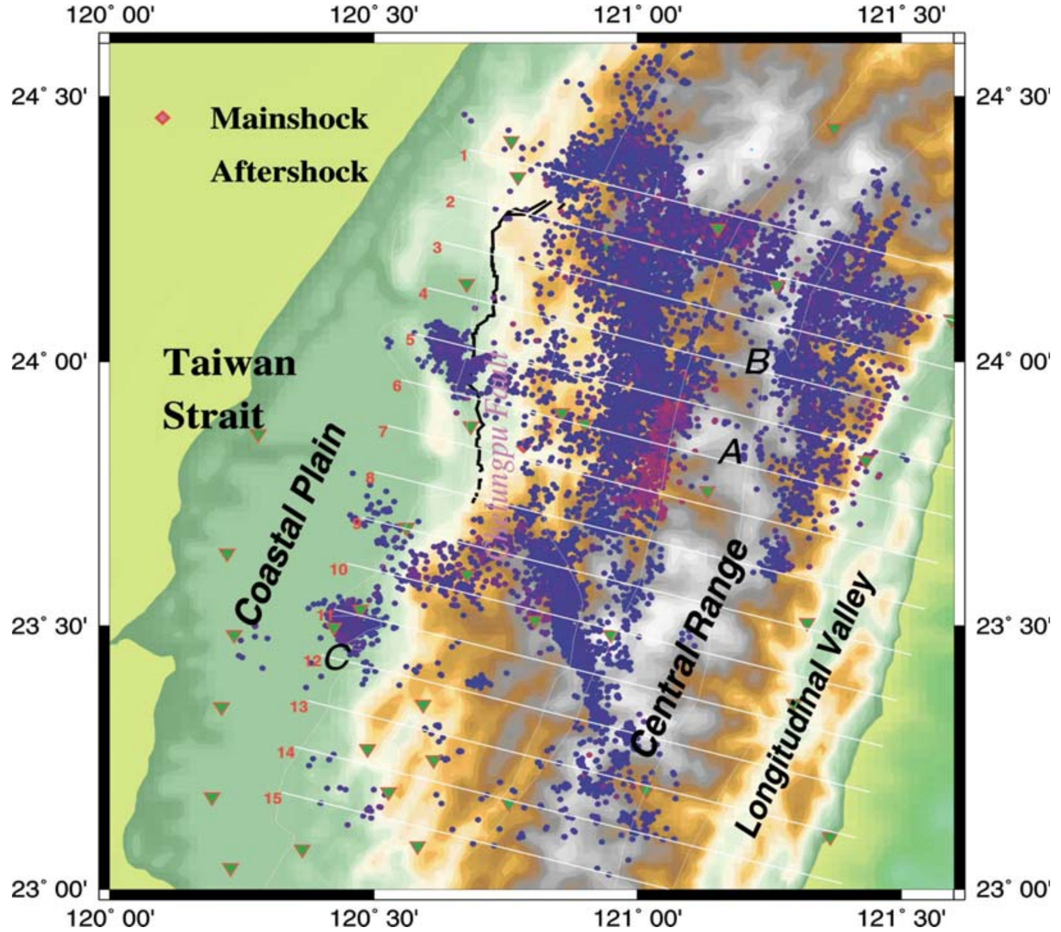
120° 00'
120° 30'
121° 00'
121° 30'
24° 30'
24° 00'
23° 30'
23° 00'
Mainshock
Aftershock
Taiwan Strait
Coastal Plain
Chelungpu Fault
Central Range
Longitudinal Valley
A
B
C
1
2
3
4
5
6
7
8
9
10
11
12
13
14
15

C1

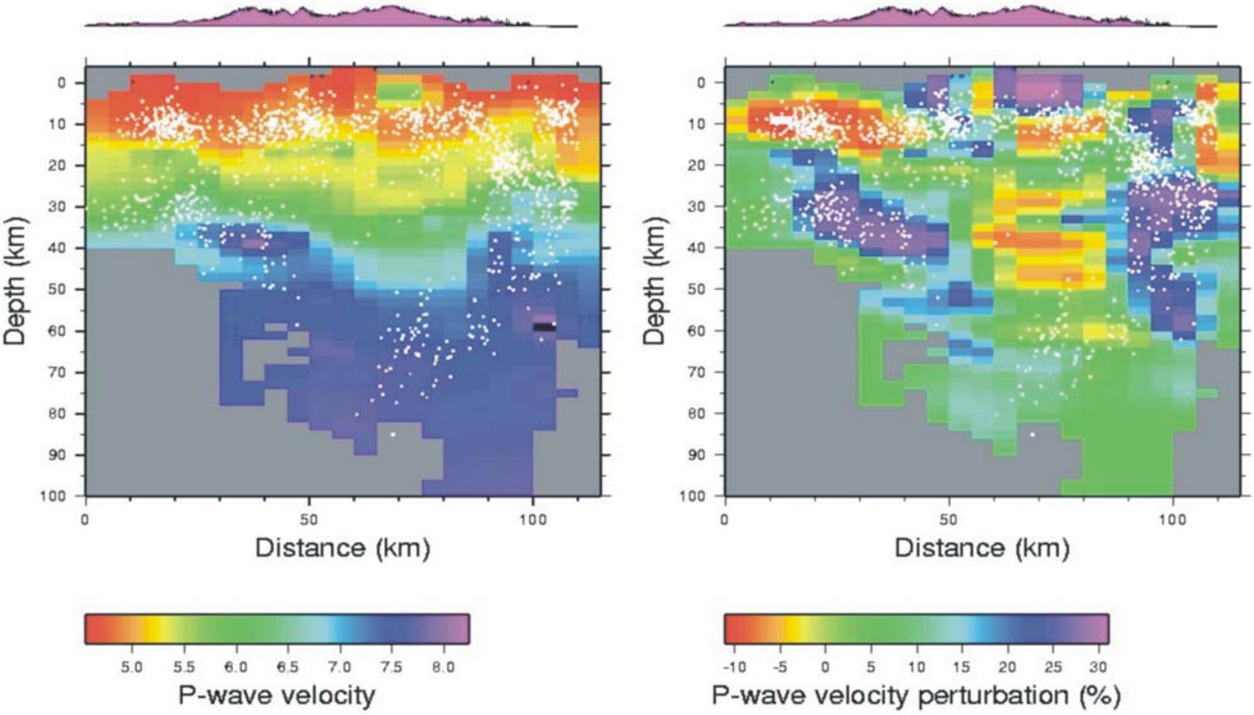

Depth (km)
0
10
20
30
40
50
60
70
80
90
100
Distance (km)
0
50
100
5.0
5.5
6.0
6.5
7.0
7.5
8.0
P-wave velocity
-10
-5
0
5
10
15
20
25
30
P-wave velocity perturbation (%)

C2

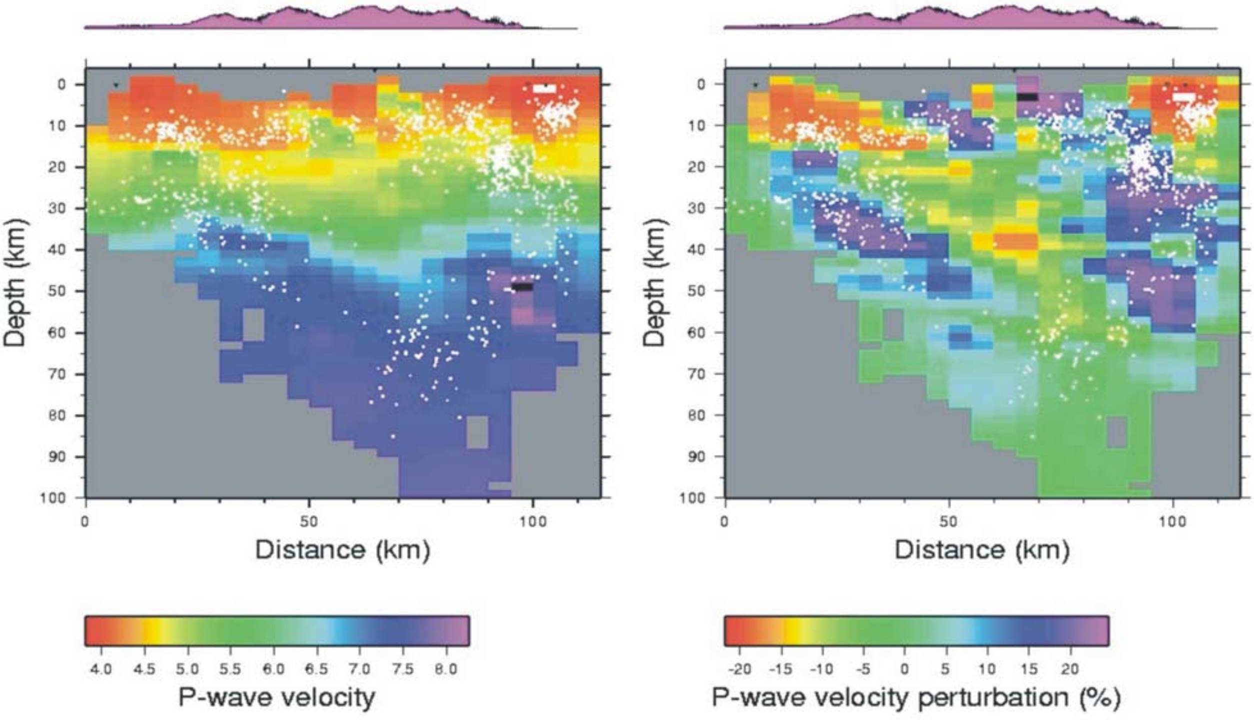

Depth (km)
0
10
20
30
40
50
60
70
80
90
100
Distance (km)
0
50
100
4.0
4.5
5.0
5.5
6.0
6.5
7.0
7.5
8.0
P-wave velocity
-20
-15
-10
-5
0
5
10
15
20
P-wave velocity perturbation (%)

C3

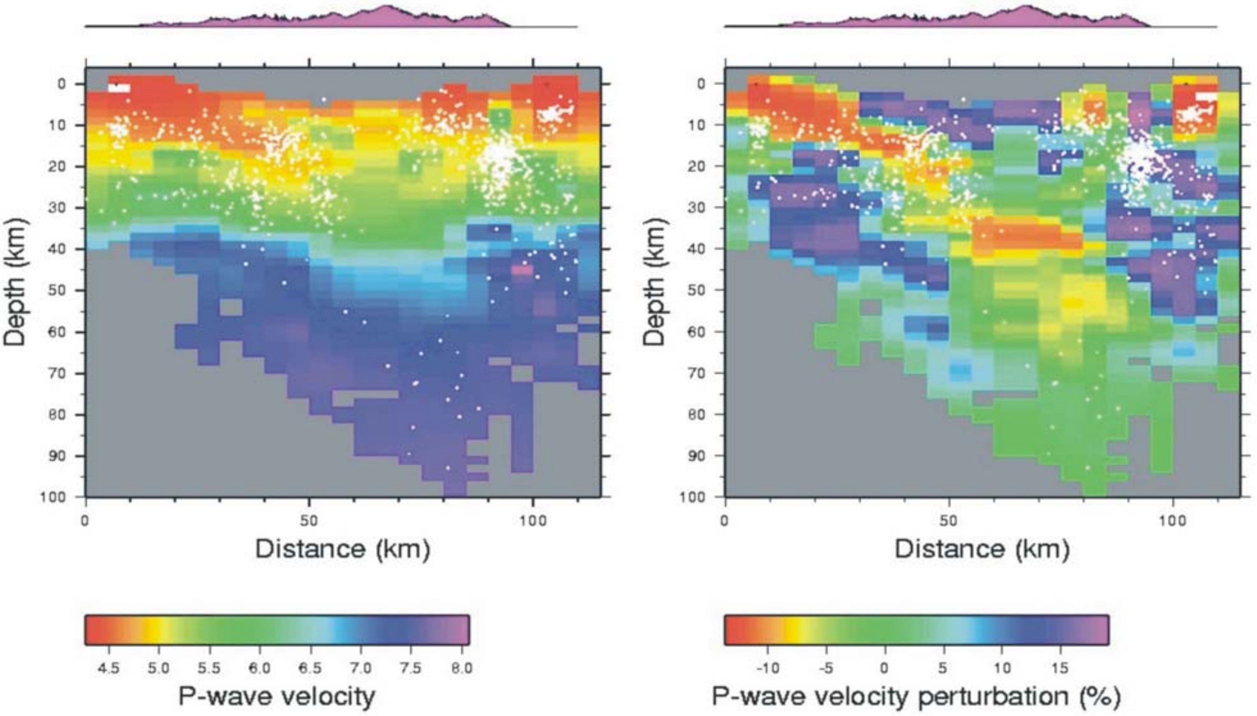
Depth (km)
0
10
20
30
40
50
60
70
80
90
100
0
50
100
Distance (km)
4.5
5.0
5.5
6.0
6.5
7.0
7.5
8.0
P-wave velocity
Depth (km)
0
10
20
30
40
50
60
70
80
90
100
0
50
100
Distance (km)
-10
-5
0
5
10
15
P-wave velocity perturbation (%)

C4

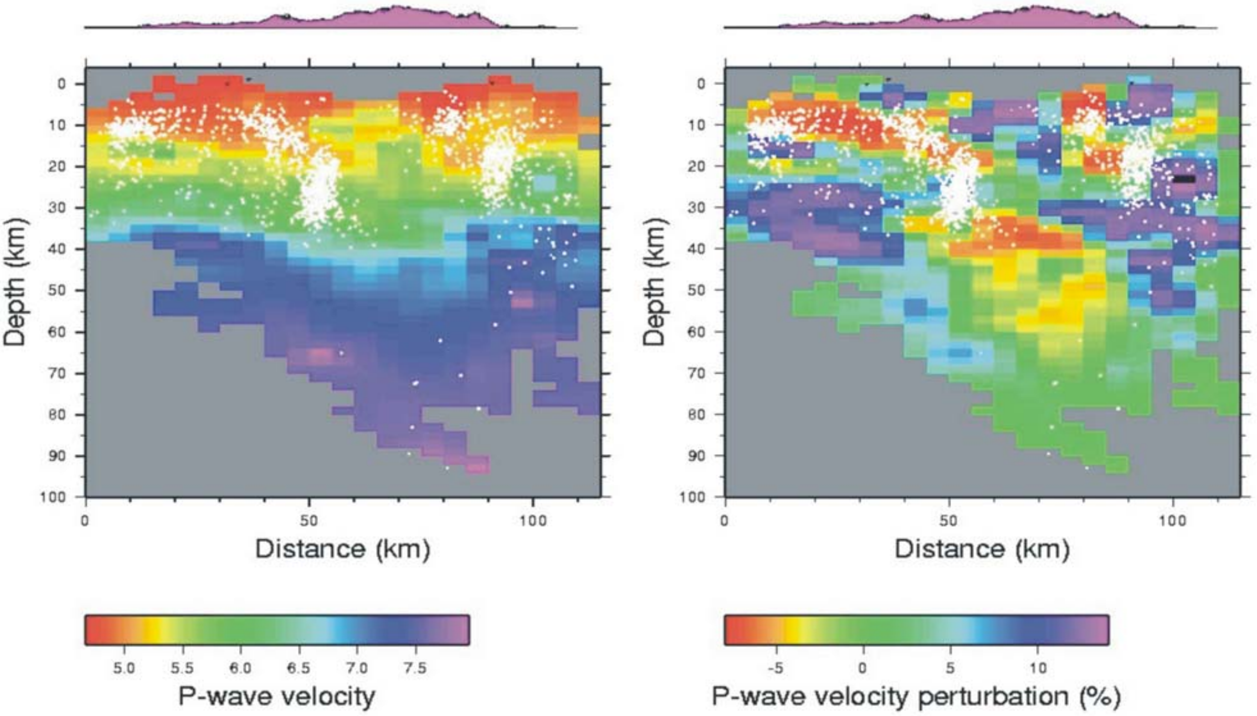
Depth (km)
0
10
20
30
40
50
60
70
80
90
100
0
50
100
Distance (km)
5.0
5.5
6.0
6.5
7.0
7.5
P-wave velocity
Depth (km)
0
10
20
30
40
50
60
70
80
90
100
0
50
100
Distance (km)
-5
0
5
10
P-wave velocity perturbation (%)

C5

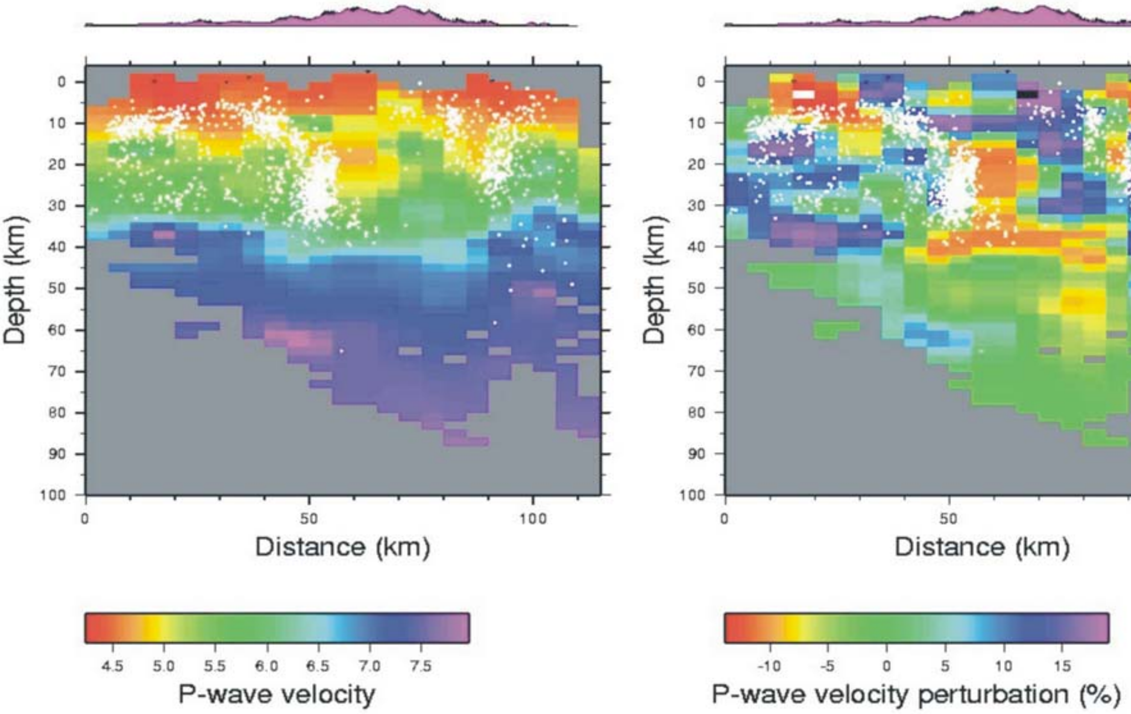
Depth (km)
0
10
20
30
40
50
60
70
80
90
100
0
50
100
Distance (km)
4.5
5.0
5.5
6.0
6.5
7.0
7.5
P-wave velocity
Depth (km)
Distance (km)
-10
-5
0
5
10
15
P-wave velocity perturbation (%)

C6

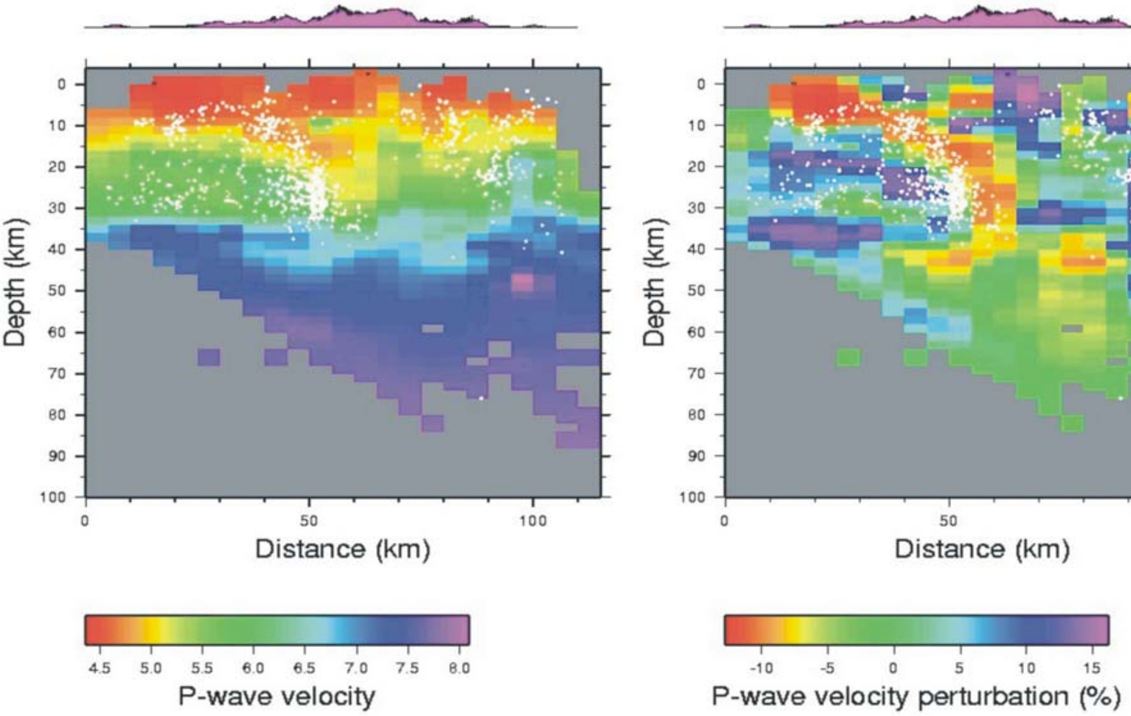
Depth (km)
0
10
20
30
40
50
60
70
80
90
100
0
50
100
Distance (km)
4.5
5.0
5.5
6.0
6.5
7.0
7.5
8.0
P-wave velocity
Depth (km)
Distance (km)
-10
-5
0
5
10
15
P-wave velocity perturbation (%)

C7

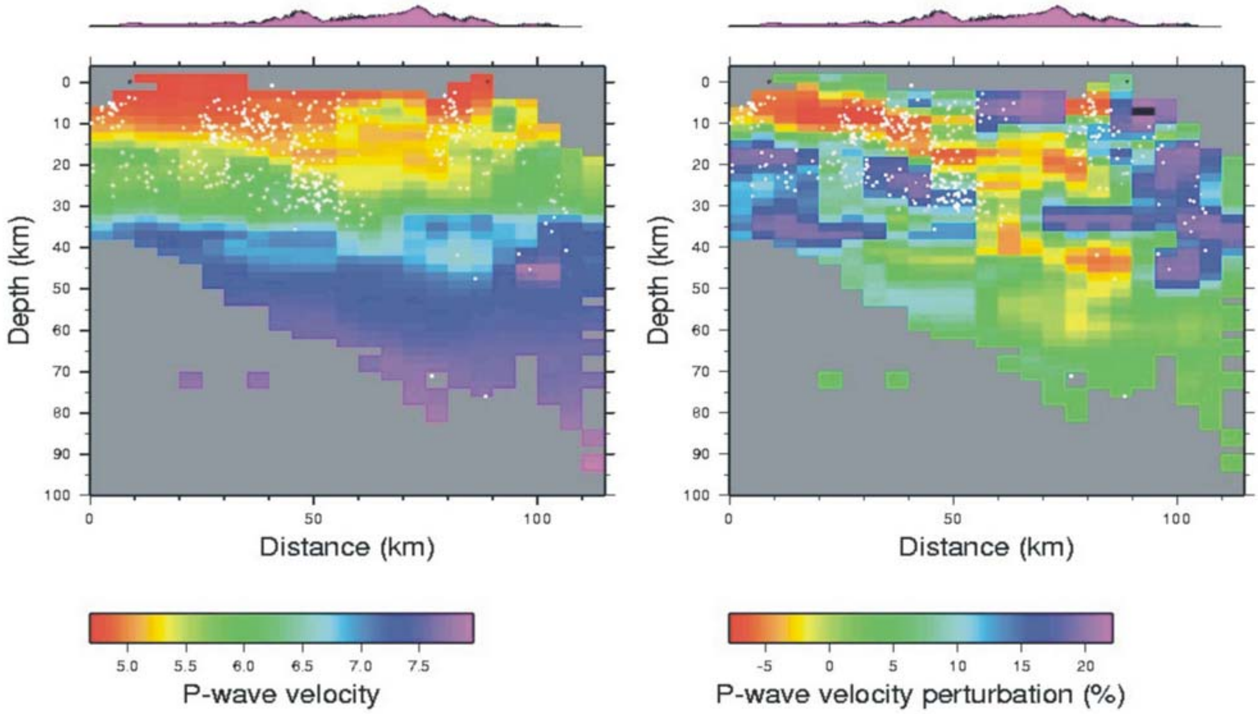
Depth (km)
0
10
20
30
40
50
60
70
80
90
100
0
50
100
Distance (km)
4.5
5.0
5.5
6.0
6.5
7.0
7.5
P-wave velocity
-5
0
5
10
15
20
P-wave velocity perturbation (%)

C8

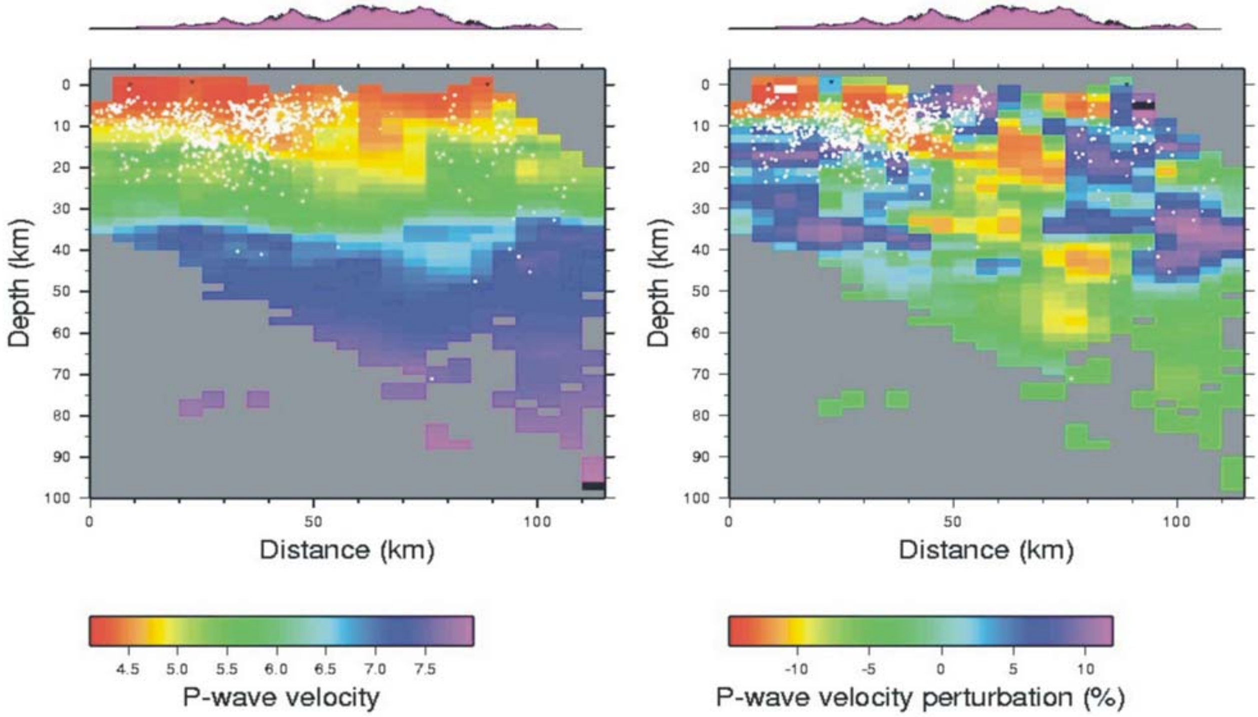
Depth (km)
0
10
20
30
40
50
60
70
80
90
100
0
50
100
Distance (km)
4.5
5.0
5.5
6.0
6.5
7.0
7.5
P-wave velocity
-10
-5
0
5
10
P-wave velocity perturbation (%)

C9

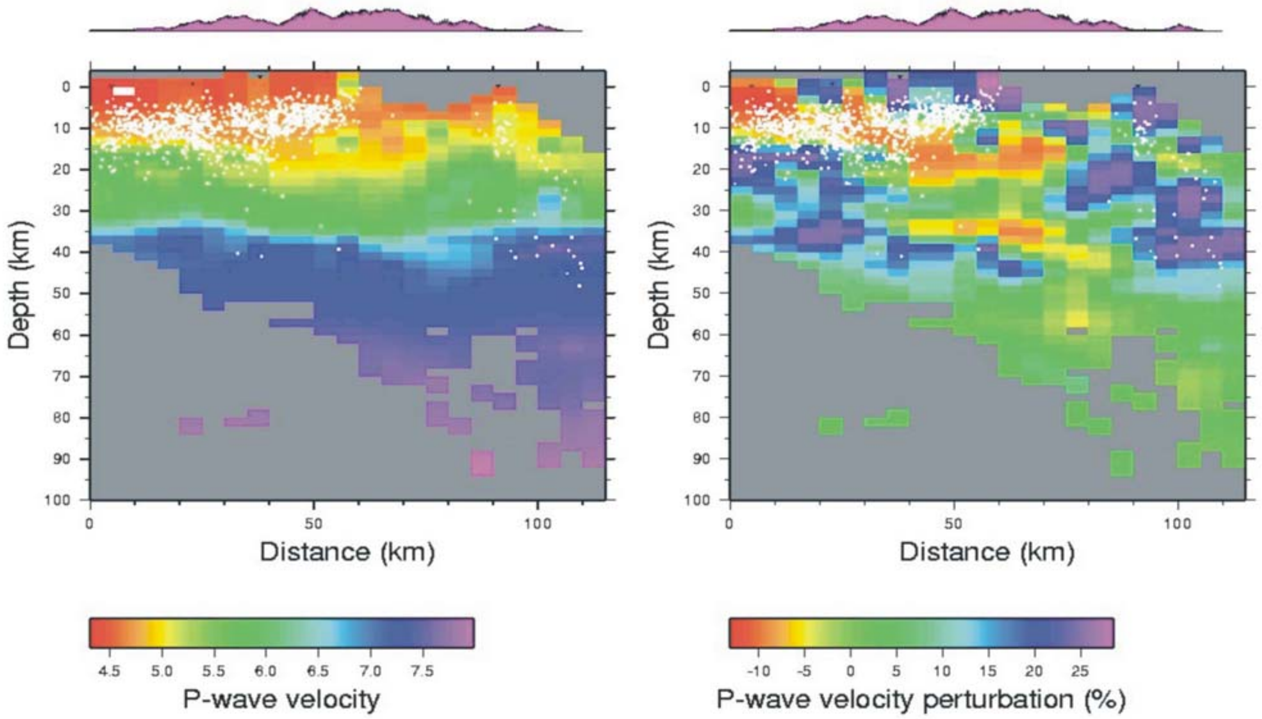
Depth (km)
0
10
20
30
40
50
60
70
80
90
100
0
50
100
Distance (km)
4.5
5.0
5.5
6.0
6.5
7.0
7.5
P-wave velocity
Depth (km)
Distance (km)
-10
-5
0
5
10
15
20
25
P-wave velocity perturbation (%)

C10

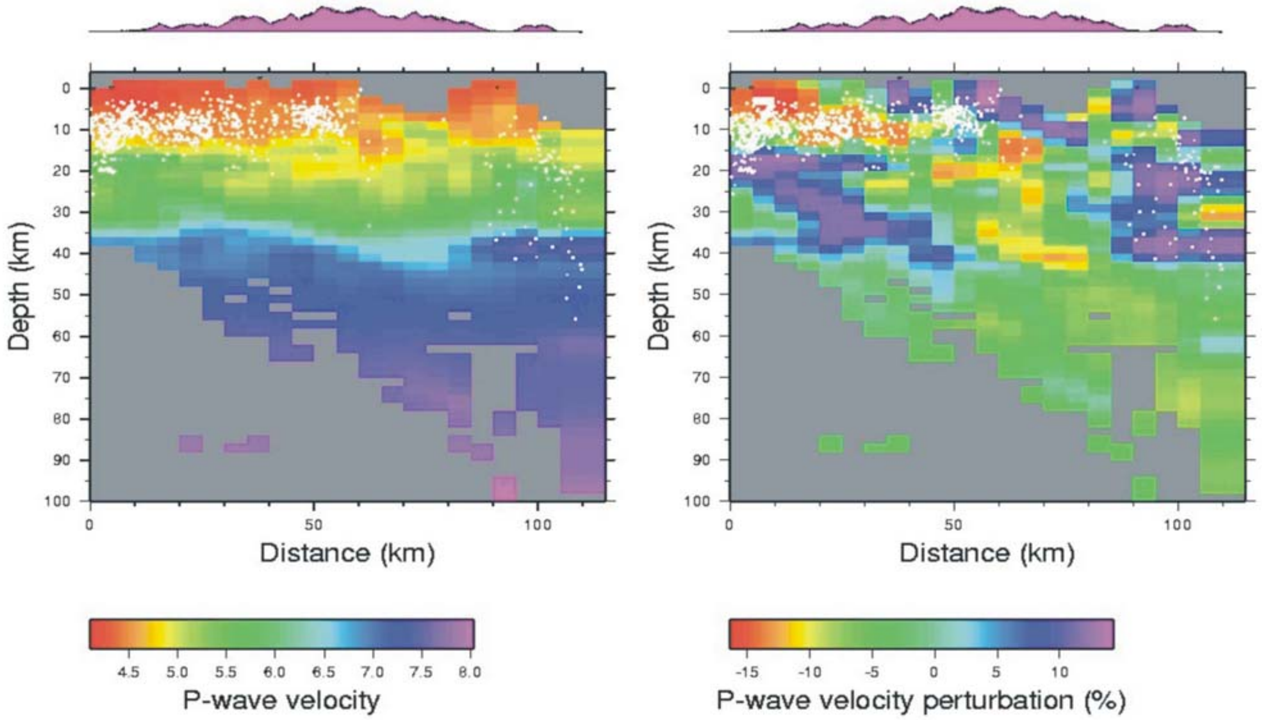
Depth (km)
0
10
20
30
40
50
60
70
80
90
100
0
50
100
Distance (km)
4.5
5.0
5.5
6.0
6.5
7.0
7.5
8.0
P-wave velocity
Depth (km)
Distance (km)
-15
-10
-5
0
5
10
P-wave velocity perturbation (%)

C11

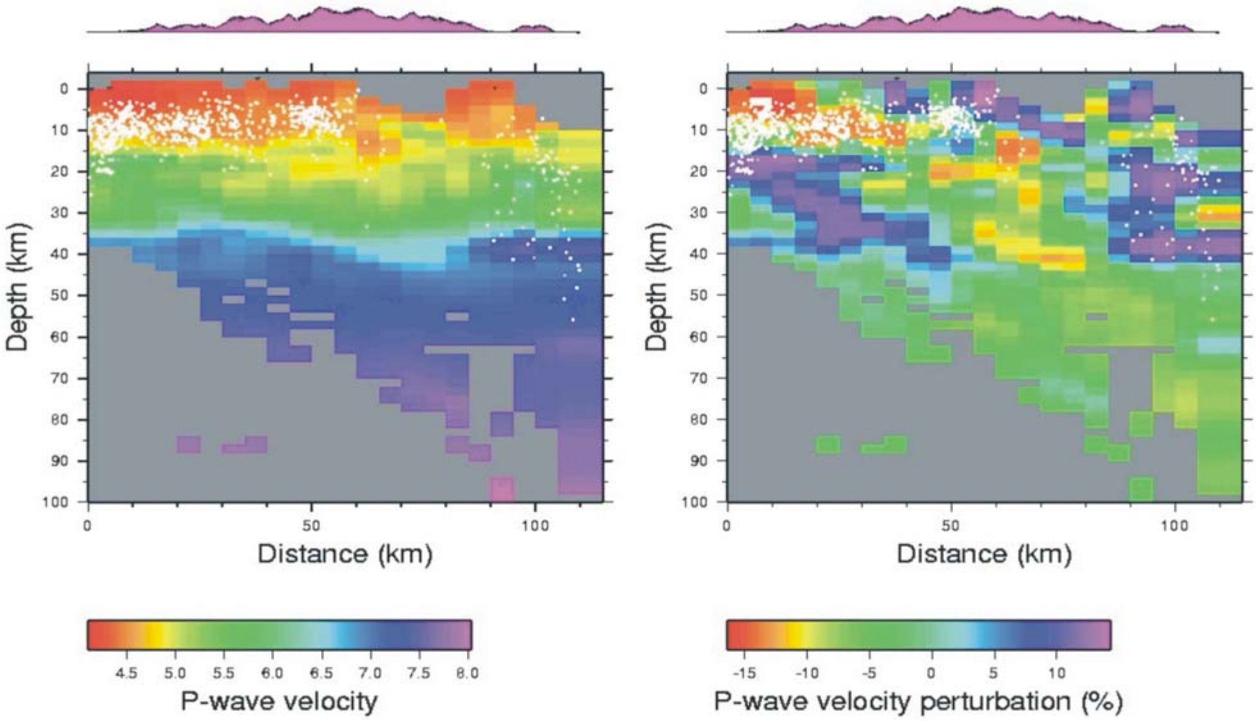
Depth (km)
0
10
20
30
40
50
60
70
80
90
100
0
50
100
Distance (km)
4.5
5.0
5.5
6.0
6.5
7.0
7.5
8.0
P-wave velocity
-15
-10
-5
0
5
10
P-wave velocity perturbation (%)

C12

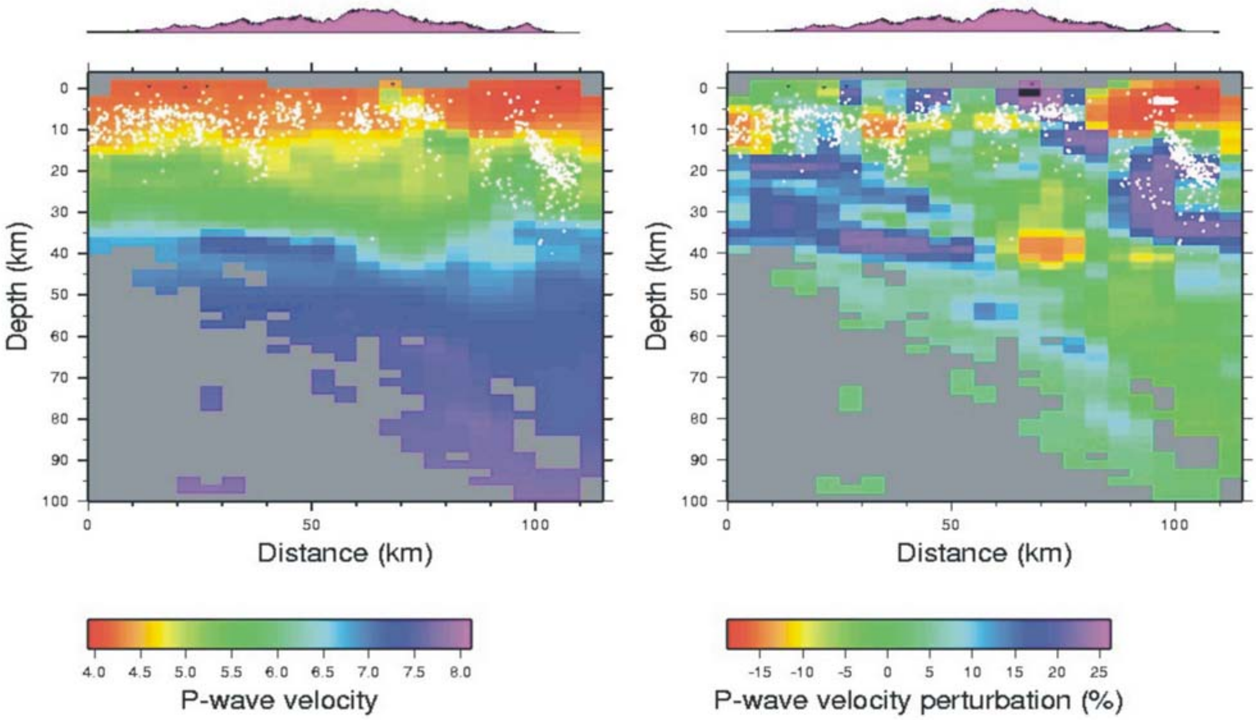
Depth (km)
0
10
20
30
40
50
60
70
80
90
100
0
50
100
Distance (km)
4.0
4.5
5.0
5.5
6.0
6.5
7.0
7.5
8.0
P-wave velocity
-15
-10
-5
0
5
10
15
20
25
P-wave velocity perturbation (%)

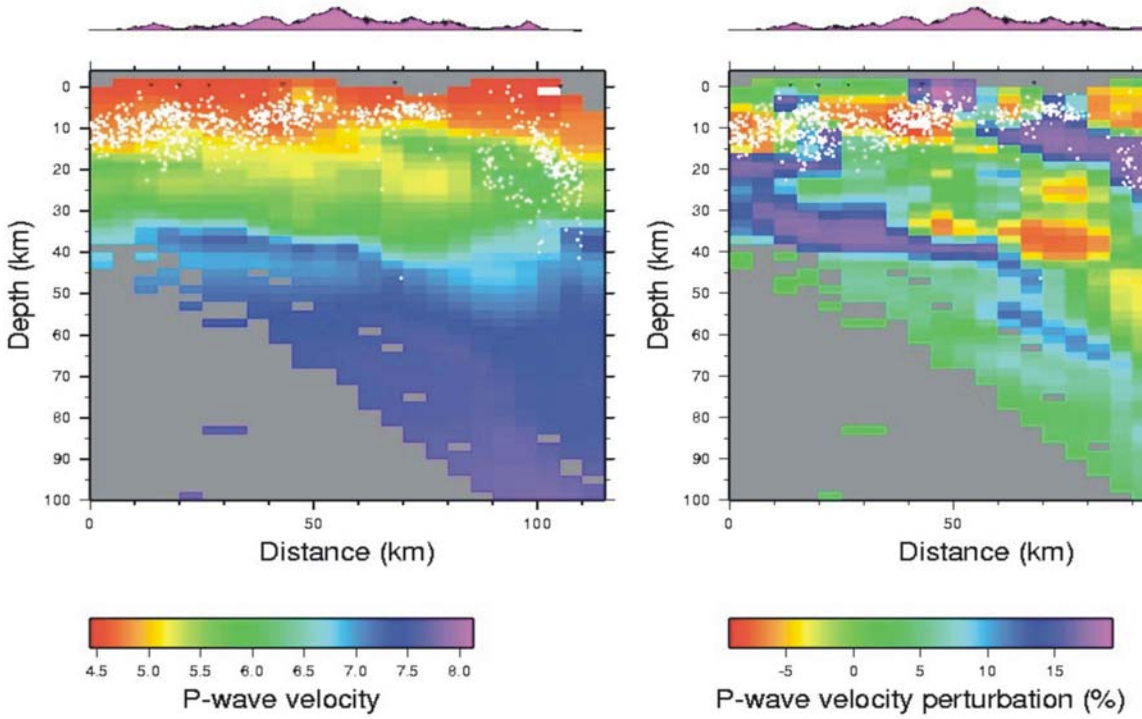
Depth (km)
0
10
20
30
40
50
60
70
80
90
100
0
50
100
Distance (km)
4.5
5.0
5.5
6.0
6.5
7.0
7.5
8.0
P-wave velocity
Depth (km)
Distance (km)
-5
0
5
10
15
P-wave velocity perturbation (%)

C14

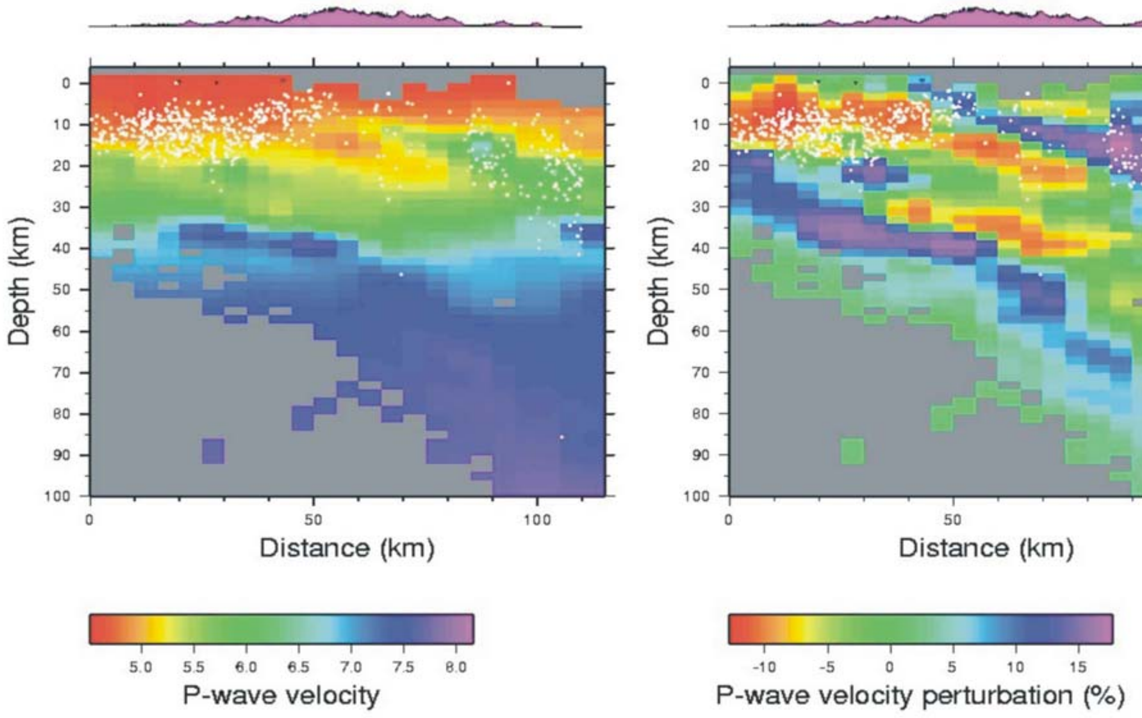
Depth (km)
0
10
20
30
40
50
60
70
80
90
100
0
50
100
Distance (km)
5.0
5.5
6.0
6.5
7.0
7.5
8.0
P-wave velocity
Depth (km)
Distance (km)
-10
-5
0
5
10
15
P-wave velocity perturbation (%)

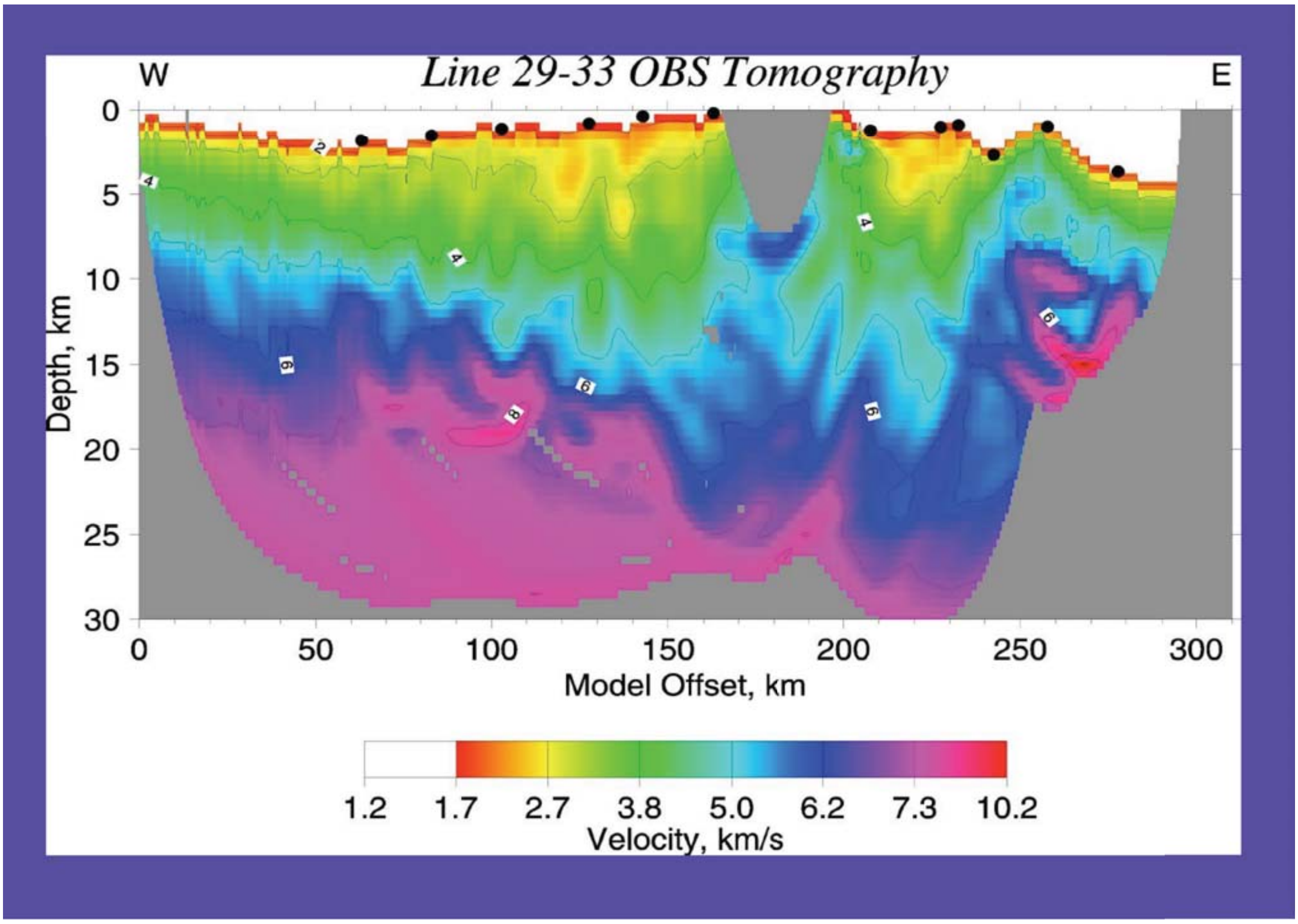

Conclusions

- Seismicity permeates the crust and upper mantle underneath the foothills
- Thrust mechanisms dominate in W Taiwan
- Much of Central Range aseismic – ductile?
- Major episode of normal faulting occurred following the 1999 Chi-Chi earthquake
- A high-angle reverse fault under the Lishan fault is consistent with root building under Central Range

- Subduction in northern and southern Taiwan have clear seismicity and velocity signatures
- Subduction in Central Taiwan has not been detected so far

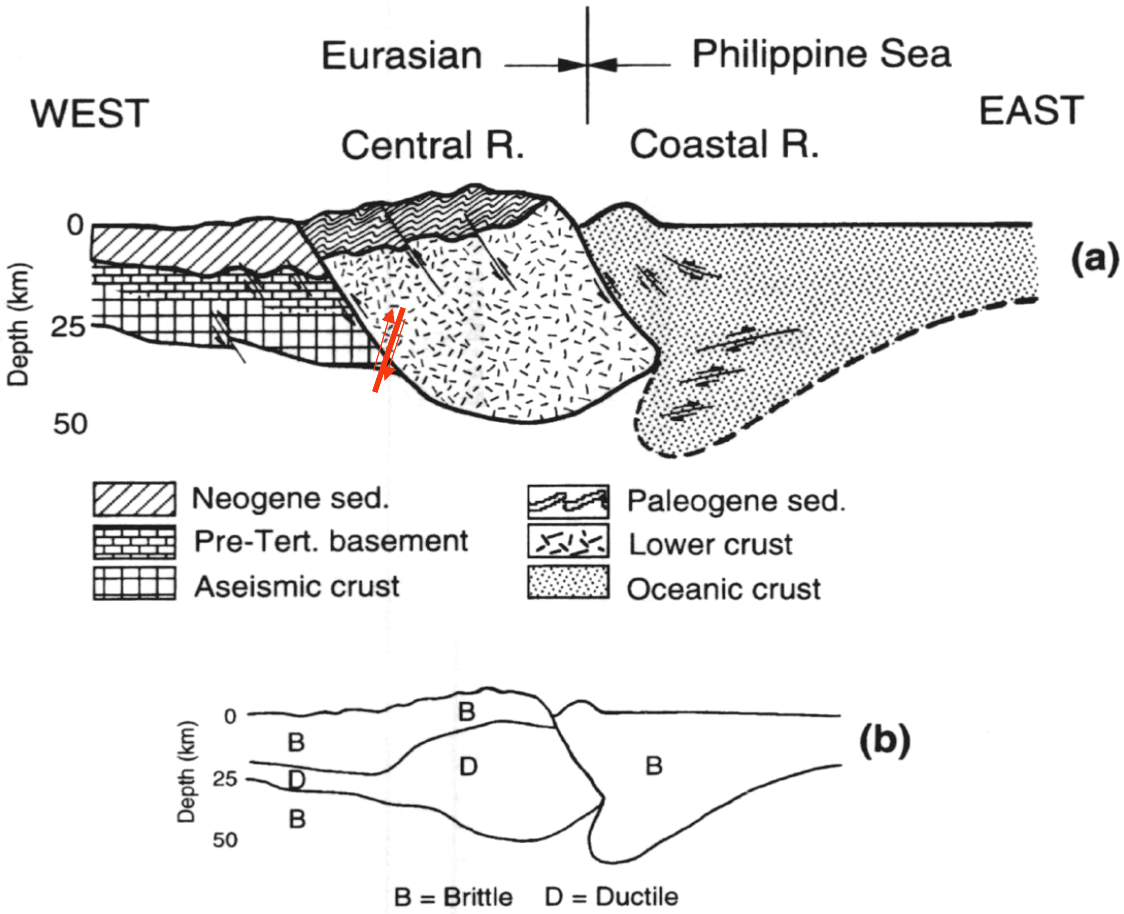

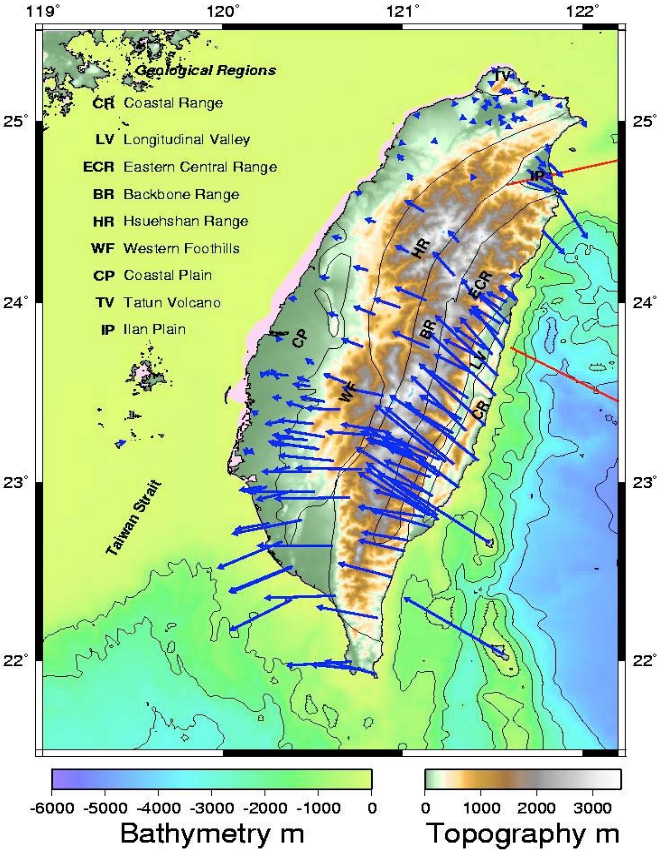

TAIGER

TAiwan Integrated GEodynamics Research

USA: Francis Wu, David Okaya, Kirk McIntosh, Yosio Nakamura, Larry Brown, Luc Lavier, Nik Christensen, Martyn Unsworth, Steve Roecker

Taiwan: Ben Tsai et al., Char-Shine Liu, C.S. Lee, Bor-shouh Huang, C.Y.Wang, Yi-ming Wu, R.J. Rau and other groups

Japan: Naoshi Hirata, Hiroshi Sato, Kanazawa

Project Themes

- Taiwan orogeny is young and very active:
  - the underlying geodynamical processes can be observed while in action
  - the orogeny is complex yet tractable
  - Younging southward ->time-space eqv.

    -> evolution of the orogen
  - Existence of currently viable Hypotheses
- Centered on the geodynamics of orogeny

Strategy

- High resolution imaging – to link details of geol obs to subsurface info
- Examine the viable geodynamic hypotheses regarding tectonics of Taiwan
- Deduce testable aspects
- Direct data acquisition to aim at testing hypotheses
- Retain, modify, discard or create new hypotheses at the end of the project

Implementation

- Data acquisition determined by the tests needed
- Geology – observation near the surface that provides boundary conditions and timing/rate information
- Geophysics – observation of Earth's interior to provide a glimpse of the ongoing processes
- Modeling and testing

Target Geodynamic Processes

- Mode of crustal deformation, *decollement*, "escape"
- Crust-upper mantle coupling
- Delamination
- Subduction – continental? lost slab?
- Upper mantle flow
- "Collision"
- "Intraplate" deformation

Existing Testable Models

- “Thin-skinned” model of Suppe
- “Thin-skinned”+subduction model of Lallemand, Malavielle….
- Lithospheric collision model of Wu et al.
- [Subduction and back-arc interaction model of Chemenda]

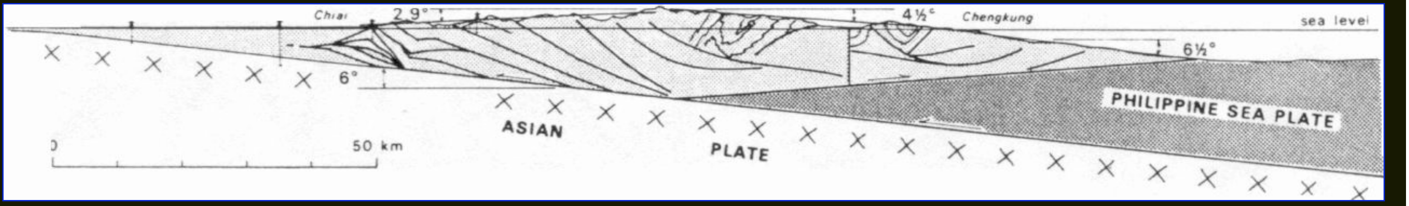

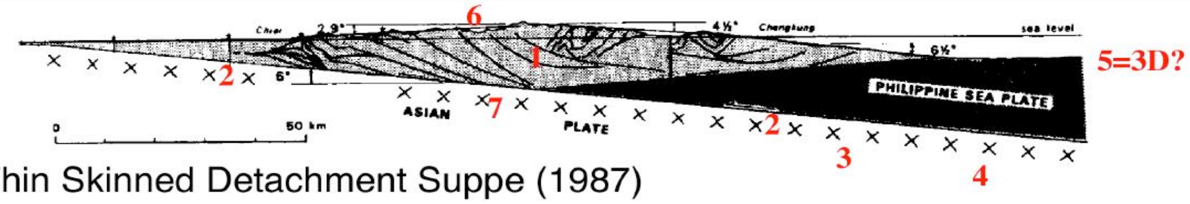

Thin Skinned Detachment Suppe (1987)

1. thick Tertiary wedge? from velocity images? gravity? reflectivity?
2. Does a decollement exist? At what dip? What physical properties such as fluid content, fault zone width?
3. Eurasian subduction beyond eastern Taiwan?
4. Eurasian continental crust subducting under Phillipine Sea oceanic crust?
5. Time-space equivalence (2-D = 3-D)?
6. Steady-state of topographic profile?
7. Isostatic response to bulldozing? Gravity?

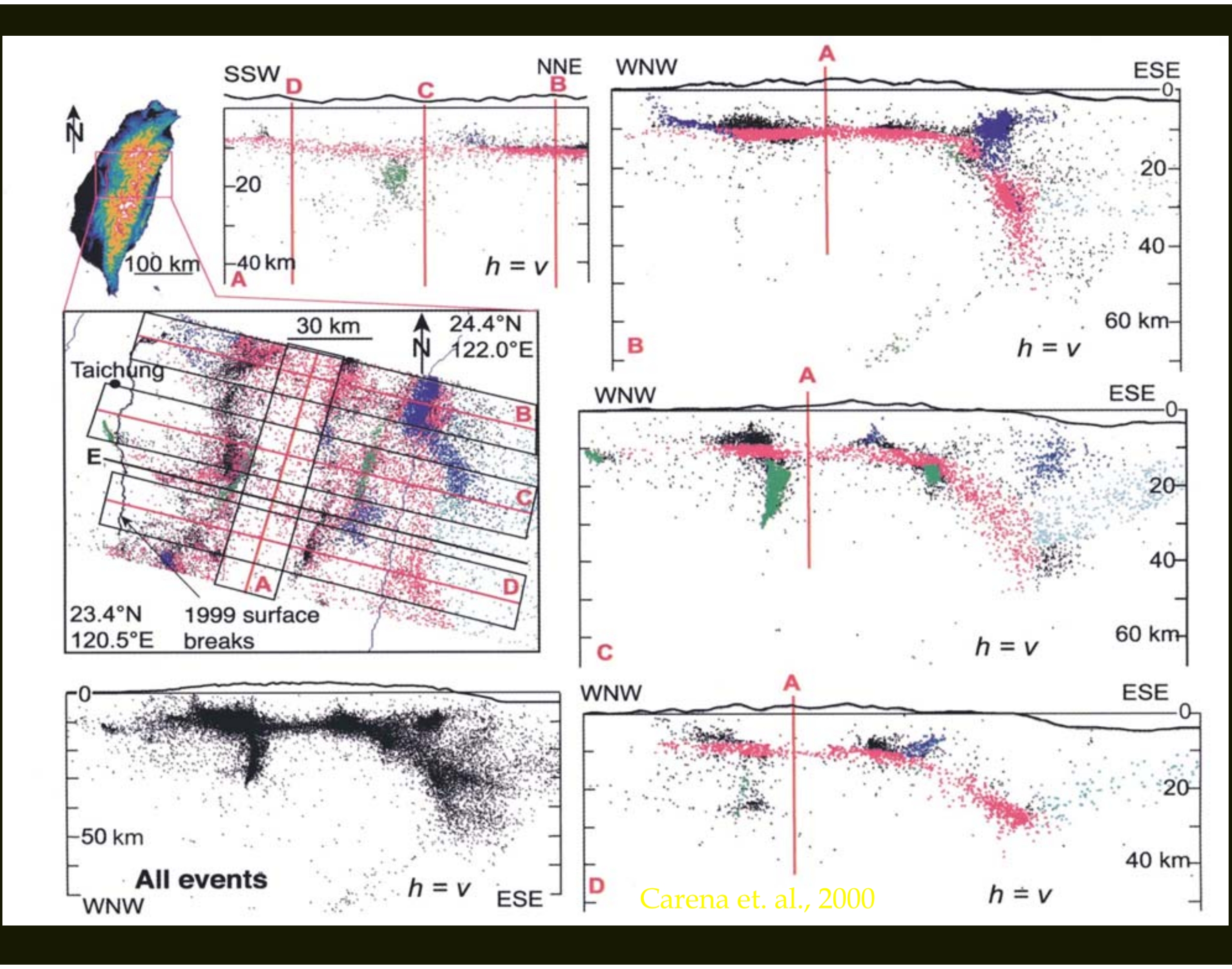

Carena et. al., 2000

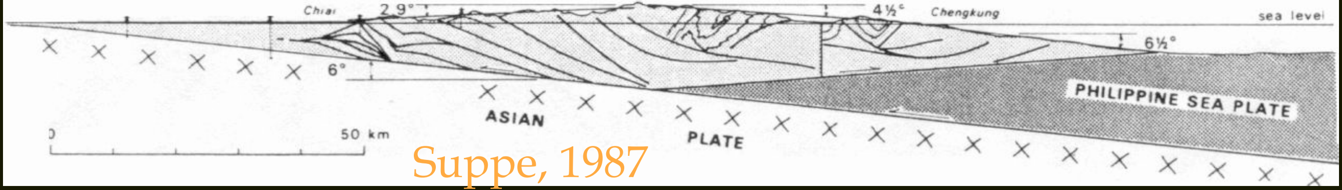

Suppe, 1987

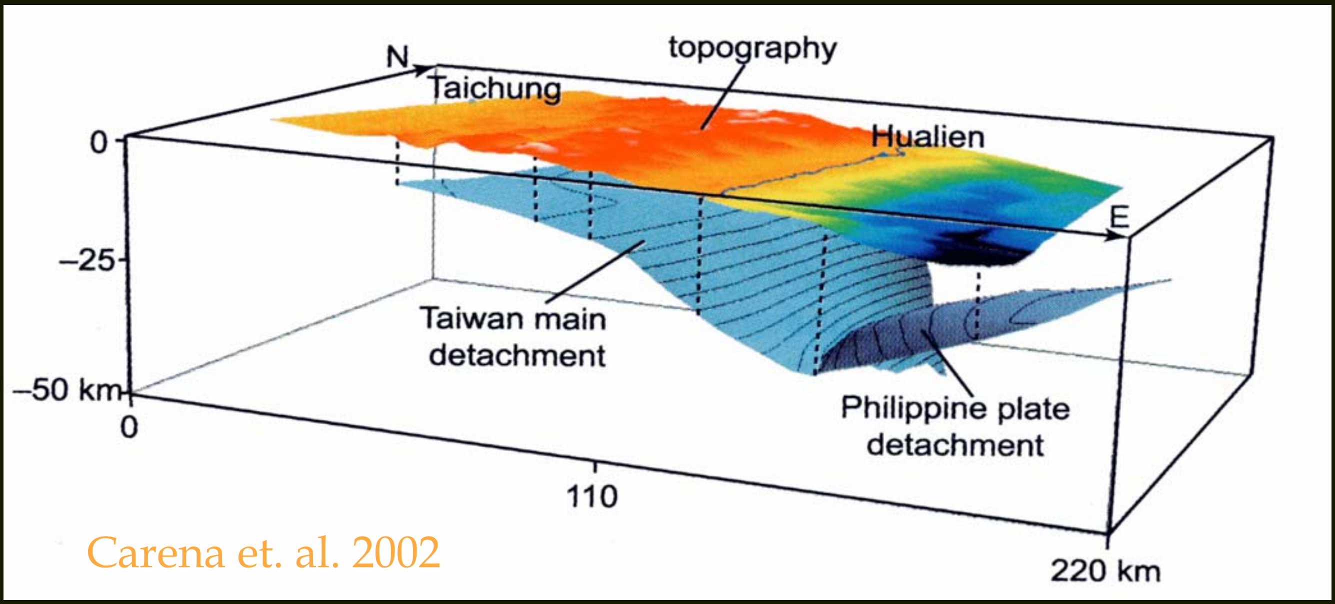

Carena et. al. 2002

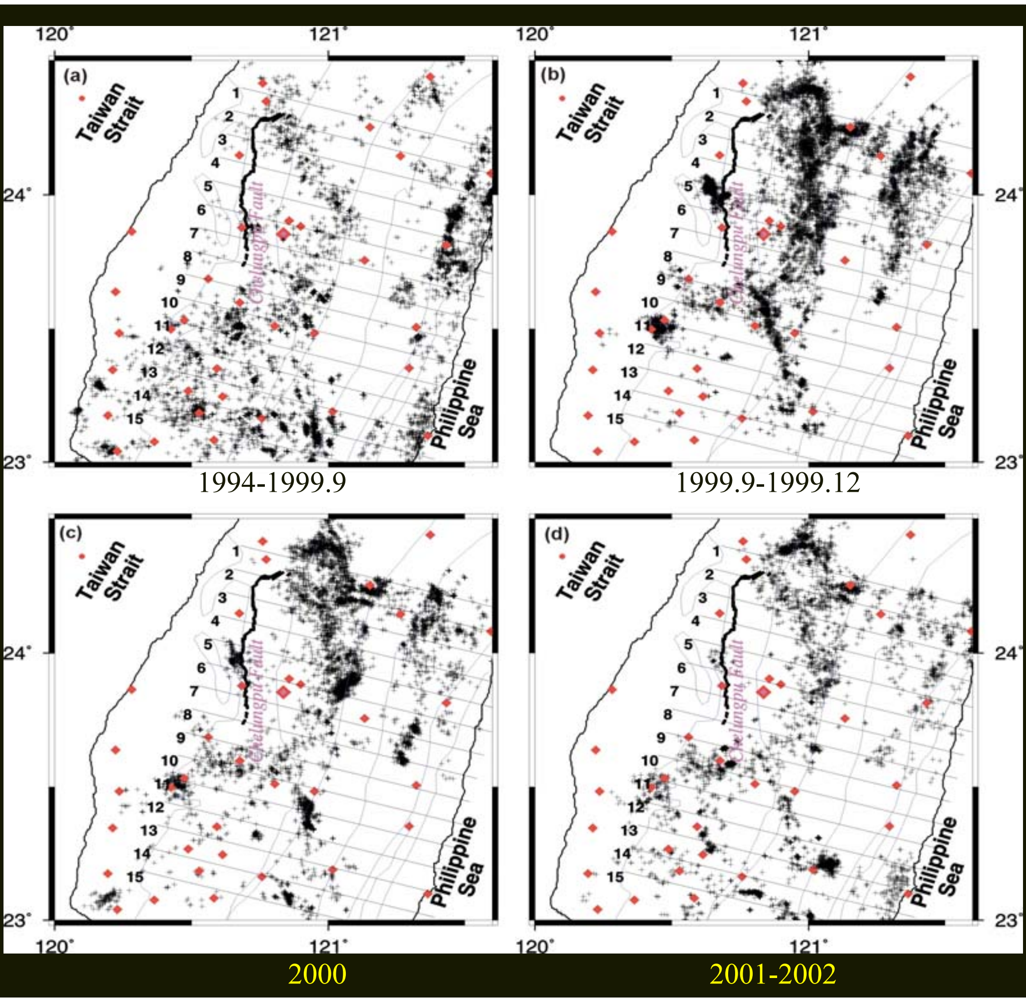

1994-1999.9

1999.9-1999.12

2000

2001-2002

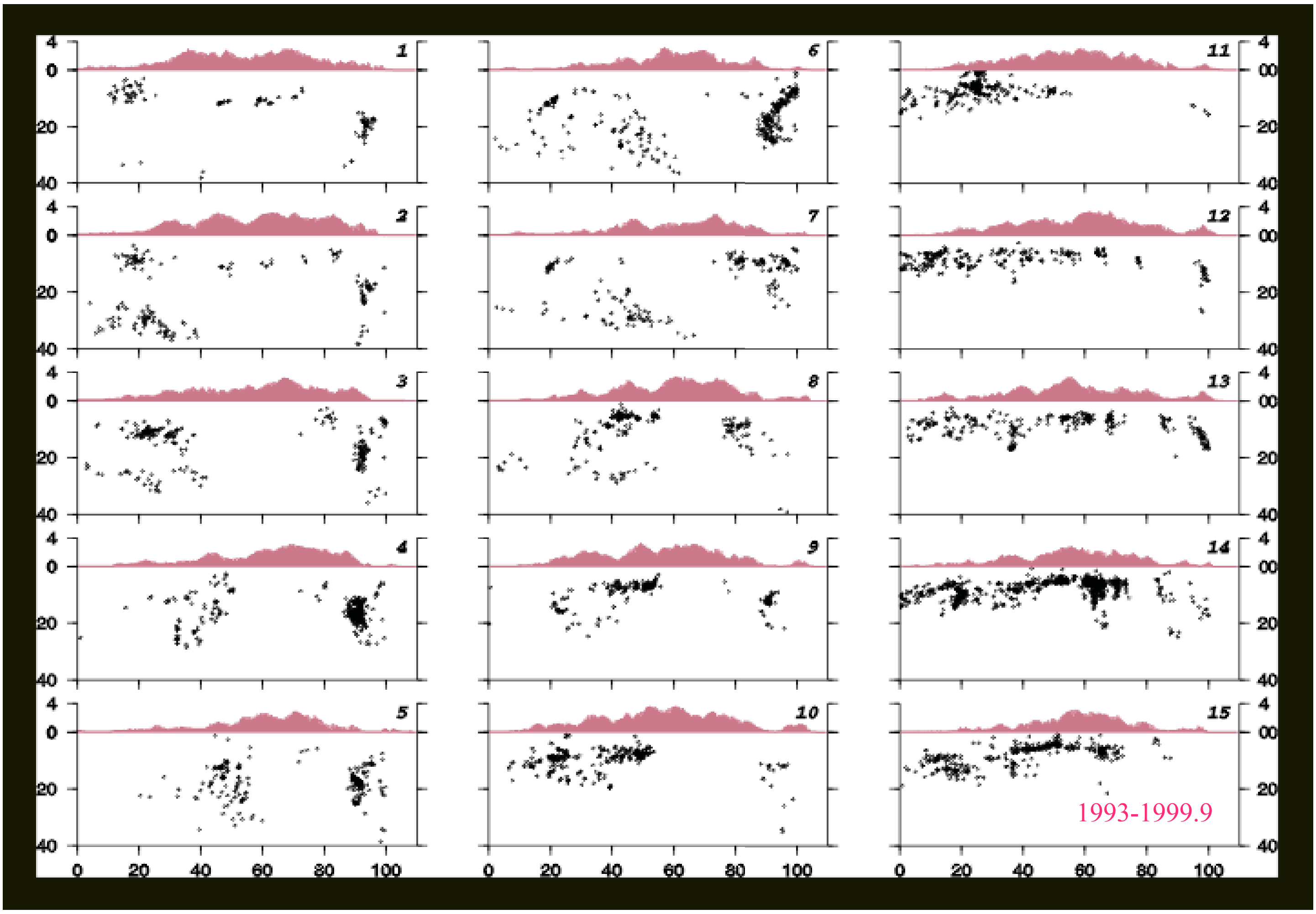

1993-1999.9

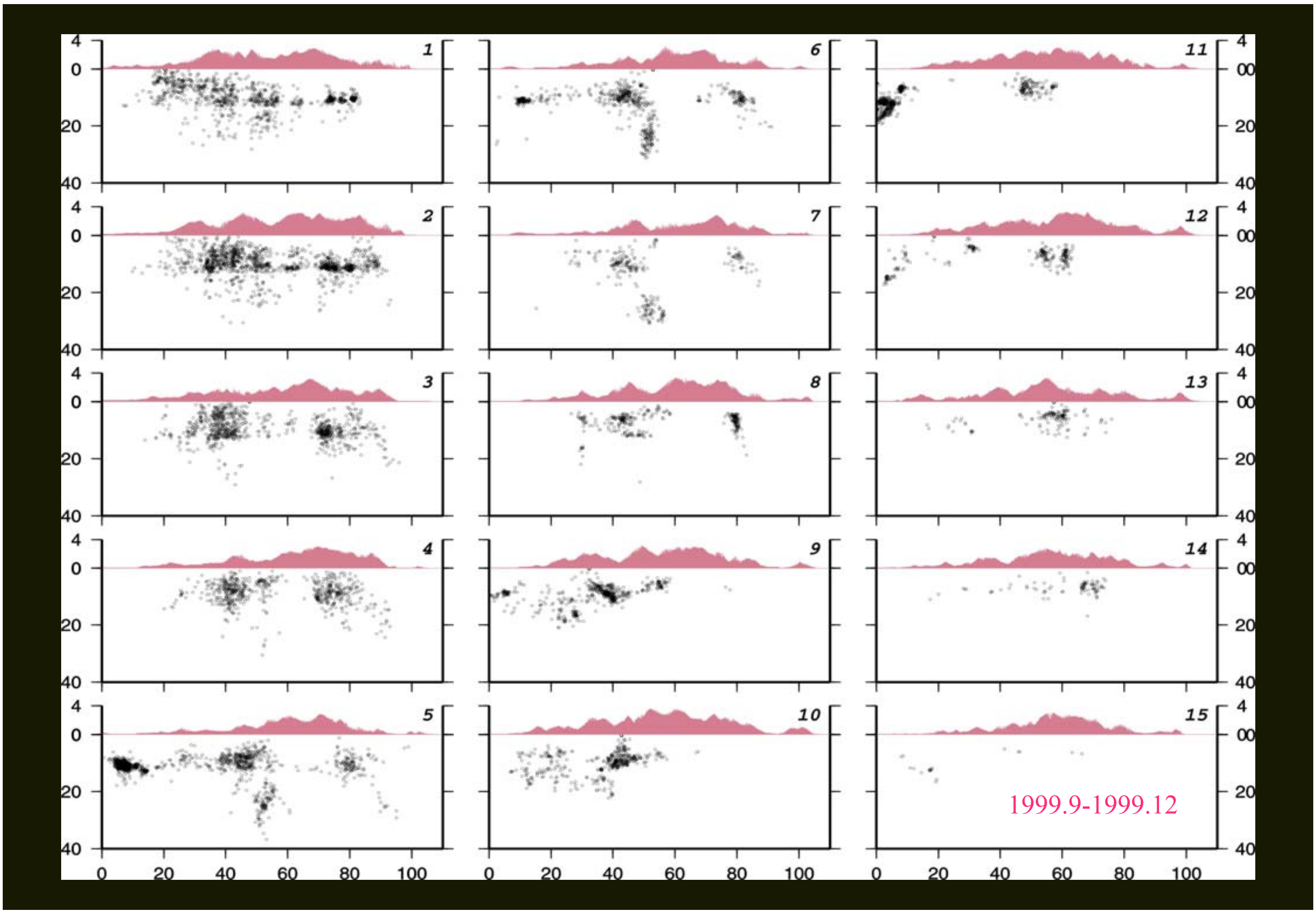

1999.9-1999.12

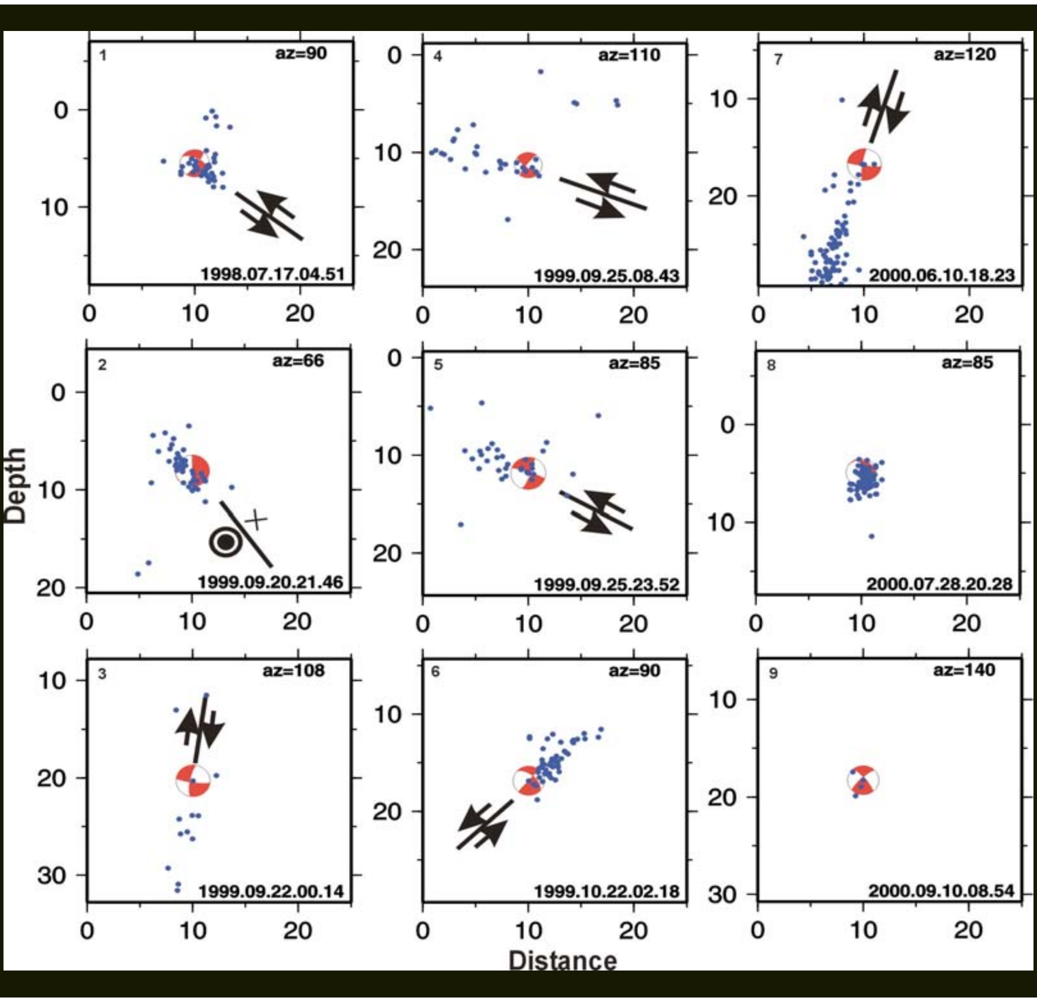
Depth
Distance
1
az=90
1998.07.17.04.51
2
az=66
1999.09.20.21.46
3
az=108
1999.09.22.00.14
4
az=110
1999.09.25.08.43
5
az=85
1999.09.25.23.52
6
az=90
1999.10.22.02.18
7
az=120
2000.06.10.18.23
8
az=85
2000.07.28.20.28
9
az=140
2000.09.10.08.54
0
10
20
30

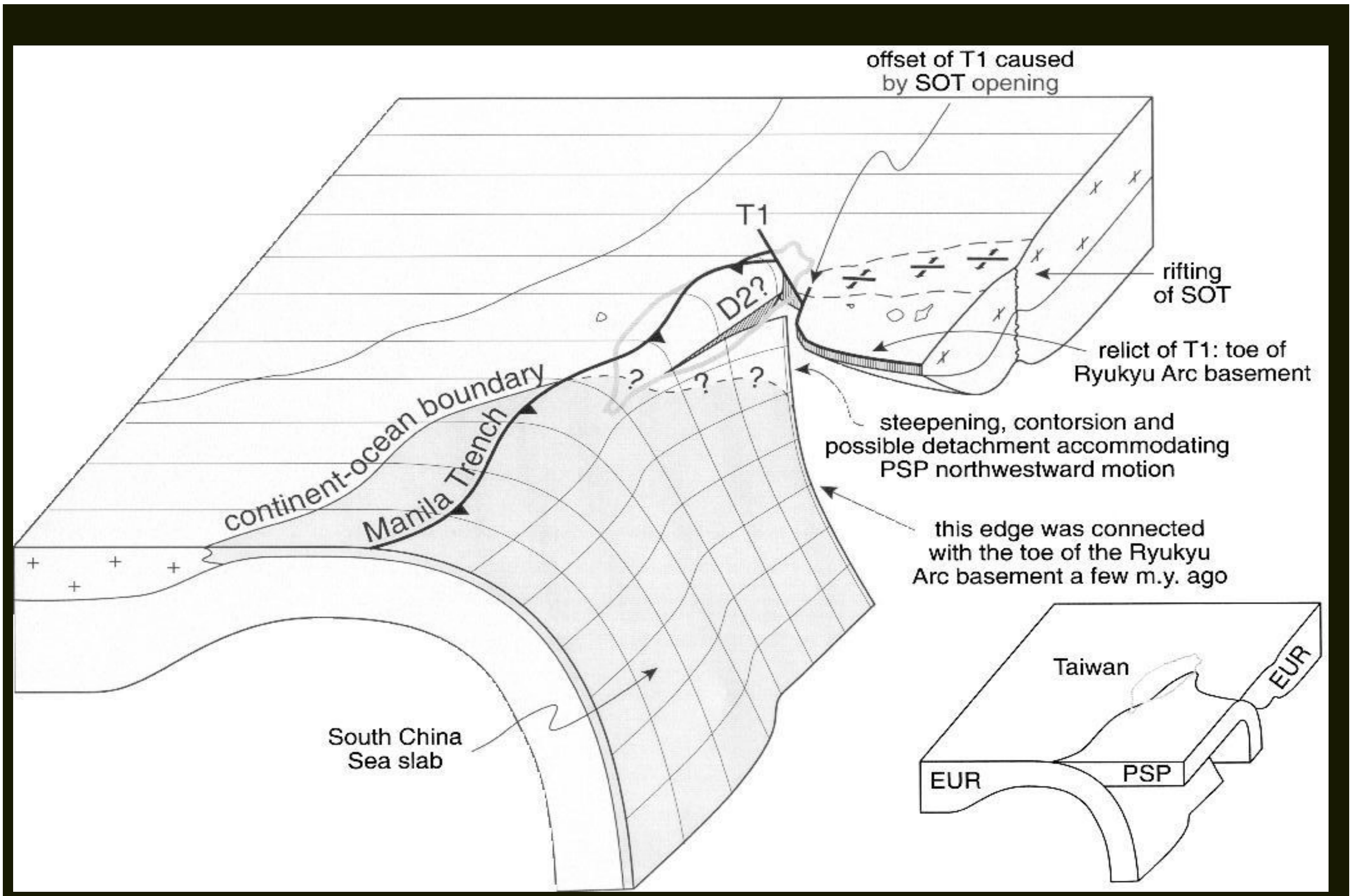
offset of T1 caused by SOT opening
T1
D2?
?
rifting of SOT
relict of T1: toe of Ryukyu Arc basement
steepening, contorsion and possible detachment accommodating PSP northwestward motion
continent-ocean boundary
Manila Trench
this edge was connected with the toe of the Ryukyu Arc basement a few m.y. ago
South China Sea slab
Taiwan
EUR
PSP
EUR

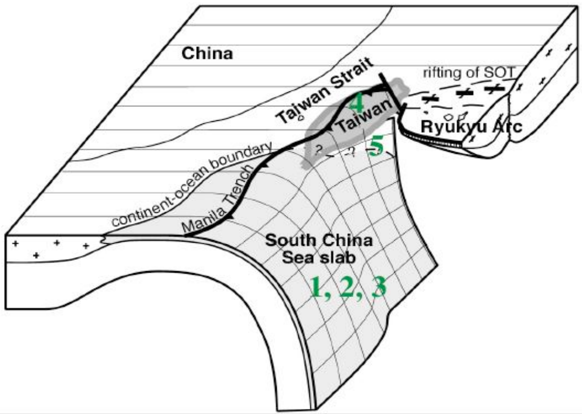

Thin Skinned
(Lallemand et al., 2000)

1. Teleseismic image resolving the slab?
2. If high velocity zone exists, what is the exact geometry? Vertical (like New Zealand)? East dip? Shallow dip? Detached slab?
3. Location bias of the slab?
4. Other questions same as above (Suppe model).
5. Used Rau & Wu (1995) tomography model as evidence for continental subduction. New high resolution tomography modeling does not show.

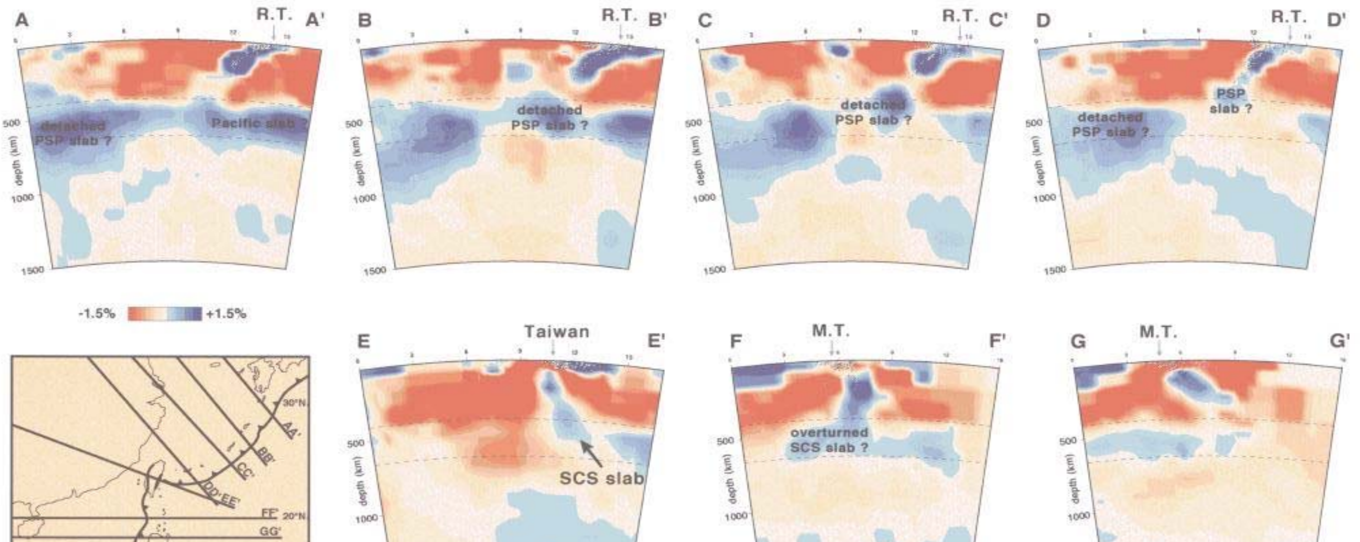

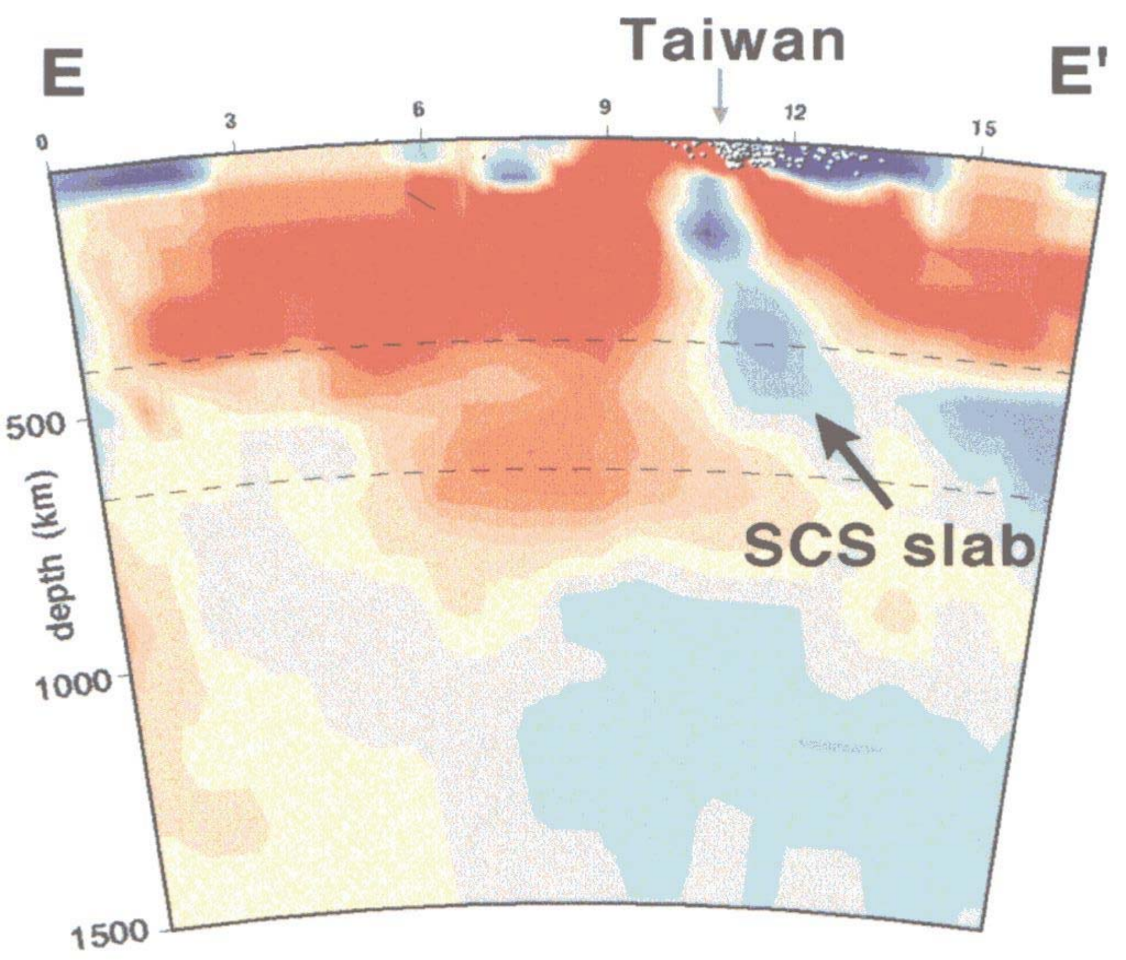
E
Taiwan
E'
0
3
6
9
12
15
500
depth (km)
1000
1500
SCS slab

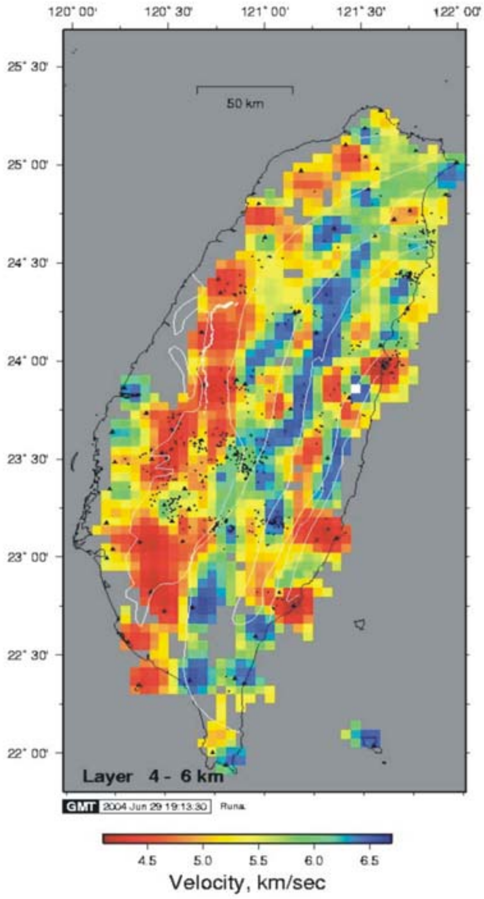
120° 00'
120° 30'
121° 00'
121° 30'
122° 00'
25° 30'
25° 00'
24° 30'
24° 00'
23° 30'
23° 00'
22° 30'
22° 00'
50 km
Layer 4 - 6 km
GMT 2004 Jun 29 19:13:30
Runa.
4.5
5.0
5.5
6.0
6.5
Velocity, km/sec

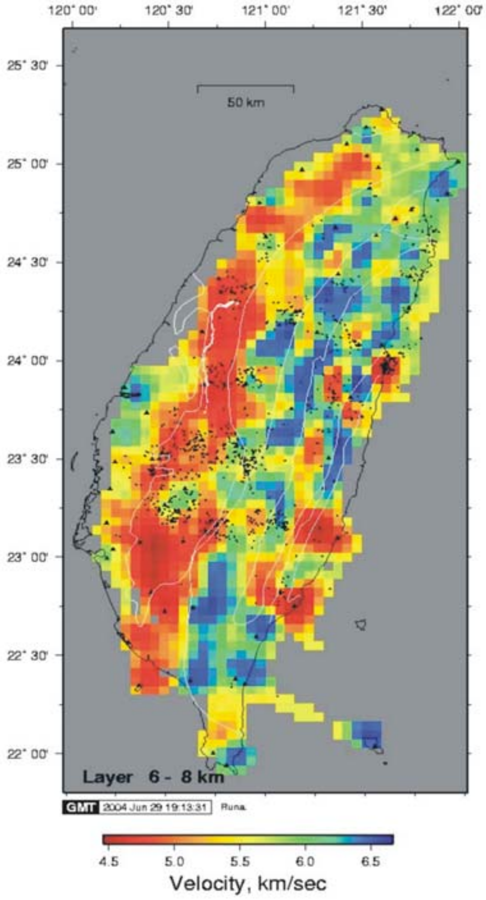
120° 00'
120° 30'
121° 00'
121° 30'
122° 00'
25° 30'
25° 00'
24° 30'
24° 00'
23° 30'
23° 00'
22° 30'
22° 00'
50 km
Layer 6 - 8 km
GMT 2004 Jun 29 19:13:31
Runa.
4.5
5.0
5.5
6.0
6.5
Velocity, km/sec

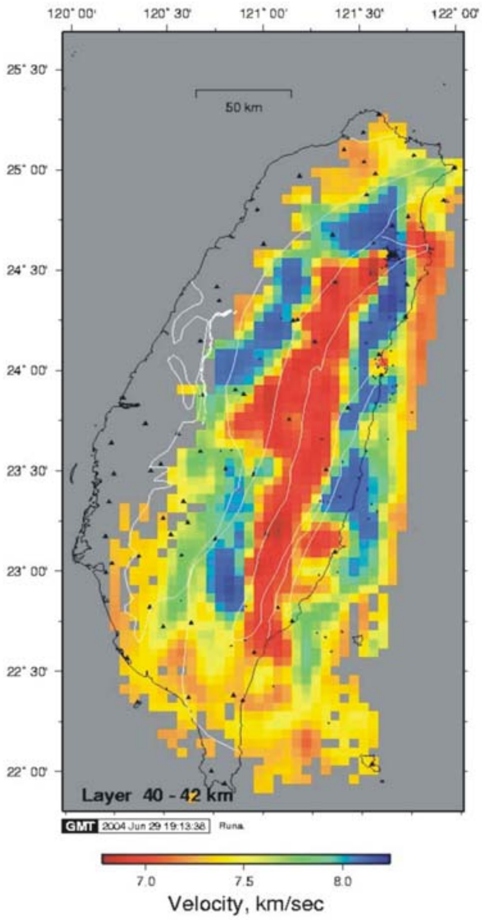
120° 00'
120° 30'
121° 00'
121° 30'
122° 00'
25° 30'
25° 00'
24° 30'
24° 00'
23° 30'
23° 00'
22° 30'
22° 00'
50 km
Layer 40 - 42 km
GMT 2004 Jun 29 19:13:38
Runa.
7.0
7.5
8.0
Velocity, km/sec

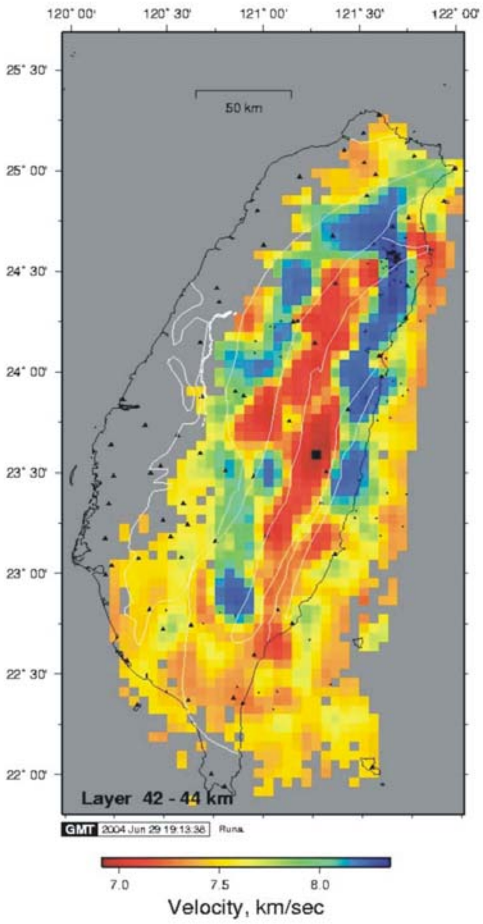
120° 00'
120° 30'
121° 00'
121° 30'
122° 00'
25° 30'
25° 00'
24° 30'
24° 00'
23° 30'
23° 00'
22° 30'
22° 00'
50 km
Layer 42 - 44 km
GMT 2004 Jun 29 19:13:38
Runa.
7.0
7.5
8.0
Velocity, km/sec

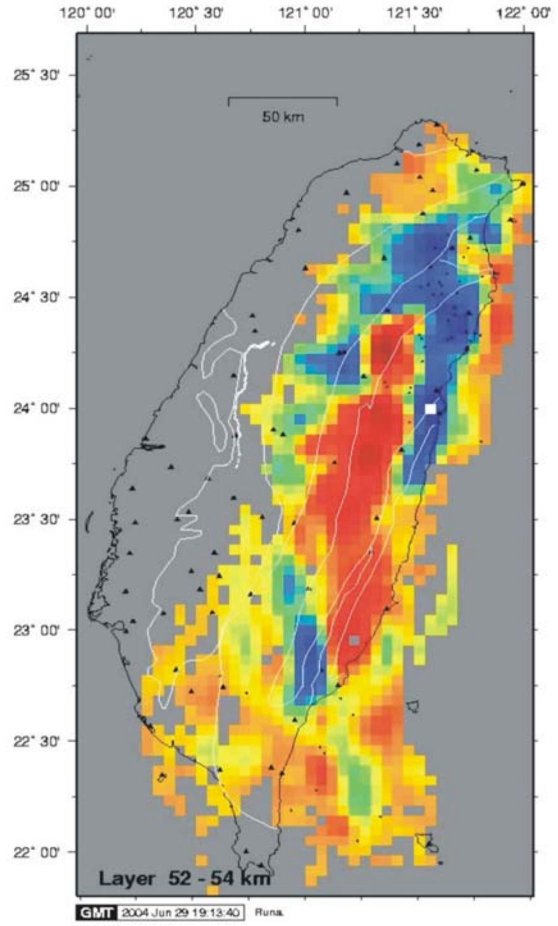
120° 00'
120° 30'
121° 00'
121° 30'
122° 00'
25° 30'
25° 00'
24° 30'
24° 00'
23° 30'
23° 00'
22° 30'
22° 00'
50 km
Layer 52 - 54 km
GMT 2004 Jun 29 19:13:40
Runa.

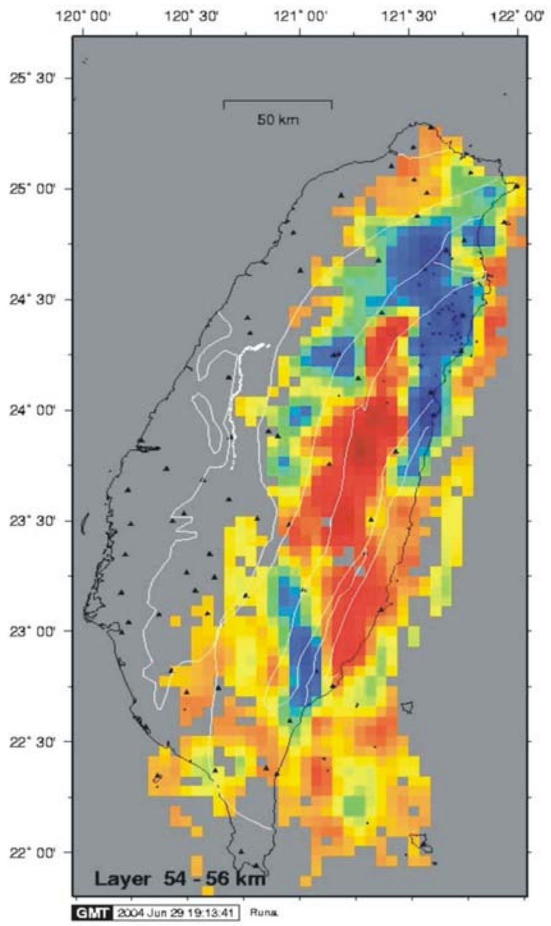
120° 00'
120° 30'
121° 00'
121° 30'
122° 00'
25° 30'
25° 00'
24° 30'
24° 00'
23° 30'
23° 00'
22° 30'
22° 00'
50 km
Layer 54 - 56 km
GMT 2004 Jun 29 19:13:41
Runa.

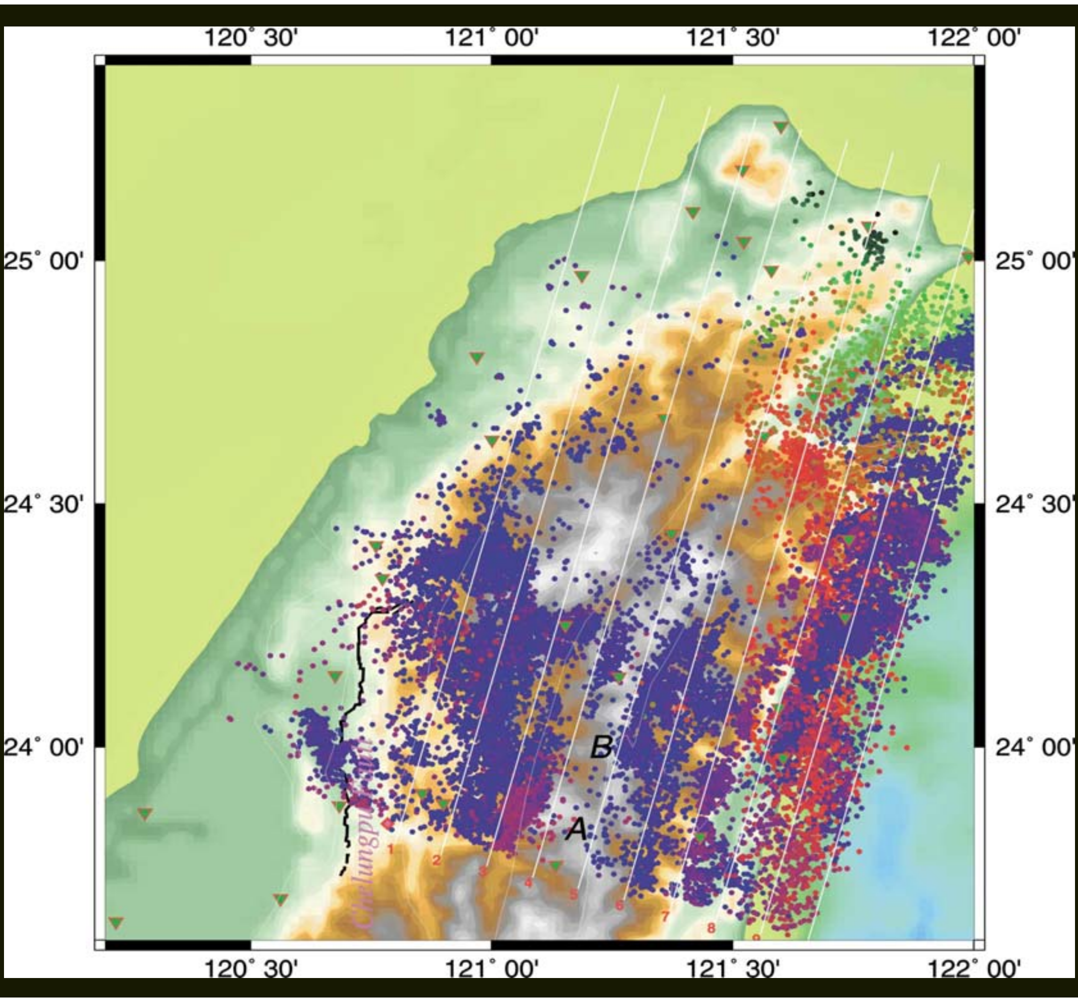
120° 30'
121° 00'
121° 30'
122° 00'
25° 00'
24° 30'
24° 00'
B
A
Chelungpu
1
2
3
4
5
6
7
8
9

N7

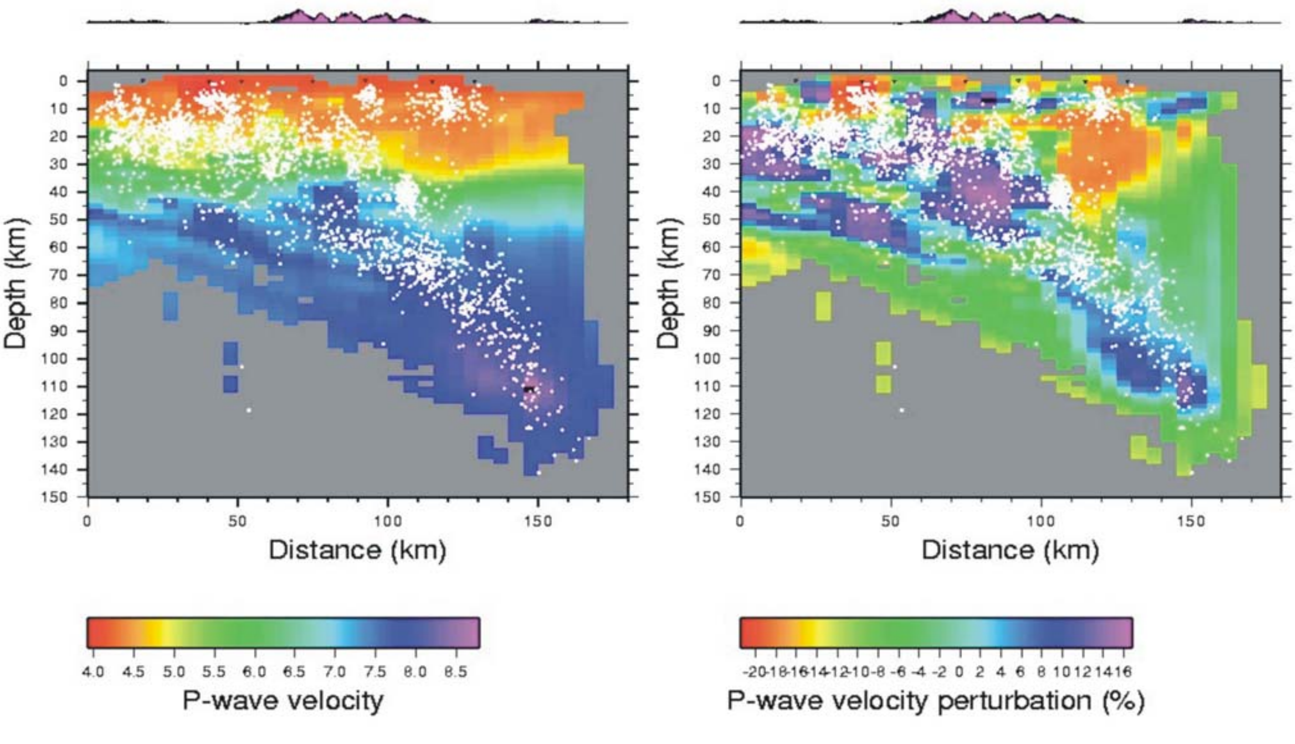
Depth (km)
0
10
20
30
40
50
60
70
80
90
100
110
120
130
140
150
Distance (km)
0
50
100
150
4.0
4.5
5.0
5.5
6.0
6.5
7.0
7.5
8.0
8.5
P-wave velocity
-20
-18
-16
-14
-12
-10
-8
-6
-4
-2
0
2
4
6
8
10
12
14
16
P-wave velocity perturbation (%)

C4

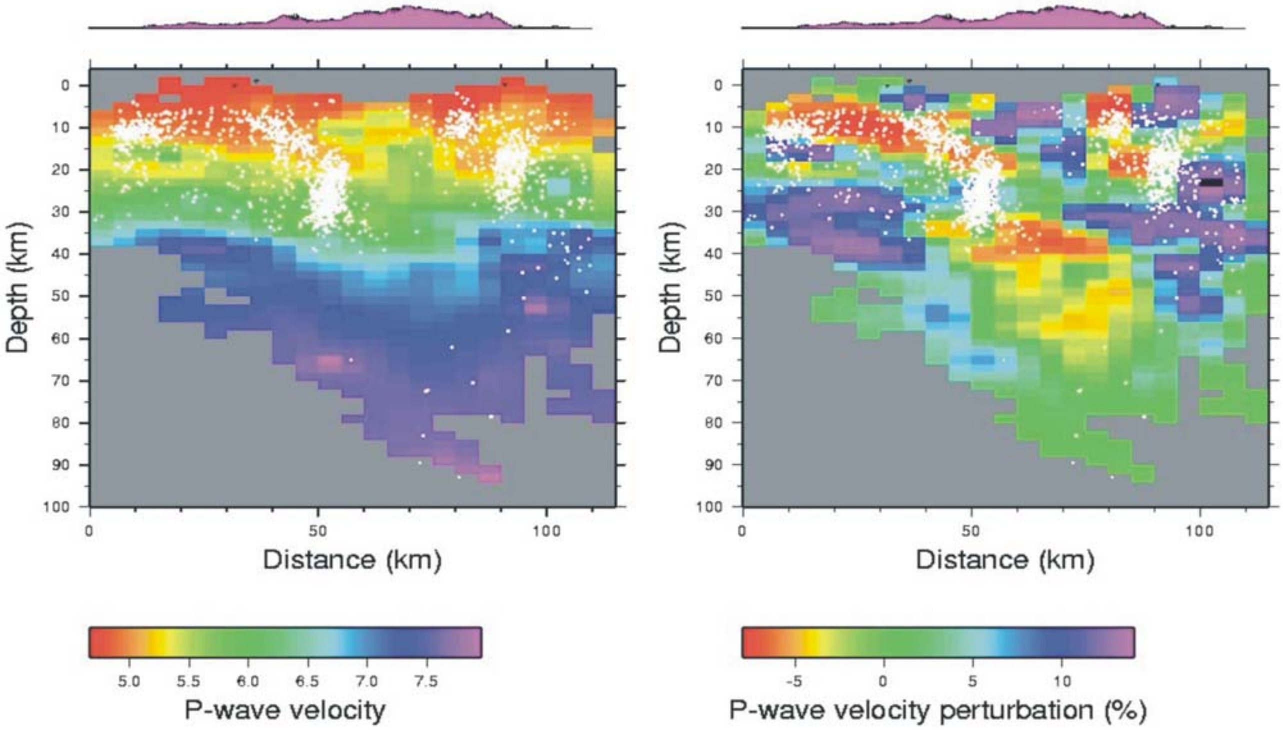
Depth (km)
0
10
20
30
40
50
60
70
80
90
100
Distance (km)
0
50
100
5.0
5.5
6.0
6.5
7.0
7.5
P-wave velocity
Depth (km)
Distance (km)
-5
0
5
10
P-wave velocity perturbation (%)

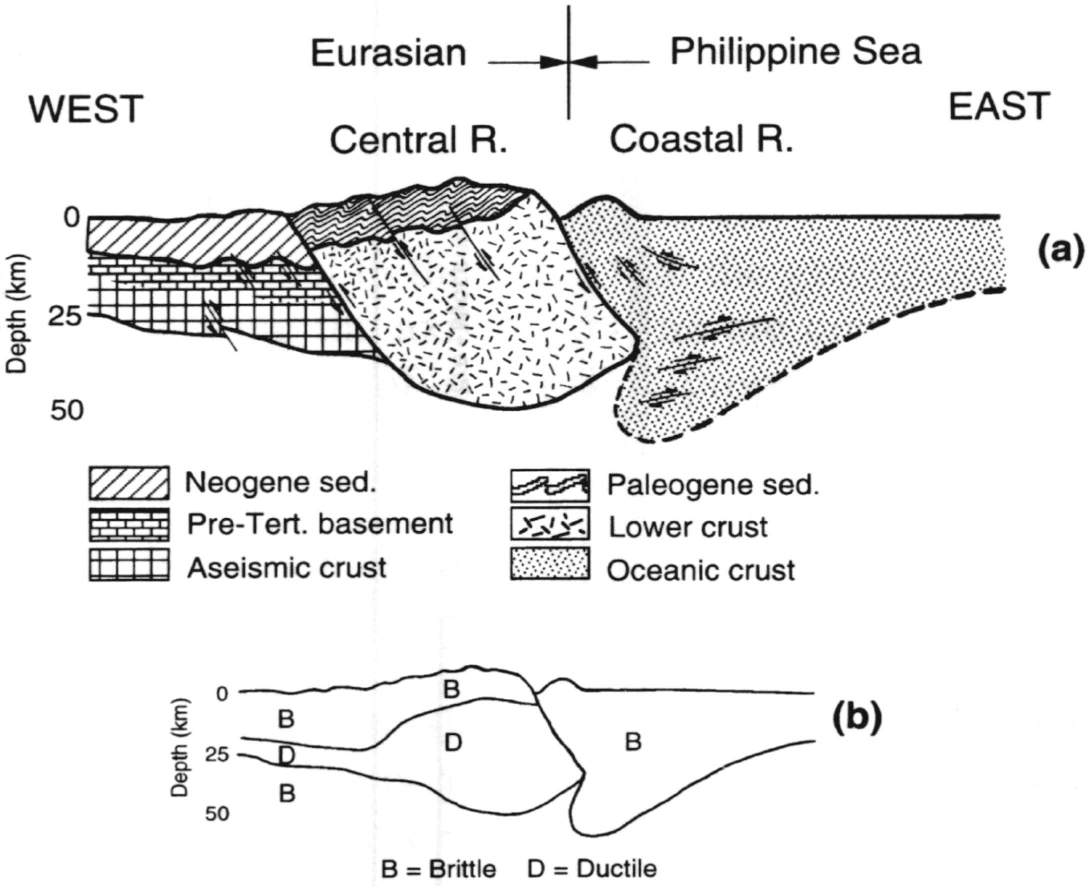
Eurasian
Philippine Sea
WEST
EAST
Central R.
Coastal R.
(a)
0
25
50
Depth (km)
Neogene sed.
Pre-Tert. basement
Aseismic crust
Paleogene sed.
Lower crust
Oceanic crust
(b)
0
25
50
Depth (km)
B
D
B
B
D
B
B = Brittle
D = Ductile

Lithospheric model (just south of 24°N) (Wu et al., 1997)

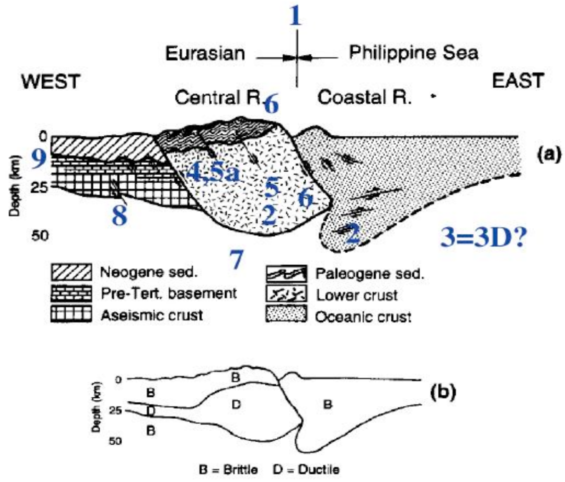

Plate geometries, configurations (what's going where), mass balance:

1. How is the 8 mm/yr convergence being accommodated in the entire system? (upper crust, lower crust, mantle, Phillipine Sea plate, Eurasian plate)
2. If there is no subduction, is shortening balanced by thickening (Moho)?
3. Is there evidence for out-of-plane escape?

Rheology:

4. Is Central Ranges block an indentor to drive western thin skinned deformation (is it rigid)?
5. Is CR block deforming aseismically?

5a. What is the boundary between CR and Foothills? Is it sharp? Indicates uplifted thermal structure in CR (heating -> softening)?

Mountain building / root building:

6. Is the CR block uplift mechanism isostatic or dynamic due to Phillipine Sea plate convergence?
7. What's the role of the mantle - does it provide support? Does it enhance root formation by mantle sinking (like New Zealand)?

Thin-skinned upper crustal deformation:

8. Is the Foothill-Plains block convergence by decollement thin-skinned thrusting or by horizontal thickening of whole lithosphere?
9. Is detachment faulting a necessary mechanism?

PROPOSED TAIGER RESEARCH

Passive Seismology (I)

- 3-D velocity structure of crust, mantle → Boundary geometry, kinematics
- Receiver function profile → variations in crustal/upper mantle discontinuities, 410/660 topography
- Teleseismic P-delays/tomography →Hunt for upper mantle slab
- Short period receiver functions over Chelungpu fault →Hunt for *decollement*.

Passive Seismology (II)

- Across-Central Ranges detailed Vp/Vs tomography → petrology, rheology
- ScS, S, SKS anisotropy → flow/shear in the upper mantle (and their relationship with surface structures)
- Land and ocean-bottom Broadband deployment for critical data

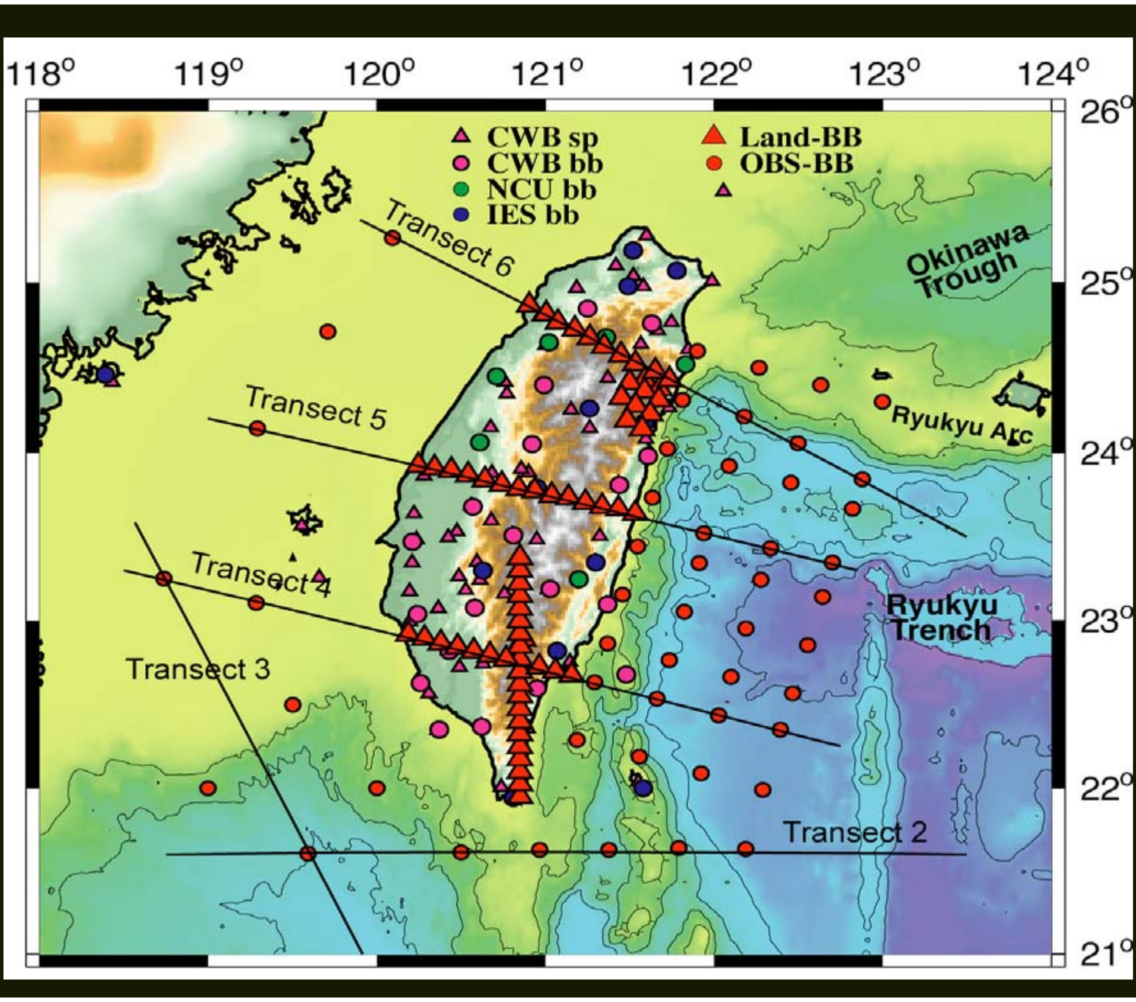

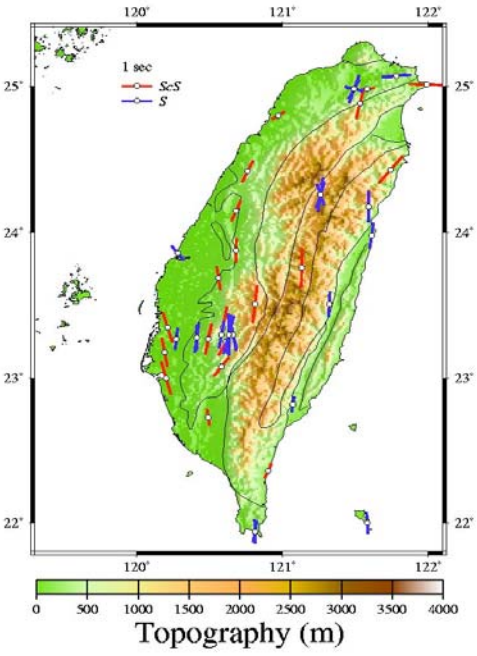

Rau et. al., 2000

South Island Splitting Measurements

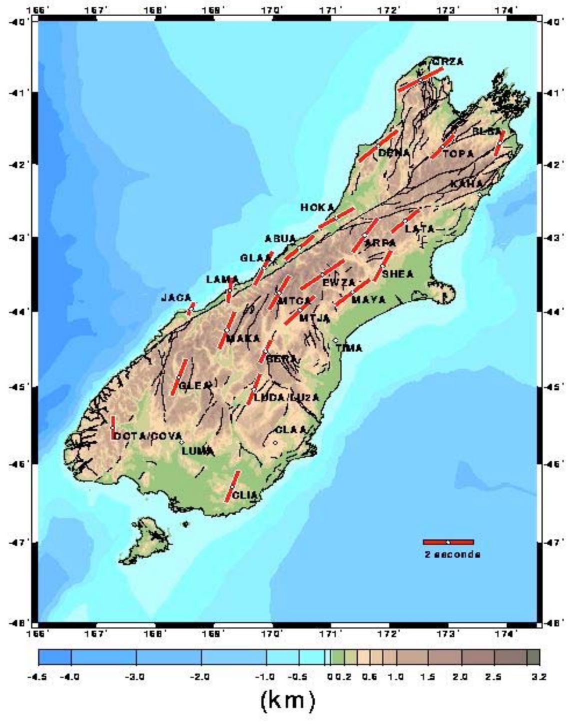

Active Seismology (I)

- **Experiments**
  - **Transects #4, #5 and #6: cross-island transects involving airguns, MCS, OBS, on-off recorders, land refraction. Airguns on both sides of island. No CDP but may be able to create low-fold using dense refraction array plus multiple land sources**

Active Seismology (II)

- Transect #1, 2 & 3: pure MCS/OBS/airgun transects
- N-S line of receivers: wide angle/airgun
- #5 could be a long line extending from Fujian Province to Philippine Sea

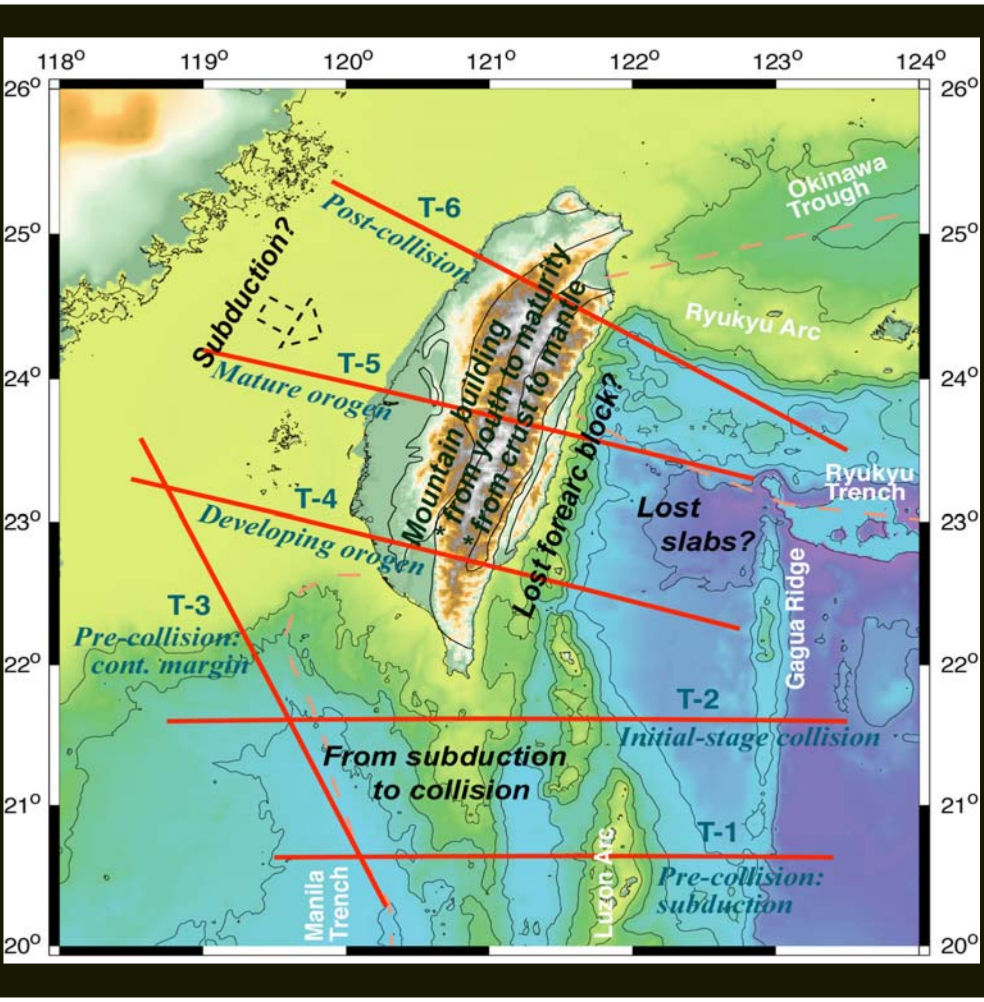
118°
119°
120°
121°
122°
123°
124°
26°
25°
24°
23°
22°
21°
20°
T-6
Post-collision
Okinawa Trough
Ryukyu Arc
Subduction?
T-5
Mature orogen
Mountain building
* from youth to maturity
* from crust to mantle
Lost forearc block?
T-4
Developing orogen
Ryukyu Trench
Lost slabs?
Gagua Ridge
T-3
Pre-collision:
cont. margin
T-2
Initial-stage collision
From subduction
to collision
T-1
Pre-collision:
subduction
Manila Trench
Luzon Arc

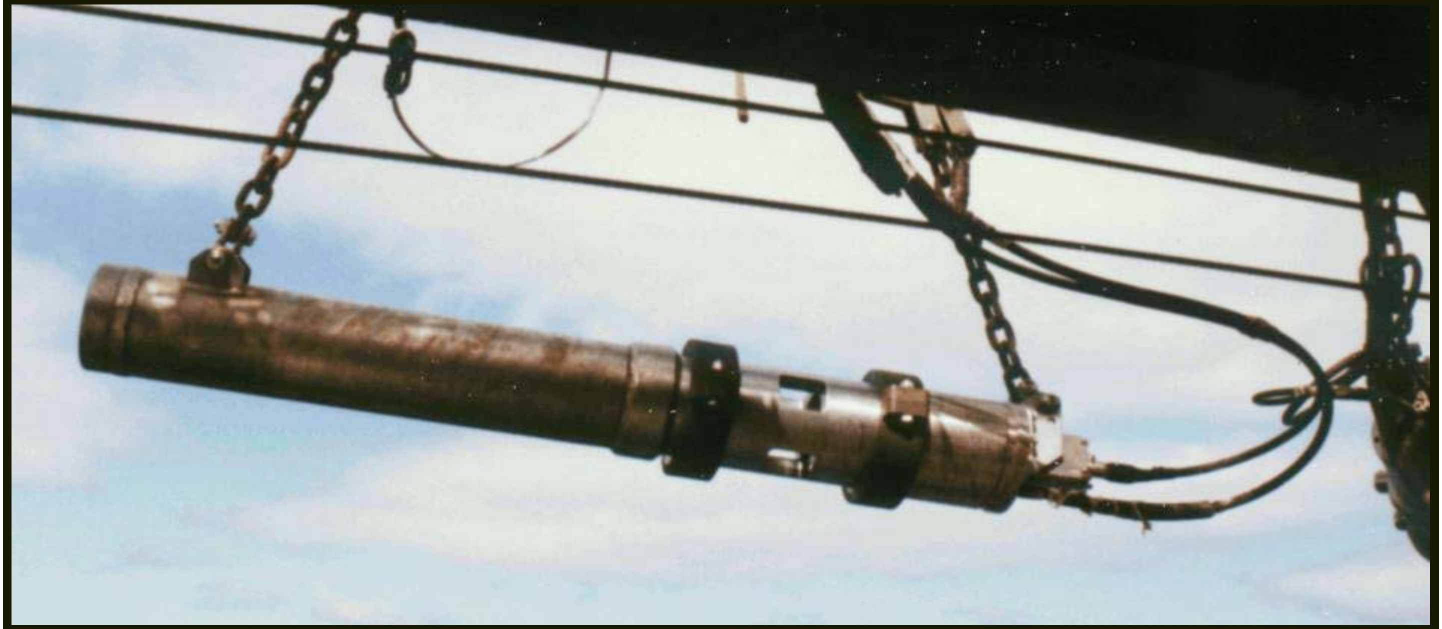

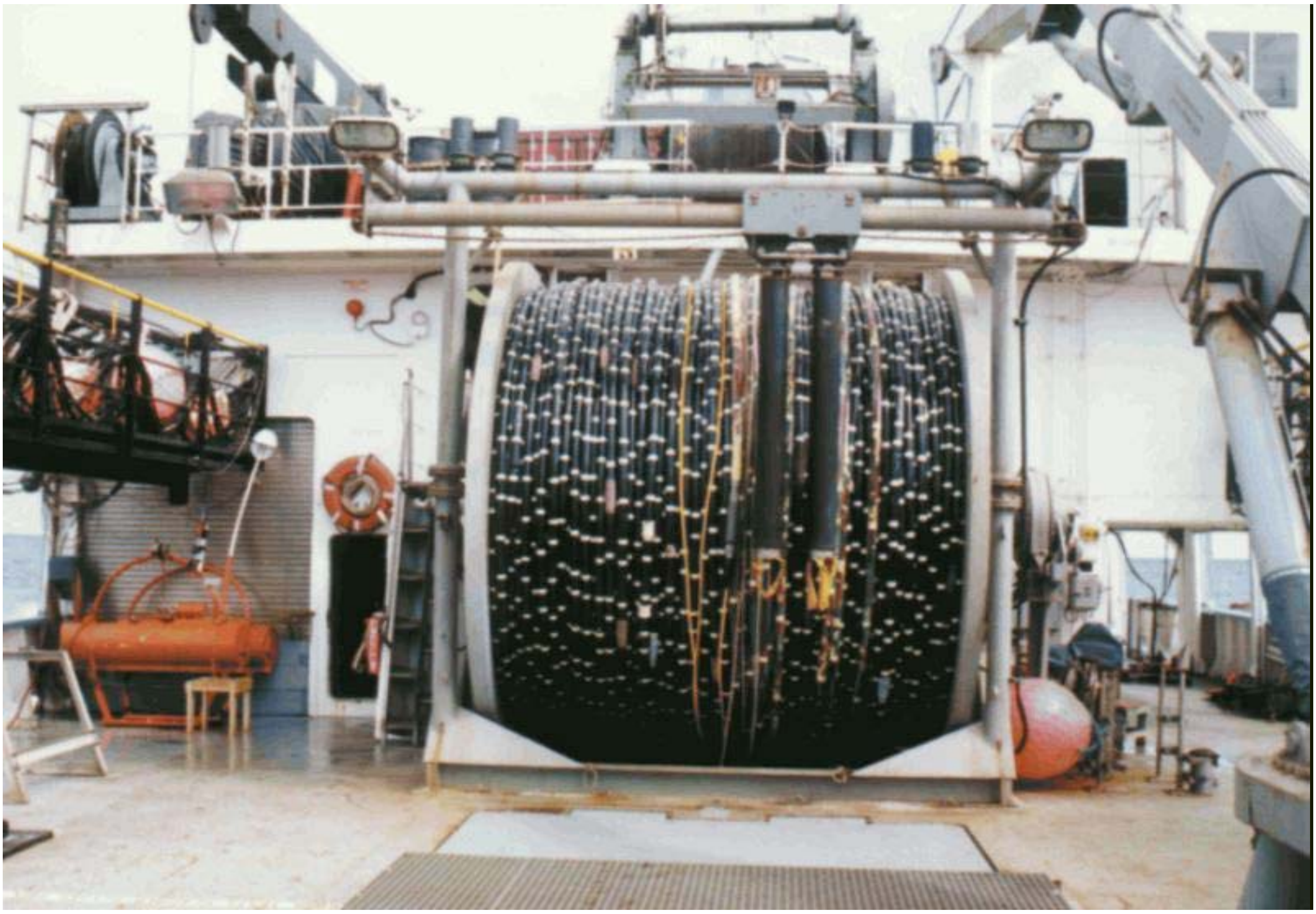

Active Seismology (III)

Studies

- velocity structure of crust and upper mantle (higher spatial resolution than passive source 3-D tomography) – internal structure of orogen
- Direct waveform imaging of Moho and slab
- Seismic reflectivity (proxy strain indicators) of upper and lower crust

---

Geology

- Fission track dating of the whole Central Range
- Dating of river terraces
- Mineral strain measurement
- Interpretation of Metamorphic structures
- Transect-oriented

Other Geophysics

- Joint seismic/gravity modeling – density ⇒ dynamics
- Rock physics measurements ⇒ velocity -> rock identification
- Magnetotellurics ⇒ composition/temp.
- GPS and Leveling; Yu, Liu ⇒ modern deformation
- Integration through geodynamic modeling

TAIWAN STRAIT

- Taiwan Strait is active – 1604 M~8 event, 1994 S. of Penghu M6.5 event (N-S T-axis), etc.
- Data from both sides of Strait needed
- MCS, OBS – difficult but possible
- CSB, IESAS, CAS, CAGS interests
- Unknown factors

Time Lines

- Preproposal submitted to CD and "blessed" April, 2001
- NSF Panel approval: April, 2004
- Beginning date: September 2004
- Pre-TAIGER research
- Magnetotellurics and petrophysics – 2004-2007

Time lines (Cont'd)

- Passive seismology
  - Land: Mar 06-May 07
  - Marine Apr 06-May 07
- Active seismology
  - Land: Jul 06
  - Marine: Apr-June, 07
- Geodynamic modeling and testing – 2004-2009

The US Group

- Larry Brown, Cornell – Imaging of Faults
- David Okaya, USC – Crustal Anisotropy
- Kirk McIntosh, UTIG – Onshore/offshore
- Yosio Nakamura, UTIG-Ocean bottom Seis.
- Steve Roecker, RPI – 3-D mantle anisotropy
- Luc Lavier, UTIG - Geodynamics

US Group (cont’d)

- Martyn Unsworth, U Alberta, MT
- N. Christenson, Wisconsin – Rock Physics
- Francis Wu, SUNY Binghamton – Overall, tomography and coordination

Studies of Active Tectonics with Seismology

Francis T. Wu
State University of New York
Binghamton, New York
USA

Lecture Notes for "7th Workshop on Three-Dimensional Modeling of Seismic Waves Generation, Propagation and Their Inversion", 2004.

Introduction

- Active tectonics involves ongoing physical processes in the Earth related to deformation under stresses.
- Earthquakes are products of the tectonic stresses and as such they can provide us information regarding the state of stresses in the Earth.
- The seismic waves produced by the earthquakes are sources of energy that can illuminate the structures – products of the physical processes - through which they propagate.

Being a comprehensive topic, active tectonic study is not the sole domain of seismology, but seismology produces critical data and can play a role in the interpretation of data. Everything discussed at this workshop can be applied for the study. High resolution works are required and thus global networks are not adequate and special networks in the area are usually needed.

- Plate boundaries in general are certainly areas where active tectonics is taking place. Although the general framework of plate tectonics explains the subduction and rifting of ocean floor quite well, myriad questions regarding the fate of the subducted lithosphere, the entrained flows generated by subduction, the flow regimes in the rift systems etc. remain. These features are mostly under the ocean and deployment of stations on the islands is not always enough. Fortunately more usable ocean bottom seismic instruments begin to accumulate and the potential of future studies is high.
- Active mountain building can be found near the plate boundaries (Himalaya, Andes, New Zealand, New Guinea, Taiwan, Zagros etc.) or away from plate boundaries (Tianshan, Kunlun, Eastern Alps, etc.). They are much easier to study, in some senses, than the last type because they are mainly on land, so that stations can be deployed around them. But the terrain may be prohibiting and logistics can still be a severe problem.

In this note we concentrate on the active mountain building. I will particularly describe my recent works in several areas and a new major study in Taiwan that will be carried out in the next five years.

1. How do we start a research project?

It is often the case there is already some idea of what is going on in a region of interest. Some of ideas may be based purely on geology and others with basis in geophysical data. These ideas are basically hypotheses regarding the physical processes that produce the regional features. It does not matter how the hypotheses (we may call it models or theories sometimes) were formulated we can always say they are not completely correct. In fact some would say that they are never going be correct. What does this mean? Practically it means that the power of the hypothesis can be judged by how good it can predict observations not yet made. For example, in mountain building, there is a widely applied geological theory that mountains are built by the "thin-skinned" tectonics – usually above a depth of 10-15 km at most, and the lower crust is "decoupled" across a decollement. If so, we would expect the processes on the surface to be totally isolated from what is happening below this detachment surface. To see whether the hypothesis is a good one data at depth can be sought; if at depth there is no evidence so far the hypothesis can be to have survived a test, but if there is evidence that the surface structures are consistent with those at depth, implying that the same stress controls structures throughout the crust and mantle, for example, then the hypothesis can be said to have been falsified.

Thus we start a project by sorting out what we can deduce from the current hypothesis and then find out whether the deductions are consistent with data not yet considered in light of the hypothesis. If there are deductions for which we have no relevant data for testing then we need to go acquire more data.

Karl Popper (e.g., www.eeng.dcu.ie/~tkpw/intro_popper) made the point strongly that induction is not a good way to do science. Rather advances are made when find critical ways to falsify existing hypotheses and thus enhance the power of prediction of a hypothesis or invalidate a hypothesis.

If a hypothesis was formulated purely on geological (surface and shallow depth information) then the testing of the hypothesis using seismological data regarding its subsurface revelations is always a good thing to do. It should be mentioned that sometimes the questions we end up asking are not the same as the starting ones, but one would have a relatively hard time convincing some agency to support your research without have asked a series of good questions regarding the current models.

2. Investigation of the orogeny of South Island, New Zealand (see accompanying powerpoint presentation for illustrations)

North Island New Zealand is along a continuation of the Tonga/Kermadec Island chain. A well-defined subduction zone underlies it. The orogenic processes probably started more than 10 million years ago, but the South Island mountains as we know today probably occurred after The west-dipping subduction zone terminates under the northern part of the South Island (the Marlborough area). In the southern part of the South Island, there is a steeply (east-)dipping subduction zone. In the middle part of the South Island, between these subduction zones no deep seismic zone can be found.

Prior to a major project on the South Island, in 1995, the common theory of the orogeny of New Zealand involves the presence of a subducting Pacific plate under the South Island.

The 1995-1997 experiment had the following elements

- A deployment of broadband (STS-2) instruments in two phases for about 15 months for the determination of SKS polarization and crust/mantle structures
- Reversed airgun shooting (R/V Ewing) for sea-land profiling to obtain crustal and upper part of upper mantle structures
- Active source (explosions) profile to tie down the upper crust structures
- An unplanned recording of teleseisms on the cross-island sea-land array to image

upper mantle high velocity zones using travel-time delays
The main conclusions of this experiment are that

1) There is no evidence of a subducting Pacific plate.
2) The crust under South Island New Zealand has thickened beyond what isostasy demands
3) There is a high velocity region in the upper mantle most probably related to the thickening of the crust. This high velocity, high density zone provide overall isostasy.
4) The seismic anisotropy is very strong (with delay time on the order of 2 seconds between the fast and slow SKS waves) and the fast directions are aligned with the general fabric of the island.
5) The thickening of the crust roughly balances the shortening of the crust for the last six million years.

As far as hypothesis regarding the orogeny is concerned, Tim Stern, one of the principal investigators of the project from New Zealand, decided that the old Pacific subduction model is falsified. Instead a new concept (Molnar et al., 1999), based on the coherence of SKS with the surface structures and the presence of the high velocity zone under the thickened crust, that the oblique convergence of the Pacific against the Australian plate created a vertically coherent tectonic zone. The transpression created the mountain, its root and the upper mantle high velocity zone from the surface to depth of 200-300 km depth.

Reference

Molnar, P. et al., *Science*, v. 286, 516-519.

3. Investigation of Himalayan tectonics

Himalaya and the Tibetan plateau are of course the most impressive structures on the Earth. It has been active since early Tertiary, perhaps some 50 millions years ago. The exact history of uplift in the Himalaya is still being debated. The prevailing model of Himalayan orogeny is summarized in the following figure:

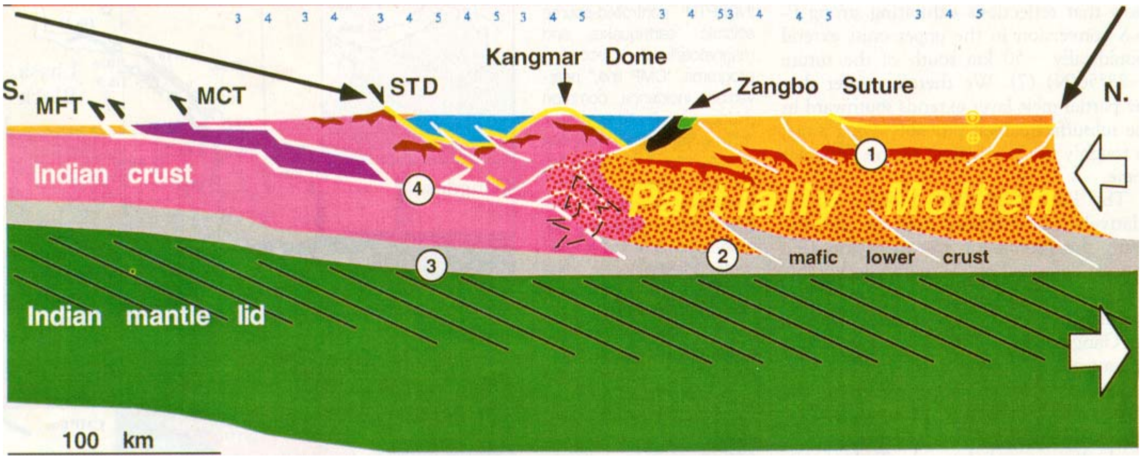

This model was derived from structural geology of the Himalaya front and an active source INDEPTH profile by Nelson et al. (1996). It describes the underthrust of the Indian lithosphere below the Asian crust. Some of the chief features are the lack of root under the high Himalaya and the raising of high Himalaya along a fault ramp. Data in the high Himalaya appropriate for testing the hypothesis is still rare. Sheehan (U. of Colorado) and I deployed a broadband network in southern Tibet and eastern Nepal in 2001-2002. The network is shown below:

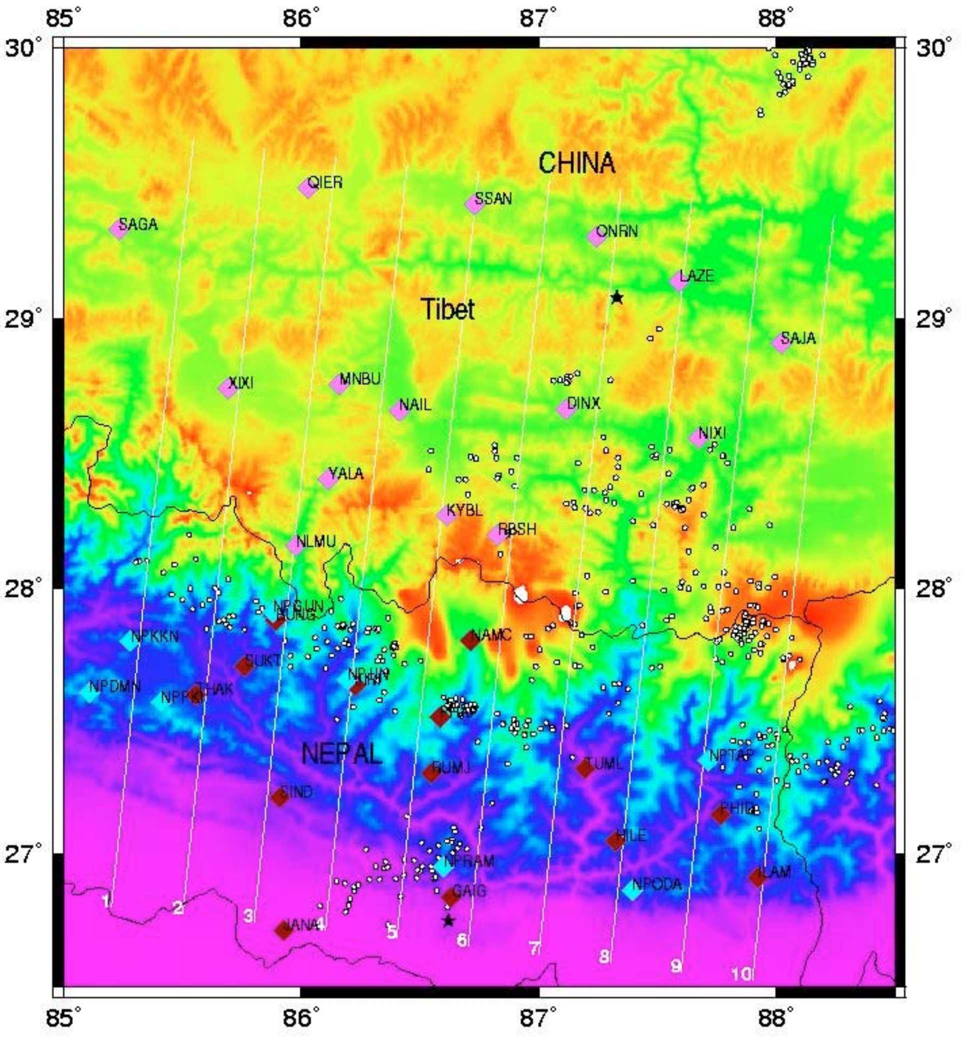

Before the deployment of the network we ask the following critical questions regarding the model below:

1. Is there a root under the high Himalaya?
2. Is the detachment (number 4 in the figure above) seismically active?
3. Does the orogeny have corresponding large trend-parallel fast direction for seismic anisotropy?

Results up to date indicates the following:

1. The stacked receiver functions across the high Himalaya appear to show Moho configuration similar to that in the figure above.
2. Earthquakes are relocated to lie under the high Himalaya at depth below Moho, down to depths of more than 100 km.
3. SKS-splitting is relatively small when compared to that in northern Tibet and to other mountain ranges (New Zealand, Tianshan, Taiwan….)
4. Earthquake in the shallower part of the crust do not seem to have any relation to the presumed detachment fault.

The results are so new and we don't yet have thought through all the implications as yet. At first glance the receiver function results seem to indicate that the Moho configuration shown in the INDEPTH model is correct.

Reference

Nelson, K.D., et al., *Science,* 274, 1684-1687.

4. **Orogeny in Taiwan; past and future research**

The orogeny in Taiwan is even younger than that of New Zealand. Similar to New Zealand in that it is bracketed by two subduction zones of "opposite polarities". In the paper by Wu, Rau and Salzberg (1997) included the basic problem of Taiwan orogeny is stated and references given. More recent works on the precise relocation of seismicity after the 1999 Chi-Chi earthquake (Mw=7.6) and high resolution tomography are shown in the powerpoint prints included here. Also included is a presentation of the planned TAIGER project (TA[iwan] I[ntegrated] GE[odynamics] R[esearch]). It is a funded project starting this September for 5 years. 3-D imaging is the main topic of this proposal.

ELSEVIER

Tectonophysics 274 (1997) 191–220

TECTONOPHYSICS

Taiwan orogeny: thin-skinned or lithospheric collision?

Francis T. Wu *, Ruey-Juin Rau, David Salzberg

Department of Geological Sciences, State University of New York, Binghamton, NY 13902, USA

Accepted 16 December 1996

Abstract

The Taiwan orogeny is young and presently very active. It provides an excellent environment for studying ongoing orogenic processes, especially since the region is monitored intensively with dense seismological and geodetic networks, and new studies aiming at deciphering shallow and deep structures in and around Taiwan have been recently conducted or are being planned. The available data can be used continually to test critically hypotheses of the Taiwan orogeny. Hypotheses dealing with the mechanics of mountain building are basic to the understanding of Taiwan orogeny and are particularly amenable to testing. The widely cited 'thin-skinned tectonics' hypothesis was formulated to explain mainly the geologic and relatively shallow (<10 km) seismic data. In various forms of this hypothesis, the mountain building involves the deformation of ready-to-fail (Tertiary) sediments in a thin (<20 km at the deepest point) wedge deformed by the advancing Philippine Sea plate; the Eurasian plate is assumed to subduct the Philippine Sea plate with the Taiwan orogenic belt on top as an accretionary wedge. We tested this hypothesis against newly acquired seismological and geophysical data and found it to be largely inadequate as a model for Taiwan orogeny, because the evidence for the participation of the lower crust and even the upper mantle in the orogeny is very strong. Rather than the result of deforming a thin wedge, the formation of the Central Range is shown to include the thickening of crust as well as the extrusion of mid- to lower crustal high-velocity materials to shallow depth. Seismicity and focal mechanisms demonstrate that significant deformation is taking place at depths far below what the thin-skinned tectonics hypothesis predicts. As an alternative, the lithospheric collision hypothesis is proposed. In this model the Eurasian and the Philippine Sea plates are colliding at least down to a depth of 60 km. This hypothesis involves not only greater depth but also greater lateral extent. It accounts for the formation of the deep-rooted Central Range on the Eurasian side, as well as the shortening and thickening of the margin of the Philippine Sea plate near Taiwan. It also asserts that the Central Range was built mainly under ductile conditions, while in the Western Foothills area, the deformation involves the whole brittle–ductile–brittle–ductile sandwiched crust and upper mantle. Furthermore, it is asserted that the collision effect is transmitted to the Taiwan Strait resulting in normal faulting striking perpendicular to the trend of Taiwan. Among the implications of this hypothesis some can be readily subjected to falsification. By critically evaluating the components and accepting or rejecting them, our understanding of the Taiwan orogeny in particular and mountain building in general can be improved.

Keywords: orogeny; Taiwan; collision; lithospheric structures; crustal rheology; tectonic model

---

* Corresponding author. E-mail: wu@sunquakes.geol.binghamton.edu.

PII S0040-1951(96)00304-6

1. Introduction

The Taiwan orogeny is geologically young; while estimates from changes in the rate of sedimentation and paleomagnetic evidence all point to a starting time of about 4 million years ago (Suppe, 1984; Lee et al., 1991), the fission-track dating puts the most rapid uplifting within the last 1 million years (Tsao et al., 1992). The rapid rate of deformation detected geodetically on the island and the high level of seismicity in and around Taiwan demonstrate its present day activity (Wu et al., 1989; Yu and Chen, 1994). It is clear that the continuous convergence of the northern part of the Luzon Arc, on the Philippine Sea plate and the Asian continental shelf was responsible for the creation of the island and the mountain ranges (Fig. 1). Because the Luzon Arc and the shelf are not parallel, the collision started near Hualien, about 4 million years ago, and moved progressively southward to reach Taitung about 1 million years ago (Lee et al., 1991); therefore a time-slice of the orogeny can be obtained by following a longitudinal profile from Hualien to Taitung, a result of diachronous collision (Suppe, 1987). That Taiwan is a product of an arc–continent collision was first recognized by Chai (1972), and since then the orogenic evolution and the plate tectonic settings have been explored by many investigators (see, for example, Wu, 1978; Biq, 1981; Suppe, 1981, 1984, 1987; Davis et al., 1983; Tsai, 1986). The ultimate aim in the study of Taiwan orogeny must be the modeling of the evolution of the geological processes underlying the orogeny. Such tasks in geosciences are inherently difficult, due to the lack of continuous geologic records and direct knowledge of the geologic processes at depth. But being one of the youngest mountain ranges on earth, the Taiwan orogeny is more amenable to detailed modeling than ones that have long ceased to be active. Here the gaps in geological records are not as long, and we are able to probe the ongoing orogenic processes.

In the studies of the Taiwan orogen, the thin-skinned tectonics hypothesis (or model) had played an integrative role. Originating as a model for Appalachian tectonics (Rich, 1934), its application to Taiwan was developed in a series of papers. The development of the basic model commenced with studies of the fold-and-thrust belt of western Taiwan (Suppe, 1976), and was completed through the incorporation of shallow (<10 km) borehole and exploration seismic data (Suppe, 1980, 1981) and the linkage between fold-and-thrust and accretionary wedge (Davis et al., 1983). It has been used frequently, either explicitly or implicitly, as a basis for interpreting the geology of Taiwan and its relation to plate motions near Taiwan (e.g., Teng, 1990; Tsao et al., 1992; Reed et al., 1992). Using the basic model, Dahlen and Barr (1989) and Barr and Dahlen (1989) solved the mechanical and thermal problem of 'critical wedge', a thinly tapered wedge with materials at failure condition. This model gives an essentially two-dimensional view of the island, although the variations in tectonic characteristics along the axis of the island have been largely taken into account by assuming a progressive younging of the collision along the whole length of Taiwan. In such a model a decollement at the base of the thin wedge is an integral part, and in Taiwan it is assumed to coincide with the top of an eastward-subducting Eurasian plate.

The thin-skinned model for Taiwan orogeny was developed when little or no deep crustal information was available. Deep seismic sounding using artificial sources had never been carried out in Taiwan. Until 1991, the quality and quantity of seismological data from natural earthquakes were insufficient for imaging the details of mid- and lower crust. Ideally, the high level of seismicity in the vicinity of Taiwan, occurring in response to the collision-induced stresses, can be utilized as an effective means for studying the orogeny. While the earthquakes, their locations and focal mechanisms, enable us to assess the state of strain, the direction of tectonic stress, the rheological properties of the crustal and upper mantle rocks as well as the plate interactions, the seismic waves generated by these earthquakes can be used to map the seismic velocity structures under the island. With an improved seismic network in place since 1991 (Rau et al., 1996), analyses of high-quality, digital data began to yield detailed 3-D velocity structures and well-constrained focal mechanisms in different parts of the orogen, such that the mechanical response of the crust and upper mantle to the collision stresses can be studied. In addition, our understanding of the orogeny is also aided significantly by the fortuitous occurrence of key earthquakes in the last few years.

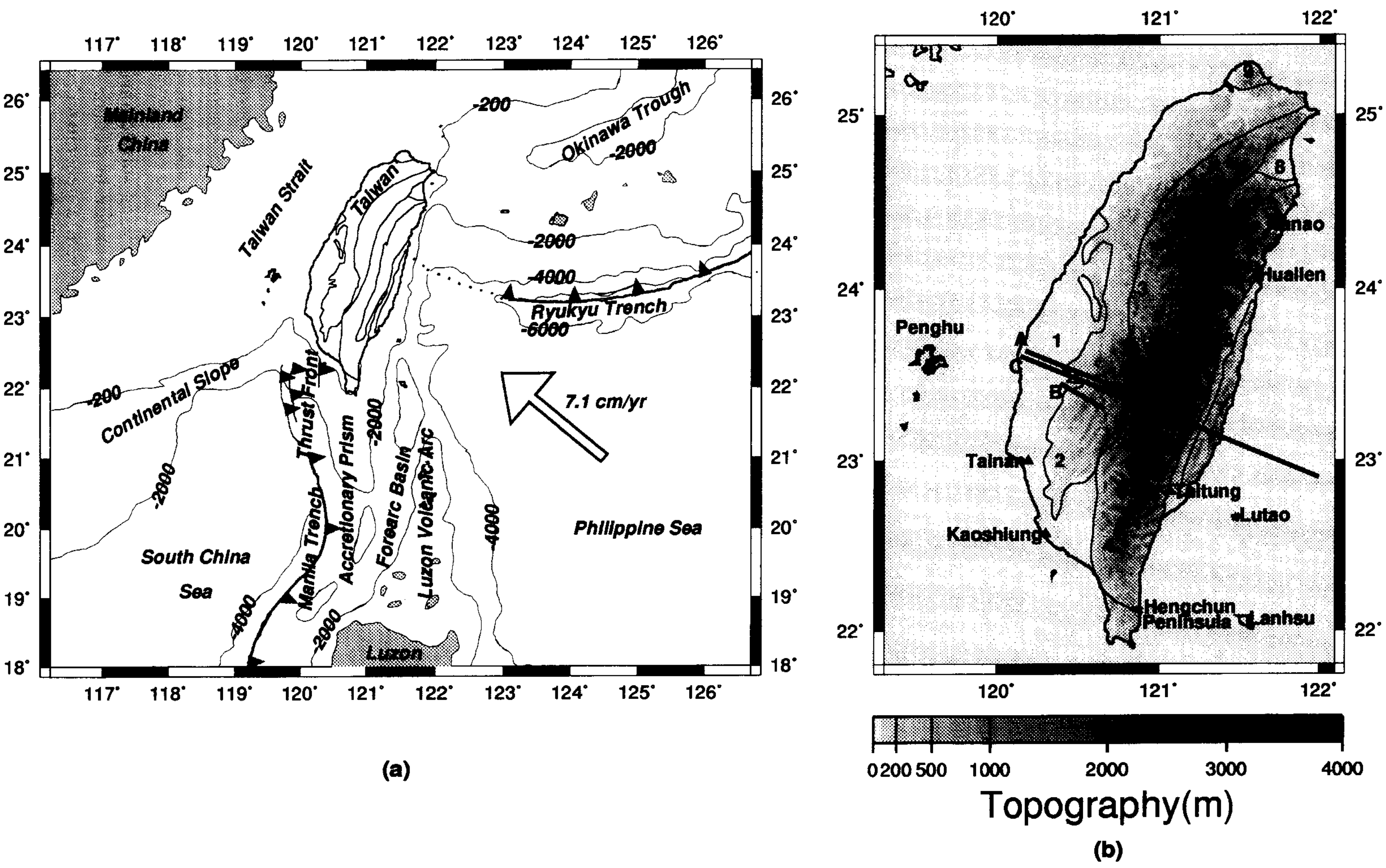

Fig. 1. (a) The overall plate tectonic environment of Taiwan (Rau and Wu, 1995). (b) Main geologic boundaries and physiographic units (Ho, 1988): *1* = western Coastal Plain (Quaternary), *2* = Western Foothills (Plio–Pleistocene), *3* = Hsueshan Range (Eocene–Miocene), *4* = Backbone Range (Eocene–Miocene), *5* = eastern Central Range (Pre-Tertiary), *6* = Longitudinal Valley (Holocene), *7* = Coastal Range (Miocene–Pleistocene), *8* = Ilan Plain (Quaternary), *9* = Tatun volcanic group (Pleistocene). Lines *A*, *B* and *C* are the locations of three schematic cross-sections of Suppe (1987) shown in Fig. 14. The place names mentioned in the main body of the paper are shown in (b).

Furthermore, in addition to the seismic data, the accumulation of other relevant data has accelerated.

With new data available, it may be useful to view the existing hypothesis in the Popperian light (Popper, 1968), i.e., attempts should be made to falsify it. Since the thin-skinned hypothesis was formulated independent of the new data, testing it using such data is suitable. In this paper we shall show that gauged against such data the thin-skinned model of Taiwan orogeny is found to be largely inadequate, mainly because the new data indicate that the orogeny is not limited to the top part of the crust. Instead, the orogeny seems to involve the participation of not only the upper crust, but also the lower crust and uppermost mantle. Also, although the shortening on the Eurasian side of the collision is well-known, the Philippine Sea plate has been considered to be the rigid indentor in the thin-skinned model; but the superposition of the Luzon volcanic arc and the accretionary wedge sediments in the Coastal Range, the high seismicity under the Coastal Range, and the presence of large earthquakes offshore of east Taiwan indicate that significant deformation has occurred on the Philippine Sea side. A recent (September 14, 1994) $M_S = 6.5$ earthquake in the Taiwan Strait even demonstrated that the orogenic effect has propagated to the area west of Taiwan. Thus, based mainly on the new seismic imaging and the distribution of earthquakes in the crust and upper mantle, and incorporating geologic and other geophysical data, we propose an alternative hypothesis that we shall call the 'lithospheric collision hypothesis'. In this hypothesis deformation of lithosphere on both sides of the plate boundary takes place to create the mountains. We purposefully avoid the term 'thick-skinned' (see for example, Hatcher and Hooper, 1992), because of its past usage, which includes the concept of a decollement at depth near the bottom of the crust.

Like other hypotheses, the lithospheric collision hypothesis is formulated with the observations with which the authors are familiar. Since a tectonic hypothesis is necessarily multifaceted, it must be tested by others with existing and new data from as many different subdisciplines as possible. Aspects of the hypothesis or the whole hypothesis can be falsified. A number of specific topics are suggested by these authors for further testing. Through testing, we hope to focus attention on specific problems of the Taiwan orogeny. It is with the same Popperian spirit that we tested the 'thin-skinned tectonics' hypothesis. This is especially useful in view of the multitude of relevant research being carried out or planned in and around Taiwan. By posing specific questions, we hope to make more systematic advances in our understanding of orogeny.

We shall begin by reviewing the available evidence, first geophysical and then geological, on which we base our testing and formulation of hypotheses. Then the thin-skinned tectonic hypothesis will be evaluated and lithospheric collision hypothesis proposed and discussed.

2. Key seismological and geophysical observations

It is probably safe to assume that before the collision began the crust under the Asian continental shelf was thinning toward the edge similar to the crust under the shelf northwest of the Okinawa Trough (Iwasaki et al., 1990) or the eastern passive margin of North America (Grow et al., 1979). Then the seismic velocity structures under Taiwan, especially any significant departures in geometry from that of a typical passive margin, can be interpreted as the results of collision-induced deformation. With the expansion and upgrading of the Taiwan seismic network in 1991 (Rau et al., 1996) the concomitant improvement in quality and increase of quantity of seismic data were significant. While more precise hypocentral locations resulted from increased station density, enhanced dynamic range of the digital recording systems broadened the magnitude range of events for which usable seismograms are recorded, and allowed the identification of more subtle first arriving phases. In addition to more detailed seismicity, tomographic imaging (Rau and Wu, 1995) using the new data now provides sufficient resolution for tectonic interpretation. With seismic velocity structures as constraints, the modeling of Bouguer anomalies of Taiwan (Yeh and Yen, 1992) is less ambiguous.

In each of the following subsections we describe the main results from relevant studies. At the end of this section we present a generalized model of the crustal and upper mantle structures under Taiwan on the basis of these results.

2.1. Crustal and upper mantle structures (tomography and refraction)

Based on refraction studies using earlier local earthquake data, Rau (1992) found the crustal velocities under the Coastal Range to be similar to those of a typical oceanic crust; however, the Moho is at about 20 km below the surface. Under the Central Range, the estimate of the average Moho depth is about 38 km, and under the Western Foothills, the Moho depth is about 28 km; typical continental velocities are obtained, and the P_n velocity is about 7.6 km/s.

Tomographic imaging using new data provides more details. In Fig. 2, C–C′ and D–D′ are two P wave velocity sections across the island near Hualien (see the index map in Fig. 2 for exact locations). First, a root appears to have already formed under the mountain. This root becomes noticeably shallower toward the south (Fig. 2, section B–B′ along the spine of the island). The reduction of the root (as marked by the 7.5 km/s contour) has been interpreted by Rau and Wu (1995) as a consequence of the mountain range being younger toward the south (Lee et al., 1991). Fig. 3 shows a juxtaposition of the northward-dipping Ryukyu subduction zone (from Fig. 2 section A–A′) with the velocity profile from section B–B′ in Fig. 2. This schematically shows the contact (cross-hatched area) between the Philippine Sea and Eurasian lithospheric plates. Note in section B–B′ (Fig. 2) that where the root deepens quickly the topography also rises sharply. Under the eastern flank of the Central Range, materials with velocities as high as 8.5 km/s are present at depths from 25 to 50 km (Fig. 2, sections C–C′ and D–D′); they probably represent a part of the oceanic lithosphere, and are in direct contact with the low-velocity materials on the continent side. Also seen in Fig. 2 (C–C′ and D–D′) are the relatively high velocities in the top 15 km under the Central Range, relative to velocities under the Foothills and the Coastal Plain; Rau and Wu (1995) has shown that the 5.5 km/s contours generally rise under the central Taiwan profiles to within a few kilometers under some part of the Range, although not always the highest part. Under the western Coastal Plain an extensive lower velocity (<5 km/s) surface layer is found to extend down to between 5 and 8 km. Unfortunately the resolution of tomographic inversion for southern Taiwan is very poor because of the narrowing of the Hengchun Peninsula and hence the paucity of stations in that area.

2.2. Seismicity, crustal rheology and focal mechanisms

Although seismicity is an indicator of ongoing deformation, the absence of earthquakes in an area within an orogenic zone does not imply a lack of deformation, because of the dependence of rheological properties of rocks under different ambient conditions. The focal mechanisms of earthquakes allow us to map the nature of faulting, and an aggregate of them the orientation of the stresses.

2.2.1. Seismicity

The pattern of seismicity and plate configuration under and around Taiwan have been studied by Wu (1970, 1978), Cardwell et al. (1980), Tsai (1986), and Wu et al. (1989). The upgraded network has yielded much improved images of seismicity. In this paper we consider mainly the seismicity within the network, using data from 1-1991 to 5-1996; seismicity in neighboring areas can be found in earlier papers. We divide the area into three subregions: in the northern region seismicity associated with the northward-subducting Philippine Sea plate dominates; in southern Taiwan the eastward-subducting Eurasian plate is quite clear; and in central Taiwan, between these two subducting regimes, seismicity is limited mostly to the top 60 km of the lithosphere.

In Figs. 4–6 sections A–A′ through G–G′ show seismicity cross-sections in the three subregions as indicated in the index map. Although the new seismicity data do not change the basic conclusions regarding the general plate configurations around Taiwan based on earlier data, the more precise hypocentral locations define the Wadati–Benioff zones under northern Taiwan (F–F′ and G–G′ in Fig. 4) and southern Taiwan (C–C′ through G–G′ in Fig. 6) much more clearly. In contrast, the section of Taiwan between Hualien and Taitung does not have significant deep seismicity either under the island (A–A′ through G–G′ in Fig. 5) or offshore (Wu et al., 1989). In Fig. 5, seismicity permeates the upper 30–40 km in western Taiwan, with some sections (e.g., A–A′

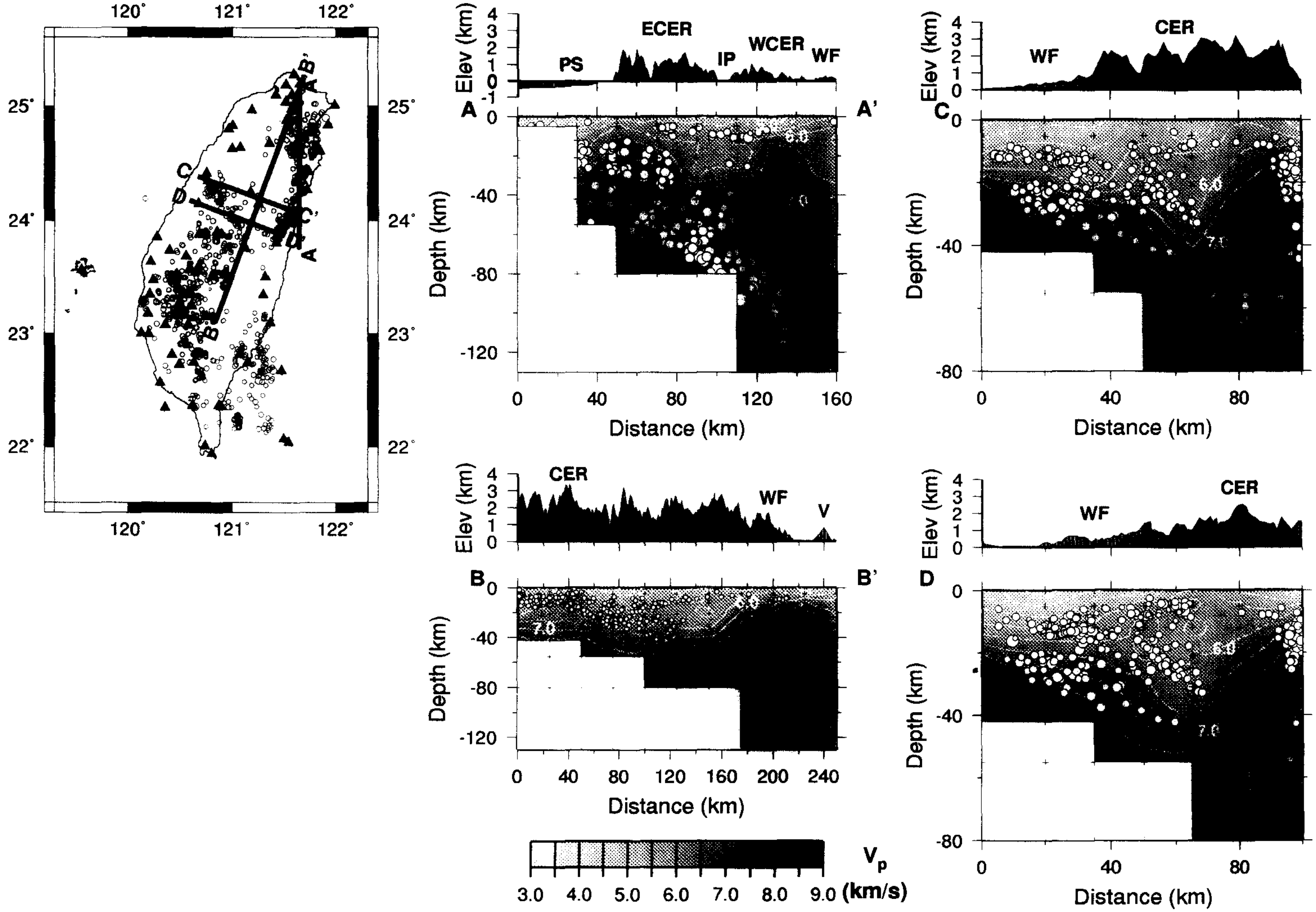

Fig. 2. Seismic P wave tomography of Rau and Wu (1995). Map shows the locations of the tomographic sections. Above each tomographic section, the topography is shown. The velocity contour interval is 0.5 km/s. The white circles are relocated hypocenters including events within ±1 grid space of the profile. The white areas mark the unsampled regions. In section *A–A′* the north-dipping subduction zone is seen clearly. It is a relatively high-velocity zone (>8 km/s) and coincides with the Benioff zone. Sections *C–C′* and *D–D′* are sections across northern-central Taiwan. Notice the presence of a root under the Central Range. Also, the seismic P velocities under the Central Range reaches 5–5.5 km/s, a velocity corresponding to relatively high-grade rocks. Section *B–B′* is along the axis of Taiwan, showing the rapid increase of the thickness of relatively low-velocity rocks (<7.5 km/s) under the northern part of the island (around the latitude of 24.5°N) and the gradual thinning from the north toward the south. *PS* = Philippine Sea; *ECER* = eastern Central Range; *IP* = Ilan Plain; *WCER* = western Central Range; *WF* = Western Foothills; *V* = Tatun volcano group; *CER* = Central Range. Note that profiles are not plotted on the same scale; in particular, B–B′ is plotted at about 50% of the other profiles — the hypocenters shown in B–B′ appear to be smaller in comparison with those shown in other profiles.

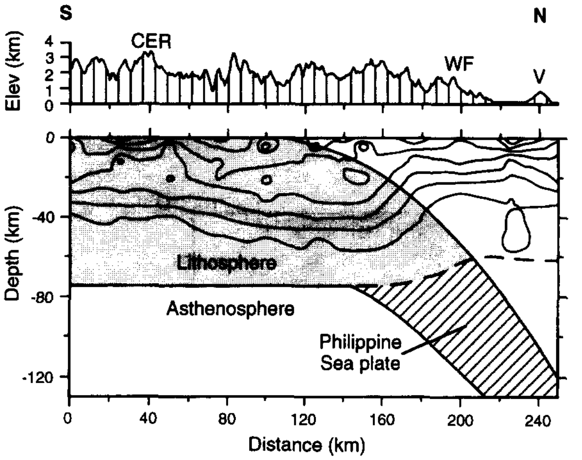

Fig. 3. Interpretation of section B–B′ in Fig. 2: the thinning of the lower velocity crust can be explained as a result of younging of the collision toward the south (Rau and Wu, 1995). The collisional contact of the Philippine Sea plate with the Eurasian plate (stippled area) decreases gradually toward the north owing to the finite thickness of the lithosphere, but the two plates are in full contact south of the contact of the Ryukyu 'Trench' with the continental shelf. Note that in the B–B′ section the Ryukyu subduction zone is not well developed (refer to seismicity sections B–B′ in Fig. 4). The dashed line in the figure is the approximate position of the bottom of the lithosphere. Symbols are the same as those in Fig. 2.

and B–B′) showing clear double seismic layers, with a zone of lower seismicity at a depth range of 15–23 km, typical of continental seismicity (Kohlstedt et al., 1995). Although double layering is not always as clearly seen in Fig. 5, curves of strain release (Benioff, 1955) as a function of depth (Fig. 7) for other cross-sections reveal such structures. Also the Central Range is generally a region of low seismicity (Wu et al., 1989), except at depth between 60 and 80 km around the 24°N latitude (Lin and Roecker, 1993; A–A′ and B–B′ in Fig. 5). In Fig. 4 (E–E′ and F′–F′) the deeper events appear to be a clump of foci just before the Benioff zone dips more sharply.

2.2.2. *Crustal seismicity and rheology under Taiwan*

Based on laboratory experiments on the flow law of quartz and olivine, the rheological properties of the crustal rocks under various crustal and upper mantle conditions have been derived. Kohlstedt et al. (1995) summarized the general relations among the composition, rheology, and seismicity. The curves in Fig. 8 show strength curves for two cases. At a 'normal' geotherm of 30 K/km (Fig. 8a), for example, the top part of a continental crust, down to a depth of 20 km, a friction law (Byerlee, 1978) operates, and at 20 km the quartz flow law begins to dominate and rocks tend to flow rather than behave brittly. Below the Moho, the olivine-rich rock will initially behave brittly, but soon the olivine flow law takes over and it becomes seismically quiescent. At 50 K/km (Fig. 8b), the flow law becomes effective at much shallower depth, essentially suppressing the crustal seismicity. In the oceanic crust, the olivine law rules, and the seismicity occurs throughout the crust and the upper mantle.

The observed seismicity under western Taiwan, under the Central Range and under the Coastal Range can be explained by these laws adequately as follows. The double-layer seismicity under western Taiwan discussed above represents behavior of continental crust with a normal geotherm. Under the Central Range, the geotherm is probably significantly higher as a result of two processes. On the one hand, as we have seen in the tomographic sections, the Central Range crust is formed most probably by extruding the mid- to lower crustal material; if the crust was rapidly exhumed as the fission-track data and recent geodetic data indicate (Tsao et al., 1992), the hotter lower crust would have risen rapidly, thus increasing the geothermal gradient. The second factor that may contribute to a high gradient is strain heating of the mountain (Barr and Dahlen, 1989). If the geotherm is as high as 50 K/km, much of the crustal and upper mantle seismicity can be suppressed as shown in Fig. 7b. This gradient is not unreasonable, judging from thermal gradients in wells in the Central Range (Lee and Chang, 1986). In any case, the wide occurrence of thermal hot springs in the Central Range (Chen, 1982) indicate it is an area of generally high heat flow and probably high thermal gradient. Under the Coastal Range, seismicity extends from very shallow depth down to a depth of 60 km. Two factors probably combine to achieve this. First, it is known (Rau, 1992) that the crust has a thickness of about 20 km, and that the velocities in the crust are closer to those of a typical oceanic crust than a continental one. Thus, the oceanic rheology applies here. But in order to have seismicity down to 60 km, the oceanic crust or the part of the upper mantle just below the

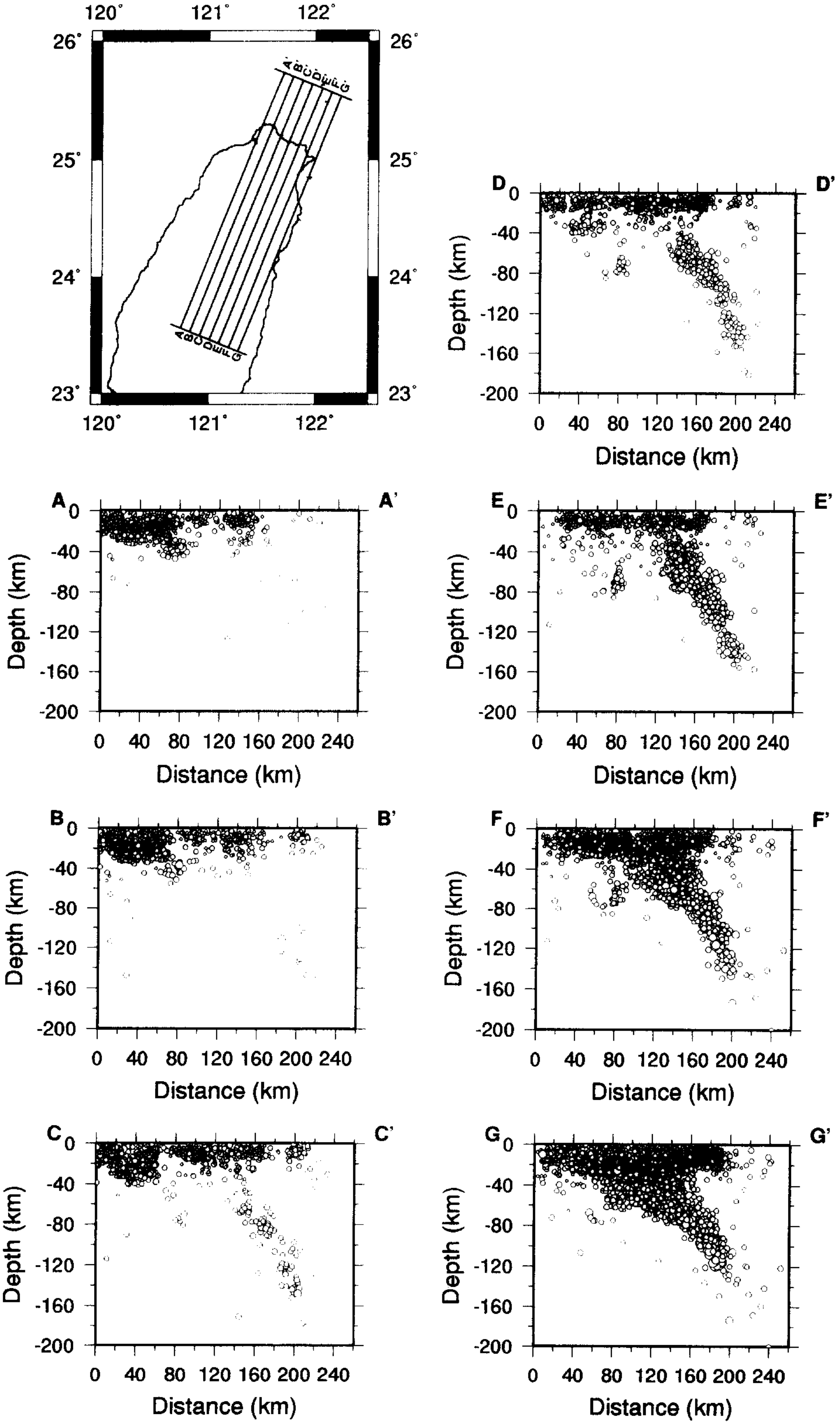
120°
121°
122°
26°
25°
24°
23°
A
B
C
D
E
F
G
A'
B'
C'
D'
E'
F'
G'
0
-40
-80
-120
-160
-200
Depth (km)
0 40 80 120 160 200 240
Distance (km)

Moho probably has to be thickened, so that brittle behavior of rocks persists to greater depth. In the northern part of the Coastal Range, where the seismicity is particularly high (see Section 2.2.7 below), the focal mechanisms of moderate earthquakes do indicate some amount of westward underthrusting, and crustal thickening could occur as a result. Note that while the Central Range in central Taiwan is a relatively quiescent zone, west and southwest of Taitung, the seismicity is high throughout the crust.

2.2.3. *A large lower crustal earthquake*

Since the establishment of the World Wide Standard Seismograph Network (WWSSN) in 1961, only one large earthquake ($m_b = 6.2$; $M_S = 6.75$; $M_W = 6.4$) took place, on January 18, 1964, under the Western Foothills. Using WWSSN seismograms, we performed a waveform inversion employing both P and SH waves (Zwick et al., 1995) and obtained the results shown in Fig. 9a (No. 1). The estimated displacement on the fault is about 1.5 m. This earthquake evidently occurred as a blind-thrust with a relatively steep dip of 40–45° under the fold-and-thrust belt of western Taiwan.

2.2.4. *Normal faulting earthquake in the Taiwan Strait*

Nearly E–W-striking faults have been mapped by seismic reflection surveys in northern and southern Taiwan Strait (Chang, 1992; Lee et al., 1993). Fig. 9b (Chang, 1992) shows the normal faults mapped by multichannel seismic data in the Tainan basin. Although the Strait is also known to be seismically active (Kao and Wu, 1996), a lack of seismic stations in the area prevents detailed studies of the minor earthquakes that occurred in the area. It should be noted that a large historical earthquake of estimated magnitude 8 occurred to the west of northern Taiwan in 1604 (Lee et al., 1976).

The first instrumentally recorded earthquake in this region large enough to be studied with world-wide data occurred on September 16, 1994 (Fig. 9a, No. 2), near the western end of the Tainan basin (22.55°N, 118.74°E, depth 13 km, and $M_S = 6.5$), in the midst of mapped normal faults (Fig. 9b). Inversion of P and SH waves (Kao and Wu, 1996) shows a high-angle, dip-slip normal faulting mechanism with both nodal planes trending approximately east–west. Such a mechanism is consistent with north–south extension in the source region. The occurrence of this earthquake demonstrates clearly that the east–west striking faults in the Taiwan Strait, including those mapped by multichannel profiling, may be active.

2.2.5. *Anomalous shallow event in northeast Taiwan*

An earthquake took place near Nanao on June 5, 1994 (Fig. 9a, No. 3). The epicenter was located just offshore, but the aftershock locations (Fig. 9c) from the Taiwan Seismic Network showed that the fault is partially under Taiwan and trends E–W. The Centroid Moment (USGS) and the local network focal mechanisms (Central Weather Bureau, Taiwan) showed that it is dominantly a strike-slip event, and is left-lateral if it strikes E–W as suggested by the aftershock distribution (Fig. 9c). It is a shallow event at about 10 km. The WNW–ESE T-axis differ from those of the earthquakes farther south in the Coastal Range area, where WNW–ESE P-axes are usually the case. We shall explain the unusual orientation of the T-axis of this earthquake later.

2.2.6. *Internal deformation of orogen based on small to moderate* ($2.7 < M_L < 5$) *focal mechanisms*

In central and western Taiwan, the seismicity is dominated by $m_b < 4.5$ events. Through the study of focal mechanisms of minor earthquakes under the active orogen, one can get a glimpse of the mechanics of mountain building, as the earthquakes are responses to the deformation within the orogen. For small to moderate earthquakes ($2.5 < m_b < 5$), the dimensions of the corresponding faults are on the order of 10's of meters to a kilometer (Slemmons

Fig. 4. Seismicity under northern Taiwan. The seismicity included in each section is that enclosed by a box centered around the section line, with its sides half as long as the distance between the section lines. The sections in the following two figures are similarly constructed. Notice the increasingly clear definition of the Benioff zone going east from sections A–A′ to G–G′. The zone becomes continuous in section F–F′; thus the Benioff zone extends to under the Coastal Range and eastern part of the Central Range. The gradual disappearance of the Benioff zone toward the west can be clearly traced.

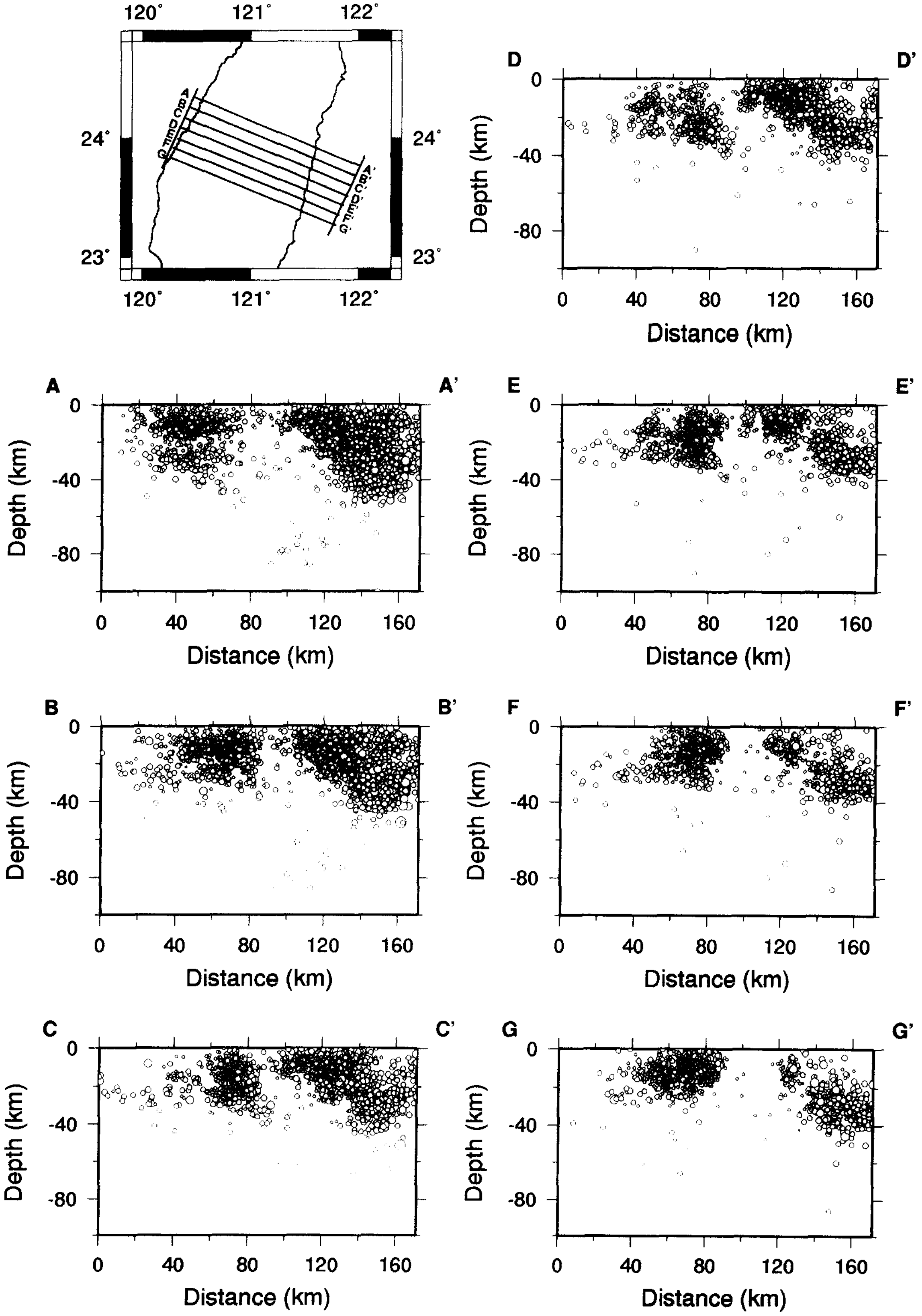

Fig. 5. Seismicity under central Taiwan. In sections A–A′ through F′–F′; a less active mid-crustal zone in western Taiwan can be discerned. The less seismically active zone under the Central Range is evident in all sections. In the eastern part of section A–A′ and B–B′ seismicity extends down to 80 km.

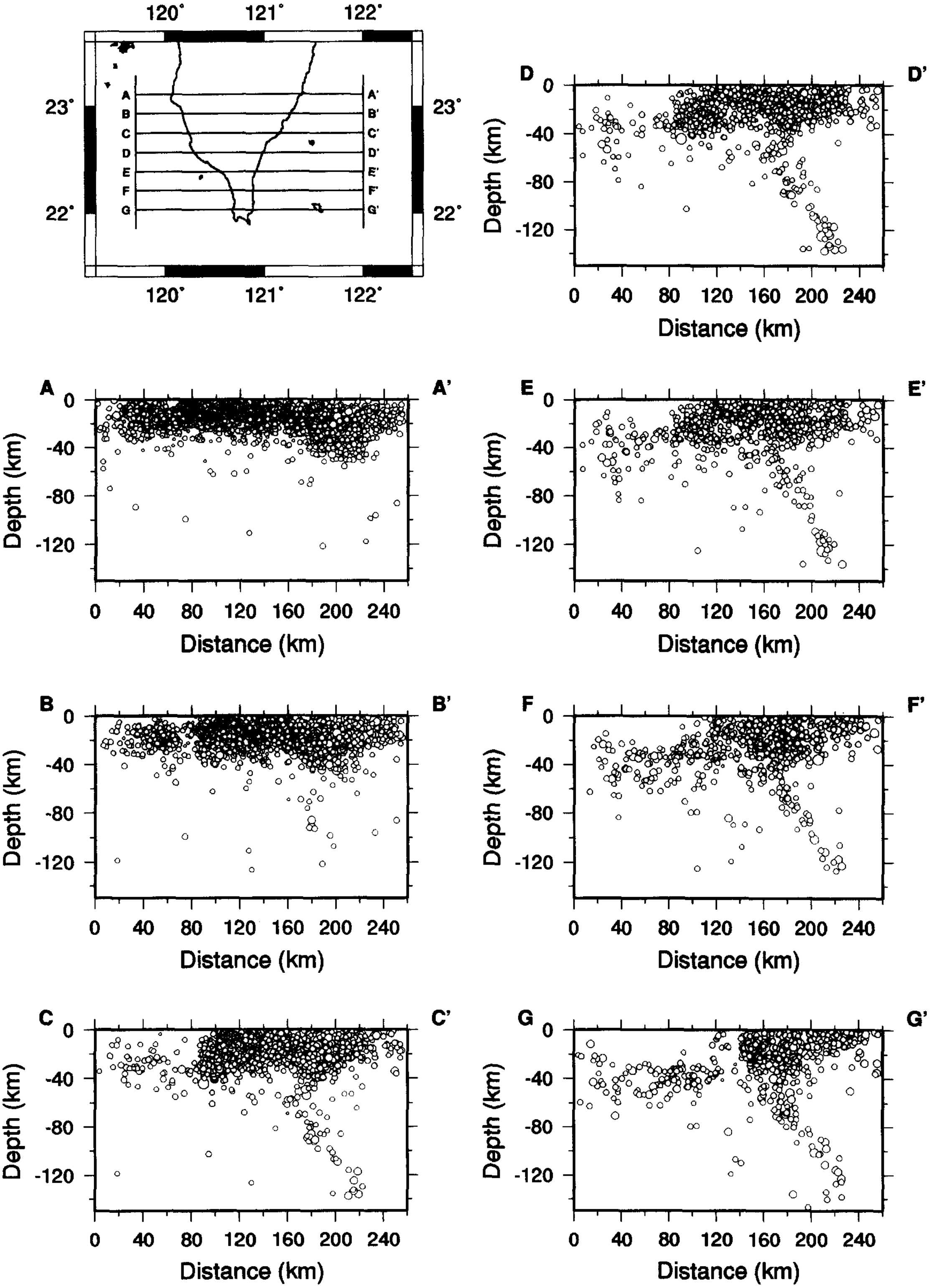

Fig. 6. Seismicity under southern Taiwan. In section C–C′ (south of Taitung) through G–G′ the east-dipping Benioff zone is well-defined. The shallow seismicity under the Hengchun ridge, the continuation of the Central Range southward, is noticeably different from the Central Range proper, i.e., no gap exists.

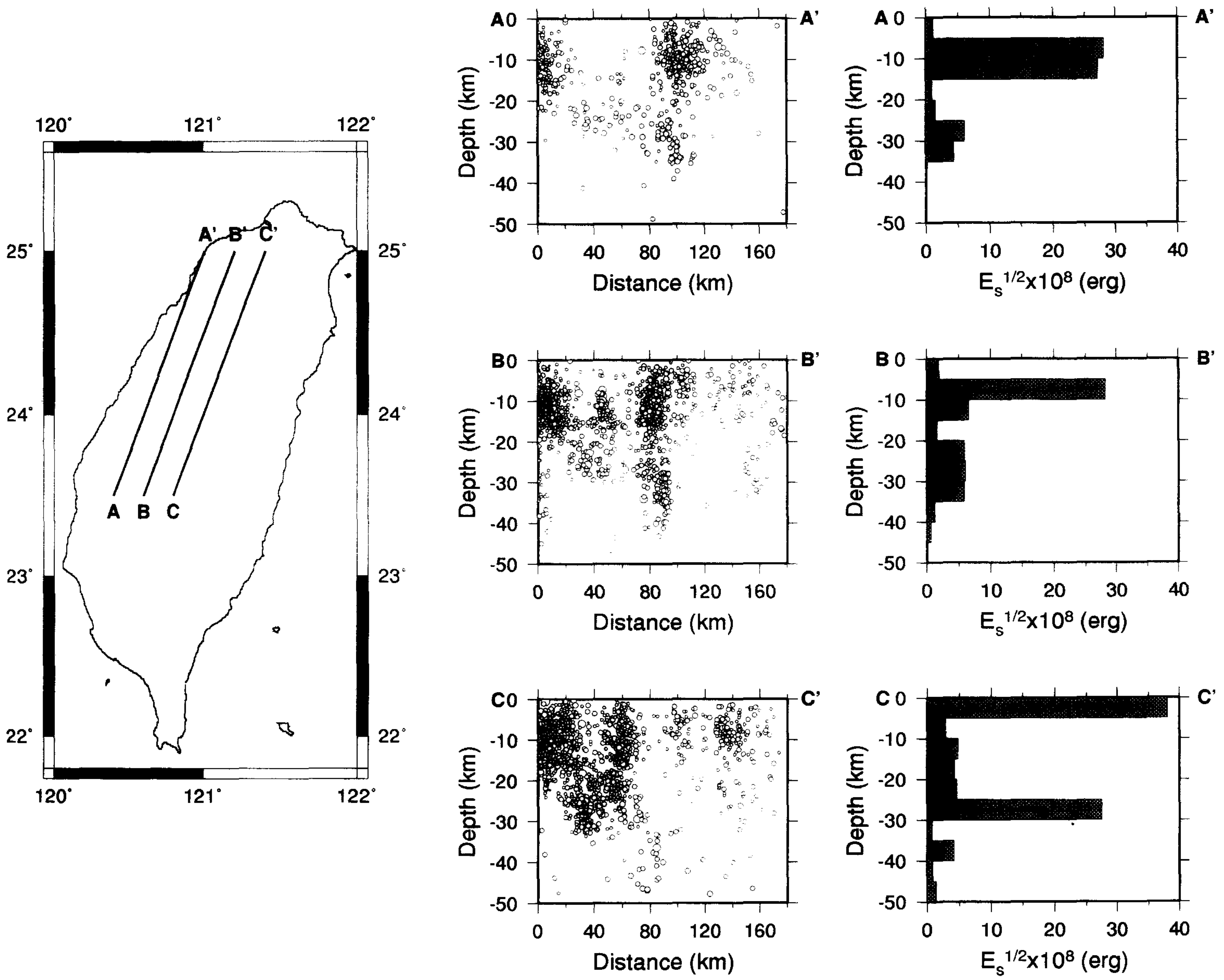

Fig. 7. Seismic double layer shown for sample sections in western Taiwan, with the locations of the sections shown on the left. From the seismicity (middle diagrams), an interval of relatively low seismicity can be seen. By looking at the energy release as a function of depth (at right), the double layering becomes clearer; energy within 5 km intervals are displayed.

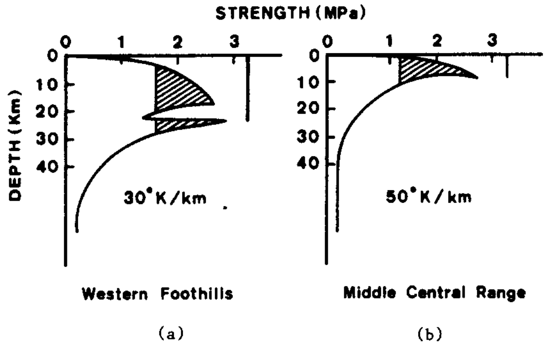

Fig. 8. Representative rheological properties of continental crust with geothermal gradients at (a) 30 K/km and (b) 50 K/km. The higher gradient is sufficient to suppress the brittle response of the lower crust below about 10 km.

and Depolo, 1986); a large number of similar mechanisms in an area probably signifies the presence of a major active structure, whereas a variety of mechanisms may indicate deformation in a highly fractured medium. Actually, the diversity of mechanism lends nicely for another purpose: the determination of local stress axes.

Using first motion polarities and SH/P amplitude ratios jointly with tomographically relocated hypocenters Rau et al. (1996) determined the focal mechanisms of 97 small earthquakes under Taiwan (Fig. 10). It is clear that mechanisms are variable even within a small region. For example, solutions 2, 6, 7, 60, and 38 are thrust faulting events at a depth range of 20–35km, and it is interesting to note that the *P*-axes are consistent, nearly horizontal and trending WNW–ESE, aligned roughly with the plate motion vector of the Philippine Sea plate (Seno et al., 1993). For another tight cluster of events at a depth range of 10–20 km (67, 82, 83, and 85–88) the mechanisms are very diverse; they are dominantly normal faulting and all of them consistent with WNW–ESE least compressive axis, instead of a WNW–ESE maximum stress axis of the last group. Three mechanism in the northern Central Range (46, 74,75) are also normal faults. That normal faulting can occur in a collision regime has been discussed extensively in a structural geologic context (Crespi et al., 1996), but the nature of faulting in situ, whether normal or otherwise, is sometimes difficult to establish. These events do indicate that normal faulting events occur in an otherwise obviously compressional regime. The occurrence of these events however, does not necessitate the occurrence of large ($M > 5.5$, say) normal faulting events, as no such events have yet occurred in the Central Range of Taiwan. In general, most of the faults are high-angle ones especially in the western Foothills, and there are a few cases where one of the planes could represent either a shallow-angle thrust (events 8, 18, and 29) or a shallow-angle normal fault (events 19, 42 59, 81, 82 and 88).

2.2.7. Seismicity and focal mechanism offshore of eastern Taiwan

The most active seismic area in the immediate vicinity of Taiwan is the area east of Hualien. The cross-section in Fig. 11 shows an WNW–ESE seismicity profile across Taiwan and the offshore area east of Hualien. The high level of seismicity under the Coastal Range down to 60 km and the decrease of hypocentral depths can readily be discerned. On the basis of rheological considerations described earlier, the deepening of the seismicity is interpreted as a result of the thickening of oceanic upper mantle. Although there have been a few magnitude-6 or above events in the Hualien region, there are not enough of them, especially at 30 km or deeper in the active zone, for deciphering the overall pattern of deformation. To utilize the more frequent $M_S = 5.3 - 6$ events Salzberg (1996) has recently implemented a combined surface and body wave inversion method. Altogether about 20 mechanisms, mostly thrusts, in this area were obtained and are shown in Fig. 11a. In depth section (Fig. 11b) they can be interpreted either as west-vergent high-angle thrusts or low-angle underthrusts. The former implies the rising of Philippine Sea materials east of the Coastal Range, and the latter provides a mechanism for thickening the Philippine Sea plate underneath the Coastal Range.

2.3. GPS results

Geodetic data provide direct evidence of current tectonic activity. Based on fixed and repeated mobile GPS results for the last four years, Yu and Chen (1994) presented the regional horizontal displacement (with respect to Penghu in the Taiwan Strait) and strain in the Taiwan orogen. The key findings are: (1) the volcanic island Lanhsu (Fig. 1) on the

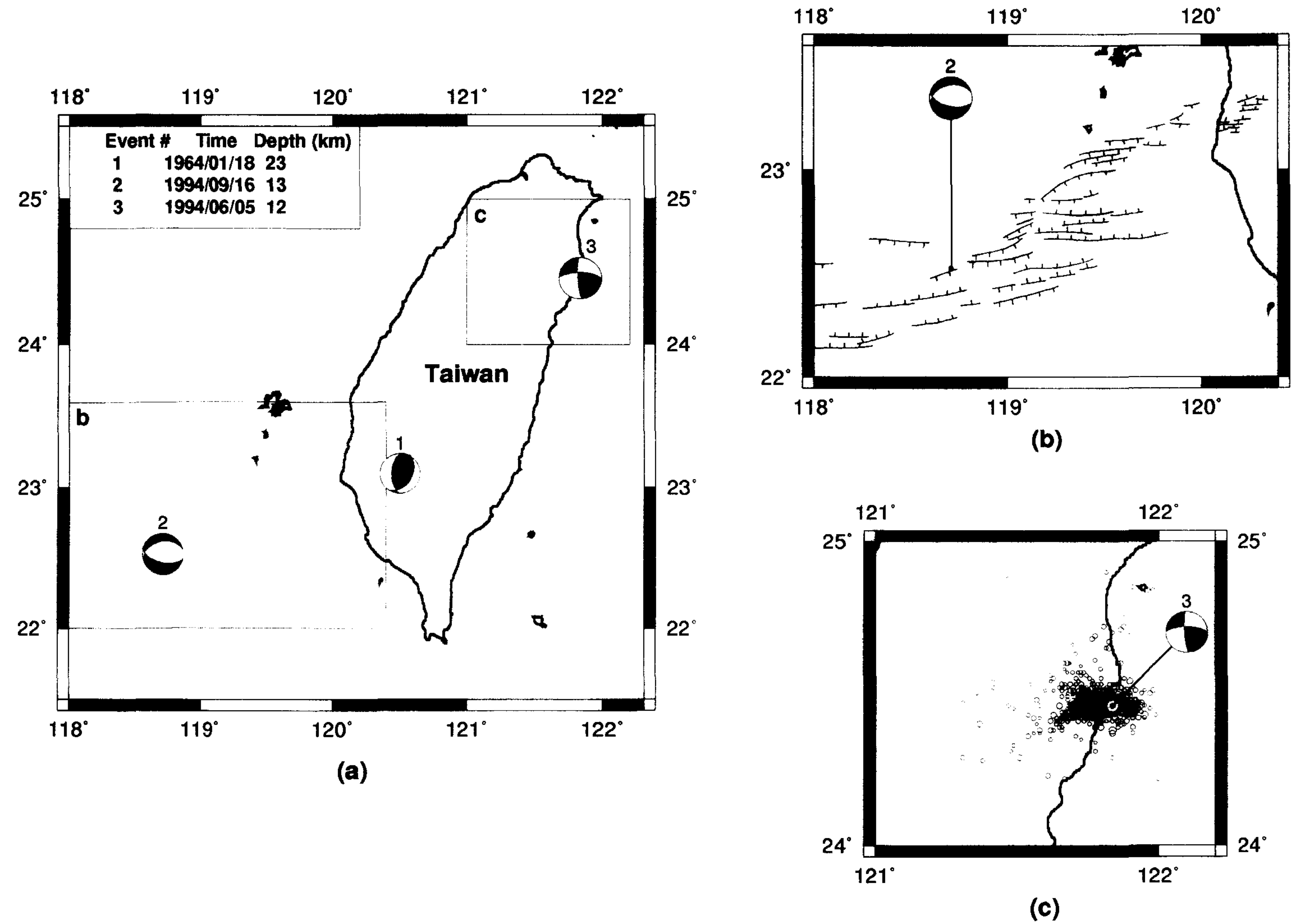

Fig. 9. (a) Focal mechanism of the three large important earthquakes in the Taiwan region; the focal mechanisms are plotted where the events are located. The focal mechanism of January 18, 1964 Tainan earthquake (*1*) derived through waveform inversion (Zwick et al., 1995). It represents a thrust fault with the centroid depth at 23 km, i.e., in the lower crust. The earthquake has a moment of 4.3×10^{18} N m. It is located under the Foothills. The focal mechanism of the June 5, 1994 Nanao earthquake (*3*) determined by waveform inversion (USGS Preliminary Determination of Epicenters, September, 1996). The focal mechanism of the September 16, 1996 Penghu earthquake (*2*) determined by Kao and Wu (1996). (b) The location of the Penghu earthquake, its mechanism, and the normal faults mapped in the Tainan basin south of Penghu (Chang, 1992). The focal mechanism of the earthquake is consistent with the prevalent E–W-striking normal faulting in this area. (c) Distribution of aftershocks that occurred within a day of the June 5, 1994 Nanao earthquake. Its trend indicates that an E–W-striking fault plane; it is thus most probably a left-lateral strike-slip event on an E–W-trending fault, with an NW–SE *T*-axis, very different from the WNW–ESE *P*-axes of the typical thrust events south of this region (Wu et al., 1989).

Philippine Sea plate is moving at the rate of nearly 8 cm/yr toward Penghu; (2) extensional strain is found in the southern Central Range; (3) there is an overall shortening across Taiwan.

2.4. Bouguer anomalies

The Bouguer anomaly of Taiwan is very conspicuous in that instead of being associated with a Bouguer low as are many older mountain ranges (e.g., Lyon-Caen and Molnar, 1983), the Central Range corresponds to a high Bouguer gradient (Yeh and Yen, 1992). The obvious low (nearly −60 mGal) in northwestern Taiwan is partially due to the thick sediments in the Taichung basin. Here we model a profile taken across central Taiwan south of Hualien (Fig. 12) where the tomographic velocity structures are well resolved. The initial density model was obtained by assigning density (Nafe and Drake, 1965) to the tomographic seismic velocities while retaining the model geometry. This 2-D density structure is then adjusted by changing slightly both the density and the boundaries until a reasonable fit to the gravity data is obtained. The boundaries in the final model have generally the same geometry as those of the initial model. From this modeling we conclude that the Bouguer anomaly profile across central Taiwan is consistent with the depression of the Moho down to a depth of 50 km and the presence of relatively high density materials at shallow depth under the Central Range. The gravitational effect of the root is balanced by the shallow high-density rocks, and the rapidly rising Bouguer anomaly in the eastern Central Range is most sensitive to the placement of the eastern flank of the root. The position of the eastern flank of the root based on gravity is offset about 7 km from that determined by tomography.

2.5. Summary of results

We synthesize the above seismological and geophysical results in Fig. 13. In this figure the interpretations are superposed on 3-D plots of seismicity; the subduction zones and the major crustal and lithospheric structures are constructed based on the data presented above. We emphasize the observations that the Philippine Sea plate subducts to the north, to the northeast of Taiwan as well as under the eastern part of northern Taiwan, and the Eurasian plate subducts to the east in southern Taiwan. But from 23°N to 24°N, there is no evidence that subduction is taking place toward the east. In the figure it is also indicated that the crust under various parts of the island has thickened as a result of collision, and that the Philippine Sea plate has begun noticeably to underplate the northern Coastal Range — in what appears to be a process of lithosphere thickening. Seismicity occurs throughout much of the lithosphere under western Taiwan and under the Coastal Range. This implies that, at least, the stress is present in the crustal volume where seismicity is detected. Based on rheological consideration, the juxtaposition of the highly seismic region under the Coastal Range, down to a depth of 60 km or more, against the seismically quiescent Central Range evidently reflects the transition from oceanic crust to continental crust. The southern tip of Taiwan, overlying a well-defined Benioff zone, is an accretionary wedge, with relatively thin crust.

3. Tectonic geology of Taiwan

3.1. Geologic framework of the island of Taiwan

The part of Taiwan west of the Longitudinal Valley (Fig. 1b) was in a passive continental margin and slope environment before the impingement of the Luzon Arc that created Taiwan (Chai, 1972). The dominant geologic variations resulting both from the orogeny and the orientation of the sedimentary basin occur in the direction perpendicular to the trend of the island, with rocks generally becoming older, more metamorphosed, and more intensely deformed when proceeding eastward. The western Taiwan Foothills (Fig. 1b) are composed of Plio–Pleistocene rocks in a fold-and-thrust belt (Ho, 1988). The source sediments of these rocks are from the Central Ranges, i.e., they are post-orogenic. To the west of the Foothills is the Coastal Plain, where recent sediments are rapidly accumulating. In the Central Ranges east of the Foothills, the older Tertiary (Paleogene) shelf and slope sediments are metamorphosed to become mostly slates and schists and are now raised to a maximum elevation of nearly 4000 m. But higher-grade metamorphic rocks of pre-Tertiary age are exposed on the eastern flank of the Range. These rocks had been subjected to

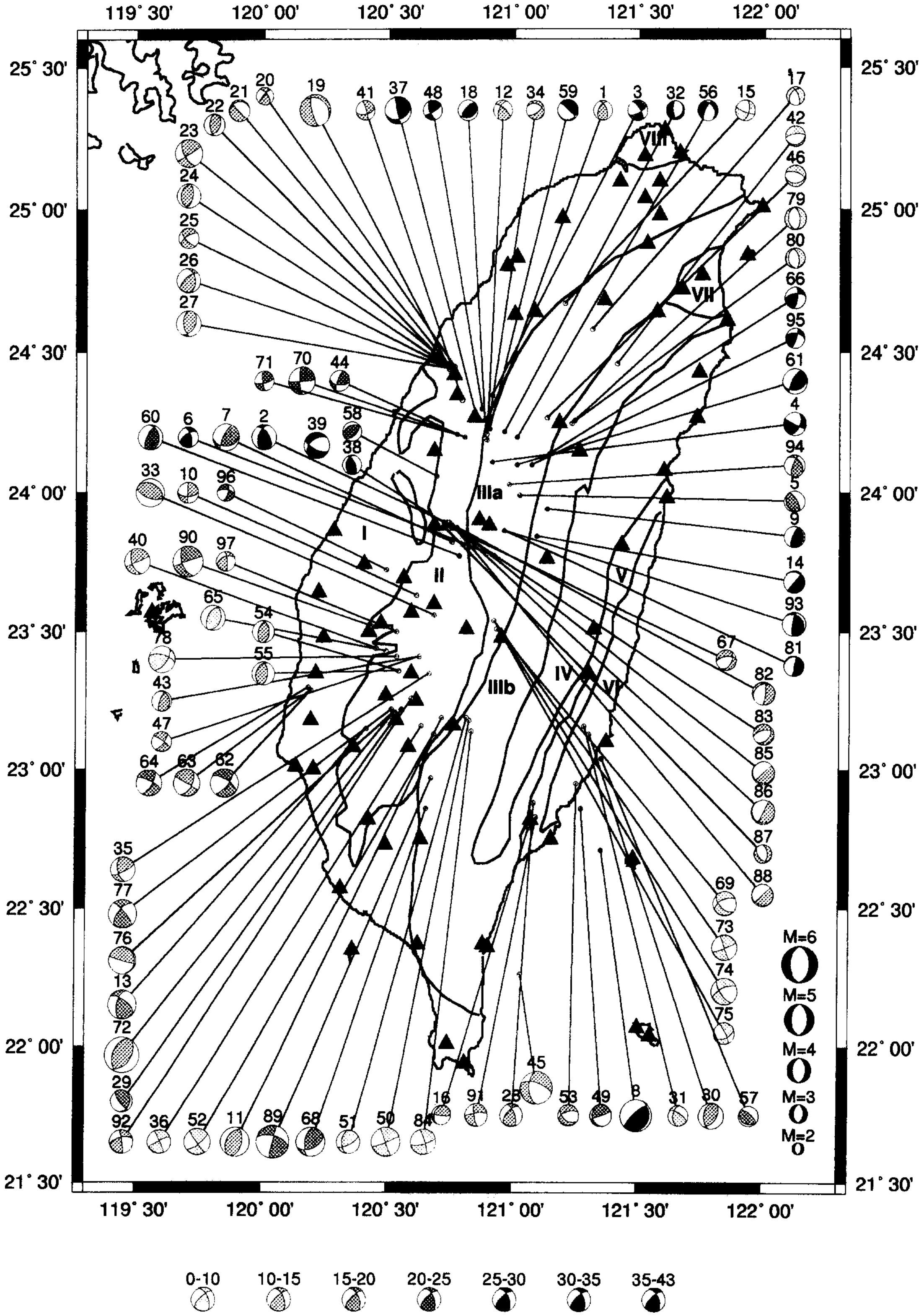
119° 30'
120° 00'
120° 30'
121° 00'
121° 30'
122° 00'
25° 30'
25° 00'
24° 30'
24° 00'
23° 30'
23° 00'
22° 30'
22° 00'
21° 30'
VIII
VII
IIIa
I
II
IIIb
IV
V
VI
20
19
41
37
48
18
12
34
59
1
3
32
56
15
17
21
22
23
24
25
26
27
42
46
79
80
66
95
61
4
94
5
9
14
93
81
71
70
44
60
6
7
2
39
58
38
33
10
96
40
90
97
65
54
78
55
43
47
64
63
62
67
82
83
85
86
87
88
69
73
74
75
35
77
76
13
72
29
92
36
52
11
89
68
51
50
84
16
91
28
45
53
49
8
31
30
57
M=6
M=5
M=4
M=3
M=2
0-10
10-15
15-20
20-25
25-30
30-35
35-43

deep burial (>10 km) and represent those of mid-crustal level. East of the high-grade metamorphics is the Longitudinal Valley, a sediment-filled, relatively linear valley separating the Central Range from the Coastal Range in eastern Taiwan. The Coastal Range is composed of a suite of rocks that were associated with the island arc on the margin of the Philippine plate. It is capped by andesites of the Luzon Arc, with the underlying sedimentary rocks consisting of deposits in the forearc basin, in the trench and on the outer rise. Considering the distance between the volcanic arc and the trench, shortening of more than 100 km of the Philippine Sea plate margin must have been accommodated.

The north–south geologic variations in Taiwan are more subtle. For example, the Central Range can be divided into the Hsueshan (in the west) and the Backbone (in the east) ranges in northern Taiwan; the Paleogene rocks in the Hsueshan Range are coal-bearing and were deposited in a typical continental shelf environment, while the rocks in the Backbone Range are finer grained and were deposited close to the continental slope. Between 22.8°N and, 23.5°N, however, only the equivalent Backbone Range is there. In other words, at that point, the orogen is moving off the shelf and onto the slope.

No detailed geologic map of southern Taiwan, south of the line connecting Kaoshiung and Taitung, has yet been published, although the melange at the southern tip of Taiwan has been a focus of attention (Ho, 1988). Generally the slates in the southern Central Range north of this area grade into unmetamorphosed rocks of the Hengchun Peninsula. Hu and Tsan (1984) mapped the structures along the southern Taiwan railroad and found them to be quite different from those of the Central Range further north. In addition to the dominant N–S-striking folds, they also mapped a number of small-scale E–W striking folds and right-lateral strike-slip faults. They concluded that after the compression under ENE-oriented stress in the Plio–Pleistocene, there had been N–S-oriented compression operating in this area. These observations point out that the area is in a tectonically very different environment from that of the Central Range.

3.2. Accretionary wedge onshore and offshore of southern Taiwan

Reed et al. (1992) mapped the offshore area of southern Taiwan, defined the accretionary wedge, and show the geometry of the wedge as well as the ubiquitous thrust faulting therein. Several investigators (e.g., Lee et al., 1993; Gong et al., 1995; Lallemand et al., 1995) have attempted to trace the northern terminus of the deformation front. While Lee et al. (1993) and Gong et al. (1995) connect it to structures on shore near Kaoshiung, Lallemand et al. (1995) prefer a more northerly location. Lee et al. (1995) used multichannel seismic data to show the continuity of the deformation front as mapped by Reed et al. (1992) to Kaoshiung and the absence of any displacement in the channel deposits west of Tainan in the Strait. At present the Kaoshiung connection seems to be better supported; Kaoshiung is also the point south of which the east-dipping northern Luzon subduction zone becomes clear (Fig. 6, C–C′). The southern part of Taiwan and offshore of southern Taiwan clearly belong to the accretionary wedge environment.

The deeper crustal structures are being studied with the 1995 R/V *Ewing* multichannel data (Don Reed, pers. commun., 1996) and wide-angle sea–land reflections (Yeh et al., 1995). From the Bouguer anomalies (Fig. 10) in southern Taiwan we can see the transition from the generally negative Bouguer values northwest of Taitung to positive values southwest of Taitung; it is quite possible that the Hengchun Peninsula is underlain by mostly oceanic crust. This is particularly an important problem in understanding how the Hengchun ridge was formed.

Fig. 10. Map of Taiwan showing the locations and fault plane solutions of 97 events studied (Rau et al., 1996). The solutions are coded for both local magnitude (2–6) and depth (0–43 km). The numbers next to the solutions indicate time sequence, the later the event the higher the number. Seventy-five TaiSeiN seismic stations are shown as solid triangles. The solid lines mark the boundaries of the major geologic units: *I* = Coastal Plain, *II* = the Western Foothills, *III* = the western Central Range, *IV* = the eastern Central Range, *V* = the Longitudinal Valley, *VI* = the Coastal Range, *VII* = the Tatun volcanic group.

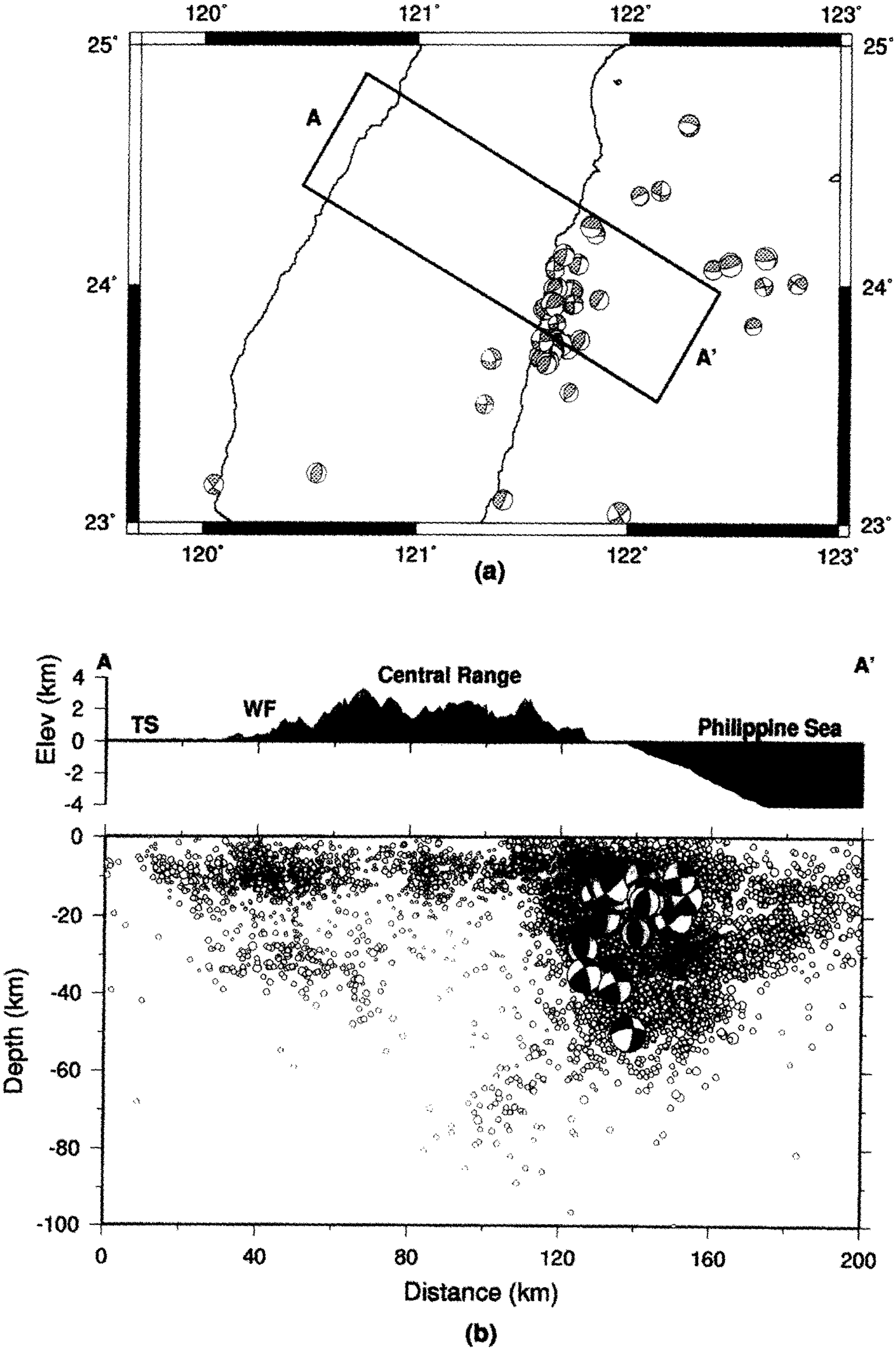

Fig. 11. (a) Focal mechanisms of $5 < M_S < 6$ events near Hualien. (b) A NWN–ESE seismicity profile across Taiwan contained in the box shown in (a) and the focal mechanism of the same events as in (a), but shown in the vertical plane parallel to the section. There is an apparent shallowing of foci toward the east, under the Philippine Sea; note that because only land-based data are used, the depth determination of offshore earthquakes may have errors up to 30 km.

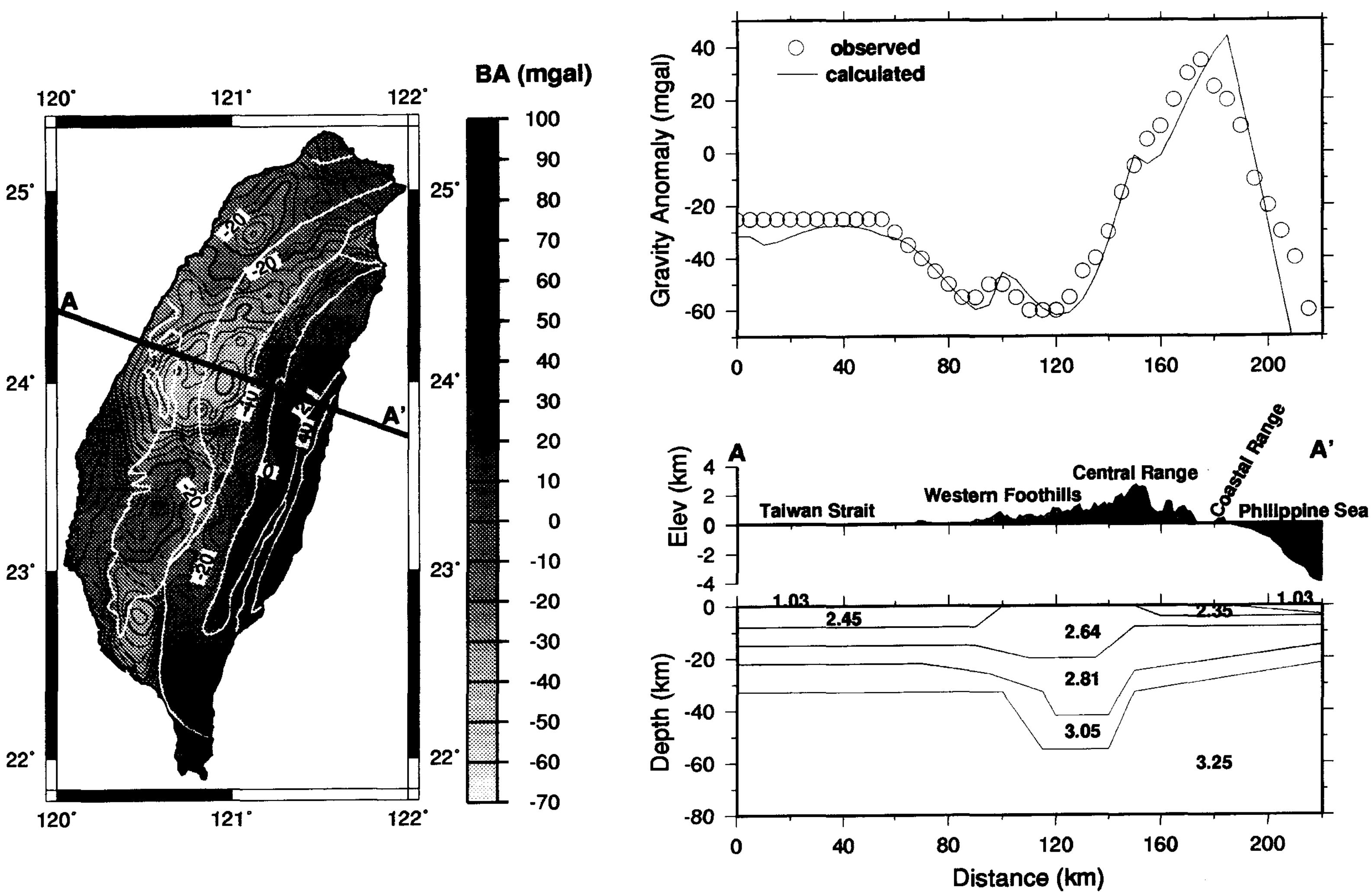

Fig. 12. 2-D Bouguer gravity interpretation constrained by a tomographic seismic velocity model. The distances between 70 and 170 km in A–A′ correspond to the D–D′ profile in Fig. 2. For lack of constraints the gravity anomalies offshore are not well modeled.

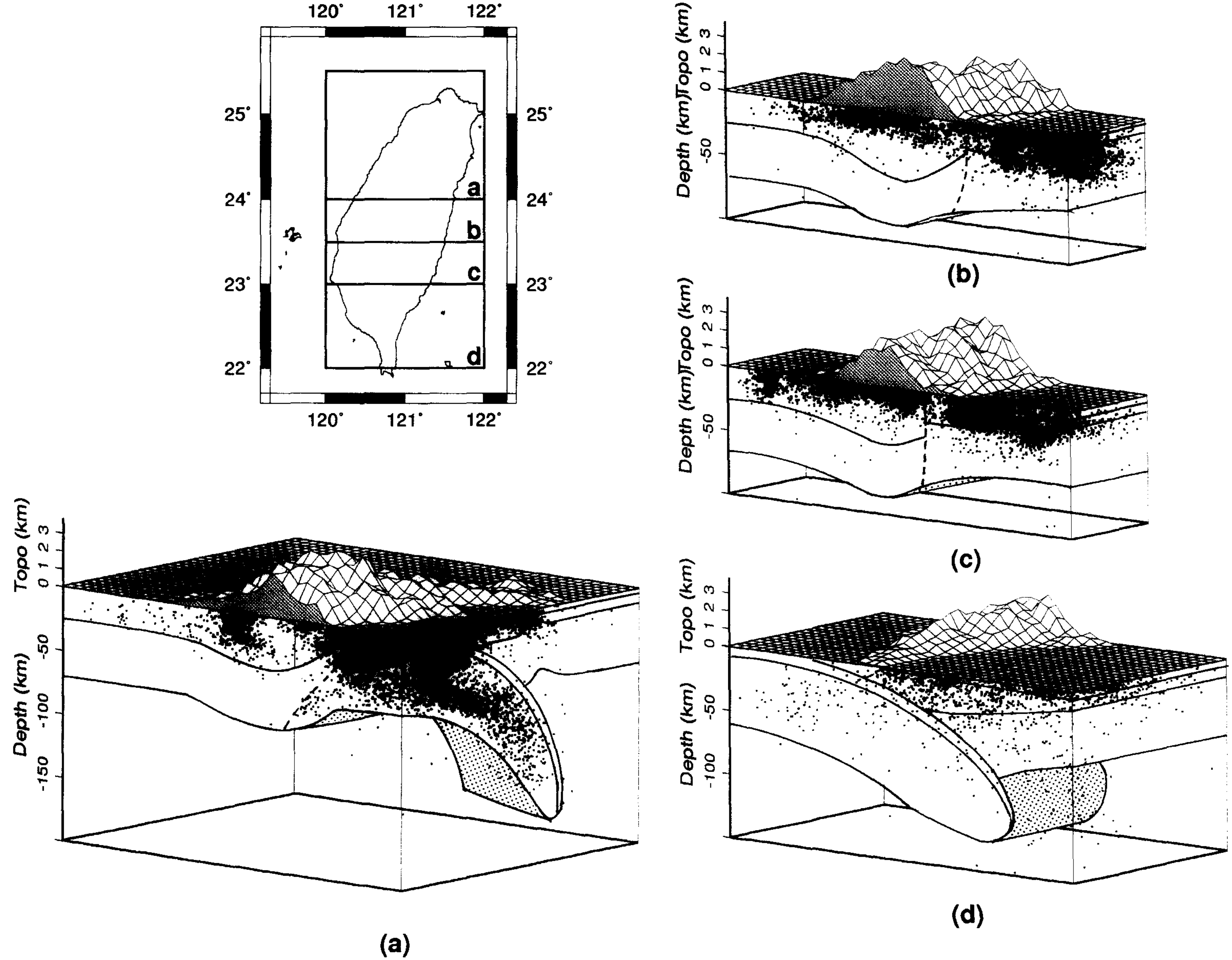

Fig. 13. Synthesis of seismological and geophysical data showing major subsurface structures. The structures are superposed on the 3-D seismic foci. The depth of the crustal features are those from seismic tomography (Fig. 2). The WNW motion of the Philippine Sea plate led to both northward subduction of the Philippine Sea plate (a) and the collision of the lithospheres of this plate and that of the Eurasian plate, resulting in the thickening of the crust and the lithospheres on both sides (b and c). In southern Taiwan, the Eurasian plate subducts eastward under the Philippine Sea plate (d). The locations of the blocks are shown in the index.

Since the deformation front west of Hengchun is not yet in contact with the Eurasian continental shelf, the Hengchun Peninsula and the ridge south of it could not have been created through collision in the same manner as the Central Range.

3.3. Geology offshore of eastern Taiwan

The area offshore of the east coast of Taiwan (between 23°N and 24.5°N and from the east coast to 123°E) is tectonically complex. A number of shallow penetration, multichannel and single-channel seismic lines have been gathered by National Taiwan University and they have been summarized and interpreted by Lin (1994). Here the deformation associated with the Ryukyu forearc and that of the collision of the Philippine Sea and Eurasian plates are evidently superposed. The Yayaema ridge (Fig. 14) is the southwest continuation of the Ryukyu forearc and appears to be a fairly typical accretionary wedge overlying the subducting Philippine Sea plate as shown in Lin's seismic sections. In approaching the Coastal Range of Taiwan, the EW-striking forearc appears to be truncated by island-parallel ridges and troughs. Southeast of the intersection of Ryukyu and Taiwan is the Hoping Basin, east of the precipitous cliff between Hualien and Nanao. This is a very curious basin as it is apparently quite deep and associated with a remarkable free-air gravity low of about −200 mGal (Yen et al., 1995). Wu (1978) interpreted this basin as having been created under E–W tension. The orientation of the *T*-axis of the June 5, 1995 earthquake described above is consistent with this interpretation. South of the Ryukyu Trench on the abyssal plain, the sedimentary layers are generally undisturbed, although several large strike-slip seismic events were located there (Wu, 1978).

3.4. Falsification of hypothesis

In terms of orogeny, a truly comprehensive hypothesis should include the space–time evolution of a

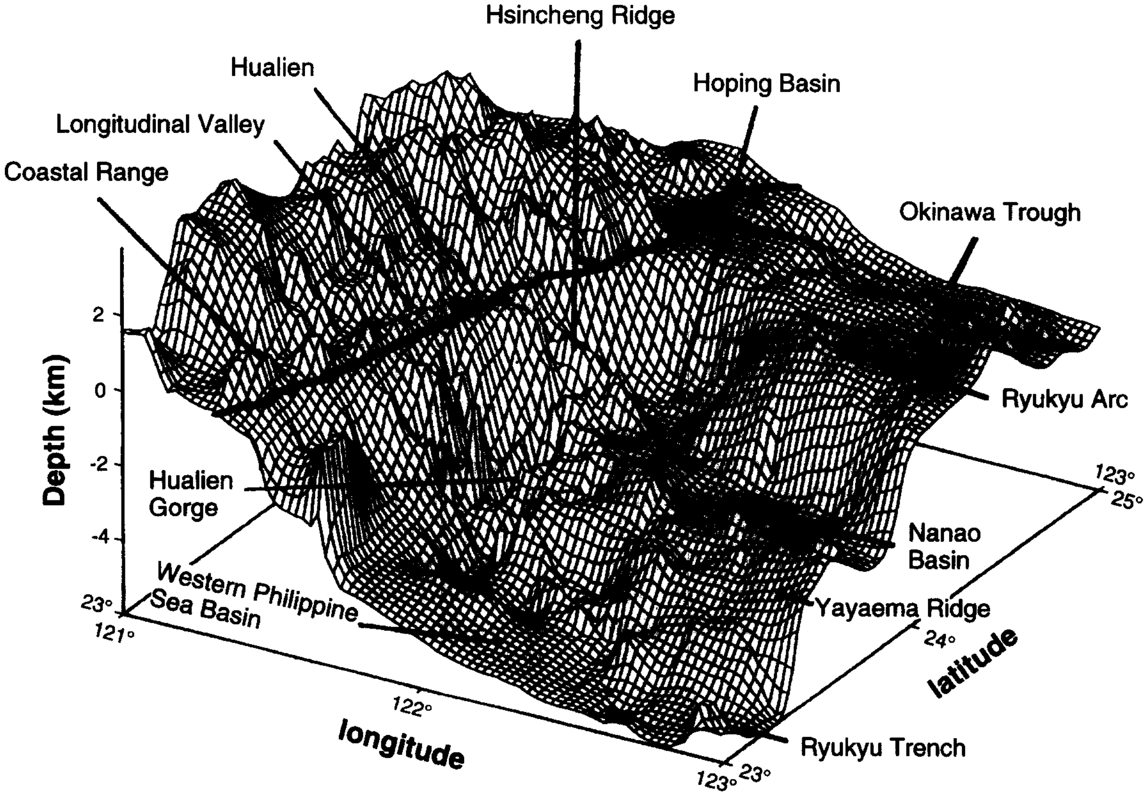

Fig. 14. 3-D view of the bathymetry offshore of northeastern Taiwan (adapted from Lin, 1994).

mountain range. Even for the young Taiwan orogeny, such a hypothesis does not seem to be within grasp yet. In the meantime, a hypothesis may center on the evolution of a mountain belt, for which dating of events are needed. The hypotheses we attempt to falsify and propose concern mainly the orogenic processes that led to the current state. The observables are the results of the processes: the geometry of boundaries and the nature of materials as interpreted from seismicity, velocity and density. Through the focal mechanisms and GPS measurements we can also map the current state of strain. Although the three dimensions of the physical space may be well sampled, the data are time-insensitive.

In this paper we follow the view of Popper (1968) that a scientific hypothesis cannot be shown to be absolutely true, and it should be subjected to constant falsification attempts. We shall use existing data as summarized above to test the thin-skinned hypothesis of Taiwan orogeny, and finding it inadequate we then offer a new hypothesis. The new hypothesis should then be subjected to tests by others. We make attempts to show what are the unsubstantiated assumptions of our hypothesis to facilitate testing. We believe that through such a process, attention can be focused on key questions of the Taiwan orogeny.

4. The thin-skinned tectonics hypothesis of the Taiwan orogeny

4.1. The thin-skinned model

Suppe (1981, 1987) pioneered the modeling of the Taiwan orogeny in terms of 'thin-skinned' tectonics. His interpretation arose primarily from mapping of the fold-and-thrust belt in western Taiwan (Suppe, 1976), and was later augmented with exploration seismics and some drilling data in western Taiwan (Suppe, 1980, 1981). Davis et al. (1983) explicitly made the fold-and-thrust belt and the accretionary wedge equivalent and Dahlen and Barr (1989) then solved the thermal–mechanical problem of a 'critical' wedge. This model is based on the following assumptions: (1) the boundary between the Eurasian and the Philippine Sea plates extends from the Manila Trench northward onto the Coastal Plain of western Taiwan, and the east-dipping subduction zone in northern Luzon also continues northward with the continental lithosphere under Taiwan subducting to the east; (2) the Taiwan orogen is wedge-shaped and is soled by a decollement, at a slope of about 6°, which coincides with the top surface of the subducting plate; and (3) the materials in the wedge follow a cohesionless friction law under supra-lithostatic fluid pressure.

More specifically (Suppe, 1987), the Tertiary sediments in Taiwan that dominate the surface geology of the mountain ranges fill the wedge; they are folded and faulted in a brittle manner above a detachment (Fig. 15A, B) such that they can be retrodeformably reconstructed. A 'bull-dozer' or indentor, the Coastal Range, came from the east and deformed the wedges on the continental shelf and the Philippine Sea plate to form the mountain range (Fig. 15C). New materials enter the wedge from the west and are moved closer to the indentor along paths that are depth-dependent; they, however, will be exhumed. The metamorphism of the materials intensifies as they move through the wedge. The rate of propagation of the apex of the wedge is assumed to be constant, and is the same as the indentor. Erosion continues to remove materials from the surface of the wedge. With the erosion rate and the rate of uplift assumed to be nearly in balance, the wedge maintains a steady-state cross-section. The wedge, at its deepest point is on the order of 10–20 km. This model is essentially two-dimensional in the sense that the geological differences along the axis of Taiwan are considered to be only a result of southward propagation of the collision.

4.2. Falsification of thin-skinned model and discussion

Whereas the thin-skinned hypothesis predicts that the Taiwan orogeny is a result of the deformation of an accretionary wedge-like body with depth not reaching beyond about 20 km, the observations outlined above indicate that the orogeny in Taiwan involved the deformation of the whole crust and upper mantle. Instead of being limited to a shallow wedge, a root as deep as 50 km under the Central Range, a result of long-term deformation, had formed. Major deformation that must be associated with the ongoing orogeny is also occurring beneath the assumed wedge. There is no evidence supporting the subduc-

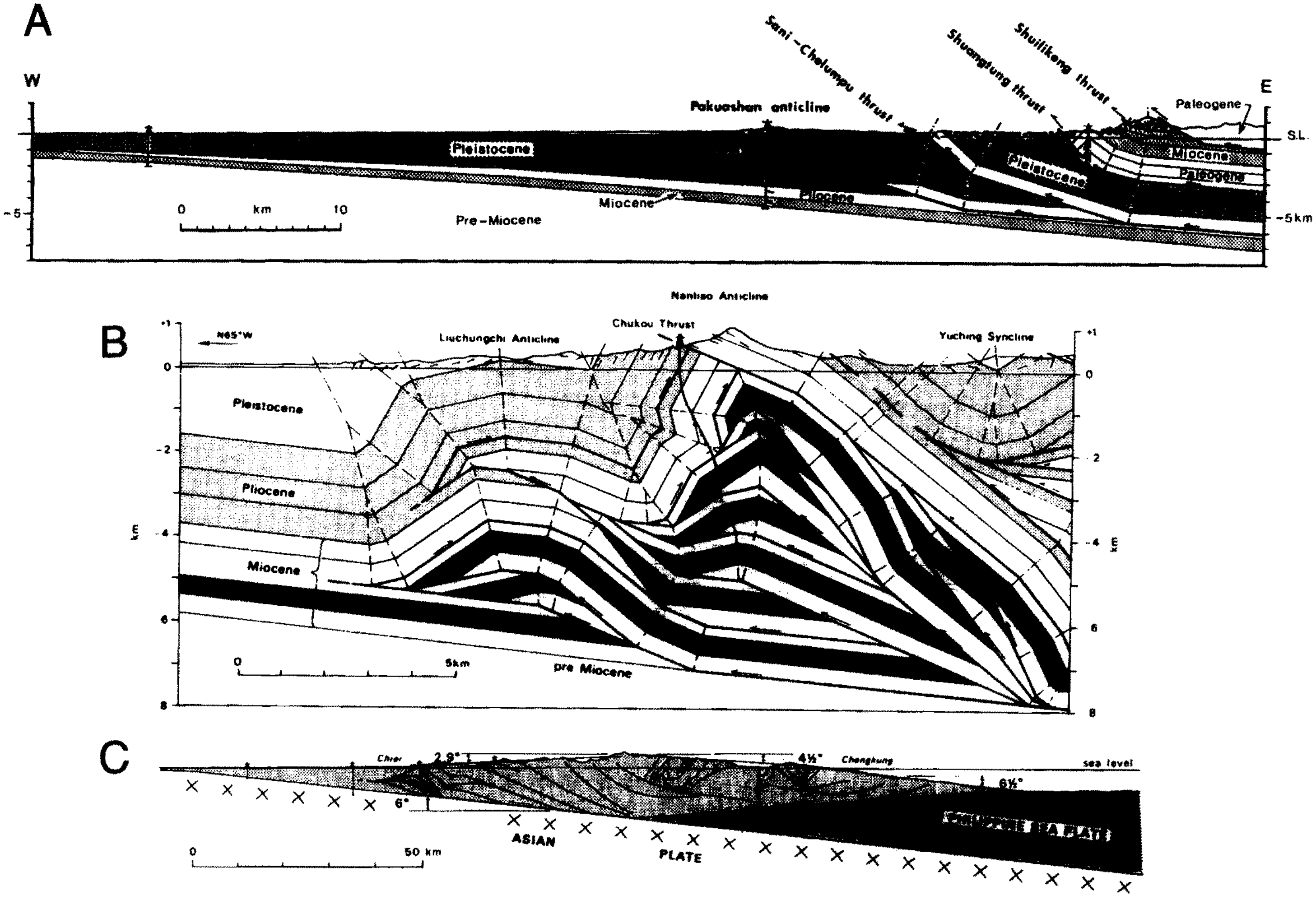

Fig. 15. (A, B) Thin-skinned tectonics of Taiwan as illustrated by a cross-section across central Taiwan (Suppe, 1987). Here a decollement underlies the Miocene sediments (shown as folded and faulted layers). (C) In this model the Central Range is created by advancing the Philippine Sea plate westward.

tion of the continental lithosphere under the Central Range, whether in terms of a dipping seismic zone, normal faulting on the outer rise (with *T*-axis perpendicular to the trend of the island), or shallow thrust events under the Foothills. Also, with seismic velocity around 5.5 km/s, the rocks at shallow depth under the Central Range are most probably metamorphic rocks similar to those exposed on the eastern side of the Central Range and not likely to be in a critical state. The Taiwan orogeny as a whole also is closely coupled to the lithospheric shortening at the margin of the Philippine Sea plate near Taiwan as well as the faulting in the Taiwan Strait. Thus the thin-skinned tectonics is not adequate or appropriate as a hypothesis for the Taiwan orogeny.

We falsify the thin-skinned hypothesis based mainly on the observations that the Central Range is not modeled correctly and important orogenic processes at depth are not included. However, there are questions concerning the fold-and-thrust belt in the Foothills that we did not address. For example, the existence of a decollement as a base for such a belt is frequently invoked in orogenic studies. Neither in the seismicity or small earthquake focal mechanisms obtained so far can a decollement be discerned. In the 'thick-skinned' tectonics of Hatcher and Hooper (1992) a decollement is defined more loosely as a zone of mechanical weakness along which faults may propagate. They propose that the decollement may exist near the transition between the brittle and ductile layers or in the ductile layer in the crust. Of course such a decollement would play a very different role from the one assigned in the thin-skinned hypothesis. There are other related aspects of the falsification, but we shall avoid repetition by discussing them later after we describe the proposed lithospheric collision model.

4.3. *The lithospheric plate collision model*

In this hypothesis the Taiwan orogeny is the result of a collision between the Eurasian and the Philippine plates with the plate edges engaged in collisional (transpressional) contact. Since the Philippine Sea plate is subducting toward the north at the same time, the contact area between the two plates is variable as shown in Fig. 3. The two plates are in contact from the surface down to a depth of more than 60 km near Taitung (23°N), but as the Philippine Sea plate begins to subduct northward near 23.5°N the top of the contact zone begins to dip northward; initially the dip is small, but it increases gradually and north of Nanao the subducting Philippine Sea plate dips under the lithosphere and encounters the asthenosphere on the Eurasian side (Fig. 3). Beyond the northern tip of Taiwan, the two plates are no longer in collision. Due to the non-parallel orientations of the Luzon Arc and the Eurasian continental shelf, the contact was first established near Hualien and moved south, toward Taitung, as a function of time; south of Taitung, collision has not yet begun as the Eurasian continental shelf has turned more sharply westward. On the continental side, the creation of the Central Range involved the thickening of the crust as well as the upward extrusion of the mid- and lower crustal materials (Fig. 16a). The fold-and-thrust belt in the Foothills region is formed by stresses transmitted across the Central Range and the deformation extends down to below the Moho. While the deformation under the Central Range is dominated by

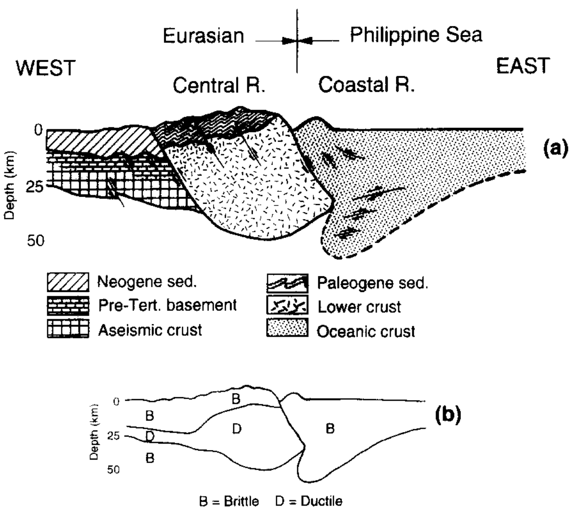

Fig. 16. (a) Schematic cross-section of the proposed lithospheric model. In this model the lithospheres (approximately 100 km thick) of the Philippine Sea plate and the Eurasian plate are engaged in collision, without subduction of either plates. The collision has resulted in the thickening of the crust, through downwarping as well as the extrusion of the mid- and lower crust, whereby the Central Range was uplifted. Note that the whole lithosphere probably has been deformed in the orogeny as indicated in Fig. 13. (b) Schematic rheological composition of the Taiwan orogen as suggested by distribution of seismic foci.

flow, the crust and upper mantle form a sandwich of strong–weak–strong–weak materials that deform by brittle deformation in the strong layer and flow in the weak layer (Fig. 16b). On the Philippine Sea plate side, thickening of the crust has accompanied shortening which has resulted in the stacking of the volcanic arc, the forearc and the trench sediments in the Coastal Range. The area west of Taiwan is dominated by N–S tension resulting from transmission of stress in the brittle layer on top or from flow in the ductile layer. A representative cross-section of the model is shown in Fig. 16, the overall plate interaction and the 3-D features are illustrated in Fig. 13.

4.4. *Discussions of the model*

The hypothesis described above is very general. The agreement with available observations described earlier can be easily established. There are many implications however that are candidates for use in falsification. We shall discuss some of the details and deductions of the hypothesis as we see it.

The oblique (N70°W) convergence between the Philippine Sea and the Eurasian plates partitions into the shortening of the margins of both plates and northward (actually NNE) subduction. The suture between these plates can be discerned in the tomographic images (Rau and Wu, 1995), and from differences in seismicity as described earlier. The convergence thickened the whole crust to form a root under the Central Range and also raised the mid- to lower crust to shallow depth to build the Range; the relatively high-velocity (5.5 km/s) and high-density rocks are probably similar to those in the Pre-Tertiary eastern Central Range. At the same time, both the crust and the upper mantle of the Philippine Sea plate margin have been thickened to build the Coastal Range. The Tertiary strata in the Central Range are not more than a few kilometers thick and lie directly on the Pre-Tertiary basement rocks similar to those now exposed on the eastern side of the Central Range. The Western Foothills are underlain by a thick sedimentary basin filled with post-Late Pliocene rocks that were shed from the Central Range. These rocks are deformed as a fold-and-thrust belt by stresses transmitted across the Central Range; folding and blind-thrust faulting occur within the brittle layers in the upper 40 km of the crust. The lithosphere is a sandwich of brittle–viscous–brittle–viscous (upper crust–lower crust–upper mantle) layers. The collisional effects are also transmitted to the western Taiwan Coastal Plain and to Taiwan Strait; E–W oblique right-lateral strike-slip/normal faults occurred in association with several earthquakes within this century and E–W-striking normal faulting in the Strait.

Based on both seismicity (Fig. 4) and tomographic imaging (Fig. 2, A–A′ and Fig. 3), it is evident that the intersection of the westward extension of the Ryukyu Trench and the Taiwan orogen is located south of Hualien. The exact location is probably not as important, as the slope of the subduction zone is initially very small. The subduction zone actually appears to underplate the eastern part of Taiwan south of Hualien. The changing geometry of the collisional contact should affect the variation of intensity of the orogeny as well as the style of deformation along the Central Range. Between Hualien and Taitung the two sides of the plate should essentially bear the full brunt of the collision and therefore this section should undergo the largest shortening. Further north, the Philippine Sea plate is impinging on the lower part of the Eurasian lithosphere. Between Hualien and Nanao, the compressional contact is placed at increasingly greater depth toward the north; the overall shortening on the Eurasian side is still expected to take place. The Eurasian plate above the Ryukyu subduction zone to the east is decoupled from the subducting Philippine Sea plate and will not be compressed. As a result, we can expect the separation of the Eurasian plate along the Hualien–Nanao line. Here WNW-trending tension is generated. That such a stress condition exists may be shown by normal faulting in the Hoping basin (Lin, 1994). The WNW–ESE-oriented tension such separation would generate is also consistent with the focal mechanism of the June 5, 1994 earthquake cited earlier.

The oblique collision of the Luzon Arc with the Eurasian margin implies a shift of the point of contact southward with time (Suppe, 1984). A rate of 90 km/m.y. was estimated by Suppe (1984) adopting the trend of Taiwan as the orientation of the Luzon Arc before collision and taking the line connecting the shelf south of Penghu to the middle of the Okinawa Trough near northeastern Taiwan as the edge of the shelf before collision. Lee et al. (1991) used the block rotation in the Coastal Range as a proxy for determining the time of contact of the Luzon Arc with the shelf and their rate is 40 km/m.y.; the contact near Hualien occurred about 3.5 m.y. ago and reached Taitung about 1 m.y. ago. This is much slower than Suppe's estimate. The two rates can be reconciled if, using Suppe's geometric construction, the trend of the present Luzon Arc (N10°W) is taken as the trend of Luzon before collision and if the shelf line is constructed by linking the shelf south of Penghu to the southern edge of the Okinawa Trough, i.e., assume that the back-arc spreading was not as extensive as previously estimated. Suppe (1984) further assumed that the propagation began in northernmost Taiwan and has now reached the southern tip of Taiwan. Part of the reason for extending the propagation to northern Taiwan is to account for the orogeny northwest of Hualien. Our hypothesis has obviated this view by invoking the finite thickness of the lithosphere, whereby the orogeny persists north of Hualien as the Philippine Sea plate continues its northward subduction as well as its collision with the Eurasian plate.

As far as the southern extent of the collision is concerned, we have seen that south of the Kaoshiung–Taitung line, the southern part of Taiwan can be described as a true accretionary wedge overlying a subduction zone, while north of this line the collision involves the deformation of the continental crust. Thus there must be a discontinuity or, more likely, a transition zone in the vicinity of this line; in the south, the materials between the volcanic arc and the deformation front is undergoing shortening while the deformation front continues to move westward to approach the Eurasian continental shelf and in the north, the orogeny described above is taking place (Wu, 1996). The transition is partly a left-lateral fault and partly the result of a southward extrusion, or escape, of the Central Range. It is possible that the GPS results in southern Taiwan (Yu and Chen, 1994) are showing that the Hengchun Peninsula is moving westward relatively to the Coastal Plain north of Kaoshiung. Recall that the Coastal Range of eastern Taiwan is actually a telescoped suite of island arc volcanics, an accretionary wedge and trench sediments, an equivalent coastal range to the west of the Hengchun Peninsula may be formed in about six million years on the continental shelf of SE China, incorporating the Lutao–Lanhsu volcanic arc, the Hengchun Peninsula and the sediments to the west of Hengchun.

The normal faulting in the Taiwan Strait is a problem of far-reaching consequence. The problem of producing normal faulting in an otherwise compressional environment has been explored (Burchfiel and Royden, 1985; Burchfiel et al., 1992; England and Molnar, 1993). In the Taiwan Strait, the strike of the fault is nearly parallel to σ_1, the maximum principal compressive stress, similar to the normal faulting on the Tibetan Plateau, north of the Himalayas. But in this case, neither collapse of a high plateau or a cessation of collision, causes invoked by England and Molnar (1993) applies. Kao and Wu (1996) proposed the following two alternatives. Analogous to the model that Zhao and Morgan (1987) proposed to explain the rising of the Tibetan Plateau, we propose that flows may be generated in the ductile layers in the lower crust and upper mantle (the aseismic layer in the lower crust or the aseismic layer in the mantle). While the flow in the lower crust may be linked to the ductile flow in the Central Range, the upper mantle flow results from the push by the Philippine Sea plate and the root formation. When either flow diverges to the north and south, local N–S-directed tension may occur. The other alternative is suggested by experiments of rock fracture under low and intermediate confining pressure, conditions satisfied in the shallow crust, in which dilatant cracks parallel to σ_1 may form. The first alternative requires the participation of lower crustal or upper mantle flow while the second alternative implies the transmission of collision-induced stress into the Strait. Although normal faulting could also occur in the outer-rise area due to the bending of the lithosphere (an implication of the thin-skinned hypothesis), we do not offer this particular interpretation because there is no evidence for the existence of active normal faults in the Strait that are parallel to the assumed plate boundary based on extensive petroleum company seismic profiles (e.g., Sun, 1985). Furthermore, the T-axis for the September 16, 1994 earthquake described earlier is perpendicular, not parallel, to the presumed subduction direction, inconsistent with the plate bending model.

It should be said that the proposed hypothesis is still limited in scope. The lack of data below about 60 km prevents us including considerations regarding the processes in the upper mantle under the Taiwan orogen. For example, as a consequence of the formation of the root, rocks under a shallower thermal regime in the upper mantle must be pushed downward to greater depth (by 20–30 km), where the ambient temperatures are higher. Thus, we may expect it to form a positive density anomaly that could lead to 'delamination', a process that has been proposed in conjunction with orogeny (Bird, 1978; Molnar, 1988). Also, we did not deal with the potentially resolvable question of how the former subduction ceased and collision began. We can answer the question partly through a search for the remnant subduction zone either through seismicity or velocity anomalies. But until the seismic network is expanded to cover the Philippine Sea area east of Taiwan, a search is not possible. We shall expand the hypothesis in the future if warranted.

4.5. Proposed falsification experiments of lithosphere collision models

In the discussion above a number of implications are described and several of them can be subjected to tests. Such tests can be performed with existing data of which the PI's are not aware, or with experiments designed specifically to falsify various aspects of the hypothesis. In the following discussion we shall suggest an initial set of tests.

Although judging from the seismicity under the Coastal Range and through rheological considerations, the Philippine Sea plate near Taiwan appears to have been thickened, with the land-based seismic network, the locations of offshore earthquakes, their depths in particular, are not very well constrained. If the crust does not thicken at the margin of the Philippine Sea plate, then a major question arises: how is the shortening of the Philippine Sea achieved? The recently acquired data in this area (C.S. Liu, pers. commun., July 1996) will most probably provide a basis for testing. In any case, the intraplate deformation of the Philippine Sea plate near Taiwan is one of the major aspects of the collision tectonics.

One of the critical elements in the proposed model is the manner in which the Central Range was created. If the mid- to lower crust extrusion model is right, then the modern deformation of the Central Range as measured in leveling or vertical GPS surveys should indicate an overall more rapid uplift in the higher ranges. The long-term deformation should be recorded in the geologic structures in the Central Range as well. Thus detailed mapping of the Range will be highly desirable. To decipher the transition from the Western Foothills to the Central Range, from a rheologically sandwiched (brittle–ductile–brittle) region to a highly mobile region will be most interesting. Here, refraction and near-vertical incidence reflection studies will likely yield pertinent data to test whether there is a marked change in seismic velocities between the two units. By extruding the deeper rocks to shallower level the thermal regime will certainly have changed. The thermal gradient at shallow level must be drastically increased, but the thermal gradient in the mid-crust would have been decreased. In terms of thermal gradients near the surface, there are many hot springs in the Central Range (Chen, 1982), and the available heat flow measurements there do indicate higher values, but they are not corrected for topography. Heat flow measurements being difficult to make and interpret in areas of extreme relief, perhaps modern magnetotelluric measurements (Park et al., 1993) may be used to obtain electric conductivities, which can in turn be interpreted in terms of thermal structures.

One of the deductions of the hypothesis that is eminently falsifiable is the existence of the transition in southern Taiwan discussed above. Limited existing data do show that the anticlinal axis near Kaoshiung (Fig. 1) undergoes a turn (Sun, 1963) that is consistent with a left-lateral motion in the transition zone. Detailed work in this area is hampered by restricted access to some key outcrops, the lack of a good geologic map (the 1:50,000 map has not yet been completed) and much of the possible evidence is to be found under the Coastal Plain. Also, the seismicity there is less frequent than further north, and therefore will require more time before we can use seismicity and focal mechanisms to look at the nature of deformation there. Further accumulation of GPS data should also clarify the relative motions between the Hengchun Peninsula and the rest of the island. If the transition zone does not exist then the difference between what we think is the collision zone and the accretionary wedge does not exist, and a major part of the hypothesis has to be modified or abandoned.

Currently the tectonics of the Taiwan Strait and its relation to that in the Coastal Plain cannot yet be completely deciphered. We hypothesized that the flow in the crust or in the upper mantle are probably responsible for the generation of the N–S tensile stress that resulted in the graben formation. If so, there are probably certain flow patterns given the boundary conditions. To falsify the flow and the stress transmission model proposed, we can map the anisotropy in the area. Also, the distribution of active normal faults in the Strait and their orientations will enable us to decipher the relation between the Taiwan orogeny and the ongoing deformation in the Taiwan Strait. When data exchange across the Strait takes place, then such studies can be done.

5. Discussion and conclusion

In that Taiwan is a prime example of active arc–continent collision and that both an established knowledge base and extensive research infrastructure exist locally, further detailed studies can provide a sound basis for testing hypotheses on orogeny. Although this orogen is relatively compact, it is not simple, and extensive analyses of recently acquired data will evidently be the immediate step needed to advance further in our understanding. Attempts to apply the Popperian concepts of scientific investigation in the study of tectonics of Taiwan can help us focus our attention on key aspects of the tectonic problem.

As far as the Taiwan orogeny is concerned, we are faced with an unprecedented opportunity in understanding the dynamics of the Taiwan orogen. Of the many proposed experiments, the reflection profiling across the Central Range will probably be the most useful in obtaining a high-resolution image of the key components of the core of the mountain. Although the vertical boundary will not be clearly imaged, the boundary between the Central Range and the Foothills could be well delineated. The infrastructures exist in Taiwan to conduct such profiling. A long-term (on the order of a year) ocean-bottom seismometer (OBS) deployment in the offshore area of eastern Taiwan to record both local seismicity and teleseisms can provide data to study more clearly the intraplate tectonics of the collisional margin of the Philippine Sea plate. OBS deployment can also address the question, 'where did the subducted slab go?', using teleseismic tomography to search for a high-velocity zone in the mantle. Data on thermal structures are also very critical. Although magnetotelluric studies can provide some constraints, a few direct heat flow measurements will eventually be necessary.

More thorough testing will enable us to establish a better conceptual model. With such a model appropriate numerical simulations can then be formulated and conducted, thus allowing us to quantify estimates of the rate of uplift, the strain rate in different areas, etc. Inconsistencies with such modeling will indicate either the weakness of the model or the inadequacy of data, thus pointing out the need of further data taking. Such iteration should place the study of orogeny on a firm basis.

Acknowledgements

This research came into focus when the senior author was on sabbatical leave from SUNY Binghamton in 1993 at the Institute of Earth Sciences (IES), Academia Sinica, in Taipei, Taiwan. A series of seminars on the tectonics of Taiwan co-convened with Dr. Y.H. Yeh was particularly stimulating. Discussions with Prof. Y.L. Yung of California Institute of Technology on science in general were useful in directing the senior author's queries. The senior author wishes to acknowledge the importance of the threatened system of sabbatical leaves. NSF grants EAR-8916159 to the senior author initiated this phase of the Taiwan research and INT-9513945 enabled him to complete it. Dr. Ray Russo's review of the manuscript greatly improved it.

References

Barr, T.D. and Dahlen, F.A., 1989. Brittle frictional mountain building, II. Thermal structure and heat budget. J. Geophys. Res., 94: 3923–3947.

Benioff, H., 1955. Seismic evidence for crustal structure and tectonic activity. Geol. Soc. Am. Spec. Pap., 62: 61–95.

Biq, C., 1981. Collision, Taiwan-style. Mem. Geol. Soc. China, 4: 91–102.

Bird, P., 1978. Initiation of intracontinental subduction in the Himalaya. J. Geophys. Res., 83: 4975–4987.

Burchfiel, B.C. and Royden, L.H., 1985. North–south extension within the convergent Himalayan region. Geology, 13: 679–682.

Burchfiel, B.C., Chen, Z., Hodges, K.V., Liu, Y., Royden, L.H., Deng, C. and Xu, J., 1992. The south Tibetan detachment system, Himalayan orogen: extension contemporaneous with and parallel to shortening in a collisional mountain belt. Geol. Soc. Am. Spec. Pap., 269, 41 pp.

Byerlee, J.D., 1978. Friction of rocks. Pure Appl. Geophys., 116: 615–626.

Cardwell, R.K., Isacks, B.L. and Karig, D.E., 1980. The spatial distribution of earthquakes, focal mechanism solutions, and subducted lithosphere in the Philippine and northeastern Indonesian islands. In: D.E. Hayes (Editor), The Tectonic and Geologic Evolution of Southeast Asian Seas and Islands. Am. Geophys. Union, Geophys. Monogr., 23: 1–35.

Chai, B.H.T., 1972. Structure and tectonic evolution of Taiwan. Am. J. Sci., 272: 389–422.

Chang, M., 1992. Integrated geological and geophysical interpretation of Penghu sedimentary basin. Pet. Geol. Taiwan, 27:237–250.

Chen, C.H., 1982. Analysis of topographic effects on ascending thermal water in the Central Range of Taiwan. Proc. Natl. Sci. Council, 6:241–249.

Crespi, J., Chan, Y.-C. and Swaim, M. S., 1996. Synorogenic extension and exhumation of the Taiwan hinterland. Geology, 24: 247–250.

Dahlen, F. A. and Barr, T. D., 1989. Brittle frictional mountain building, 1. Deformation and mechanical energy budget. J. Geophys. Res., 94: 3906–3922.

Davis, D., Suppe, J. and Dahlen, F.A., 1983. Mechanics of fold-and-thrust belts and accretionary wedges. J. Geophys. Res., 88: 10,087–10,101.

England, P. and Molnar, P., 1993. Cause and effect among thrust and normal faulting, anatectic melting and exhumation in the Himalaya. In: P.J. Treloar and M.P. Searle (Editors), Himalayan Tectonics. Geol. Soc. London Publ., 74: 401–411.

Gong, S.Y., Lee, T.Y., Wu, J.C., Wang, S.W. and Yang, K.M., 1995. Possible links between Pliocene–Pleistocene reef development and thrust migration in the southwestern Taiwan. In: H.H. Tsien (Editor), International Conference and 3rd Sino–French Symposium on Active Collision in Taiwan, Program and Extended Abstracts. Geol. Soc. China Publ., pp. 113–119.

Grow, J.A. and Bowin, C.O., 1979. Multichannel seismic depth sections and interval velocities over outer continental shelf and upper continental slope between Cape Hatteras and Cape Cod. In: J.S. Watkins, L. Montadert and P.W. Dickerson (Editors), Geological and Geophysical Investigations of Continental Margins. Am. Assoc. Pet. Geol., Mem., 29: 65–83.

Hatcher, R.D. and Hooper, R.J., 1992. Evolution of crystalline thrust sheets in the internal parts of mountain chains, In: K.R. McClay (Editor), Thrust Tectonics. Chapman and Hall, London, pp. 217–233.

Ho, C.S., 1988. An Introduction to the Geology of Taiwan: Explanatory Text of the Geologic Map of Taiwan. Ministry of Economic Affairs, Taipei, 192 pp.

Hu, H.N. and Tsan, S.F., 1984. Structural study of the slate formation along the south link railroad, Taiwan. Spec. Publ. Central Geol. Surv., 3: 25–43.

Iwasaki, T., Hirata, N., Kanazawa, T., Melles, J., Suyehiro, K., Urabe, T., Moller, L., Makris, J. and Shimamura, H., 1990. Crustal and upper mantle structure in the Ryukyu island arc deduced from deep seismic sounding. Geophys. J. Int., 102: 631–651.

Kao, H. and Wu, F.T., 1996. The 16 September earthquake ($m_b = 6.5$) in the Taiwan Strait and its tectonic implications. Terr. Atmos. Ocean Sci., 7: 13–29.

Kohlstedt, D.L., Evans, B. and Mackwell, S.J., 1995. Strength of the lithosphere: constraints imposed by laboratory experiments. J. Geophys. Res., 100: 17585–17602.

Lallemand, S.E., Liu, C.S. and Lin, S.J., 1995. Behavior of the Ryukyu sliver in the wave of the indenting northern Luzon arc (east of Taiwan). In: H.H. Tsien (Editor), International Conference and 3rd Sino–French Symposium on Active Collision in Taiwan, Program and Extended Abstracts. Geol. Soc. China Publ., pp. 167–175.

Lee, C.R. and Chang, W.T., 1986. Preliminary heat flow measurements in Taiwan. In: Circum-Pacific Energy and Mineral Resources Conference, 4th, Singapore, Proceedings.

Lee, T.Q., Kissel, C., Barrier, E., Laj, C. and Chi, W.R., 1991. Paleomagnetic evidence for a diachronous clockwise rotation of the Coastal Range, Eastern Taiwan. Earth Planet. Sci. Lett., 104: 245–257.

Lee, T.-Y., Tang, C.-H., Ting, J.-S. and Hsu, Y.-Y., 1993. Sequence stratigraphy of the Tainan basin, offshore southwestern Taiwan. Pet. Geol. Taiwan, 28: 119–158.

Lee, T.Y., Hsu, Y.Y. and Tang, C.H., 1995. Structural geometry of the deformation front between 22°N and 23°N and migration of the Penghu Canyon, offshore of southwestern Taiwan arc–continent collision zone. In: H.H. Tsien (Editor), International Conference and 3rd Sino–French Symposium on Active Collision in Taiwan, Program and Extended Abstracts. Geol. Soc. China Publ., pp. 219–227.

Lee, W.H.K., Wu, F.T. and Jacobson, C., 1976. A catalog of historical earthquakes in China compiles from recent Chinese publications. Bull. Seismol. Soc. Am., 66: 2003–2016.

Lin, C.H. and Roecker, S.W., 1993. Deep earthquakes beneath central Taiwan: mantle shearing in an arc–continent collision. Tectonics, 12: 745–755.

Lin, S.C., 1994. Bathymetry and seismic Characteristics Offshore Eastern Taiwan, and its Tectonic Implication. M.S. Thesis, Institute of Oceanography, National Taiwan University, 77 pp.

Lyon-Caen, H. and Molnar, P., 1983. Constraints on the structure of the Himalaya from an analysis of gravity anomalies and a flexural model of the lithosphere. J. Geophys. Res., 88: 8171–8183.

Molnar, P., 1988. A review of geophysical constraints on the deep structure of the Tibetan Plateau, the Himalaya and the Karakoram, and their tectonic implications. Trans. R. Soc. London, A, 327: 33–88.

Nafe, J.E. and Drake, C.L., 1965. Density vs velocity curve. In: F.S. Grant and G.F. West (Editors), Interpretation Theory in Applied Geophysics. McGraw-Hill Book Company, New York, pp. 199–200.

Park, S.K., Johnston, M.J.S., Madden, T.R., Morgan, F.D. and Morrison, H.F., 1993. Electromagnetic precursors to earthquakes in the ULF band: a review of observations and mechanisms. Rev. Geophys., 31: 117–132.

Popper, K.R., 1968. The Logic of Scientific Discovery. Harper Torchbooks, Harper and Row, New York.

Rau, R.J., 1992. Flexure Modeling and Taiwan Tectonics. Master thesis, State University of New York at Binghamton, 131 pp.

Rau, R.J. and Wu, F.T., 1995. Tomographic imaging of lithospheric structures under Taiwan. Earth Planet. Sci. Lett., 133: 517–532.

Rau, R.J., Wu, F.T. and Shin, T.C., 1996. Regional network focal mechanism determination using 3-D velocity model and SH/P amplitude ratio. Bull. Seismol. Soc. Am., in press.

Reed, D., Lundberg, N., Liu, C.S. and Kuo, B.Y., 1992. Structural relations along the margins of the offshore Taiwan accretionary wedge: implications for accretion and crustal kinematics, Acta Geol. Taiwan., 30: 105–122.

Rich, J.L., 1934. Mechanics of low-angle overthrust faulting as illustrated by Cumberland thrust block, Virginia, Kentucky and Tennessee. Amer. Assoc. Pet. Geol. Bull., 18: 1584–1594.

Salzberg, D.H., 1996. Simultaneous Inversion of Moderate Earthquakes Using Body and Surface Waves: Methodology and Applications to the Study of the Tectonic of Taiwan. Ph.D. Thesis, State University of New York, Binghamton, NY.

Seno, T., Stein, S. and Gripp, A.E., 1993. A model for the motion of the Philippine Sea plate consistent with NUVEL-1 and geological data. J. Geophys. Res., 98: 17941–17948.

Slemmons, D.B. and Depolo, C.M., 1986. Evaluation of active faulting and associated hazards. In: R.E. Wallace (Editor), Active Tectonics. U.S. Geol. Surv., Menlo Park, Calif., pp. 45–62.

Sun, S.C., 1963. The reef limestones and the geologic structures in the vicinity of Kaohsiung city, Taiwan. Pet. Geol. Taiwan, 2: 47–64.

Sun, S.C., 1985. The Cenozoic tectonic evolution of offshore Taiwan. Energy, 10: 421–432.

Suppe, J., 1976. Decollement folding in western Taiwan. Pet. Geol. Taiwan, 13: 25–35.

Suppe, J., 1980. Imbricate structure of western Foothills belt, south-central Taiwan. Pet. Geol. Taiwan, 17: 1–16.

Suppe, J., 1981. Mechanics of mountain building and metamorphism in Taiwan. Mem. Geol. Soc. China, 4: 67–89.

Suppe, J., 1984. Kinematics of arc–continent collision, flipping of subduction, and back-arc spreading near Taiwan. Mem. Geol. Soc. China, 6: 21–33.

Suppe, J., 1987. The active Taiwan mountain belt. In: J.P. Schaer and J. Rodgers (Editors), The Anatomy of Mountain Ranges. Princeton Univ. Press, Princeton, N.J., pp. 277–293,

Teng, L.S., 1990. Geotectonic evolution of late Cenozoic arc–continent collision in Taiwan. Tectonophysics, 183: 57–76.

Tsai, Y.B., 1986. Seismotectonics of Taiwan. Tectonophysics, 125: 17–37.

Tsao, S., Li, T.C., Tien, J.L., Chen, C.H., Liu, T.K. and Chen, C.H., 1992. Illite crystallinity and fission-track ages along the east central cross-island highway of Taiwan. Acta Geol. Taiwan., 30: 45–64.

Wu, F.T., 1970. Focal mechanisms and tectonics in the vicinity of Taiwan. Bull. Seismol. Soc. Am., 60: 2045–2056.

Wu, F.T., 1978. Recent tectonics of Taiwan. J. Phys. Earth, 26: S265–299.

Wu, F.T., 1996. A proposed transition between the collisional orogen and the accretionary wedge in southern Taiwan. Manuscript to be submitted.

Wu, F.T., Chen, K.C., Wang, J.H., McCaffrey, R. and Salzberg, D., 1989. Focal mechanisms of recent large earthquakes and the nature of faulting in the Longitudinal Valley of eastern Taiwan. Proc. Geol. Soc. China, 32: 157–177.

Yeh, Y.H. and Yen, H.Y., 1992. Bouguer anomaly map of Taiwan. Inst. Earth Sci., Acad. Sin., Taipei.

Yeh, Y.H., Lin, C.H., Liu, C.C., Yeh, H.Y., Huang, B.S., Liu, C.S., Wu, F.T. and Shi, R.C., 1995. Wide-angle deep seismic profiling in Taiwan. EOS, Trans. Am. Geophys. Union, F635.

Yen, H.-Y., Liang, W.-T., Kuo, B.-Y., Yeh, Y.-H., Liu, C.-S., Reed, D., Lundberg, N., Su, F.-C. and Chung, H.-S., 1995. A regional gravity map for the subduction–collision zone near Taiwan. Terr. Atmos. Ocean Sci., 6: 233–250.

Yu, S.B. and Chen, H.Y., 1994. Global positioning system measurements of crustal deformation in the Taiwan arc–continent collision zone. Terr. Atmos. Ocean Sci., 5: 477–498.

Zhao, W.L. and Morgan, W.J.P., 1987. Injection of Indian crust into Tibetan lower crust, a two-dimensional finite element model study. Tectonics, 6: 489–504.

Zwick, P., McCaffrey, R. and Abers, G., 1995. Earthquake moment tensor analysis from inversion of teleseismic body waves. Manuscript, RPI, Troy, New York, 118 pp.